Common Accommodation Mechanisms for Mutualistic and Detrimental Fungi in *Oryza sativa* (Rice) Roots

Nkechi Carol Ibe

Newnham College, University of Cambridge

Submission Date: 30th September 2019

Declaration: This dissertation is submitted for the degree of Doctor of Philosophy

DECLARATION

This thesis is the result of my own work and includes nothing which is the outcome of work done in collaboration except as declared in the Preface and specified in the text.

It is not substantially the same as any that I have submitted, or, is being concurrently submitted for a degree or diploma or other qualification at the University of Cambridge or any other University or similar institution except as declared in the Preface and specified in the text. I further state that no substantial part of my dissertation has already been submitted, or, is being concurrently submitted for any such degree, diploma or other qualification at the University of Cambridge or any other University or similar institution except as declared in the Preface and specified in the text

It does not exceed the prescribed word limit for the relevant Degree Committee.

Nkechi Carol Ibe

September 2019

Common Accommodation Mechanisms for Mutualistic and Detrimental Fungi in Oryza sativa (Rice) Roots

Nkechi Carol Ibe

ABSTRACT

Rice roots engage in symbiosis with ancient symbiotic fungi such as *R. irregularis*, whilst resisting invasion of the detrimental fungus *M. oryzae*, a major causative agent of the rice blast (leaf) disease. *M. oryzae* can also invade rice roots with simple non-melanised hyphopodia formed on the rice root surface, very similar to *R. irregularis*. This similarity in behaviour has raised questions whether the biotrophic pathogen adopts an endophytic lifestyle during rice root colonisation, possibly as a disguise to bypass the plant defence machinery whilst entering the host. Identifying shared plant genes and development programmes utilised by *M. oryzae* and *R. irregularis* during rice root invasion will provide a better understanding of how the host plant responds to and accommodates both fungi in its root.

The work presented here, describes a novel function of three *Oryza sativa* plasma membrane receptors (*Chitin Elicitor Receptor Kinase 1, CERK1*; *Nod Factor Receptor 5, NFR5* and *Chitin Elicitor Binding Protein, CEBiP*) in enabling *M. oryzae* invasion of rice roots. It also demonstrates, for the first time, a role of OsNFR5 as a compatibility factor, rather than a defence receptor during *M. oryzae* rice leaf infection. Unexpectedly, OsCEBiP was found to be involved in rice root colonisation by *R. irregularis*, challenging existing reports while presenting a different perspective on the possible co-functioning of the LysM-RLP with OsCERK1 during AM symbiosis. Excitingly, OsCERK1 emerged as a common co-receptor for AM symbiosis, immunity signalling and rice root invasion by *M. oryzae*, supporting a diverse role of the LysM-RLK in the perception of an array of signalling molecules.

Lastly, transcriptome comparison analysis performed in this study revealed a new set of co-induced rice genes (*Exo70-H3b* exocyst, *Lectin Receptor-Like Kinase, LecRLK* and *DUF538* genes encoding 'proteins of unknown function) that may be commonly required for the invasion of rice roots by both symbiotic and detrimental fungi. These findings lend strong support to the long-standing hypothesis that plant pathogens exploit genetic pathways established in the ancient arbuscular mycorrhizal symbiosis to facilitate their invasion of the host plant. They also have significant implications for effective crop improvement and disease control strategies, which will contribute to global food security.

ACKNOWLEDGEMENTS

First, I would like to thank Prof. Uta Paszkowski for being a great supervisor during my PhD. I appreciate your support and professional guidance, which has made me a better scientist. Thank you for welcoming me into your lab and sharing your wealth of scientific knowledge with me. It's been an amazing experience, not one without challenges, but one that has contributed to my science career. Thank you so much. I am very grateful!

To my second supervisor, Prof. Nick Talbot, thank you so much for your wonderful support during my PhD. I appreciate you giving me the opportunity to do some of my experiments in your laboratory with the help of your postdoctoral researchers, Vincent Were and Lauren Ryder. I always felt so welcomed in your laboratory and I won't forget the time you took out from your very busy schedule to give me great advice about my work. I greatly appreciate your support and thank you all so much!

Being part of the Department of Plant Sciences has been a wonderful experience and contribution to my personal and professional life. I have thoroughly enjoyed meeting so many amazing scientists, staff and colleagues, many of whom I can call 'friend'. I would like to thank members of the Paszkowski laboratory, especially Jen McGaley, Craig MacKenzie and Roza Bilas who were particularly very helpful and supportive with watering my plants, getting me coffee and giving time to listen and laugh at my silly jokes, towards the end of my PhD. I appreciate you all.

There are so many people in the Department of Plant Sciences and the university that I would like to thank for their support and contribution towards the African science initiatives that I have been so honoured and blessed to organise during my time in the department. Special thanks to Trisna Tungadi, Leonie Luginbuehl, Conor Simpson, Emily Servante, Jen McGaley, Noor Agip (MRC-MBU), Chloe Orland, Greg Reeves, Greg Mellers (may his soul rest in peace), Del Hawtin, Catherine Butler, Barbara Landamore, Prof. John Carr, Prof. Jim Haseloff, Prof. Sir David Baulcombe and others. Thank you so much for believing in our cause to empower African scientists to help lift millions of Africans out of hunger and poverty through research and innovation. It's been a wonderful experience and I don't know what I would have done without your support. Thanks again!

I also would like to thank the Gates Cambridge Scholarship and uncle Bill Gates for funding my PhD. I call him my uncle even though I do not know him personally, but he has funded my PhD, something that I don't know how it would have come about, except for his kind and generous heart. As an African who came from a family that is not wealthy, there is no way I would have gotten this

far if not for people like Mr Gates, who continue to be a blessing to many. I am deeply humbled and grateful. Thank you, Sir!

May I also use this opportunity to thank members of the Cambridge University Gospel Choir, a student society that I was so blessed and honoured to serve during my PhD. There, I met people from different nations, who I call friends, sisters and brothers. The inspiration, the words of encouragement and the uplifting songs and performances kept me going throughout my PhD. It gave me the opportunity to meet people within the university and the community that I may never have met. I cherish every moment of my time with the choir and will carry these unforgettable memories into the future. Thank you!

To my dear friends! Where do I start? I have so many of you and I thank and appreciate each one of you for your kindness and support throughout my PhD. Special thanks to my dearest friend, Alma Ogunbode, who helped me with childcare and preparing those special Jamaican delicacies, including my favourite jerk chicken. Oh! What would I have done without you? Thank you so much. And to Patience James and Dean Eton, my friends and singing partners, thank you so much for inspiring me throughout this journey. It has been a blessing to meet you all in Cambridge.

And to my family! Ah! Where do I start to thank the most special people in my life? My dear husband (Ifeanyi) and sons (David and Daniel), who have been more than supportive and understanding throughout this journey. I call them my 'money-can't-buy' support system. Daniel is still in my tummy as I write this, but we have all done this PhD together. Thank you so much for showing me so much love, affection and kindness. I love you all forever!

To my dearest parents, and siblings and their families, you all know how it started. It's been an incredible and fruitful journey that we all have looked to see come through and it has. Thank you so much for your unconditional love and support. You are the best and I will forever cherish you as my family.

I wouldn't end without thanking my God, for He has been so good to me. I have run on your strength and vision, and I know that it would have been so easy for me to give up at any point in this journey, if not for your special grace and love to me. I return all the glory to You!

DEDICATION

I dedicate this work to my creator, the One who has touched my heart to look beyond myself and to do the things I do to make a difference in the lives of others, no matter how difficult, no matter how tiring, and no matter how inconvenient. As a person of colour, a black woman in science, it would be impossible for me to compete here with great minds in science and students from educationally privileged backgrounds, considering my own background and the 'impossibilities' that surround me. But with the support and understanding of many good people, I have made it this far, hence why I dedicate this work to people from disadvantaged communities, especially black minority students, who have the right attitude, the right passion and the right talents to make a difference, but often give up due to inadequate institutional preparation and support. I salute your courage and encourage you to keep going, keep dreaming and keep doing good, no matter how hard, no matter how odd and no matter how lonely it might get along the way. If I could do it, you can too! So, don't stop!

To African agricultural scientists, especially those in Africa, who continue to toil in the lab and in the field under unfavourable conditions, to make the continent a better place, with little or no resources, I understand your struggle and I believe in you. I know what hunger and poverty look like, and I know how much your hard work, passion and absolute dedication to science and to humanity can do to change things. I dedicate this work to your efforts, and encourage you to keep working hard, look beyond personal gain and accolades, and always find a way to use your education, talents and good offices to make a difference to those around you.

And finally, to everyone who has supported me in one way or the other, I dedicate this work to you. I do not forget where I have come from and the opportunities that I have been given to be where I am today. There is no way I would have done it without your inspiration, prayer and kind support, so thank you so much for everything. This is our success!

TABLE OF CONTENTS

LIST OF ABBREVIATIONS

AM	Arbuscular mycorrhiza
bp	Base pair
BiFC	Bimolecular fluorescence complementation
CCaMK	Calcium- and calmodulin-dependent protein kinase
cDNA	Complementary DNA
CNGC	Cyclic nucleotide-gated channels
C_t	Threshold cycle
CERK1	Chitin elicitor receptor kinase 1
CEBiP	Chitin elicitor binding protein
CO	Chitin oligosaccharide
CRISPR	clustered regularly interspaced short palindromic repeats
Cas9	CRISPR-associated protein 9
DMI	Does not make infections
DNA	Deoxyribonucleic acid
dNTP	Deoxynucleotide triphosphates
dpi	Days post inoculation
d.i.	Distilled water
EIHM	Extra-invasive hyphal membrane
ETI	Effector-triggered immunity
Exo	Exocyst
FDA	Fluorescein diacetate
g	Gram
GFP	Green fluorescent protein
GlcNAc	N-acetylglucosamine
h	Hour
HMGRI	3-Hydroxy-3-Methylglutaryl CoA Reductase 1
IPD3	Interacting protein of DMI3
LB	Lysogeny broth
LCO	Lipochitooligosaccharides
Lj	*Lotus japonicus*
LRR-RLK	Leucine-rich repeat receptor-like kinase

M	Milli
M	Micro
M	Molar
Mt	*Medicago truncatula*
NFR5	Nod factor receptor 5
NSP1	Nodulation Signalling Pathway 1
NSP2	Nodulation Signalling Pathway 2
Nod	Nodulation
NIN	Nodulation Inception
SbtM1	Secreted subtilisin protease
RAD1	Required for Arbuscule Development 1
Os	*Oryza sativa*
PI	Propidium iodide
IH	Invasive hypha
PAMP	Pathogen Associated Molecular Pattern
PAM	Periarbuscular membrane
PAS	Periarbuscular space
PPA	Pre-penetration apparatus
PTI	PAMP-triggered immunity
Fls2	Flagellin-Sensitive 2
BIK1	Botrytis-Induced Kinase 1
RBOHB/D	Respiratory burst oxidase homologue protein B/D
ROS	Reactive Oxygen Species
GlcNAc	N-acetylglucosamine
R	Cognate resistance
AVR	Avirulence
Slp1	Secreted LysM Protein 1
RLP	Receptor-like protein
PRRs	Pattern Recognition Receptors
LysM	Lysine motif
RNAi	RNA interference
CLSM	Confocal laser scanner microscopy
Kb	Kilobase
EDTA	Ethylenediaminetetraacetic acid
LiCl	Lithium chloride

HPT	Hygromycin phosphotransferase
CTR	Control
-ve	Negative
PCR	Polymerase chain reaction
qRT-PCR	Quantitative reverse transcription PCR
RNA	Ribonucleic acid
s	Seconds
sg	Single guide
SEM	Standard error of the mean
T1	Offspring of transformed plants
T2	Offspring of T1 generation
WGA	Wheat germ agglutinin
WT	Wild type
WPI	Weeks post inoculation
SL	Strigolactone
Myc	Mycorrhiza
Mag	*Magnaporthe*

CHAPTER 1

General Introduction

According to the United Nations Food and Agriculture Organisation (FAO), rice is a major staple food for more than half of the world population, and of significant importance for food security in many low-income food deficit countries. As the consumption of rice has exceeded production in many developing countries, especially in sub-Saharan Africa (FAO, 1996), there is an urgent need to increase rice production and to develop rice cultivars that can better adapt to low input rice agro-ecosystems. Developing effective biofertilization systems alongside modern disease control strategies against rice pathogens such as *Magnaporthe oryzae*, the causative agent of the rice blast disease (Wilson and Talbot, 2009) is crucial for improving rice production and global food security.

1.1. The arbuscular mycorrhizal (AM) symbiosis

Plants are colonised by a plethora of microorganisms including bacteria, viruses and fungi, and this results in different types of associations, which may be competitive, mutualistic or parasitic. In either of these associations, plants can benefit from the microbes, suffer from the interaction or provide a habitat for microbial communities (for review, see Schirawski and Perlin, 2017). In mutualistic plant-microbe interactions, both organisms often benefit from nutrient and other signalling exchange that contributes to either of the organism's growth and metabolism. For instance, many plant roots associate with symbiotic microorganisms such as specific fungi (e.g., arbuscular mycorrhizal fungi), rhizobia bacteria or actinobacteria (*Streptomycetes* in particular) which provide the plant with soil mineral nutrients (Smith and Read, 2008).

The roots of many terrestrial plants form mutualistic associations with fungi of the Glomeromycotina (e.g., *Rhizophagus irregularis*) in a process known as arbuscular mycorrhizal (AM) symbiosis. AM symbiosis dates back ~450 million years and is believed to have evolved to help the earliest terrestrial plants to absorb nutrients in the absence of complex vascular root systems (Simon et al., 1993). Under limited soil nutrient conditions, plants such as rice (*Oryza sativa*) (Nakagawa and Imaizumi-Anraku, 2005), tomato (*Solanum*

lycopersicum) (David-Schwartz et al., 2001) and the legume *Medicago truncatula* (Sagal et al., 1995) engage in symbiosis with the AM fungus *R. irregularis*, which facilitates the uptake of phosphorus, and to a lesser extent, nitrogen and other mineral nutrients from the soil to the plant. In some cases, AM colonisation improves the plant's resistance to root pathogens (Newsham et al., 1995). In return, the fungus receives photosynthetic carbon which it uses for its own metabolism (Smith and Read, 2008).

AM symbiosis is initiated by a bi-directional exchange of signalling molecules between the symbiotic partners, which stimulates fungal hyphal growth towards the plant root surface where initial contact is made. Following this initial contact, the fungal hypha differentiates and forms an attachment structure called the hyphopodium on the root surface. From the hyphopodium forms a penetration hypha which the fungus uses to penetrate the rhizodermal layer of the plant, allowing it to enter the root where it grows, and forms highly branched hyphae called arbuscules within cortical cells (Figure 1.1). Arbuscules are housed in an apoplastic compartment surrounded by the peri-arbuscular membrane, which is considered the site of nutrient and signal exchange in symbiosis (for review, see Gutjahr and Parniske, 2013; Lanfranco et al., 2018).

Once inside the root, the fungus can colonise the plant root using two different strategies; an Arum-type or Paris-type colonisation (Dickson, 2004). In the Arum-type colonisation, fungal hyphae spread between cortical cells before penetrating an inner cortical cell to form arbuscules, whereas in the latter type, fungal hyphae grow through the intracellular passage of cortical cells where it forms hyphal coils or arbuscules (for review, see Luginbuehl and Oldroyd, 2017). Studies have found that plants colonised by the AM fungus generally show more resilience and tolerance to biotic and abiotic stresses compared to non-mycorrhizal plants, not solely due to a better nutritional status (Jung et al., 2012; Auge et al., 2015). AM fungus also improves soil quality and increases plant biodiversity (Rilling et al., 2015; Van der Heijden et al., 1998).

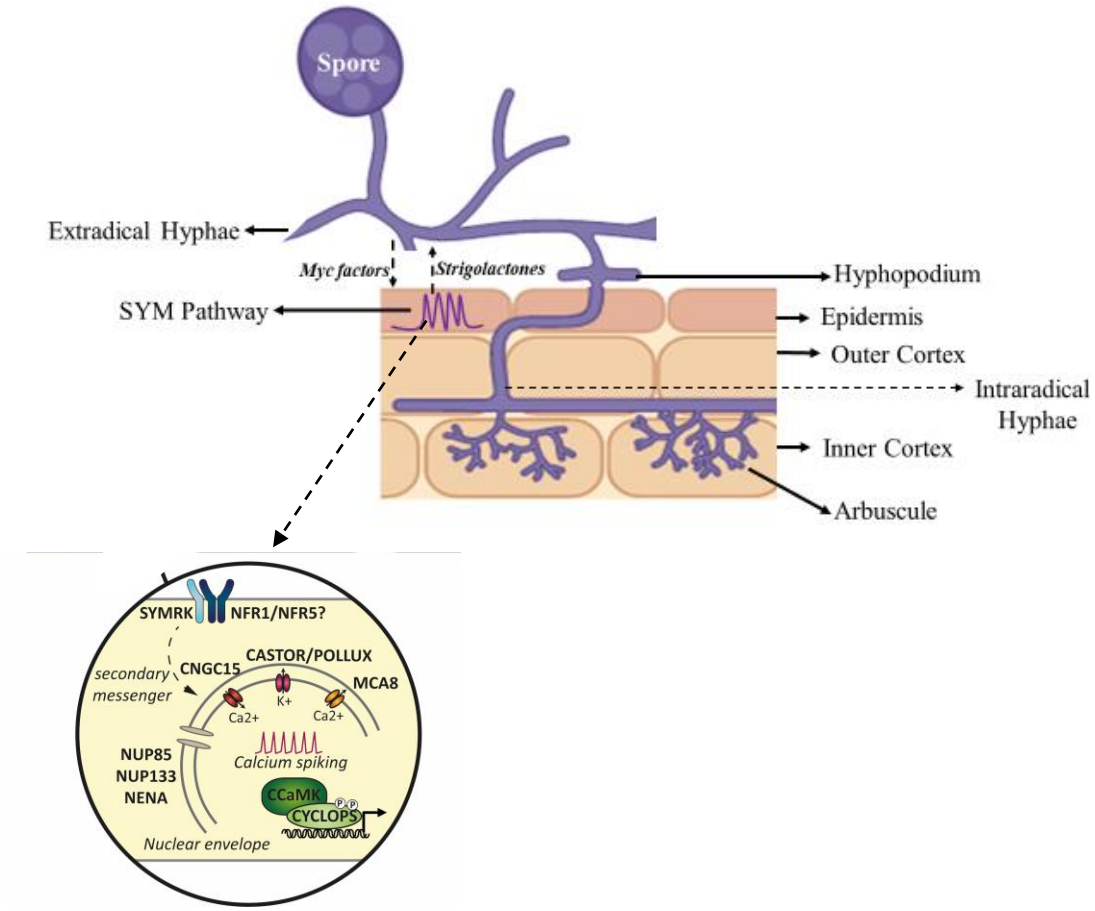

Figure 1.1: Stages of intracellular colonization of rice roots by *Rhizophagus irregularis*. The host plant releases strigolactones which stimulate AM fungal spore germination and intense hyphal branching. The hyphopodium is formed on the plant root surface followed by a pre-penetration apparatus (PPA), which allows the fungus to enter the plant host cell. The fungus grows intracellularly within cortical cells where it forms arbuscules, which is surrounded by a plant-derived peri-arbuscular membrane, the site of nutrient exchange during symbiosis. Arbuscules are surrounded by a plant-derived peri-arbuscular membrane (PAM). AM fungus releases signalling molecules known as Myc factors, which are recognised at the plasma membrane by unidentified Myc factor receptors that act in conjunction with SYMRK (Symbiosis Receptor-Like Kinase). The signals are transduced by putative secondary messengers to the nucleus to activate perinuclear calcium spiking, a process involving several proteins (e.g. CASTOR, POLLUX, MCA8, NUP85, NUP133, NENA and putative calcium channel. The calcium response is decoded by CCaMK, which phosphorylates and activates the transcription factor, CYCLOPS. (Image modified from Luginbuehl and Oldroyd, 2017).

1.1.1. Establishment of AM symbiosis: the pre-symbiotic phase

The establishment of AM symbiosis involves several successive steps. First is the mutual recognition of both plant and fungal partners within the rhizosphere. This is initiated by a molecular dialogue involving the exchange of signalling molecules between the fungus and host plant before any physical or direct contact is made via the formation of the hyphopodium. Plant-derived signals induce spore germination and intense hyphal branching to enable contact

with the plant root (Akiyama and Hayashi, 2006). In return, the fungus releases signalling molecules that elicit symbiotic responses in the root. This mutual exchange in molecular communication is crucial at the pre-contact phase but is also likely to occur during intra-radical colonisation by AM fungi. Notably, survival of AM fungi largely depends on efficient spore germination and rapid colonisation of the host plant. The spores inhabit the soil and can germinate spontaneously, independent of plant-derived signals, although root exudates and volatiles can promote or suppress spore germination, possibly due to spore receptors that respond to changes in the environmental chemical composition (for review, see Paszkowski 2006). Without a host plant, fungal hyphal growth is restricted and eventually ceases. This phenomenon occurs due to low amounts of stored carbon, although the spore can retain enough carbon that enables it to germinate again and find a new host (for review, see Paszkowski 2006).

1.1.2. Plant to fungal communication

In AM symbiosis, root exudates play a crucial role in enabling the fungus to enter an active state, whereby fungal metabolism and extensive hyphal branching are induced to enable the fungus to locate the host root (Besserer et al., 2006; Akiyama et al., 2005). Under conditions of nutrient starvation, especially when phosphorus is depleted in the soil, plant roots synthesize and release strigolactones and other signalling molecules such as flavonoids and 2-hydroxy fatty acids into the rhizosphere (Nagahashi and Douds, 2011; for review, see Nadal and Paszkowski, 2013; Schmitz and Harrison, 2014; Carbonnel and Gutjahr, 2014). Present in the root exudates of many monocotyledonous and dicotyledonous plant species are very low concentrations of strigolactones (Xie, 2016), which are involved in the communication between plants and a variety of parasites (Cook et al., 1966), arbuscular mycorrhizal fungi (Akiyama et al., 2005), and more recently, the legume-rhizobia symbiosis (De Cuyper et al., 2015; Foo and Davies, 2011).

Strigolactones are a group of sesquiterpenes first isolated as seed-germination stimulants for the root-parasitic weeds *Striga* and *Orobanche* (Cook et al., 1966; Bouwmeester et al., 2003; Akiyama and Hayashi, 2006). When exuded from the root, strigolactones induce hyphal branching in AM fungi (Akiyama and Hayashi, 2006; Besserer et al., 2006). They also have diverse functions in mycorrhizal symbiosis, including the activation of oxidative metabolism, mitochondria division and the release of fungal-derived symbiotic signalling molecules (Besserer et al., 2006; Genre et al., 2013; Tsuzuki et al., 2016). Following their release into the

rhizosphere, strigolactones become rapidly hydrolysed, with the resulting steep gradient concentration thought to provide a directional cue to the AM fungus (Nadal and Paszkowski, 2013; Ruyter-Spira et al., 2013). Parasitic plants have also been shown to utilise strigolactones to trigger seed germination and as a guiding signal to locate their host (Bouwmeester et al., 2007).

Strigolactones are synthesised from carotenoids through the action of an iron-binding protein encoded by D27 (DWARF27), Carotenoid Cleavage Dioxygenase 7 (CCD7), CCD8 and More Axillary Growth 1 (MAX1) (Schwartz et al., 2004; Alder et al., 2012). In the plastids, the precursor of strigolactones known as all-*trans*-β-carotene is converted into carlactone by the β-carotene isomerase D27 and CCD7 and CCD8 (Bruno et al., 2017; Seto et al., 2014; Kohlen et al., 2014; Alder et al., 2012). In the cytosol, MAX1 aids the catalysis of carlactone oxidations to carlactonic acid. Carlactonic acid is methylated, and subsequently oxidised into a biologically active form of strigolactone-like compounds by the Lateral Branching Oxidoreductase, an oxidoreductase-like enzyme of the 2-oxoglutarate and Fe (II)-dependent dioxygenase superfamily (Brewer et al., 2016; Zhang et al., 2014; Seto et al., 2014; Kohlen et al., 2014; Alder et al., 2012). Despite a broad understanding of strigolactone biosynthesis, it remains unclear whether canonical strigolactones or carlactone-derived molecules are synthesised in *Arabidopsis thaliana* (for review, see De Cuyper and Goormachtig, 2017) and which ones are endogenous hormones (Alder et al., 2012).

Understanding how strigolactones are secreted from the root into the soil for plant-microbe communication in the rhizosphere is crucial. So far, the only well-characterised strigolactone transporter is the *Petunia hybrida* ATP-Binding Cassette (ABC)-transporter Pleotropic Drug Resistance 1 (PDR1) (Kretzschmar et al., 2012), a member of the G-type subfamily of ABC transporters involved in the transport of phytohormones such as cytokinin, abscisic acid and auxin (Borghi et al., 2015). The export of strigolactones into the environment by PDR1 produces a strigolactone gradient which activates fungal metabolism, as well as provides a positional cue for the fungus to locate the host root (Kretzschmar et al., 2012). *P. hybrida pdr1* mutants showed a defect in exuding strigolactone from their roots, which resulted in reduced symbiotic interactions. At the same time, an enhanced branching phenotype, indicative of impaired strigolactone allocation was seen in *pdr1* mutants above ground (Kretzschmar et al., 2012). Strigolactone export from the cell has been attributed to the asymmetrical localisation of PDR1 at the plasma membrane. For instance, the localisation of PDR1 at the apical membrane of root hypodermal cells in the root tip suggests an active strigolactone export from

the root tip to the shoot. Conversely, PDR1 localisation at the outer lateral membrane of hypodermal passage cells above the root tip, where AM fungi enters the root, indicates an active outward traffic into the rhizosphere (Sasse et al., 2015; Sharda and Koide, 2008).

By inducing extensive fungal hyphal branching, strigolactones enable the formation of a large network of mycelia, which extend beyound the root rhizosphere, thus allowing soil nutrients to be captured from expanded soil areas. This has been proven by experiments showing a reduction in root colonisation by two arbuscular mycorrhizal fungi *R. irregularis* and *Gigaspora rosea* in strigolactone-deficient *Solanum lycopersicum* (tomato) and *Zea mays* (maize) mutants, respectively (Gomez-Roldan et al., 2007; Koltai et al., 2010). What is still unknown is how strigolactones are perceived by the host. Inside the plant, strigolactones are recognised by the α/β hydrolase DWARF 14 (D14). This leads to a complex formation involving the Skp1-Cullin-F-box (SCF) complex with the F-box protein MAX2, members of the Suppressor of MAX2 1-Like (SMXL) protein family and Topless repressors (for review, see De Cuyper and Goormachtig, 2017). It is expected that as strigolactone binds, the SCF^{MAX2} complex ubiquitinate the SMXL proteins, leading it to proteasomal degradation, which then activates downstream signalling (for review, see De Cuyper and Goormachtig, 2017).

Cutin monomers such as the *Medicago truncatula* RAM2 (*Required for Arbuscular Mycorrhization 2*) were initially identified as plant signals with a role in AM symbiotic dialogue (Wang et al., 2012). However, recent studies suggest that RAM2, a glycerol-3-phosphate acyl transferase (GPAT), involved in the biosynthesis of hydroxylated aliphatic acid, alongside FatM (Fat thioesterases M) are involved in lipid biosynthesis in colonised cells to secrete enough lipids for use by the AM fungus (Bravo et al., 2017). In addition, the *Zea mays* (maize) and *Oryza sativa* (rice) NOPE1 (NO PERCEPTION1) was discovered as a plant signal required for pre-symbiotic fungal reprogramming (Paszkowski et al., 2006; Nadal et al., 2017). Mutants of ZmNOPE1 failed to support hyphopodia formation by the AM fungus *Gigaspora mosseae* (Paszkowski et al., 2006), as well as *osnope1* mutants, which showed a significant reduction in *R. irregularis* rice root colonisation and the formation of aberrant hyphopodia on the root surface (Nadal et al., 2017), suggesting that NOPE1 is required for pre-symbiotic signal exchange. Further analysis suggested that NOPE1 may be specifically required for interaction with AM fungi as *osnope1* mutants inoculated with the pathogens *Piriformospora indica* and *Magnaporthe oryzae* showed normal root invasion relative to the wild-type (Gutjahr et al., 2008; Marcel et al., 2010). Notably, NOPE1 encodes an N-acetylglucosamine (GlcNAc)

transporter, a function described in the fungal commensal pathogen *Candida albicans*, where it induces morphological budding to hyphal growth (Alvarez and Konopka, 2006).

1.1.3. Fungal to plant communication

In response to strigolactones and other molecules released by the plant, arbuscular mycorrhizal fungi produce symbiotic signalling molecules that are recognised by the host plant. Germinating spore exudates (GSEs) from AM fungi have been shown to trigger several cellular, metabolic and development changes thought to prepare plant cells for fungal colonisation. Some of these different responses in the host root include extensive transcriptional regulation of AM symbiotic genes, promotion of lateral root development, starch accumulation and rapid nuclear-related calcium oscillations (Kosuta et al., 2003; Gutjahr et al., 2009; Kuhn et al., 2010; Maillet et al., 2011; Mukherjee and Ane, 2011; Chabaud et al., 2011; Maillet et al., 2011; Czaja et al., 2012; Genre et al., 2013; Bonfante and Genre, 2015). Interestingly, studies aiming to delineate the structure of mycorrhizal (Myc) signals found that the AM fungus *Rhizophagus irregularis* secretes a mixture of sulphated and non-sulphated lipochitooligosaccharides (LCOs) that resemble Nod (nodulation) factors released by rhizobia bacteria (Maillet et al., 2011). The chitin oligosaccharidic backbone of both Nod- and Myc-factors is made up of four or five N-acylated glucosamine residues, but compared to the Nod factors, *R. irregularis* Myc factors or signals have a much simpler structure (Dénarié et al., 1996; D'Haeze et al., 2002). Research findings show that rhizobial mutants that produce simple LCOs like Myc-LCOs were unable to penetrate their host and form nodules (Ardourel et al., 1994).

Unlike rhizobia bacteria which produce Nod-LCOs, the AM fungus also produces short chain chitin oligosaccharides (CO4/CO5) in addition to Myc-LCOs (Genre et al., 2013). It has been shown that these GlcNAc-based signalling molecules differ in their ability to elicit symbiotic responses, which can be influenced by various factors such as their concentration, host plant species, the root cell type, and the combination with other fungal signals (Sun et al., 2015). This was demonstrated by experiments showing the activation of nuclear calcium oscillations in rice atrichoblasts by CO4 but not Myc-LCOs, whereas a mixture of CO4 and Myc-LCOs activated calcium oscillations in rice trichoblasts (Sun et al., 2015). On the other hand, lateral root growth occurred in *M. truncatula* following treatment with Myc-LCOs but not CO4, whereas both CO4 and Myc-LCOs were active in rice (Sun et al., 2015).

1.1.4. Establishment of AM symbiosis: the symbiotic phase

Following the release of strigolactone and other molecules at the pre-symbiotic stage, fungal hyphae attach to the epidermal layer of the plant root, where hyphal tips differentiate to form hyphopodia. The perception of mechanical and chemical signals, including cutin monomers emanating during hyphopodium formation (Wang et al., 2012) facilitate fungal penetration and entry into the host root. When the fungus is attached to an epidermal cell, the plant cell nucleus moves to the site of hyphal contact prior to its migration across the cell to the opposite side. As this nuclear movement takes place, the plant cell forms a pre-penetration apparatus (PPA), which permits fungal penetration and entry (Genre et al., 2005). Notably, the PPA is formed from the accumulation of a dense network of ER cisternae, actin filaments and microtubules and is associated with both fungal entry of epidermal cells and root colonisation. Formation of the PPA defines the subsequent path of hyphal infection and may be responsible for the synthesis of apoplastic compartment required for hyphal containment (Genre et al., 2005). Only when the PPA is formed does the fungal hypha enter the cell lumen, where it grows longitudinally through the apoplast and form branches, which initiate arbuscule formation in inner cortical cells (Genre et al., 2005). Notably, arbuscules are transient structures, which degenerate and collapse after 2-4 days after development.

1.1.5. Arbuscule development and the peri-arbuscular membrane (PAM)

Arbuscules are formed in inner root cortical cells and are surrounded by a plant-derived peri-arbuscular membrane (PAM), which is considered to be the site of nutrient exchange in the symbiosis (dotted white lines in Figure 1.2). Arbuscule development involves a severe reorganization of the cortical cells. Interestingly, hyphal penetration does not result in the breaching of the plasma membrane but rather produces invaginations which extend to form the PAM. The PAM separates the fungal hypha from the host cytoplasm (Harrison, 2005).

The PAM consists of two domains; the branch and trunk domains, which have defined positions and protein composition (Pumplin and Harrison, 2009). The trunk domain is located at the base of the PAM, whereas the branch domain surrounds the fine hyphal branches of the arbuscule and contains a specialized set of proteins involved in the mediation of nutrient exchange in the symbiosis (Pumplin and Harrison, 2009). In between the PAM and the fungal hypha is the peri-arbuscular space, which contains plant cell wall material in direct contact with the fungal cell walls surrounding the hypha (Balestrini and Bonfante, 2014).

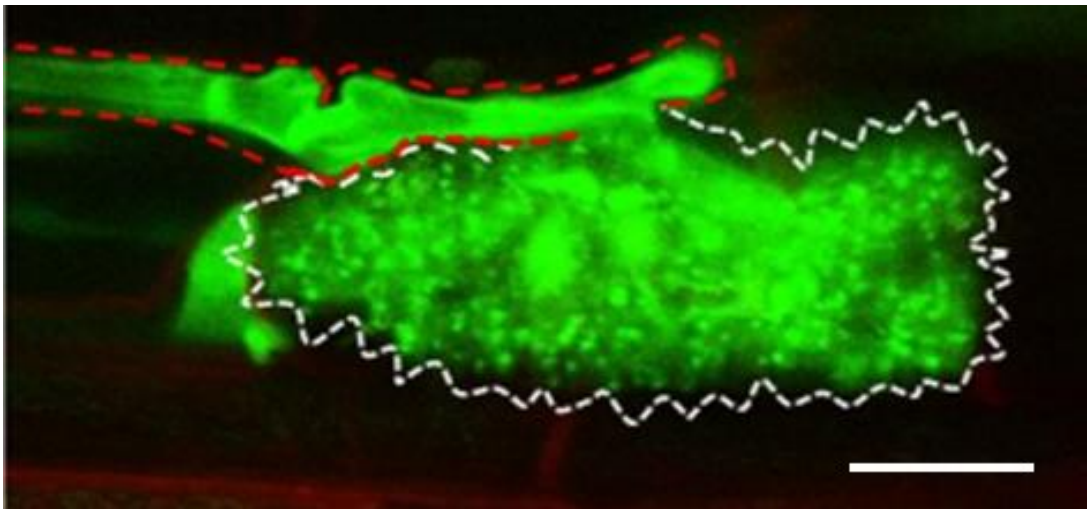

Figure 1.2: Microscopic image of a fully developed arbuscule formed by *R. irregularis* in rice root cortical cells. The intraradical hypha (outlined in red) grows intercellularly until it reaches the inner cortical cells of the root, where it then forms an arbuscule. Arbuscules are surrounded by a plant-derived peri-arbuscular membrane (PAM) (white dotted line) where nutrient exchange in the symbiosis takes place. (Scale bar = 50µm). Micrograph obtained using a modified protocol described in Kobae and Ohtomo (2016).

Cytoplasm and organelles such as the endoplasmic reticulum, Golgi bodies, plastids and mitochondria accumulate within the area surrounding arbuscule branches. In addition, tonoplast invagination and multiple small vacuole compartments are also seen in the host cell during arbuscule development (Harrison, 1999). Although the continuation of the PAM with the plasma membrane suggests that it arises by *de novo* membrane synthesis, the origin of the membrane material and secretion/signalling pathways, including lipid and protein compositions involved in the process are still unknown. The development of the PAM is critical for nutrient transport in the symbiosis and understanding how nutrient exchange occurs has been an area of focus. In *M. truncatula*, two SNAREs (soluble N-ethylmaleimide sensitive factor attachment protein receptor), VAMP721d and VAMP721e have been associated with PAM development as knockdown of both proteins blocked arbuscule and symbiosome formation during AM symbiosis and nodulation, respectively (Ivanov et al., 2012). VAMP721d/e are members of the family of SNAREs, which are located on the membranes of exocytotic vesicles. In conjunction with tSNAREs located on the target membrane, they mediate the fusion of vesicles and target membranes (Harrison et al., 2002). Expressed in inner cortical cells, VAMP721d/e vesicle cargo is thought to include PAM-resident proteins (MtPT4), an ABC transporter (STR1/STR2) and a secreted subtilisin protease (SbtM1) (Harrison et al., 2002; Zhang et al., 2010; Gutjahr et al., 2012; Takeda et al., 2009).

The exocyst complex, which is involved in vesicle trafficking has been associated with arbuscule development (Genre et al., 2012). In support of this is the *M. truncatula* Exo70I exocyst protein shown to be required for normal development of the branch domain of the PAM during AM symbiosis (Zhang et al., 2015). Mutants of MtExo70I showed a major defect in arbuscule development. More specifically, arbuscule branching was reduced and hyphal branches were aberrant and frequently distorted in shape. This defect was followed by premature maturation of the septa and arbuscule collapse, which consequently resulted in smaller arbuscules (Zhang et al., 2015). In addition, *MtExo70I* mutants failed to efficiently incorporate two important arbuscule branch domain-specific ABC transporters, STR and STR2, indicating that the Exo70I exocyst activity is crucial for the early branching phase of the arbuscule (Zhang et al., 2015).

Another interesting observation about the function of Exo70I during arbuscule PAM development is its co-localisation with Vapyrin, a plant-specific protein of unknown function required for arbuscule formation (Zhang et al., 2015). Vapyrin is a cytoplasmic protein found in cells containing AM fungal hyphae, where it accumulates in small puncta moving through the cytoplasm (Pumplin et al., 2010). It contains two domains; a major sperm protein (MSP) domain associated with VAMP proteins (VAP) and an ankyrin-repeat domain, both of which mediate protein-protein interactions (Pumplin et al., 2010). Putative vapyrin orthologues exist widely in the plant kingdom, and although its molecular function has not been determined, it is thought to be involved in mediating interactions between proteins and in enabling AM fungi to enter plant cells (Pumplin et al., 2010). In *Petunia hybrida*, mutations in the Vapyrin-encoding gene homologue, PAM1 (Penetration and Arbuscule Morphogenesis 1) showed defects in the intracellular stages of AM development (Feddermann et al., 2010), as well as legume plants with mutated Vapyrin genes, which exhibited abnormal rhizobial infection threads and fewer nodules (Murray et al., 2011). These observations further support the notion that Vapyrin may act as a scaffold protein to recruit MtExo70I, and perhaps other proteins during arbuscule development.

Other plant genes or proteins associated with arbuscule development include phosphate and ammonium transporters, which are crucial for symbiotic phosphate uptake (Javot et al., 2007; Yang et al., 2012). Following uptake into fungal mycelium, phosphate and nitrogen from ammonium are transported in the form of polyphosphates and arginine, respectively, into the peri-arbuscular space (PAS) of arbuscules, where they are released (Hijikata et al., 2010).

Extensive studies have identified various plant phosphate transporters that mediate the uptake of phosphate across the PAM (Harrison et al., 2002; Paszkowski et al., 2002; Nagy et al., 2005; Maeda et al., 2006; Javot et al., 2007; Yang and Paszkowski, 2011; Tamura et al., 2012; Yang et al., 2012; Xie et al., 2013; Breuillin-Sessoms et al., 2015). The phosphate transporters belong to a family of phosphate transporter 1 (Pht1) proton symporters and many of them were able to complement yeast phosphate transport mutants, confirming their ability to transport phosphate in other plants (Harrison et al., 2002; Paszkowski et al., 2002; Tamura et al., 2012; Xie et al., 2013). The *M. truncatula* Phosphate Transporter 4 (PT4) and its homologues in rice and soybean are localised at the branch domain of the PAM and are required to transport phosphate from the fungus to the plant, as well as to maintain AM symbiosis. Mutations or knockdown of MtPT4 resulted in premature degeneration of arbuscules and aborted symbiosis (Javot et al., 2007), whereas dramatically low levels of colonisation and arbuscules were seen in mutants of *O. sativa pt11* phosphate transporter (Yang et al., 2012). In addition, a mutation in another rice phosphate transporter, PT13, which is exclusively expressed in arbusculated cells produced very similar phenotypes to *pt11* mutants, but irrespective of this phenotype, PT11 was shown to be the only transporter involved in symbiotic phosphate uptake in rice (Yang et al., 2012).

1.1.6. Recognition of symbiotic signals by lysine motif (LysM) receptors

LysM domains are present in prokaryotic and eukaryotic proteins where they bind N-acetylglucosamine (GlcNAc)-containing carbohydrates, such as chitin, chitin-oligosaccharides and peptidoglycan (Buist et al., 2008). They were first discovered in the lysozyme of *Bacillus* phage phi-29 as C-terminal direct repeat composed of about 50 amino acids (Garvey et al., 1986; Buist et al., 2008). Multiple LysMs can be found within one LysM domain, but these are separated by spacing sequences, mostly consisting of Serine, Threonine and Aspartic acid or Proline residues, which allow a flexible region between the LysMs (for review, see Buist et al., 2008). Unlike prokaryotic proteins with repeated LysM domains, the intervening sequences between the LysMs of a family of receptor-like kinases in plants contain a conserved cysteine-X-cysteine (CxC) motif (Madsen et al., 2003; Radutoi et al., 2003; Arrighi et al., 2006), which is involved in the formation of disulphide bridges important for correct protein folding and localisation (Lefebvre et al., 2012). All available LysMs contain a well-conserved motif, at least, over the first 16 amino acid residues; however, the central region is poorly conserved except for Isoleucine/Leucine at positions 23 and 30 and the well-conserved asparagine at position 27 (Buist et al., 2008).

Originally found in bacteria, LysMs are a prevalent protein family in fungi, which produce various LysM domain-containing proteins with a diversified amino acid spectrum (Akcapinar et al., 2015). In plants, LysM domains are found in LysM receptor-like kinases (RLKs) located on the plasma membrane. LysM-RLKs are pattern recognition receptors (PRRs) that perceive various types of microbial signals, which may lead to symbiosis or immunity (Gust et al., 2012). In rice, the LysM-RLK, *Chitin Elicitor Receptor Kinase 1* (CERK1) functions with an unknown interactor to perceive chitin-oligosaccharides leading to AM symbiosis (Miyata et al., 2014; Zhang et al., 2015). This was supported by experiments showing that *oscerk1* mutants treated with GSE from *R. irregularis* failed to efficiently trigger calcium spiking (Carotenuto et al., 2017), as well as suffered reduced colonisation at the early stages of infection, emphasizing the role of OsCERK1 in early symbiotic signalling (Miyata et al., 2014; Zhang et al., 2015). In addition, OsCERK1 is involved in immunity signalling, where it cooperates with the LysM receptor-binding protein, OsCEBiP to perceive defence-related chitin signals (Kaku et al., 2006; Shimizu et al., 2010). The Arabidopsis CERK1, a homologue of OsCERK1, is also involved in immunity signalling in conjunction with another LysM-RLK known as AtLYK5 (Miya et al., 2007). However, in contrast to the role of OsCERK1 in AM symbiosis, its immunity LysM receptor-like protein (RLP) partner was found not to be required for AM symbiosis as *cebip* mutants triggered calcium spiking in response to AM GSEs (Miyata et al., 2014) and established normal symbiosis with the AM fungus *R. irregularis* (Miyata et al., 2016). This indicates that there is still an unknown symbiotic co-receptor of CERK1 in rice.

Moreover, NFR1 (in *Lotus japonicus*) and LYK3 in (*Medicago truncatula*), the closest homologues of OsCERK1, are required for Nod factor recognition during rhizobia symbiosis. Here, LjNFR1/MtLYK3 form hetero-complexes with LjNFR5/MtNFP to activate the common symbiosis pathway (Gough and Cullimore, 2011; Gust et al., 2012; Madsen et al., 2003; Radutoiu et al., 2003). Loss-of-function of either LjNFR1 or LjNFR5 led to a complete abolishment of all known symbiotic responses to *Mesorhizobium loti* and to purified Nod factors (Madsen et al., 2003; Radutoiu et al., 2003), suggesting that the key kinase activity of NFR1 but not NFR5, which lacks an active kinase, is important for transducing intracellular signalling required for rhizobia symbiosis. In contrast, LjNFR5, OsNFR5 is not required for AM symbiosis as *osnfr5* mutants were unable to trigger chitin oscillations in response to AM GSEs (Miyata et al., 2014) and established AM symbiosis normally (Miyata et al., 2016). Interestingly, the function of another homologue of NFR1/CERK1 known as SILYK10 in *Solanum lycopersicum* (tomato) has been implicated in AM symbiosis (Buendia et al., 2016),

suggesting the diverse role of LysM-RLKs in the perception and recognition of Myc- and Nod-factors.

1.1.7. The common symbiosis signalling pathway (CSSP)

The successful establishment of AM symbiosis in roots requires the activation of a chain of signalling events which lead to extensive transcriptional reprogramming of host cells and promotion of AM colonisation. This signalling process is required for both AM and rhizobia-legume symbioses, and is therefore called the Common Symbiosis Signalling Pathway, CSSP (Kistner and Parniske, 2002). Central to the CSSP is the generation of nuclear calcium spiking in the host cell in response to symbiotic (Myc-factors from AM fungi or Nod-factors from rhizobia bacteria) signal perception at the plasma membrane by lysine-motif (LysM) receptor kinases. This leads to the activation of the calcium-and calmodulin-dependent protein kinase (CCaMK) in the nucleus, which in turn, activates transcriptional changes downstream of the CSSP (for review see Gutjahr and Parniske 2013; Oldroyd 2013). Interestingly, plants carrying a mutation in components of the CSSP often do not establish successful symbioses with AM fungi or rhizobia bacteria (Catoira et al., 2000; Kistner et al., 2005), emphasizing the crucial role of the CSSP in establishing symbiosis.

The common symbiotic signalling pathway involves an early signal transduction cascade mediated by several shared components. In *Lotus japonicus*, these components include SYMRK (a receptor-like kinase), three nucleoporins (NUP85, NUP133 and NENA), CASTOR and POLLUX (cationic channels located on the nuclear envelope) and CCaMK (a nuclear calcium- and calmodulin-dependent kinase) and CYCLOPS (a substrate of CCaMK) (for review, see Oldroyd 2003). Additional CSSP components characterized in *Medicago truncatula* include 3-Hydroxy-3-Methylglutaryl CoA Reductase 1, HMGRI, a key enzyme in the mevalonate biosynthetic pathway (Kevei et al., 2007) and MCA8, a nuclear envelope-localised SERCA-type Ca^{2+}ATPase (Capoen et al., 2011; for review, see Genre and Russo, 2016). Both mevalonate and Ca^{2+} act as secondary messengers with the CSSP, either as a product of HMGRI or an activator of CCaMK, respectively (Levy et al., 2004; Venkateshwaran et al., 2015). During arbuscular mycorrhizal or legume rhizobia symbiosis, nuclear-associated Ca^{2+} oscillations mediate plant responses to the beneficial microbial partners. In the legume *Medicago truncatula*, cyclic nucleotide-gated channels (CNGC15) located at the nuclear envelope, and which are permeable to Ca^{2+} are required for nuclear-localised Ca^{2+} oscillations and symbiotic responses occurring thereafter (Charpentier et al., 2016). It is possible that the location of the

CNGC15 proteins permits a targeted nuclear release of the endoplasmic reticulum (ER) Ca^{2+} store (Charpentier et al., 2016).

The symbiosis receptor-like kinase, SYMRK acts upstream of the Nod factor- and Myc factor-induced calcium signatures occurring in and around the nucleus (Endre et al., 2002; Stracke et al., 2002; Kosuta et al., 2008). Notably, calcium signatures are transient elevations in cytosolic calcium caused by certain stimuli (Whalley and Knight, 2012). Also known as DMI2 (or NORK) in the legume *Medicago truncatula*, SYMRK encodes a receptor-like kinase that has an enzymatically functional kinase domain. Considering its structure and the symbiotic phenotypes observed in *symrk* mutants, SYMRK is thought to be the major entry point into the common symbiotic signalling pathway (Reid et al., 2014). As a receptor kinase positioned in the plasma membrane, SYMRK can directly or indirectly perceive symbiotic microbial signals, which it then transduces *via* its intracellular kinase domain. Although the exact ligand has not been identified, SYMRK responds to different types of extracellular ligands during AM and rhizobia symbiosis (for review, see Oldroyd 2013).

Nuclear pore complexes within the CSSP mediate transport of proteins, RNAs and ribonucleoprotein particles in and out of the nucleus. Specifically, the nucleoporins, NUP85, NUP133 and NENA located in the nuclear pore complex seem to play a role in controlling the import of an unknown key CSSP protein. This was demonstrated by mutations in all three nucleoporins, which resulted in strong symbiotic phenotypes. For example, mutation in NUP133 resulted in a temperature-sensitive nodulation deficient phenotype and absence of mycorrhizal colonisation, suggesting that it is involved in a rapid nuclear-cytoplasmic communication after host-plant recognition of symbiotic microbes (Kanamori et al., 2006). Mutants of NUP85 showed defects in calcium spiking, fungal and bacterial symbioses, as well as seed production in *Lotus japonicus* (Saito et al., 2007), whereas mutation in NENA resulted in impaired symbiotic responses of the rhizodermis, where CCaMK-dependent responses were abolished (Groth et al., 2010). Other components bound to the nuclear envelope and which contribute to calcium spiking (a signal transduction mechanism whereby an external stimuli triggers the mobilization of calcium from outside the cell or from intracellular storage pools to the cytoplasm) in both AM and Rhizobia symbiosis, are MCA8, the ATP-powered Ca^{2+} pump (Capoen et al., 2011) and the potassium-permeable channels, CASTOR and POLLUX (Charpentier et al., 2008). CASTOR and POLLUX set the voltage to open the Ca^{2+} channel and are thought to compensate for the charge imbalance resulting from the release of calcium during calcium spiking from CNGC15 proteins (Charpentier et al., 2016) and perhaps, other

unidentified nuclear envelope lumen-channels. MCA8 activity helps to re-establish basal nuclear Ca^{2+} concentration at the end of each peak (for review, see Genre and Russo, 2016).

Within the nucleus, CCaMK forms a complex with the phosphorylation substrate, CYCLOPS, and in conjunction with calmodulin, the CCaMK-CYCLOPS complex may decode the symbiotic calcium signatures (Shimoda et al., 2012; Miller et al., 2013; Poovaiah et al., 2013; Yano et al., 2008). When phosphorylated, CYCLOPS can regulate gene expression either directly such as through NIN (NODULE INCEPTION) promoter (Singh et al., 2014) or through the action of other transcription factors such as NSP1, NSP2 and RAM1 (Oldroyd, 2013). The essentiality of CCaMK for both nodulation and AM symbiosis was demonstrated by the induction of symbiotic processes during CCaMK activation as gain-of-function mutants of CCaMK induced nodulation in the absence of Rhizobia, as well as promoted pre-penetration structures associated with mycorrhizal colonisation (Gleason et al., 2006; Tirichine et al., 2006; Takeda et al., 2012). Considering other effects initiated by CCaMK activation, such as the redundancy of upstream components of the CSSP, CCaMK activation is deemed the sole purpose of the symbiotic calcium oscillations (Hayashi et al., 2010; Madsen et al., 2010; Oldroyd, 2013). Notably, CCaMK activation requires direct calcium binding to EF hand motifs at the carboxyl terminus of the protein and calcium binding in a complex with calmodulin through a calmodulin-binding domain located adjacent to the kinase domain (for review, see Oldroyd, 2013).

In AM symbiosis, the common symbiosis pathway controls fungal penetration and entry into the epidermal cell, as well as subsequent entry into the root cortex. Gutjahr et al. (2008) showed impairments in AM interactions and alterations in AM-specific gene expression patterns in *Oryza sativa* (rice) mutants defective in genes upstream (CASTOR and POLLUX) and downstream (CCaMK and CYCLOPS) of the central calcium-spiking signal in the common symbiosis signalling pathway. This result demonstrated functional conservation of common symbiosis signalling between distant plant species.

Furthermore, the involvement of CCaMK and CYCLOPS in downstream signalling processes leading to symbiosis has been proposed. It is thought that both components act in conjunction with the GRAS (Gibberellic-Acid Insensitive, Repressor of GAI and SCARECROW)-domain regulatory protein, DELLA, to positively regulate symbiosis (Floss et al., 2013; Jin et al., 2016). As repressors of gibberellin responses, DELLA proteins are central to the regulation of gibberellin signalling. This was demonstrated by the inhibition of AM formation upon treatment

with gibberellin, which resulted in *della* mutant-like phenotypes in *Pisum sativum* (El Ghachtouli et al., 1996), *Medicago truncatula* (Floss et al., 2013), and *Lotus japonicus* (Takeda et al., 2015).

Studies have indicated that DELLA probably functions at multiple stages of arbuscule development, especially since the AM phenotypes of the *M. truncatula della1-della2* double mutants and the *della1-della2-della3* triple mutants were indistinguishable, in that both allowed the formation of intra-radical hyphae but hardly any arbuscules (Floss et al., 2013; Floss et al., 2017). The very few arbuscules seen in the mutants showed a wild-type-like degree of branching, indicating that mutations in the DELLA proteins affect arbuscule initiation rather than branching (Floss et al., 2013). Although, it is still not very clear at what stage (e.g. the pre-penetration apparatus, PPA or trunk formation or first order branching stages), DELLA proteins act in arbuscule initiation, findings by Ivanov and Harrison (2014) showed that DELLA proteins are not required for signalling leading to repositioning and enlargement of the nucleus during hyphal entry into cortical cells. During AM symbiosis, nuclei in the cortical cells, which are in contact with intracellular hyphae move towards the site of contact with hypha. This repositioning, which is accompanied by the nuclear enlargement is found to be independent of CCaMK (Genre et al., 2005), and perhaps, the CCaMK-CYCLOPS-DELLA complex, possibly due to its independence of transcriptional regulation (for review see Pimprikar and Gutjahr, 2018).

DELLA proteins also promote nodule development and the formation of infection threads during root nodule symbiosis (Jin et al., 2016). Jin et al. (2016) showed that DELLAs can promote CCaMK-IPD3/CYCLOPS complex formation and increase the phosphorylation of IPD3/CYCLOPS. Phosphorylated CYCLOPS was shown to bind the promoter of NIN (Nodule Inception Protein) and induce nodulation in the absence of rhizobia (Singh et al., 2014). Interestingly, DELLAs were found to form a protein complex with NSP2 (Nodulation Signalling Pathway 2)-NSP1(Nodulation Signalling Pathway 1) and shown to bridge a protein complex containing IPD3/CYCLOPS and NSP2 (Jin et al., 2016). NSP1 and NSP2 encode GRAS domain transcription factors and function downstream of the CSSP. They were previously thought to have nodulation-specific functions until a recent study showed that NSP2 is also required for LCO signalling during arbuscular mycorrhization. *nsp2* mutants showed a much slower onset of AM colonisation (Maillet et al., 2011), whereas Medicago *nsp2* mutants showed more severe phenotypes including absence of infection and cortical cell division following inoculation with *Sinorhizobium melloti* (Oldroyd and Long, 2003). These differences

in the severity of phenotypes point towards the possible redundancy of NSP2 function during AM symbiosis, which then implies that there are other GRAS domain transcription factor genes that may play a similar role to NSP2 during AM colonisation. In contrast to this is NSP1, which has a specific function during nodulation and Nod factor signalling and has not been found to function during mycorrhizal colonisation (Catoira et al, 2000). Despite the differences, both NSP1 and NSP2 regulate strigolactone biosynthesis in *Medicago* and rice (Liu et al., 2011), although this does not explain the phenotypic differences seen in their respective mutants. A possible explanation is that both transcription factors have very closely associated roles associated with AM and rhizobia symbiosis (for review, see Oldroyd 2013).

Other transcription factors required for symbiosis include *Reduced Arbuscular Mycorrhization 1*, RAM1 (Gobbato et al., 2012), *Required for Arbuscule Development*, RAD1 (Xue et al., 2015), *Ethylene Response Factor 1*, ERF1 (Devers et al., 2013), and *Mycorrhiza Induced GRAS1*, MIG1 (a DELLA-interacting protein) (Yu et al., 2014). RAM1 was the first transcription factor found to specifically function in mycorrhizal signalling (Gobbato et al., 2012). RAM1 encodes a GRAS transcription factor and is located downstream of CCaMK, CYCLOPS and DELLA. Plants carrying a mutation in RAM1 failed to be colonised by mycorrhizal fungi and suffered a defect in hyphopodia formation on the root surface (Gobbato et al., 2012). Similar to NSP2, RAM1 was found to be important for Myc-LCO-induced root branching (Maillet et al., 2011; Gobbato et al., 2012), but did not seem to have a role in Nod factor signalling, suggesting that the transcription factor only acts in mycorrhizal signalling. RAM1 regulates the expression of RAM2 (*Required for Arbuscule Mycorrhization 2*), a glycerol-3-phosphate acyltransferase that promotes cutin biosynthesis, which enhances hyphopodia formation (Wang et al., 2012). However, recent studies have shown that RAM1 is not absolutely required for initial entry and spreading of fungal hyphae in roots but is definitely required for arbuscule development in inner cortical cells at later stages of colonisation (Rich et al., 2015; Xue et al., 2015; Pimprikar et al., 2016). Interestingly, the interaction of RAM1 and NSP2 supports the notion that the regulation of GRAS domain complex formation precedes activation of mycorrhizal or nodulation responses. A possibility is that a complex formation between NSP1-NSP2 may promote rhizobium-specific responses, whereas a RAM1-NSP2 complex promotes mycorrhiza-specific responses (Oldroyd, 2013). Recent findings also suggest that RAM1 is required for the up-regulation of genes involved in lipid biosynthesis and export during development of the AM symbiosis (Luginbuehl et al., 2017).

1.2. Plant-parasitic microbe interactions

Plants have distinct associations with detrimental microorganisms, which fully exploit the capacity of plants to produce photosynthetic products for their own growth and proliferation. Plant pathogens remain a major challenge to global food security because of their consequential effects on crop yield and quality. Plant roots are surrounded by a wide range of pathogens, which can range from bacteria to fungi to oomycete pathogens. Although some pathogens only interact with specific crops *via* the leaf or root, the filamentous ascomycete foliar pathogen *Magnaporthe oryzae* can associate with rice *via* the leaf and the root. Designated a foliar pathogen, *M. oryzae* seems to preferentially invade rice through the leaf, where it causes necrotic disease lesions within a short time. This is unlike in the root, where it appears to adopt an endophytic lifestyle, invading rice root cells with no loss of host cell viability, at least, for a prolonged period (Sesma and Osbourn, 2004; Marcel et al., 2010). The fact that *M. oryzae* can colonise rice roots, makes it an attractive root-infecting fungus to compare genetic commonalities with the symbiont *R. irregularis.*

1.2.1. *Magnaporthe oryzae* rice leaf infection strategy

Magnaporthe oryzae is a devastating pathogen that infects the aerial parts of rice plants causing rice blast, a major deleterious disease that can destroy up to 30% of cultivated rice in the field annually (Wilson and Talbot, 2009; Fisher et al., 2012). It can also cause disease on a variety of alternative hosts such as finger millet *Eleusine coracana*, a major source of nutrition and essential minerals such as calcium, phosphorous and iron in rural communities in poorer countries of the world. In finger millet, *M. oryzae* causes finger millet blast, which leads to a complete harvest loss before grain formation. It also causes disease in wheat, which is a major challenge in wheat fields in countries such as Brazil (for review, see Talbot, 2003).

M. oryzae is a hemi-biotrophic pathogen, which combines both biotrophic and necrotrophic features during rice leaf infection. Its infection developmental pattern on the leaf are similar to those observed in many foliar fungal pathogens, whereby tissue infection is initiated when an asexual spore or conidium is attached to the cuticle of the rice leaf surface by a spore tip mucilage or adhesive found in an apical compartment of the spore (Tucker and Talbot, 2001; Hamer et al., 1988, Talbot 2003). Mature conidia are three-celled, pyriform with a basal appendage at the point of attachment to the conidiophore. Spore germination is facilitated by the presence of free water, and conidiophores are carried from plant to plant by dewdrops

(Hamer et al., 1988). Upon germination of the conidium with two hours of landing on the plant leaf surface, a polarized germ tube is formed, typically from one of the apical cells of the conidium. The germ tube then develops into a heavily melanized special infection cell called an appressorium. It is thought that the developmental processes between the formation of the germ tube and appressorium constitutes the recognition phase because the characteristics of the substratum are monitored prior to commitment to appressorium development (Bourett and Howard, 1990). *M. oryzae* invades rice tissues using a penetration peg which develops from the appressorium to pierce the cell surface and enter the epidermal cell (Tucker and Talbot, 2001; Wilson and Talbot, 2009). As the fungus spreads within and between plant cells, it swells and within four days, it produces eyespot-shaped lesions containing thousands of spores, which invade new tissues daily (Hamer and Talbot, 1998; Valent, 2004).

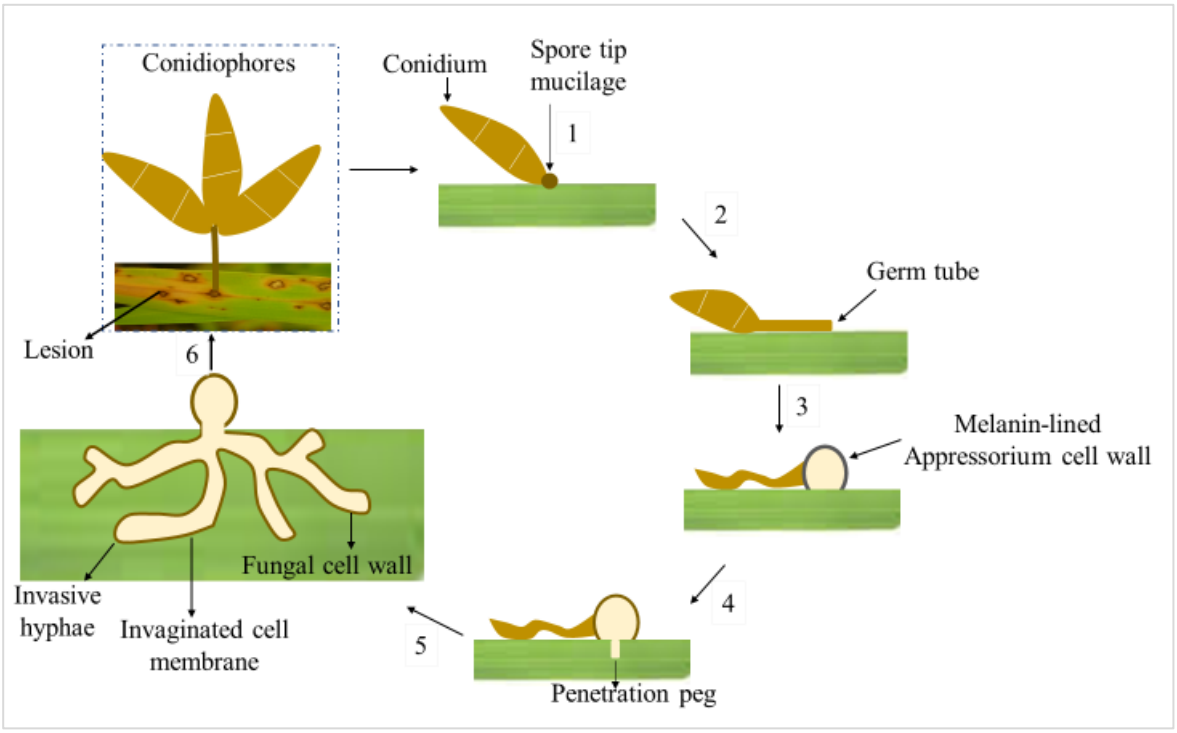

Figure 1.3: **Life cycle of the rice blast fungus *Magnaporthe oryzae*.** Fungal infection begins when conidium (1) attaches itself to the leaf surface by the spore tip mucilage. This leads to the formation of a germ tube (2), which then forms a melanized appressorium (3). From the appressorium develops a penetration peg (5), which pierces the leaf surface and allows fungal entry and proliferation inside host tissue cells (5). As the fungus spreads within and between plant cells, it swells and within four days, it produces eyespot-shaped lesions containing thousands of spores, which invade new tissues daily (6). (Image modified from Wilson and Talbot, 2009).

1.2.2. Appressorium formation

The appressorium is a key infection structure used by *M. oryzae* to penetrate rice leaf tissue and cause disease in the plant. It utilizes a mechanical force to rupture the leaf cuticle, which allows a narrow hypha to enter the underlying epidermal cells. Appressorium development involves a highly coordinated process involving the perception of both physical and chemical cues from the plant leaf surface, as well as both nuclear and cell division (Ryder and Talbot, 2015). Perception of hydrophobicity and surface hardness is necessary to initiate appressorium development, but also, fungal response to wax monomers such as 1,16-hexadecanediol can induce the development of an appressorium on the leaf surface (Wilson and Talbot, 2009). In addition, cell cycle control is crucial to the development of appressoria (Veneault-Fourrey et al., 2006). This is seen with the conidium, which consists of three cell layers, each with a single nucleus and the cell from which the germ tube emerges. Prior to appressorium development, each of these cell layers undergoes a single round of nuclear division whereby the conidial nucleus enters into the DNA replication or the S-phase (Saunders et al., 2010). Subsequent entry of the nucleus into G2 and mitosis leads to appressorium maturation and melanisation. Without mitosis, appressorium development will be hindered (Veneault-Fourrey et al., 2006). After mitosis, nuclear migration and appressorium formation, the conidium undergoes autophagic, programmed cell death, at which point the nuclei are degraded (Veneault-Fourrey et al., 2006; Kershaw and Talbot, 2009).

The final and functionally significant stages of appressorium development is the deposition of a cell wall layer containing melanin. Melanin is located outside the plasma membrane and deposits a dark pigmentation to the appressorium as observed microscopically (Howard and Valent, 1996). After appressorium expansion and melanisation, the penetration peg emerges and perforates the host surface, allowing the contents of the appressorium into cells of the leaf epidermis. Following penetration of the leaf cuticle and cell wall, the penetration peg swells and becomes the primary infection hypha, which eventually differentiates into a highly branched bulbous secondary hypha that aids fungal proliferation inside the host tissue (Koga, 1994).

1.2.3. The Extra-Invasive Hyphal Membrane (EIHM)

During biotrophic growth, the proliferating fungal hyphae, also known as the extra-invasive hyphae become surrounded by the plant plasma membrane. This forms the extra-invasive hyphal membrane (EIHM), a highly specialized plant plasma membrane-independent compartment (Kankanala et al., 2007) believed to be the site for fungal nutrient uptake, fungal modulation of plant metabolism and cell signalling through effector secretion (Martin-Urdiroz et al., 2016). Effectors are secreted proteins that can shield the fungus or pathogen, suppress the host immune response or manipulate host cell physiology (for review, see Presti et al., 2015).

The availability of vital stains such as fluorescein diacetate (FDA) and propidium iodide (PI) has facilitated investigation of the fungal-host cell membrane dynamics, especially during the biotrophic and necrotrophic phases of *M. oryzae* rice leaf infection. During the biotrophic phase, the fungus occupies single living rice cells without any evidence of loss of host cell viability, but when it switches to the necrotrophic phase, rice cells lose viability and quickly form disease lesions, which contain viable spores that eventually germinate and allow the fungal life cycle to start again (Perfect and Green, 2001; Talbot, 2003, for review, see Xia and Talbot, 2016). *M. oryzae* expresses many low molecular-weight biotrophy-associated secreted (Bas) proteins including known effectors that suppress plant immunity and promote pathogen growth during the early stages of infection (Valent and Khang, 2010). Using two distinct secretion systems, *M. oryzae* targets two effectors during plant infection (Giraldo et al., 2013). Cytoplasmic effectors are delivered into the host cells, and preferentially accumulate in the biotrophic interfacial complex or BIC, whereas apoplastic effectors are generally dispersed and retained within the extra-invasive hyphal membrane (EIHM) compartment, where they outline the entire invasive hyphae (Figure 1.4) (Giraldo et al., 2013). Notably, BIC is a new plant membrane-rich structure associated with invasive hyphae (IH) and linked to a new form of secretion involving exocyst components and the *Saccharomyces cerevisiae* Sso1 t-SNARE protein (Giraldo et al., 2013).

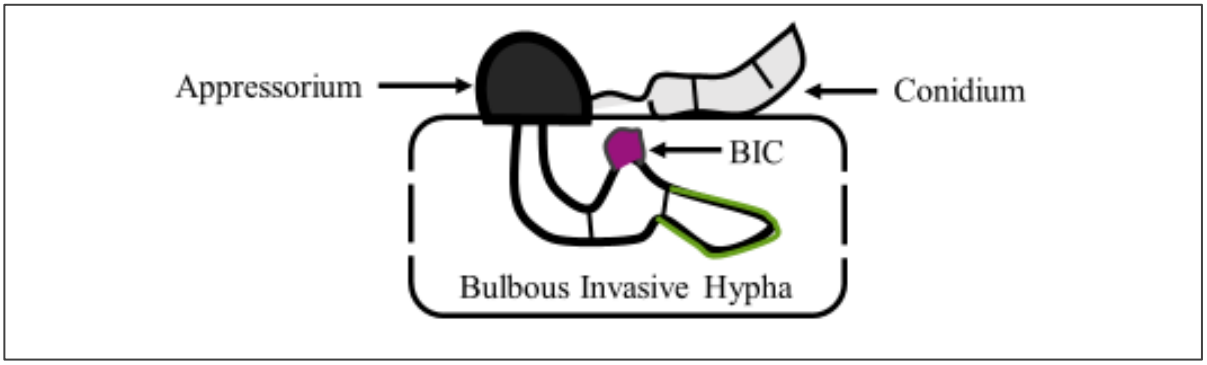

Figure 1.4: Schematic representation of a pseudohyphal-like bulbous invasive hypha in a first-invaded rice cell. Cytoplasmic effectors show preferential accumulation in the BIC (magenta), which is first located in front of the growing primary hyphal tips, and then remains behind beside the first-differentiated bulbous invasive hyphae (IH) cell (not shown). Typical accumulation patterns for cytoplasmic (magenta) and apoplastic (green) effectors are shown within the EIHM compartment enclosing the IH. (Image modified from Giraldo et al., 2013).

The distinct localisation patterns of cytoplasmic and apoplastic effectors within the EIHM compartment has been linked with filamentous fungal apical hyphal tip growth, which involves the Spitzenkörper. The spitzenkörper is considered to be the organising centre where growing fungal hyphal tips are fed with vesicles. Vesicle transport to the growing hyphal tips is aided by an exocyst complex *via* a process known as exocytosis. Notably, exocysts are known to tether post-Golgi vesicles to the target membrane before exocytic fusion. However, although it was thought that hyphal growth and secretion in filamentous fungi occurred exclusively at the hyphal tips, advanced live-imaging studies suggest that other processes including non-tip directed exocytosis may be involved (Hayakawa et al., 2011; Read, 2011). It is unclear whether *M. oryzae* secretes effectors during intracellular growth in rice roots, but this can be determined with live-cell imaging of *M. oryzae* transformed with cytoplasmic and apoplastic effector markers (Giraldo et al., 2013).

1.2.4. Rice root colonisation by *Magnaporthe oryzae*

In addition to colonizing rice leaf tissue, *M. oryzae* can also colonise rice root cells. *M. oryzae* belongs to the family Magnaporthaceae, which includes two other detrimental ascomycete pathogens (*Gaeumannomyces graminis* var. *tritici* and *Magnaporthe poae*) of great economic importance. *M. oryzae* causes the devastating rice blast disease, whereas *G. graminis* leads to the take-all disease in wheat and other grasses and *M. poae* causes the summer patch disease in turf grasses. For a long time, it was thought that *M. oryzae* rice tissue invasion was solely *via*

leaf infection, however, experimental studies showed that the fungus can undergo a range of developmental processes that are typical of root pathogens and successfully colonise the root tissue (Sesma and Osbourn, 2004). Using green fluorescent protein (GFP)-tagged *M. oryzae* strains and chlorazole black E staining, Sesma and Osbourn (2004) investigated the developmental processes associated with root infection and observed the formation of hyphal swellings on the root surface. The hyphal swellings resembled hyphopodia, which are formed on root surfaces by root-infecting fungi such as *Rhizophagus irregularis*. However, unlike the appressorium formed on leaf surfaces by foliar pathogens, which were melanised, the hyphopodia-like structure formed by *M. oryzae* on the root surface was melanin-deficient.

Since melanised appressoria are a requirement for successful penetration of leaf tissue by *M. oryzae* (Chumley and Valent, 1990), it was crucial to investigate whether melanin is also required for successful root penetration. By inoculating barley leaves with green fluorescent protein (GFP)-expressing transformants of melanin-deficient non-pathogenic (Chumley and Valent, 1990) and pathogenic (Valent et al., 1991) strains of *M. oryzae*, it was found that the non-pathogenic mutant was unable to form a melanised appressorium, and therefore, could not penetrate barley leaves. However, both strains caused disease lesions on barley root, and both the wild-type and melanin-deficient mutant strains penetrated the root with simple hyphopodia-like structures (Sesma and Osbourn, 2004).

Furthermore, unlike in leaf infection where *M. oryzae* simultaneously combines both biotrophic and necrotic features, the pathogen exhibits a prolonged biotrophic life style in the root. *M. oryzae* can proliferate intracellularly and with no symptoms in the root for a prolonged period (at least eight days post inoculation), spreading across the root tissue without causing any loss of host cell viability (Marcel et al., 2010). Fungal root infection was associated with the plant-derived extra-invasive hyphal membrane (Figure 1.5) that envelopes the fungus throughout intracellular growth (Marcel et al., 2010).

Figure 1.5: Live-cell confocal image of a GFP-expressing *M. oryzae* inside rice root cells. Invasive hypha is surrounded by a plant-derived EIHM (white dotted line), which envelopes the fungus throughout intracellular growth. The fungus crosses over from cell to cell, with slight constrictions at cell wall junctions, but with no loss of host cell viability. Propidium iodide (PI, red) was used to stain the plant cell walls. (Scale bar = 10µm). Micrograph obtained using the protocol described in Marcel et al., 2010.

When compared with other root-infecting fungi such as *G. graminis* (take-all fungus), *M. oryzae* exhibited similar features including the formation of an extensive surface colonisation and dark runner hyphae on barley roots. Both intra- and intercellular growth of *M. oryzae* were seen in the epidermal and cortical cell layers of the root following penetration. Thick and bulbous intracellular hyphae were also seen inside the root, with constrictions at junctions where the fungus crossed the plant cell wall (Sesma and Osbourn, 2004). Interestingly, the fungus spread from rice roots to the aerial tissues where it caused disease, an observation that was consistent with the blast symptoms seen in the aerial parts of up to 10% of the rice seedlings under laboratory conditions (Sesma and Osbourn, 2004). Further investigation with the root-infecting fungus *Fusarium oxysporum* confirmed that *M. oryzae* has a common shared genetic mechanism with other root-infecting fungi. For instance, the deletion of MgFOW1, a predicted mitochondria carrier protein shown to condition root infection in *R. oxysporum*, led to a significant reduction of root browning and colonisation of rice root surface by *M. oryzae* in the mutant relative to the wild-type. However, unlike in the wild-type where fungal hyphal growth progressed normally beyond the root surface to the interior layers, *mgfow1* mutant hyphal growth was restricted at the second cell layer. This phenotype (along with the reduced root browning) was restored by complementation with the *MgFOW1* gene, emphasizing a genetic similarity between *M. oryzae* and other root-infecting pathogens (Sesma and Osbourn, 2004). These findings highlight the similarities and differences between *M. oryzae* rice root versus leaf infection, and *M. oryzae* versus other root-infecting pathogens. The challenge though, is to identify shared genetic elements for rice root invasion by *M. oryzae* and the endosymbiont *R.*

irregularis as this will help us to better understand whether the pathogen has possibly recruited plant programmes established in the ancient symbiosis to advance its invasion of the host cell.

1.2.5. Shared genetic elements between mutualistic and parasitic plant-microbe interactions

Except for knowledge about the non-melanised hyphopodia formation on rice root surface prior to invasion by both fungi, not much is known about genetic commonalities in both interactions. This also applies widely within the field of plant-microbe interactions, where very few examples of shared elements between mutualistic and parasitic root interactions have been provided. The few known examples have mainly been cited in legume-parasitic microbe interactions (e.g. *Nod Factor Perception* or NFP, *Reduced Arbuscular Mycorrhization 2* or RAM2, and *Required for Arbuscule Development 1* or RAD1) with one in rice (CERK1). Accordingly, NFP is required for symbiotic signalling in *M. truncatula* and resistance against the pathogen *Aphanomyces euteiches* (Rey et al., 2013), a soilborne biotrophic oomycete pathogen responsible for pea root rot disease (Gaulin et al., 2007). RAM2 functions in hyphopodia and arbuscule development during AM symbiosis, as well as appressoria formation in the oomycete pathogen *P. palmivora* (Wang et al., 2012; Gobbato et al., 2013), and RAD1 is implicated as a host susceptibility factor required for root colonisation by unrelated filamentous symbionts and pathogens (Rey et al., 2017). In the monocotyledonous plant, *O. sativa*, CERK1 serves as a common co-receptor for both symbiosis (Miyata et al., 2014; Zhang et al., 2015) and plant immunity signalling (Kouzai et al., 2014). These findings support the existence of a shared genetic role between symbiotic and pathogenic microbe interactions, but studies in rice, a major staple cereal for more than half of the world's population, will provide useful insight that may contribute to the development of more effective disease control strategies against rice diseases.

1.3. Research Hypothesis

Based on information available in the literature and insights provided by my experimental results, I propose that 'Common mechanisms of accommodation exist for both mutualistic (*Rhizophagus irregularis*) and pathogenic (*Magnaporthe oryzae*) fungi in rice roots'. This hypothesis will be tested under two major experimental objectives.

1.4. Research Objectives

The aim of this project was to identify common genetic requirements for the accommodation of both mutualistic (*Rhizophagus irregularis*) and detrimental (*Magnaporthe oryzae*) fungi in rice roots. It involved two comparative approaches. First, a targeted approach to investigate the role of *Oryza sativa* CERK1 and other plasma membrane receptor kinases (OsNFR5) and protein (OsCEBiP) during rice root colonisation by *R. irregularis* and *M. oryzae* (Chapter 2). Second, an untargeted approach to identify genes of functional relevance for the accommodation of both fungi in rice roots (Chapter 3). To better understand the role of the plant plasma membrane receptors, OsCERK1, OsNFR5 and OsCEBiP during rice root invasion by *R. irregularis* and *M. oryzae*, a phenotypic examination was performed using corresponding loss-of-function mutant roots (*oscerk1*, *osnfr5* and *oscebip*) colonised by both fungi, respectively. This included mycorrhizal quantification experiments to determine the level of fungal colonisation in wild-type and mutant roots and live-cell confocal imaging to identify possible morphological aberrations in both fungi during rice root invasion. In addition, quantitative PCR-based molecular analysis was performed to monitor the expression levels of arbuscular mycorrhizal (AM) marker genes as well as to measure the biomass of *M. oryzae* in colonised and non-colonised wild-type and mutant roots.

The second experimental objective focused on identifying genes of functional relevance for the accommodation of *R. irregularis* and *M. oryzae* in rice roots (Chapter 3). It involved a computational comparison of whole genome transcriptomics data from rice roots during interaction with *R. irregularis* and progressive root infection by *M. oryzae*. It led to the selection of five candidate genes that are strongly co-upregulated during rice root colonisation by both beneficial and detrimental fungi. The functional roles of the gene candidates were then assessed using a reverse genetics approach utilising T-DNA insertion mutants for two gene candidates (*OsExo70-H3b* and *OsLecRLK*) and self-generated multiplex CRISPR (Clustered Regularly Interspaced Short Palindromic Repeats)-CRISPR-associated protein (Cas9) mutants for three rice gene candidates (*OsDUF538_07g02880*, *OsDUF538_07g02920* and *OsDUF538_11g38210*). Notably, the *OsDUF538* genes are members of a superfamily of genes. Using a single guide RNA, up to nine *OsDUF538* genes were successfully edited in one plant, followed by genotypic and phenotypic characterisation with *R. irregularis* and *M. oryzae*, respectively.

Taken together, the experimental approaches applied in this study led to the identification of the novel roles of three plant plasma membrane receptors, OsCERK1, OsNFR5 and OsCEBiP as potential regulators of *M. oryzae* rice root invasion. It also led to the identification of a new common set of genes that are associated with rice root colonisation by both beneficial and detrimental fungi. Findings made here will facilitate our understanding of new and/or existing plant accommodation programmes shared between symbiotic and detrimental fungi and how this may be optimised or modified to improve crop improvement and disease control strategies against rice diseases.

CHAPTER 2

The Role of Chitinaceous Signal Receptors during Rice Root Invasion by *Rhizophagus irregularis* and *Magnaporthe oryzae*

2.1. Introduction

Plants recognize pathogen species through the perception of the main components of their cell wall, which are chitin in fungi and β-glucans in oomycetes (Boller and Fellix, 2009). Similarly, flagellin, elongation factor Tu (EF-Tu), lipopolysaccharides and peptidoglycans are archetypal bacterial molecules recognized by the plant immune system (Boller et al., 2009). During bacterial infection, PAMP (Pathogen Associated Molecular Pattern)-Triggered Immunity (PTI) is initiated through the perception of bacterial flagellin protein *via* an induced receptor complex consisting of the leucine-rich repeat (LRR) receptor kinases, Flagellin-Sensitive 2 (FLS2) and BRI1-Associated Kinase 1 (BAK1) (Gómez-Gómez and Boller, 2000; Heese et al., 2007; Chinchilla et al., 2007). FLS2 was first discovered in the model plant *Arabidopsis thaliana*, and is involved in the recognition of flagellin through the direct binding of the elicitor-active epitope, flg22, a peptide spanning a conserved stretch of 22 amino acid residues situated close to the N terminus of flagellin (Felix et al., 1999; Chinchilla et al., 2006; Sun et al., 2013).

Most higher plants seem to recognize flg22 (Boller and Felix, 2009), and functional orthologues of FLS2 have been found in a wild relative of tobacco (*Nicotiana benthamiana*) (Hann and Rathjen, 2007), rice (*Oryza sativa*) (Takai et al., 2008), tomato (*Solanum lycopersicum*) (Robatzek et al., 2007), and grapevine (*Vitis vinifera*) (Trdá et al., 2014). In rice, OsFLS2 is highly homologous to AtFLS2 and functions in flg22 recognition (Takai et al., 2008). The expression of OsFLS2 in *Arabidopsis fls2* mutants restored the induction of immune responses after treatment with flg22, indicating the conservation of flg22-FLS2 signalling in monocotyledons and dicotyledons (Takai et al., 2008). Following FLS2 recognition of bacterial flagellin, FLS2 forms a receptor complex with BAK1 to initiate immune signalling. Although it is unclear how the FLS2-BAK1 receptor complex functions to activate downstream intracellular signalling cascades, a receptor-like cytoplasmic kinase BIK1 (Botrytis-Induced Kinase 1) is identified as an essential component in the MAMP signal transduction (Lu et al., 2010). Activation of the FLS2-BAK1 complex leads to the subsequent phosphorylation of BIK1. In return, BIK1 phosphorylates BAK1 and FLS2 (Lu et al., 2010), and then disassociates

from the BAK1-FLS2 receptor complex. Upon disassociation, BIK1 phosphorylates the respiratory burst oxidase homologue protein B/D (RBOHB/D), which activates its function and stimulates the production of reactive oxygen species (ROS). Elevation of ROS triggers the initiation of Ca^{2+} influx, which is perceived and decoded by Ca^{2+} binding proteins serving as Ca^{2+} sensors (Yuan et al., 2017).

Calcium is an essential signal for PAMP-triggered immunity in plants (Zipfel and Oldroyd, 2017; Yuan et al., 2017). In *Arabidopsis*, two genes encoding cyclic nucleotide-gated channel (CNGC) proteins, *CNGC2* and *CNGC4* have been linked to PAMP-induced calcium signalling (Yuan et al., 1998; Ali et al., 2007; Tian et al., 2019). In the absence of pathogens, *CNGC2* and *CNGC4* assemble into a functional calcium channel that is blocked by calmodulin at the resting state (Tian et al., 2019). However, in response to flg22, the channel becomes phosphorylated and activated by BIK, triggering an increase in the concentration of cytosolic calcium, and thereby activating calcium-based defence responses (Lu et al., 2010; Li et al., 2014; Ranf et al., 2014). This CNGC-mediated calcium entry is believed to provide a useful link between the PAMP-PRR complex and calcium-dependent events in the PTI signalling pathway (Tian et al., 2019).

Furthermore, the perception of chitin oligosaccharides (β-1,4-linked polymers of N-acetylglucosamine, GlcNAc with various degrees of polymerization) can induce symbiotic or immunity signals, and the induction of either of the signals depends on the length or lipid modification on the chitin oligosaccharide backbone. For example, chitin oligosaccharide hexamers or octamers are potent inducers of immune responses (Boller et al., 2009), whereas tetramers (CO4) and pentamers (CO5) induce symbiotic responses for AM and Rhizobia symbiosis, respectively (Genre et al., 2013; Liang et al., 2014). Notably, Myc- and Nod-factors are derivatives of chitin oligosaccharides, but with a lipid tail on the chitin oligosaccharide backbone, giving rise to lipo-chitooligosaccharides (LCOs). Rhizobia bacteria, for instance, produce a variety of modified Nod-LCOs, which differ in their chitin oligosaccharide chain, lipid acylation, and the presence of modifications (e.g. sulfation, acetylation and fucosylation), which possibly contribute to the plant host specificity (for review, see Zipfel and Oldroyd, 2017). Unlike Rhizobia symbiosis, which is established upon perception of Nod-LCOs, initiation of AM symbiosis is thought to involve a well-coordinated perception of a mixture of LCO and chitin oligosaccharide molecules. These unique characteristics continue to raise questions about how plants discriminate between chitin oligosaccharide-containing molecules that lead to immunity or symbiosis.

During pathogen attacks, plants launch at least two lines of active defence. The first line of defence is a basal defence against all potential pathogens known as PAMP-triggered immunity (PTI) and the second is the Effector-Triggered Immunity (ETI). ETI is triggered once the basal defence system is overcome by pathogens. It involves the perception of fungal effector proteins by cognate resistance (R) proteins, which activates ETI, and consequently, elicits a rapid and robust defence response in plants, including hypersensitive responses (Flor 1942; for review see De Wit et al., 2009). To counter or suppress ETI responses in plants, pathogens mutate their effectors or evolve new ones, which are also recognized by novel R proteins produced by the plant (De Wit, 2007; Jones and Dangl, 2006). Over the last two decades, successful molecular cloning of avirulence (AVR) genes from different microorganisms, including bacteria, fungi and oomycetes have increased our understanding of plant-microbe interactions. For example, an *M. oryzae* non-AVR effector protein named Secreted LysM Protein 1 (Slp1) was found to overcome the first line of plant defence during *M. oryzae* leaf infection (Mentlak et al., 2012). Slp1 accumulates at the interface between the fungal cell wall and the rice plasma membrane and can bind chitin, as well as suppress chitin-induced plant immune responses, including the generation of reactive oxygen species and plant defence gene expression (Mentlak et al., 2012). Interestingly, Slp1 competes with the LysM receptor-like protein (RLP), Chitin Elicitor Binding Protein (CEBiP) for chitin oligosaccharides, thereby preventing PTI in rice, consequently, accelerating fungal tissue invasion and disease lesion expansion (Mentlak et al., 2012).

PTI involves the recognition of PAMPs *via* their corresponding Pattern Recognition Receptors (PRRs), which are situated on the surface of the plant's plasma membrane, and this activation prevents further colonisation and infection of the host plant (De Wit, 2007; Jones and Dangl, 2006). Chitin is one of the best-known fungal PAMPs. In both monocotyledonous and dicotyledonous plants, chitin oligosaccharides can be recognized by surface receptors such as the lysine motif (LysM) receptor-like kinases (RLKs), CERK1 or receptor-like proteins (RLPs) such as CEBiP. Excitingly, CERK1 has been shown to be indispensable for the perception of chitin oligosaccharides and related signals that lead to symbiosis or immunity (Miyata et al., 2014; Zhang et al., 2014).

In *Arabidopsis*, AtCERK1 forms a heteromeric complex with another LysM-RLK known as AtLYK5 (and LYK4, a paralogue of LYK5) to perceive and elicit chitin signals (Miya et al., 2007; Zipfel and Oldroyd, 2017). AtCERK1 is a receptor kinase localized in the plant plasma membrane and consists of three lysine motifs in the extracellular region and the Ser/Thr kinase

domain in the intracellular region (Miya et al., 2007). Miya et al. (2007) showed that knockout mutants of *atcerk1* lost their ability to respond to chitin, and this hampered MAP kinase activation, generation of reactive oxygen species and gene expression. Although several studies suggest that AtCERK1 is the primary chitin receptor (Miya et al., 2007; Wan et al., 2008; Iizasa et al., 2010; Petutschnig et al., 2010; Liu et al., 2012; Shinya et al., 2012), Cao et al. (2014) strongly suggested that AtLYK5 is the primary receptor for chitin. Mutants of AtLYK5 showed a significant reduction in chitin response, suggesting that AtLYK5 is the primary chitin receptor, which forms a complex with AtCERK1 to induce plant innate immunity (Cao et al., 2014).

In rice, OsCERK1 and OsCEBiP form a heteromeric complex to perceive chitin oligosaccharides in the case of defence responses (Shibuya et al., 2001; Shimizu et al., 2010, Kouzai et al., 2014). During symbiosis, OsCERK1 interacts with an unknown partner to induce early symbiotic signalling responses. By inoculating *oscerk1* knockout (Miyata et al, 2014) and RNAi (Zhang et al., 2015) mutant roots with the AM fungus *R. irregularis*, a reduction in the level of fungal colonisation in the mutant was observed at the early stages (15 days post inoculation, dpi) of colonisation. Phenotypically, Miyata et al. (2014) observed frequent formation of a cluster of hyphopodia from one extraradical hypha on the root surface, but no internal hypha or arbuscule development in the roots at 15 dpi. The study however, claimed that all observed phenotypes vanished with prolonged AM fungi and *oscerk1* root cultivation, suggesting that OsCERK1 functions in early AM symbiotic signalling processes. In contrast, *oscebip*, as well as *osnfr5* established AM symbiosis normally (Miyata et al., 2014; Miyata et al., 2016), suggesting that both OsCEBiP and OsNFR5 are not required for AM symbiosis.

CEBiP is a plasma membrane glycoprotein consisting of three lysine motifs, with the ability to directly bind chitin oligosaccharides. It lacks an intracellular region, and must therefore, interact with a receptor kinase that has an intracellular region for immunity signal transduction. Functional studies show that CEBiP plays a major role in the perception and signalling of chitin elicitors in rice (Kouzai et al., 2014), although two of its orthologues, the lysine motif-containing protein 4 (OsLYP4) and 6 (OsLYP6) are involved in the recognition of both chitin and peptidoglycan (Liu et al., 2012). Following recognition and binding to chitin elicitors, CEBiP forms a complex with CERK1, which has an intracellular region and can phosphorylate the target protein(s) to trigger downstream defence responses (Shimizu et al., 2010). RNAi mutants of *cebip* showed a significant reduction in disease resistance against *M. oryzae*, whilst

increased hyphal growth in rice leaf sheath cells was seen in *M. oryzae* inoculated *oscerk1* mutants (Kouzai et al., 2014b).

Unlike AM symbiosis, the role of plant surface receptor-like kinases and receptor-like proteins during rice root invasion by *M. oryzae* has not been studied. It is intriguing that as a hemi-biotrophic pathogen, *M. oryzae* exhibits features peculiar to *R. irregularis* and some root-infecting pathogens such as *Fusarium oxysporum* (Sesma and Osbourn, 2004), whilst retaining its robustness to cause necrotic disease lesions on rice leaves. It forms simple hyphopodia on rice root surface and maintains a prolonged biotrophic hyphal growth phase in the root like an endophyte (Marcel et al., 2010). It also causes root browning and microsclerotia typical of root infecting fungi (Sesma and Osbourn, 2004), whilst utilizing both mechanical (turgor pressure) and chemical (enzymes and effectors) forces to invade and infect rice leaf tissue, causing necrosis (Talbot, 2019).

The unique ability of *M. oryzae* to change or combine multiple lifestyles to facilitate its invasion of the host plant *via* different organs, increases our curiosity to understand what plant programmes are involved in its recognition and accommodation in rice roots. Considering the dual role of OsCERK1 in AM symbiosis and immunity signalling, its role during *M. oryzae* invasion of rice roots is unclear. A possibility is that OsCERK1 partners with OsCEBiP to perceive signals that enable accommodation of the pathogen in the root. It is also possible that it cooperates with OsNFR5 as another receptor kinase. These are the key objectives of this chapter. To investigate the function of OsCERK1, OsNFR5 and OsCEBiP during rice root colonisation by *M. oryzae*, and to compare their role, side-by-side during *M. oryzae* rice leaf infection. These aims will be addressed using a combination of live-cell confocal imaging and molecular and cell biology techniques to identify possible overlaps in plant programmes utilized by symbiotic and parasitic microbes to invade and proliferate in rice roots.

2.2. Results

2.2.1. Examining the role of OsCERK1 in rice root colonisation by *Rhizophagus irregularis* and *Magnaporthe oryzae*

To test this hypothesis, we first determined arbuscular mycorrhizal colonisation by inoculating wild-type (Nipponbare) and *cerk1* knockout mutant rice roots with *R. irregularis* to monitor fungal invasion and intracellular colonisation. Knockout mutant seeds were obtained from Miyata et al. (2014) and genotyped with self-generated PCR primers (see Table 13 and appendix) to confirm loss-of-function of *CERK1*. Although prior information is available (Miyata et al., 2014; Zhang et al., 2015), the aim of this experiment was to determine the reproducibility of the published results under our own experimental conditions.

Inspecting fungal colonization at an early and later time point post inoculation of wild-type (WT) and *cerk1* mutant rice roots with *R. irregularis*, clusters of hyphopodia (still attached to extraradical hyphae) were ubiquitously seen across *cerk1* mutant root surface compared to the wild-type. These hyphopodia clusters appeared to be significantly more abundant on the mutant root surface relative to the WT at 3 weeks post inoculation (wpi), with very little arbuscule and vesicle formation (Figure 2.1B, 2.1C). With prolonged co-cultivation however, internal fungal structures such as hyphopodia, arbuscules, intraradical hyphae and vesicles were seen in both WT and *cerk1* mutant roots at 5 wpi, although fungal colonisation seemed to be unevenly distributed in the mutants, with clusters of hyphopodia (attached to extraradical hyphae) still present in some parts of the root surface (Figure 2.1D-F). These results suggest that fungal colonisation is delayed in *cerk1* mutants compared to the WT. Notably, although several experiments were set-up, only one complete experiment was performed utilising the same plant materials for different assays including trypan blue and mycorrhizal quantification assay, Wheat Germ Agglutinin or WGA staining, and quantitative real-time PCR assays. More experiments utilising at least, two mutant alleles are recommended for more robust experimental outcomes.

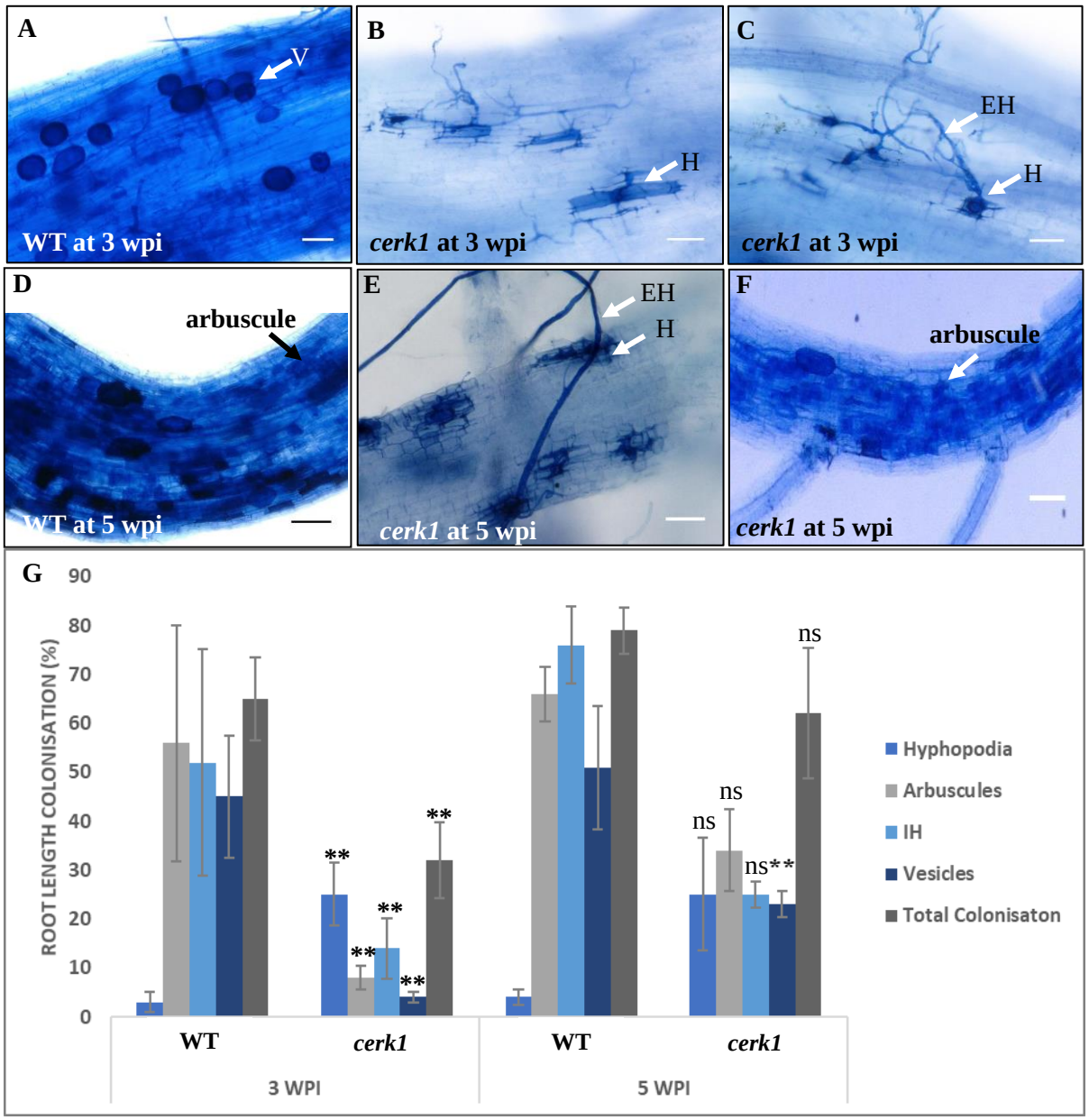

Figure 2.1: OsCERK1 is required for efficient penetration and intracellular colonisation of *Rhizophagus irregularis* in rice roots. Phenotypic observation of trypan blue stained WT and *cerk1* mutant rice roots colonised by *R. irregularis* at 3- and 5-weeks post inoculation (wpi), respectively (**A-F**). The fungus forms hyphopodia (H) on the root surface but is compromised in intra-radical proliferation during early colonisation (3 wpi) (**C**). However, with prolonged co-cultivation (5 wpi), fungal colonisation structures such as arbuscules, intra-radical hyphae (IH) and vesicles (V) became apparent in the mutants (**E-F**), but still less than in the WT as seen under the microscope (**D**). Root length colonisation shows a 31% reduction in total colonisation in *cerk1* mutants compared to the WT at 3 wpi. However, at 5 wpi, fungal colonisation slightly increased in *cerk1* mutants resulting in a 17% overall reduction compared to the WT (**G**). Bars represent the average of three biological replicates (n = 1) ± SEM. Asterisks indicate significant differences between the wild type and *cerk1* at two time points, 3- and 5 wpi. (Multiple *t*-test; *, $P < 0.05$; **, $P < 0.01$; ***, $P < 0.001$, ns = not significant). Representative of ~9 images per genotype (with at least two biological replicates) in one time-course experiment. Scale bar = 10µm.

To determine the level of fungal colonisation in WT and *cerk1* mutant roots, internal fungal colonisation structures (including hyphopodia, arbuscules, intra-radical hyphae and vesicles) observed in trypan blue stained roots were quantified under the microscope. This revealed a 31% reduction ($P < 0.01$) in fungal colonisation in *cerk1* mutants compared to the WT during early colonisation (3 wpi). With prolonged cultivation (5 wpi), total fungal colonisation in the mutant increased to WT level, (Figure 2.1G). suggesting that OsCERK1 functions in early AM signalling as previously reported. Next, we asked whether the morphology of *R. irregularis* is compromised in colonised *cerk1 versus* WT rice roots. To answer this question, colonised rice roots were stained with Wheat Germ Agglutinin (WGA) and the morphological structure of the fungus investigated by confocal laser scanner microscopy (CLSM). No aberration in fungal morphology was seen in either the mutant or WT at the early and later time points (Figure 2.2B, 2.2D), indicating that OsCERK1 is not required for the development of AM fungal structures such as arbuscules during intracellular colonisation.

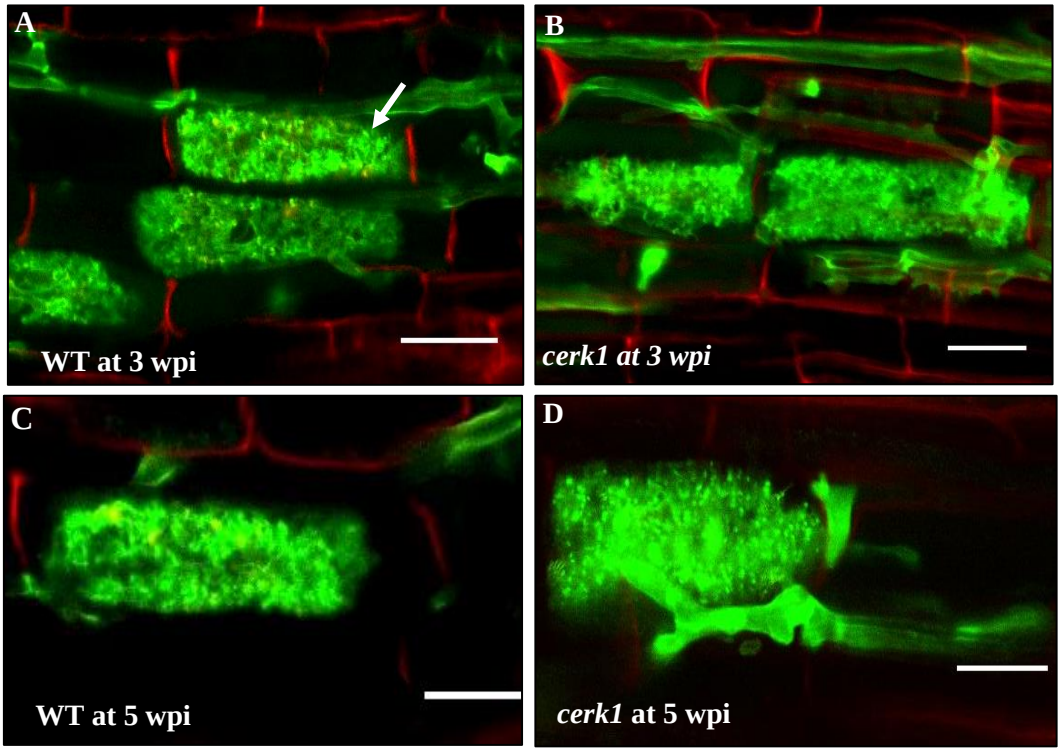

Figure 2.2: Fungal morphology is not compromised in *R. irregularis* colonised wild-type and *cerk1* mutant rice roots. Confocal microscopic images of WGA-stained WT and *cerk1* mutant roots colonised by *R. irregularis* at 3 wpi (top panel) and 5 wpi (bottom panel), respectively (**A-D**). Normal arbuscules (arrows) and intra-radical hyphae are seen in both WT and mutant roots at both time points. Propidium iodide (red) highlights the plant cell wall structures. (Scale bar = 50µm). Micrograph obtained using a modified protocol described in Kobae and Ohtomo (2016). Representative of ~9 images per genotype (at least two biological replicates) in one time-course experiment.

Lastly, to confirm that fungal colonisation is reduced in *cerk1* mutants, molecular quantification was performed to monitor the expression of AM marker genes and the *R. irregularis* Elongation Factor (RiEF) in WT and *cerk1* mutant roots of the microscopically inspected tissue. A significant reduction of RiEF and other tested AM marker genes in *cerk1* mutants at 3 wpi (Figure 2.3A, 2.3B, 2.3C) but not at 5 wpi, was observed relative to the level of induction in the WT (Figure 2.3D, 2.3E, 2.3F, 2.3G, 2.3H), thereby confirming the microscopic data. Notably, AM markers genes are genes that are induced upon mycorrhizal colonisation (Guimil et al., 2005). They code for specific proteins such as high-affinity phosphate transporters (OsPT11 and OsPT13), putative peroxidase (OsAM1), serine/threonine receptor-like kinase (OsAM14 or ARK1), germin-like proteins (OsAM4) and other hypothetical proteins (OsAM3) (Guimil et al., 2005).

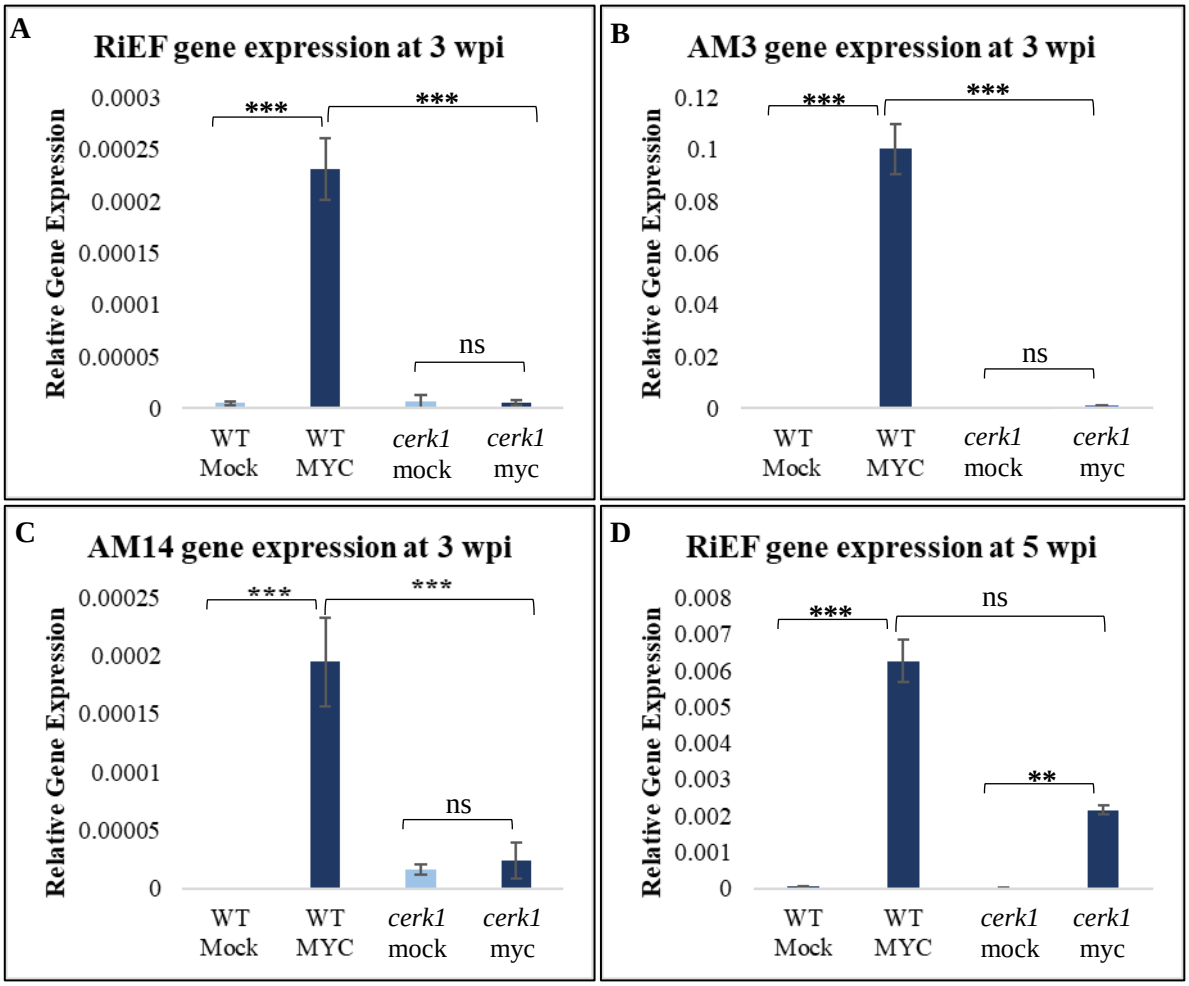

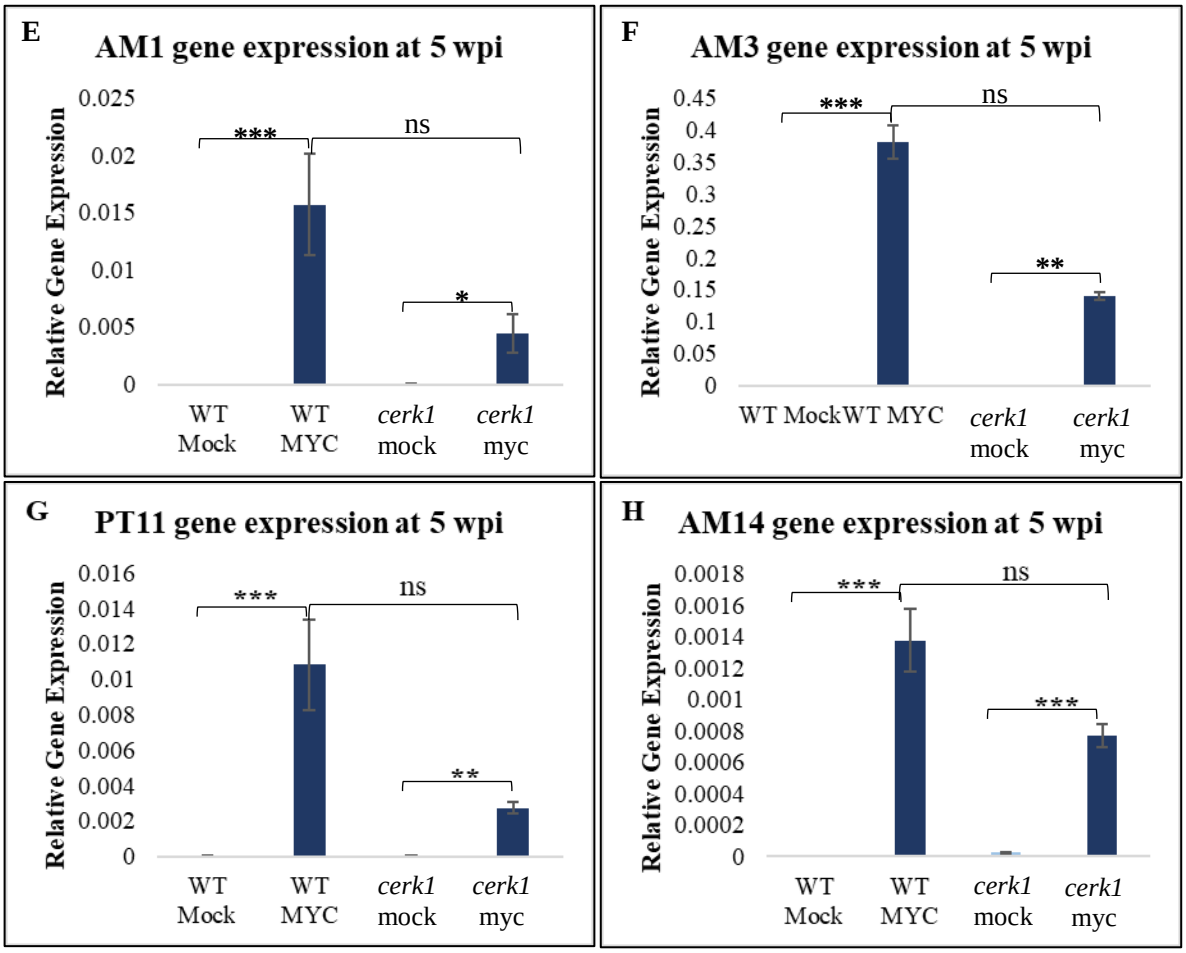

Figure 2.3: Molecular quantification of Arbuscular Mycorrhiza (AM) marker gene expression in *R. irregularis* colonised and non-colonised *cerk1* and WT rice roots. A significant reduction in AM fungal marker gene expression is seen in *cerk1* mutants compared to the WT at early colonisation (3 wpi) (**A-C**) but not at the later stages of colonisation (5 wpi) (**D-H**). Error bars represent the average of three biological replicates (n = 1) ± SEM and asterisks indicate significant differences between the WT and *cerk1*. MYC = mycorrhized roots; mock = non-mycorrhized roots. (Student's *t*-test; *, $P < 0.05$; **, $P < 0.01$; ***, $P < 0.001$).

2.2.2. OsCERK1 is required for rice root cell invasion by *M. oryzae*

To investigate whether OsCERK1 is required for intracellular colonisation of *M. oryzae* in rice roots, WT and *cerk1* rice roots were co-cultivated with GFP-expressing *M. oryzae* and monitored by live-cell imaging. Two time points, early (4 dpi) and late (7 dpi) were considered for this experiment to enable us to follow the fungus microscopically and to better understand how rice roots are responding to the pathogen in the absence of OsCERK1. Interestingly, a striking phenotype was observed in *cerk1* mutants, where the invasive fungal hyphae appeared to be trapped and/or dead inside rice root cells at both 4 and 7 dpi (Figure 2.4). Notably, dead fungal hyphae were stained with propidium iodide (arrow in Figure 2.4B, 2.4F, 2.4H), which is known to stain dead cells (Boulos et al., 1999).

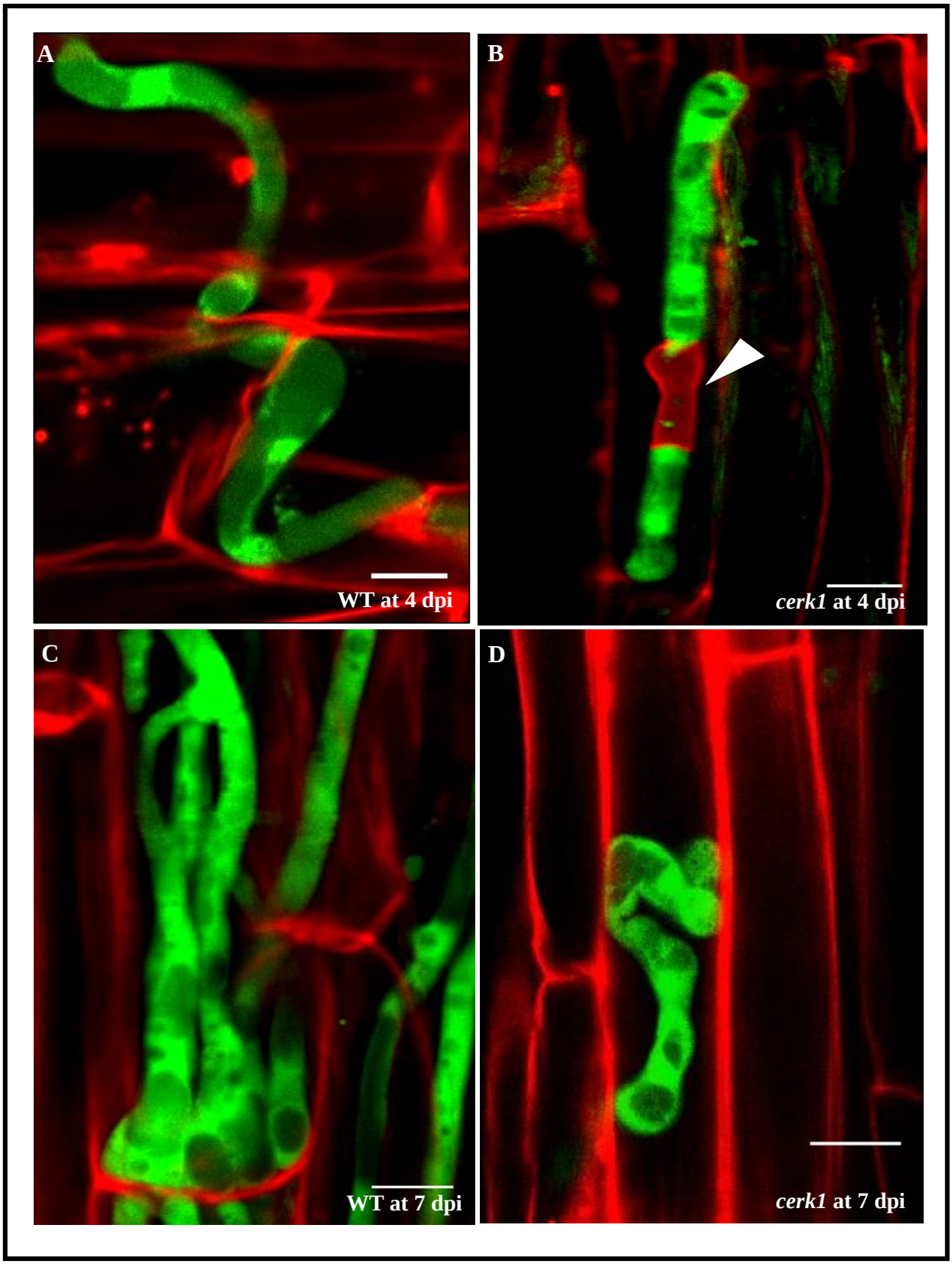
A
WT at 4 dpi
B
cerk1 at 4 dpi
C
WT at 7 dpi
D
cerk1 at 7 dpi

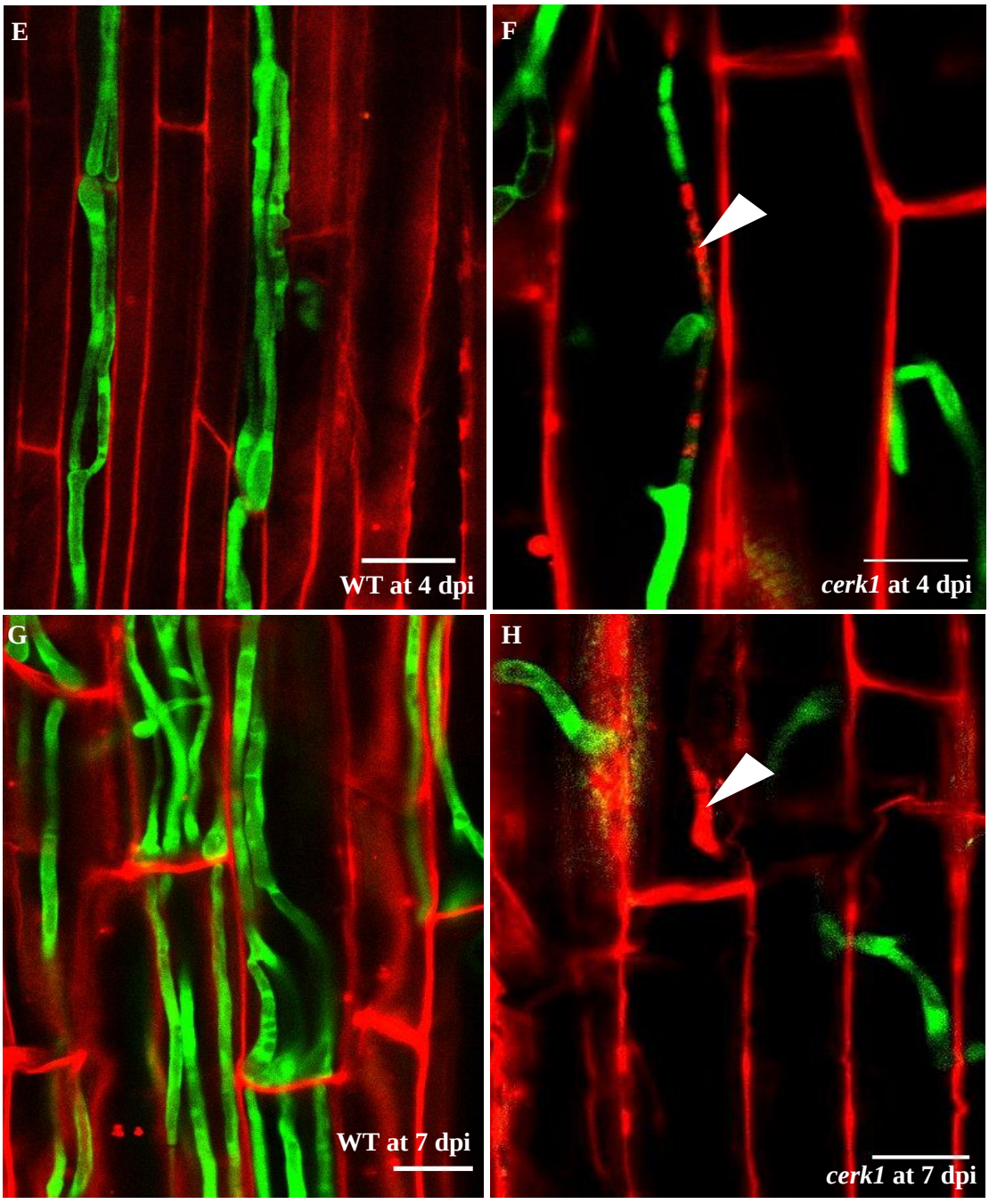

Figure 2.4: **Live cell confocal imaging of wild-type (Nipponbare) and *cerk1* mutant rice roots colonised by GFP-expressing *M. oryzae* (Guy11 strain).** *M. oryzae* proliferates normally, crossing from cell to cell in the WT but is trapped and dead (arrow) in *cerk1* mutants at both 4 dpi (**A, B, E, F**) and 7 (**C, D, G, H**) dpi, respectively. Increased fungal proliferation is observed in the WT compared to a visual reduction of fungal biomass in *cerk1* mutants at 7 dpi. Images in the top panel were taken at 63x (zoom 1.6) magnification on the SP8, whereas the bottom panel was taken 63x (zoom = 1). Propidium iodide stain (red) highlights the dead cells, as well as the plant cell walls. Representative of 70 (WT) and 67 (*cerk1*) images with 3 biological replicates per experiment in at least four experiments. Micrograph obtained using protocol described in Marcel et al., 2010. Scale bar = 50µm.

To quantify the number of dead and/or trapped fungal hyphae seen inside rice root cells, images of colonised WT versus *cerk1* mutant roots produced by confocal microscopy (from more than three independent experiments) were collected and analysed. Out of a total of 70 images, 22 (31%) dead or restricted *M. oryzae* invasive hyphae were seen in rice root cells compared to 3 (5%) out of 67 total fungal hyphae in the WT (Table 1), suggesting CERK1 may be required for compatibility and intracellular accommodation of *M. oryzae* in rice roots.

Phenotypic quantification of *M. oryzae* hyphal death in WT and *cerk1* rice roots		
Genotype	**WT**	***cerk1***
Total number of images analysed	67	70
Number of dead and/or trapped fungal hyphae inside rice root cells	3	22
Estimated Average Total (%)	**5%**	**31%**

Table 1: Phenotypic quantification of *M. oryzae* invasive hyphae, dead or trapped inside rice root cells. The total number of dead or restricted invasive hyphae seen in confocal images of colonised WT and *cerk1* mutant roots was calculated to determine the severity of phenotype observed in the mutant. Images were analysed with three biological replicates (root tips from three plants) *per* experiment in an average of four experiments.

Next, to confirm whether the extent of *M. oryzae* colonisation of *cerk1* mutant roots is reduced relative to the WT, qPCR-based quantification was performed using three *M. oryzae* housekeeping genes (*Mo-Actin*, *Mo-Tubulin* and *Mo-40s8*, encoding a ribosomal protein). An overall reduction in the expression of all three housekeeping genes was observed in colonised *cerk1* mutants at early and late time points (Figure 2.5), which correlates with the phenotypic observations (Table 1).

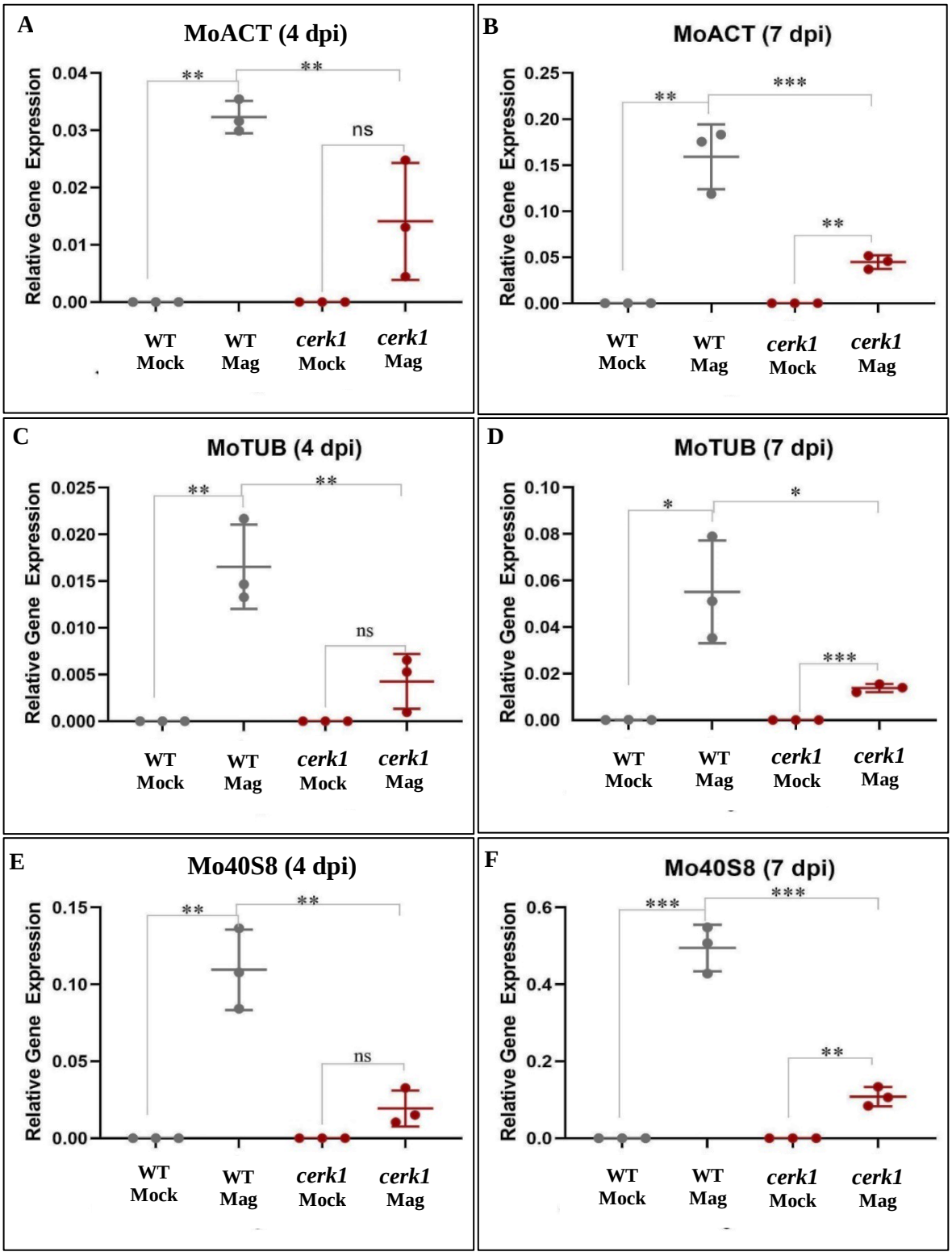
A
MoACT (4 dpi)
Relative Gene Expression
0.04
0.03
0.02
0.01
0.00
**
**
ns
WT Mock
WT Mag
cerk1 Mock
cerk1 Mag
B
MoACT (7 dpi)
Relative Gene Expression
0.25
0.20
0.15
0.10
0.05
0.00
**
***
**
WT Mock
WT Mag
cerk1 Mock
cerk1 Mag
C
MoTUB (4 dpi)
Relative Gene Expression
0.025
0.020
0.015
0.010
0.005
0.000
**
**
ns
WT Mock
WT Mag
cerk1 Mock
cerk1 Mag
D
MoTUB (7 dpi)
Relative Gene Expression
0.10
0.08
0.06
0.04
0.02
0.00
*
*
***
WT Mock
WT Mag
cerk1 Mock
cerk1 Mag
E
Mo40S8 (4 dpi)
Relative Gene Expression
0.15
0.10
0.05
0.00
**
**
ns
WT Mock
WT Mag
cerk1 Mock
cerk1 Mag
F
Mo40S8 (7 dpi)
Relative Gene Expression
0.6
0.4
0.2
0.0
***
***
**
WT Mock
WT Mag
cerk1 Mock
cerk1 Mag

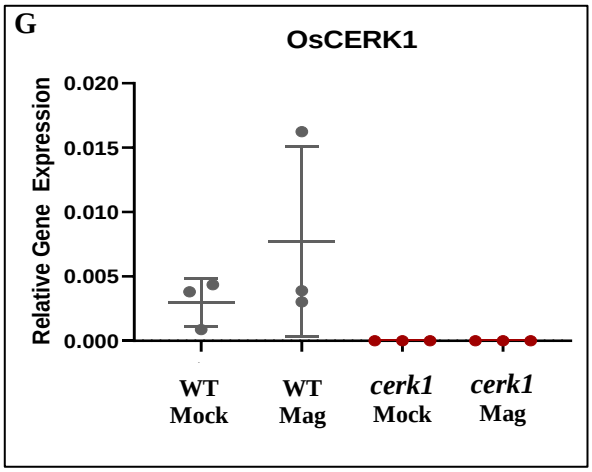

Figure 2.5: Molecular quantification of *M. oryzae* biomass in colonised and non-colonised WT and *cerk1* mutant rice roots. Expression levels of three *M. oryzae* housekeeping genes (*MoACT* - actin, *MoTUB* – tubulin and *Mo40S8* - ribosomal protein) and *OsCERK1* in colonised and non-colonised *cerk1* and WT roots at 4 and 7 dpi, respectively, are shown (**A-G**). Expression levels were measured by qRT-PCR and normalized to the geomean of three *O. sativa* housekeeping genes - *Cyclophilin, GAPDH* and *Ubiquitin* expression. Bars represent the means of three biological replicates ± SEM (n = 1). Asterisks indicate significant differences between expression levels in colonised and non-colonised roots of the same and different genotypes (e.g. WT colonised *versus* WT non-colonised, *cerk1* colonised vs *cerk1* non-colonised, and WT vs *cerk1* colonised) at the corresponding time point (one-way ANOVA and *t*-test, *, $P < 0.05$; **, $P < 0.01$; ***, $P < 0.001$, n.s., $P \geq 0.05$).

2.3. Is OsCEBiP required for rice root colonisation by *Rhizophagus irregularis* and *Magnaporthe oryzae*?

To verify the mycorrhizal phenotype of rice lines mutated in *CEBiP*, fungal colonisation was monitored at early (3 wpi) and later (5 wpi) time points. Knockout mutants of *cebip* were obtained from Miyata et al. (2014) and genotyped using self-generated PCR primers (Table 13) to confirm the loss-of-function of CEBiP (see appendix). Surprisingly, at 3 wpi, efficient penetration of the fungus seemed to be compromised. Like in *cerk1* mutants, clusters of hyphopodia with attached extra-radical hyphae were observed (Figure 2.6B, 2.6C), especially during early colonisation, however, they were more sparsely distributed than in *cerk1* mutants at 3 wpi. With prolonged co-cultivation of the fungus and *cebip* mutant roots, internal AM colonisation structures such as arbuscules, intra-radical hyphae, vesicles were seen (Figure 2.6E, 2.6F) but significantly reduced compared to the WT at 5 wpi (Figure 2.7B).

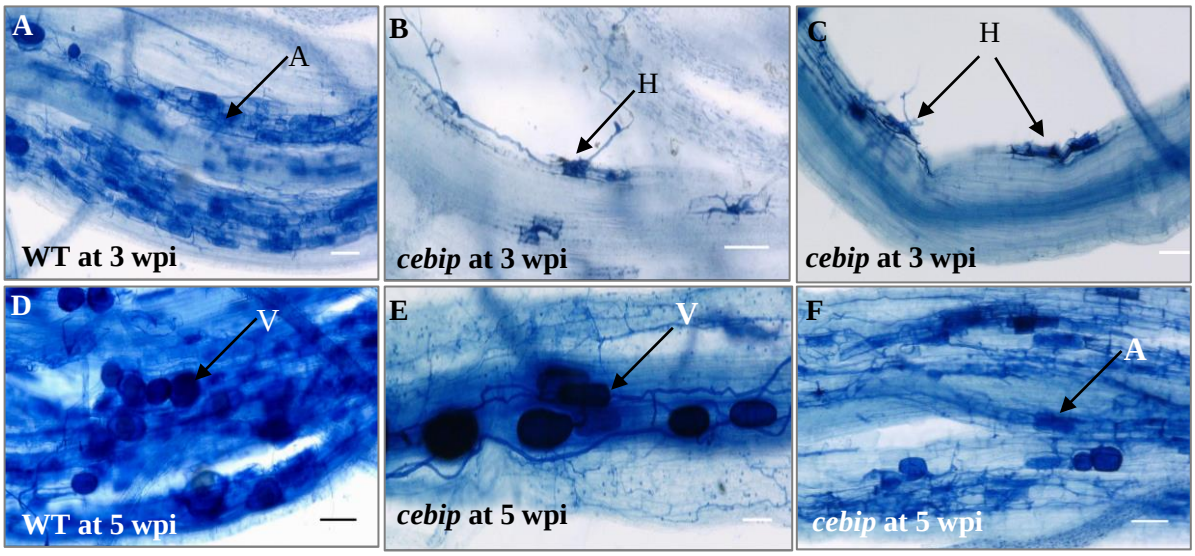

Figure 2.6: Phenotypic observation of *R. irregularis* colonised WT and *cebip* mutant rice roots. The fungus forms hyphopodia (H) on the root surface but intra-radical proliferation is compromised in *cebip* mutants (**B-C**) compared to the WT (**A**) at 3 wpi. At 5 wpi, fungal colonisation structures such as arbuscules (A), intra-radical hyphae and vesicles (V) become apparent in the mutants (**E-F**) but remain relatively less than in the WT (**D**). Roots were stained with trypan blue to enable the microscopic visualization of fungal structures. Representative of ~9 images per genotype (with at least two biological replicates) in one time-course experiment. Scale bar = 10µm.

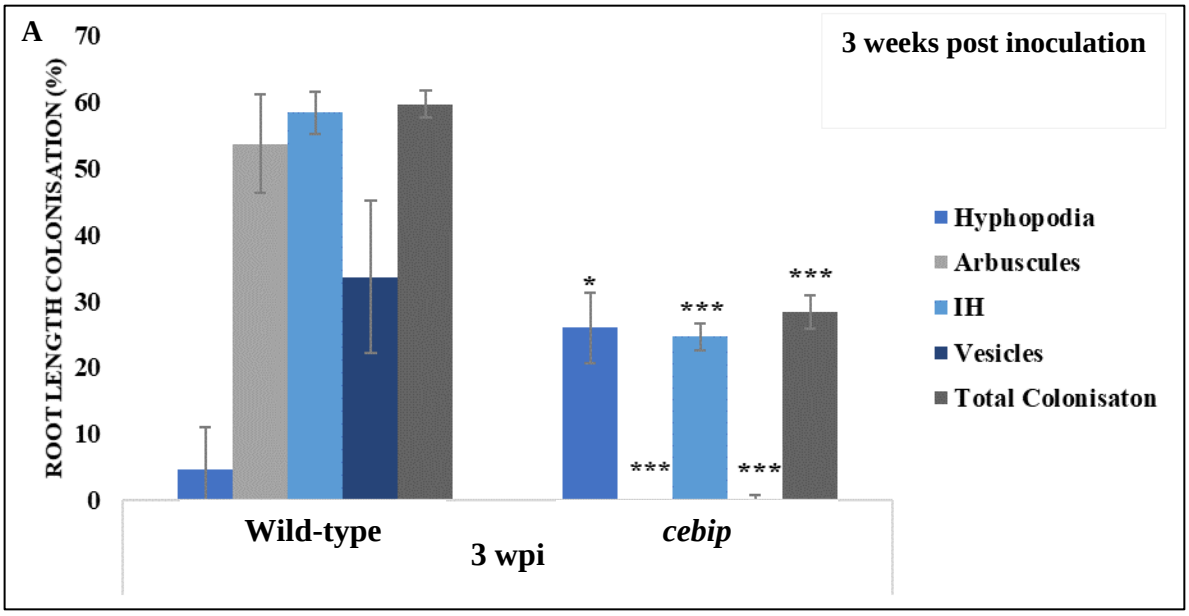

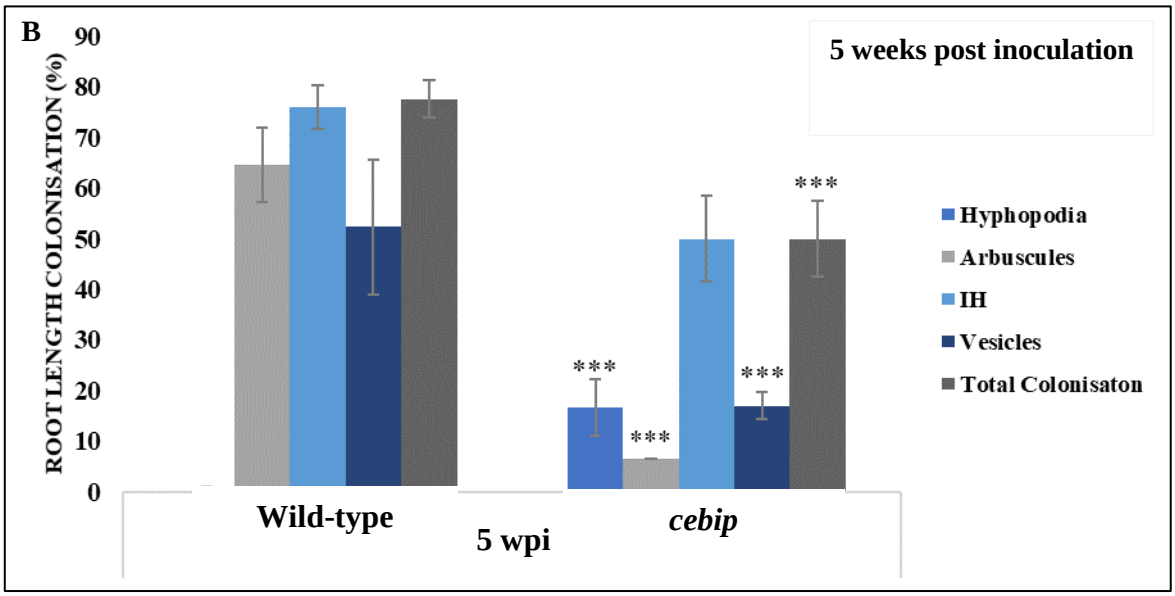

Figure 2.7: Quantification of fungal infection structures in *R. irregularis* colonised WT and *cebip* mutant roots. The presence of hyphopodia, arbuscules, intra-radical hyphae (IH) and vesicles in trypan blue stained WT and *cebip* mutant root pieces is shown as percentage of the total number of root pieces examined. Fungal colonisation was quantified at 3 wpi (**A**) and 5 wpi (**B**). Bars represent the average of three biological replicates ± SEM. Asterisks represent significant differences between the wild type and *cebip* at each time point. (Multiple *t*-test; *, $P < 0.05$; **, $P < 0.01$; ***, $P < 0.001$.

To investigate whether *R. irregularis* morphology was compromised in *cebip* mutants, colonised WT and *cebip* rice roots were stained with WGA. Compared to the WT, where fungal intra-radical hyphae grow intercellularly and then form arbuscules in inner cortex cells (Figure 2.8A, 2.8C, 2.8E), it appears that the trunk domain (TD) of the arbuscule is formed in the mutant, but with reduced branching (Figure 2.8B, 2.8D, 2.8F).

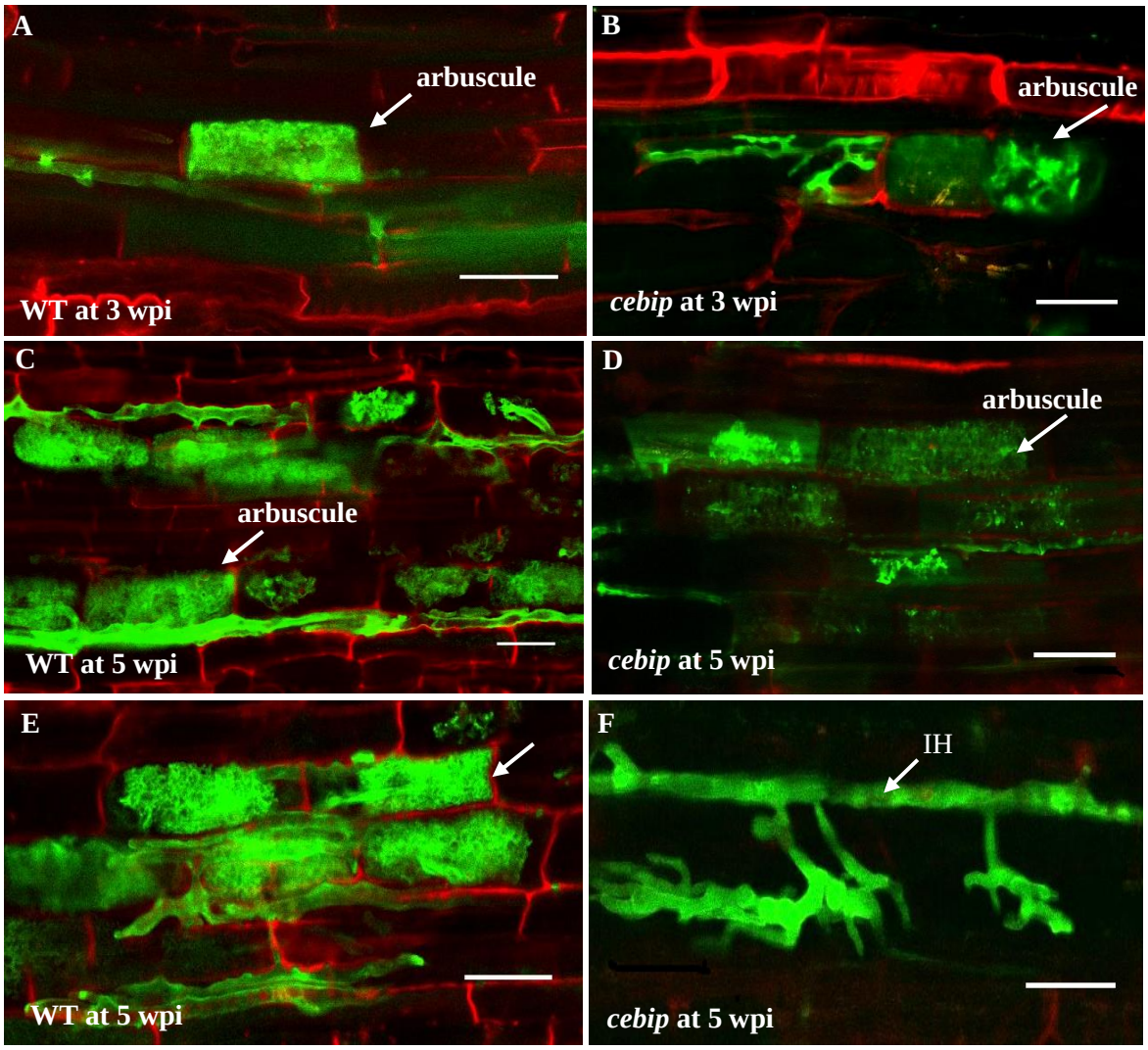

Figure 2.8. Morphological characterization of *R. irregularis* colonised WT and *cebip* mutants. Confocal imaging revealed fungal colonisation structures such as arbuscules and intra-radical hyphae (IH) in WGA-stained colonised WT and *cebip* mutant roots at 3 and 5 wpi, respectively (**A-F**). Fully formed arbuscules (A) are seen in the WT (A, C, E), whereas arbuscules with possible reduced branching are seen in *cebip* mutants (D, F). Fungal structures were stained with WGA (green) and propidium iodide (red) was used to highlight the plant cell wall structure). Representative of ~9 images per genotype (with at least two biological replicates) in one time-course experiment. Scale bar = 50µm.

Following phenotypic characterization, the expression levels of arbuscular mycorrhizal (AM) marker genes such as *AM1*, *AM3*, phosphate transporter 11 (*PT11*) and *AM14* were measured by qRT-PCR at 3 and 5 wpi, respectively. Experimental results revealed a significant reduction of all AM marker genes in *cebip* mutants at 3 wpi (Figure 2.9A-D) but not at 5 wpi, except for *AM3* expression, which was significantly reduced in the mutant at 5 wpi (Figure 2.9F). The extremely low transcript level at both time points differ from the microscopic data, where overall colonisation of fungal internal structures was 30% at 3 wpi and 50% at 5 wpi (Figure

2.7 A, 2.7B). With this level of colonisation, especially at 5 wpi, it is expected that all marker genes would be expressed, although at reduced levels. This discrepancy between the microscopic and gene expression data may be due to an unequal distribution of root material collected for the different experiments (trypan blue staining, WGA and qPCR). It is possible that more fine lateral roots, which are not colonised by *R. irregularis* (Gutjahr et al., 2015), were inadvertently collected for RNA extraction and the qPCR experiments, and perhaps, more large lateral and crown roots for the other experiments. More experiments will help to clarify this discrepancy.

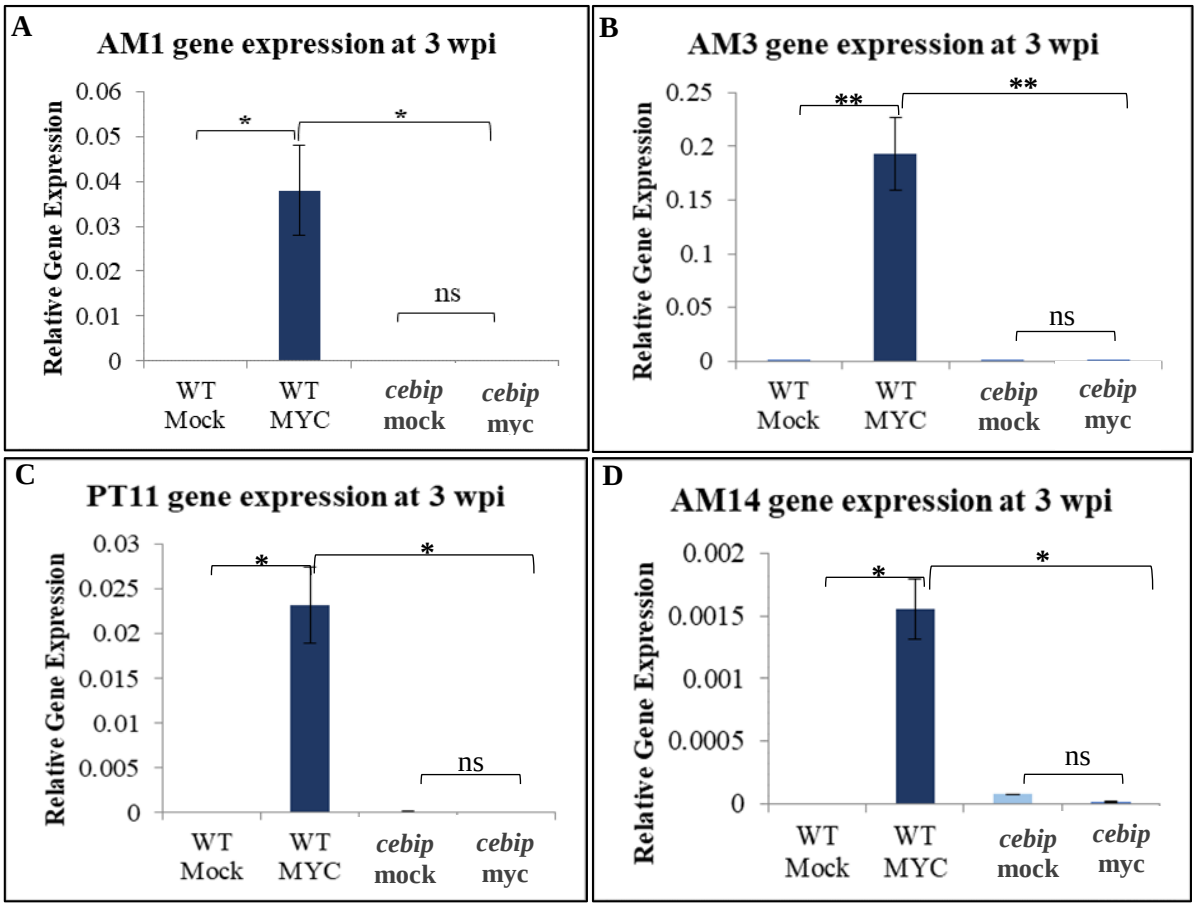

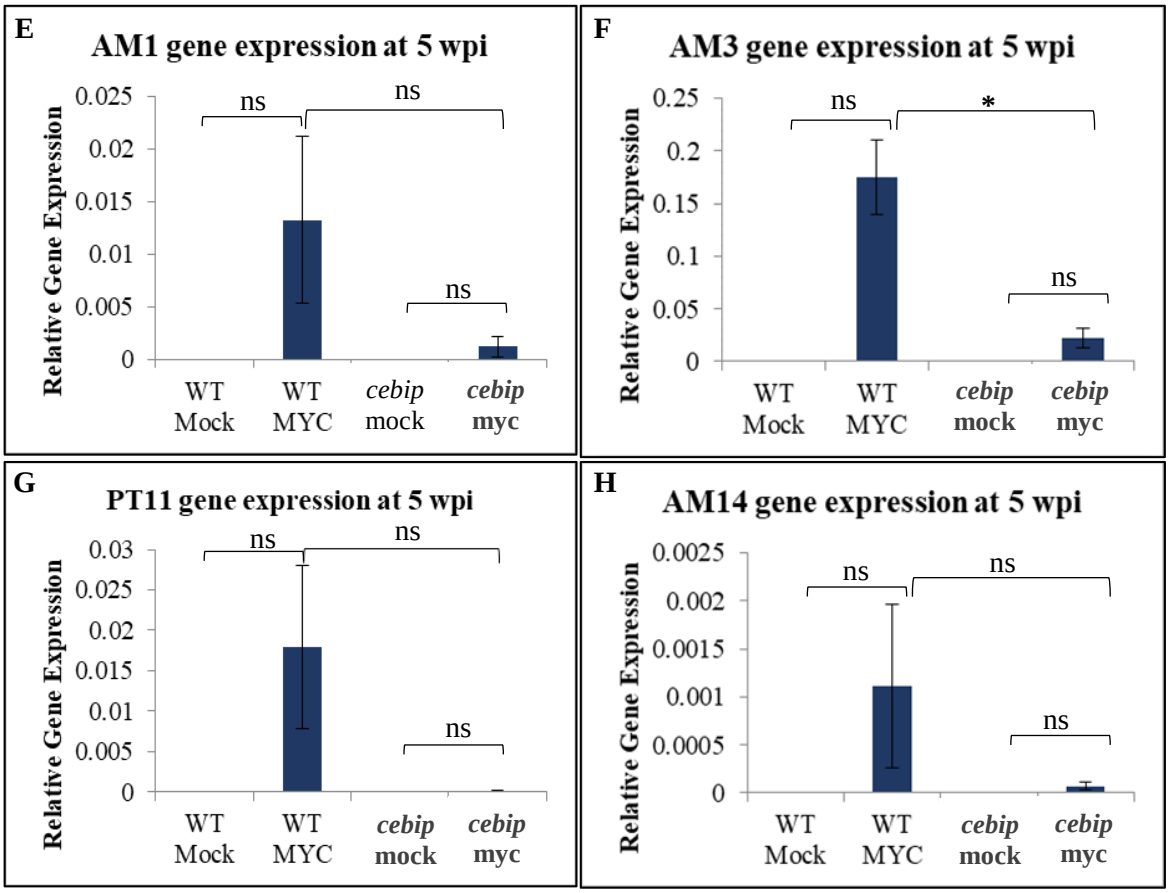

Figure 2.9: Molecular quantification of AM marker gene expression in *R. irregularis* colonised and non-colonised WT and *cebip* mutant roots. Expression levels of AM marker genes in colonised and non-colonised rice roots at 3 and 5 wpi, respectively are shown (**A-H**). Expression levels were measured by qRT-PCR and normalized to the geomean of three *O. sativa* housekeeping genes - *Cyclophilin, GAPDH* and *Ubiquitin* expression. Bars represent the means of three biological replicates (n = 1) ± SEM. Asterisks indicate significant differences between expression levels in colonised and non-colonised roots of different genotypes (e.g. WT colonised vs *cerk1* colonised) at two time points (*t*-test, *, $P < 0.05$; **, $P < 0.01$; ***, $P < 0.001$, n.s., $P \geq 0.05$).

2.3.1. OsCEBiP is required for rice root colonisation by *M. oryzae*

To investigate whether OsCEBiP is necessary for rice root colonisation by *M. oryzae*, WT and *cebip* mutant rice roots were inoculated with GFP-expressing *M. oryzae*. Root invasion was monitored in a time-course manner, early (4 dpi) and late (7 dpi) colonisation. Interestingly, live-cell confocal imaging revealed the presence of less fungus in *cebip* mutant roots than in the WT (Figure 2.10A-D). However, unlike in *cerk1* mutants, where fungal hyphal cell death was observed, the number of dead or trapped invasive fungal hyphae in *cebip* mutant roots was comparable to the WT (Table 2).

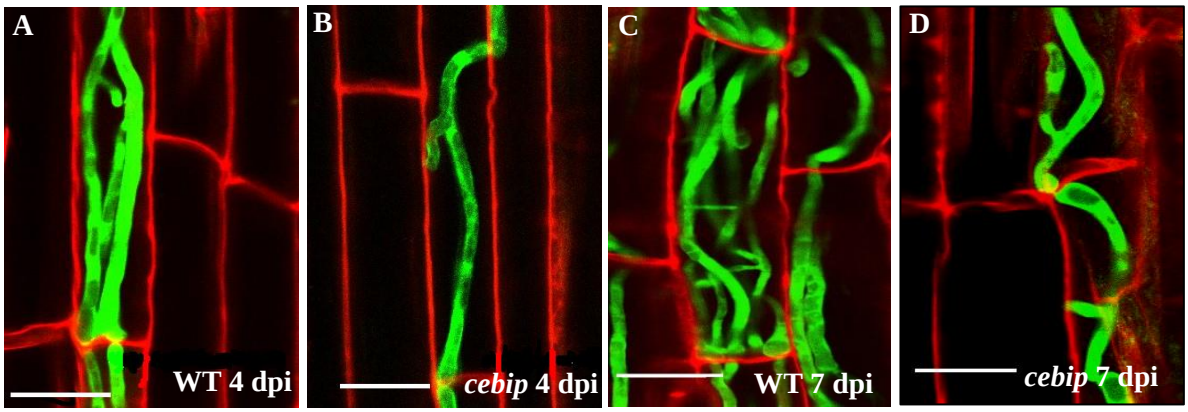

Figure 2.10: Intracellular colonisation of *M. oryzae* in WT and *cebip* mutant rice roots. Live-cell confocal imaging shows GFP-transformed *M. oryzae* (Guy11) proliferating inside WT (Nipponbare) and *cebip* mutant rice roots at 4 and 7 dpi, respectively (**A-D**). Less fungus is seen in *cebip* mutants (B, D) compared to the WT (A, C) at both time points, respectively. The plant cell wall was stained with Propidium iodide (red). Representative of 67 (WT) and 57 (*cebip*) images with 3 biological replicates per experiment in at least four experiments. Micrograph obtained using protocol described in Marcel et al., 2010. Scale bar = 50µm. Micrograph obtained using protocol described in Marcel et al. (2010).

Phenotypic quantification of *M. oryzae* hyphal death in WT and *cebip* rice roots		
Genotype	**WT**	***cebip***
Total number of images analysed	67	57
Number of dead and/or trapped fungal hyphae inside rice root cells	5	3
Estimated Average Total (%)	**5%**	**5.3%**

Table 2: Phenotypic quantification of *M. oryzae* in colonised rice roots. No difference in the number of dead or restricted invasive fungal hyphae in *M. oryzae* colonised WT and *cebip* mutant roots was found. Images were analysed from three biological replicates (root tips from three plants) *per* experiment in an average of four independent experiments.

Interestingly, molecular quantification by qRT-PCR confirmed the reduction of *M. oryzae* biomass by the consistently reduced transcript levels of the three housekeeping genes (*MoACTIN*, *Moβ-tubulin* and *Mo40s8* ribosomal RNA) in *cebip* mutants compared to the WT at 4 and 7 dpi, respectively (Figure 2.11). The significant overall reduction ($P < 0.05$) confirmed the microscopic results (Figure 2.10).

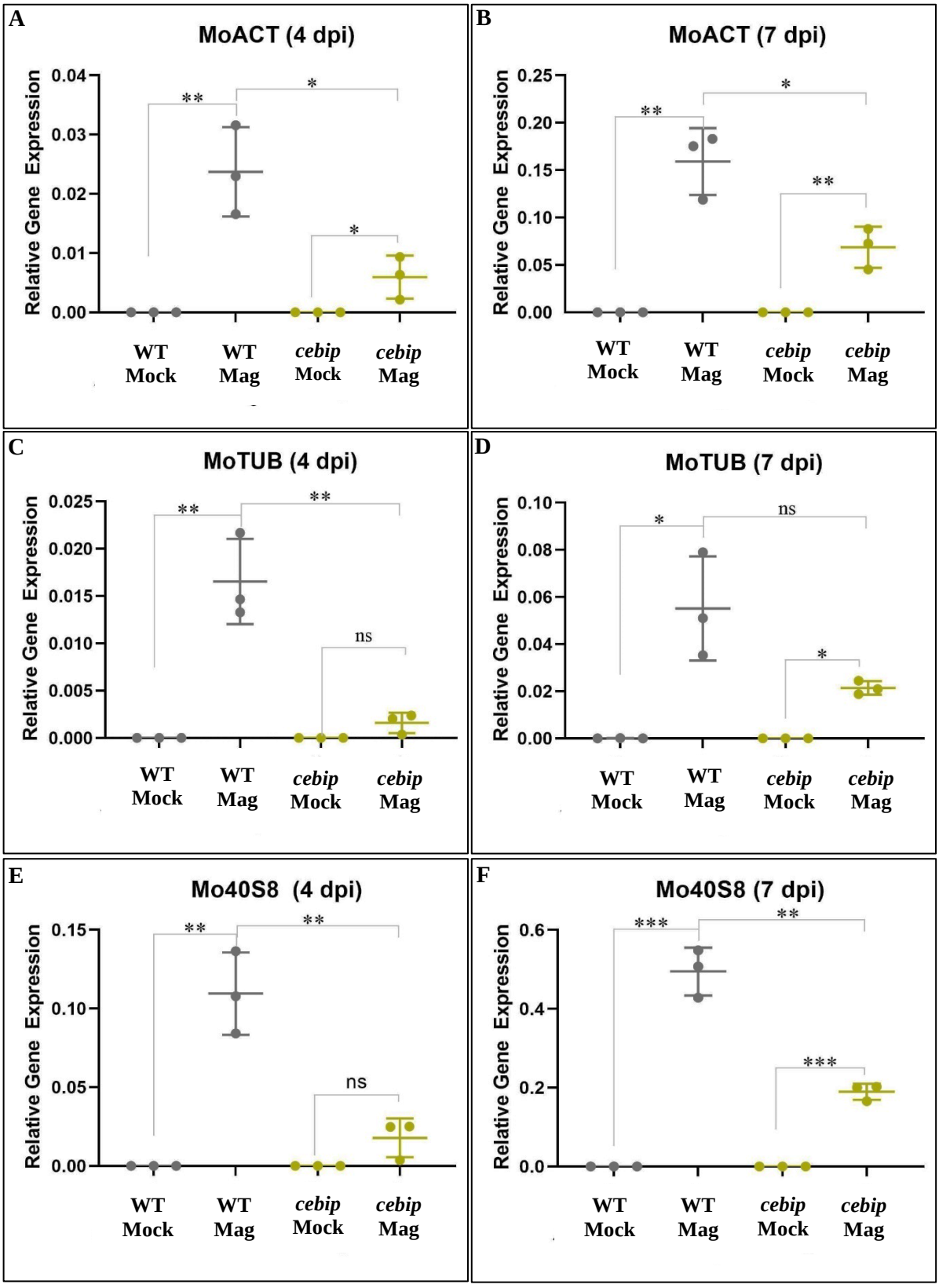
A
MoACT (4 dpi)
Relative Gene Expression
0.04
0.03
0.02
0.01
0.00
**
*
*
WT Mock
WT Mag
cebip Mock
cebip Mag
B
MoACT (7 dpi)
Relative Gene Expression
0.25
0.20
0.15
0.10
0.05
0.00
**
*
**
WT Mock
WT Mag
cebip Mock
cebip Mag
C
MoTUB (4 dpi)
Relative Gene Expression
0.025
0.020
0.015
0.010
0.005
0.000
**
**
ns
WT Mock
WT Mag
cebip Mock
cebip Mag
D
MoTUB (7 dpi)
Relative Gene Expression
0.10
0.08
0.06
0.04
0.02
0.00
*
ns
*
WT Mock
WT Mag
cebip Mock
cebip Mag
E
Mo40S8 (4 dpi)
Relative Gene Expression
0.15
0.10
0.05
0.00
**
**
ns
WT Mock
WT Mag
cebip Mock
cebip Mag
F
Mo40S8 (7 dpi)
Relative Gene Expression
0.6
0.4
0.2
0.0
***
**
***
WT Mock
WT Mag
cebip Mock
cebip Mag

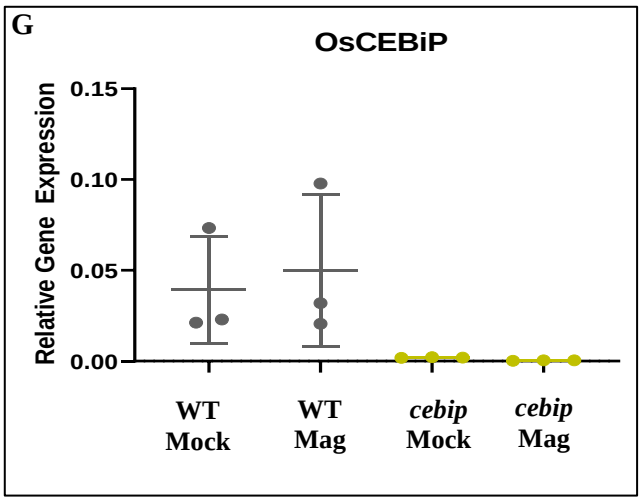

Figure 2.11: Quantifying the molecular biomass of *M. oryzae* in colonised and non-colonised WT and *cebip* mutant rice roots. The graphs represent the expression levels of three *M. oryzae* housekeeping genes (*MoACT, MoTUB,* and *Mo40S8* ribosomal protein) and OsCEBiP in colonised and non-colonised WT and *cebip* mutants at 4 and 7 dpi, respectively (**A-G**). Expression levels were measured by qRT-PCR and normalized to the geomean of three *O. sativa* housekeeping genes - *Cyclophilin, GAPDH* and *Ubiquitin* expression. Bars represent the means of three biological replicates (n = 1) ± SEM. Asterisks indicate significant differences between expression levels in colonised and non-colonised roots of the same and different genotypes (e.g. WT colonised vs WT non-colonised, *cerk1* colonised vs *cerk1* non-colonised, and WT vs *cerk1* colonised) at the corresponding time point (one-way ANOVA and *t*-test, *, $P < 0.05$; **, $P < 0.01$; ***, $P < 0.001$, n.s., $P > 0.05$).

2.4. A role of OsNFR5 for rice root cell invasion by *Magnaporthe oryzae*

NFR5 has been generally studied in the context of Nod-factor signal perception of legumes, where it cooperates with NFR1 to perceive and transduce signals leading to rhizobia symbiosis. However, unlike in rhizobia symbiosis, OsNFR5 is not required for AM symbiosis (Miyata et al., 2016). It has also been found that *L. japonicus* NFR1 and NFR5 do not participate in general long-chain chitin signalling as the expression of selected chitooligoaccharide-responsive genes was similarly induced in response to chitooctaose treatment in *L. japonicus* WT and *nfr1* and *nfr5* mutant plants (Zhang et al., 2007). Although LjNFR5 proteins seem to have evolved a specific function in Nod factor perception and signalling, the role of its homologue in rice, OsNFR5, during rice root invasion by *M. oryzae* has not been studied. To investigate this, WT (Nipponbare) and *nfr5* mutant rice roots were co-cultivated with *M. oryzae* conidia and cellular invasion was monitored after 4 and 7 dpi. Live-cell confocal imaging revealed interesting morphological phenotypes in the mutants, where the fungal hyphae appeared bulbous, deformed, and occasionally trapped inside rice cells (Figure 2.12B, C). The bulbous shape of the invasive fungal hyphae seen in the mutants did not resemble the normal bulge (arrow, Figure

2.12A, E) often found at cell wall junctions when the fungus constricts and crosses over to the neighbouring cells.

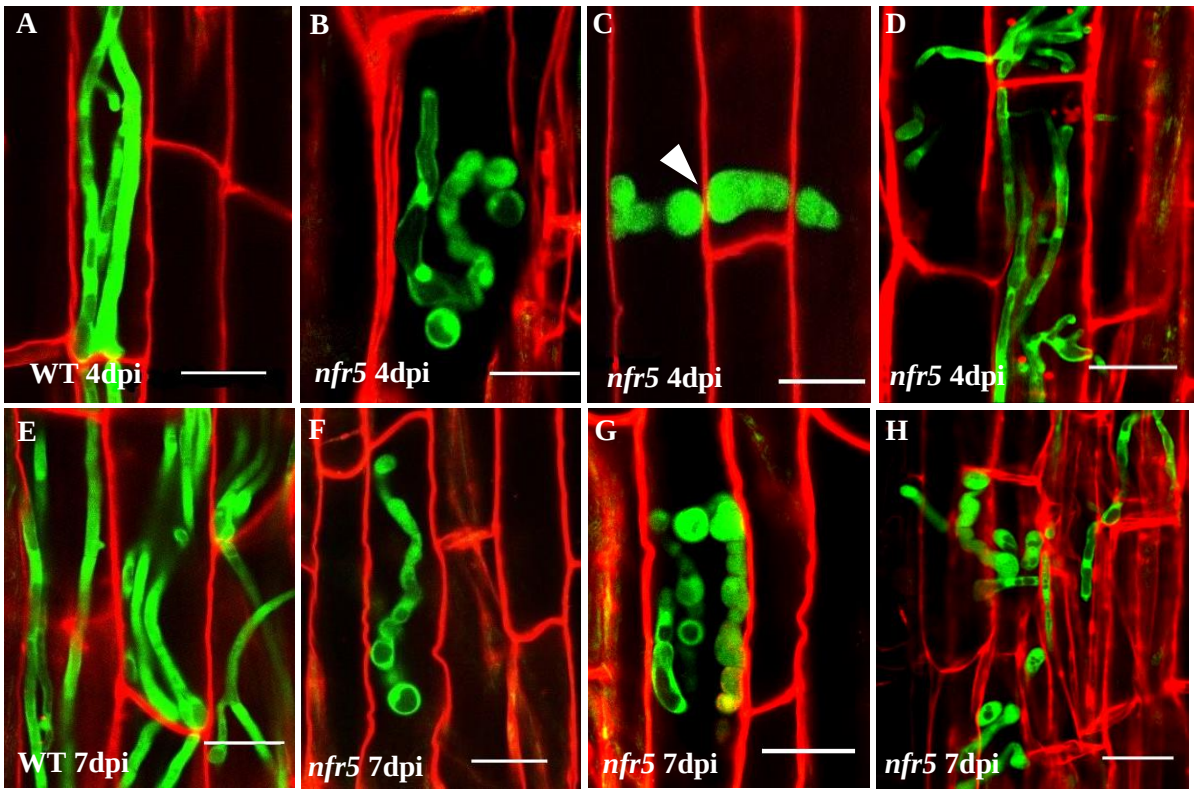

Figure 2.12: Live-cell confocal imaging of *M. oryzae* invading WT and *nfr5* mutant rice root cells. Normal fungal proliferation is seen in WT rice roots, with slight constriction and bulging of the hypha as it crosses the cell wall junctions at 4 and 7 dpi, respectively (**A, E**). In *nfr5* mutants, *M. oryzae* invasive hyphal morphology seems to be compromised as they appear bulbous, deformed and trapped inside root cells at both time points (**B, C, F, G**). Occasionally, fungal hyphae proliferate from cell to cell in the mutant, although they still appear bulbous in some parts (**D, H**). Propidium iodide (red) stain highlights the plant cell walls. Representative of 67 (WT) and 60 (*nfr5*) images with 3 biological replicates per experiment in at least four experiments. Micrograph obtained using protocol described in Marcel et al., 2010. Scale bar represents 50µm. Micrograph obtained using protocol described in Marcel et al. (2010).

Phenotypic quantification of *M. oryzae* hyphal death in WT and *nfr5* rice roots		
Genotype	**WT**	*nfr5*
Total number of images analysed	67	60
Number of dead and trapped fungal hyphae inside rice root cells	5	3
Estimated Average Total (%)	**5%**	**5%**

Table 3: Phenotypic quantification of *M. oryzae* invasive hyphae dead and trapped inside rice root cells. No difference in the number of dead invasive fungal hyphae is seen in *nfr5* mutants versus the WT. Images were analysed from three biological replicates (root tips from three plants) *per* experiment in an average of four independent experiments.

To determine whether *M. oryzae* rice root colonisation is reduced in *nfr5* mutants relative to the WT, molecular quantification experiments by qRT-PCR was performed. The level of fungal colonisation was significantly reduced ($P < 0.05$; $P < 0.01$) at both time-points (Figure 2.13A-F), suggesting that OsNFR5 may be required for *M. oryzae* colonisation of rice root cells.

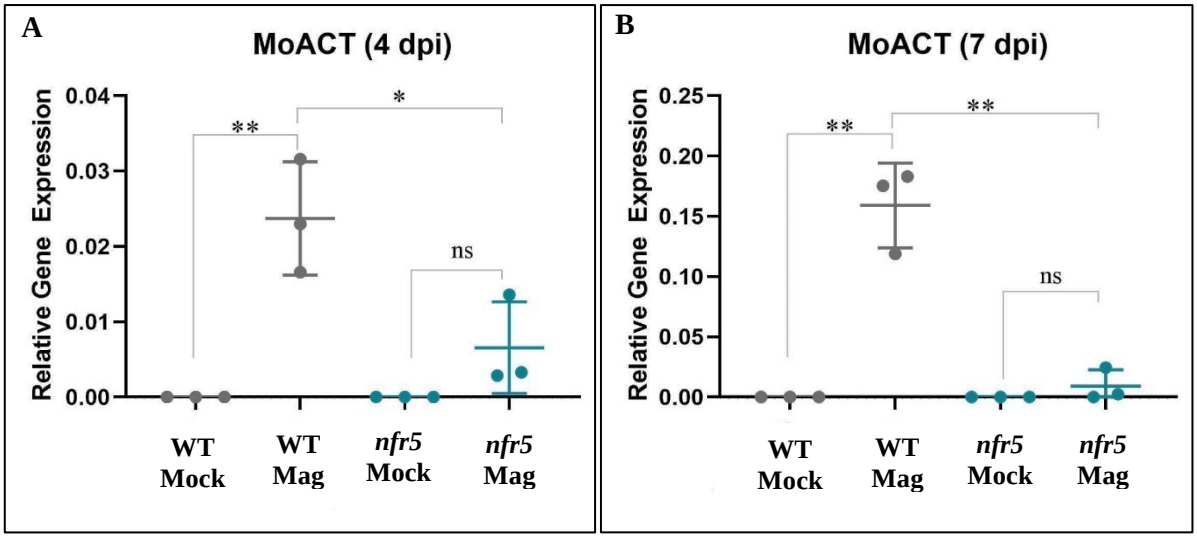

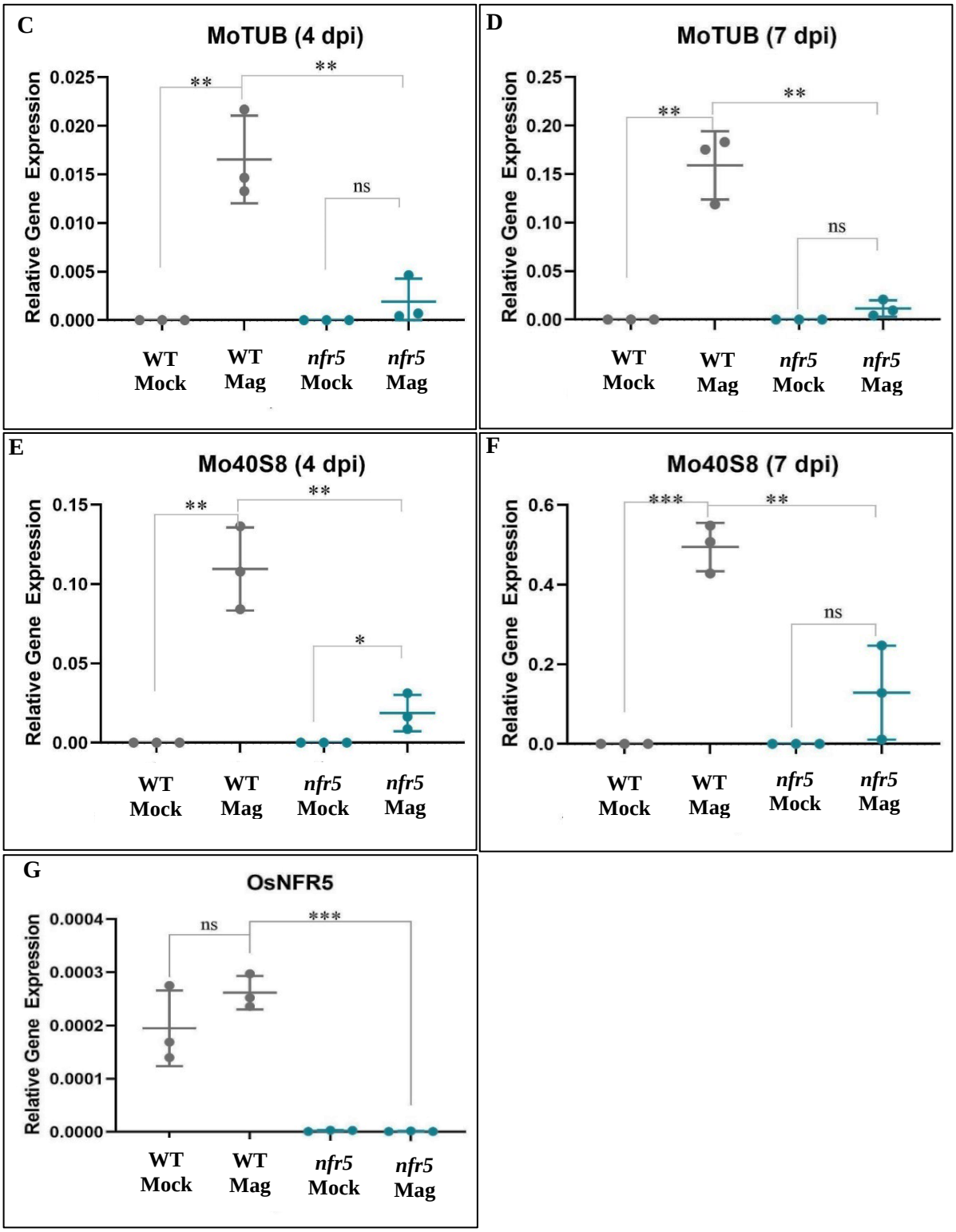

Figure 2.13: Quantification of *M. oryzae* molecular biomass in WT and *nfr5* mutant rice roots. Gene expression analysis revealed an overall reduction in *M. oryzae* colonisation in *nfr5* mutants compared to the WT at 4 and 7 dpi, respectively. The graphs represent the expression levels of three *M. oryzae* housekeeping genes (*MoACT*, *MoTUB*, and *Mo40S8* ribosomal protein) and OsNFR5 in colonised and non-colonised WT and *nfr5* mutants at both time points (**A-G**). Expression levels were measured by qRT-PCR and normalized to the geomean of three *O. sativa* housekeeping genes - *Cyclophilin*, *GAPDH* and *Ubiquitin* expression. Bars represent the means of three biological replicates (n = 1) ± SEM. Asterisks indicate significant differences between expression levels in colonised and non-colonised roots of the same and different genotypes (e.g. WT colonised vs WT non-colonised, *nfr5*

colonised vs *nfr5* non-colonised, and WT vs *nfr5* colonised) at the corresponding time point (one-way ANOVA and *t*-test, *, P < 0.05; **, P <0.01; ***, P < 0.001, n.s., P > 0.05).

2.5. A novel role of OsNFR5 during rice leaf infection by *M. oryzae*

Although the role of LjNFR5/OsNFR5 has been studied in the context of Rhizobia and AM symbioses, respectively, where it is required for the former (Rhizobia symbiosis) but not the latter (AM symbiosis), its involvement in immunity signalling has not been investigated. My findings from subchapter 2.4 indicate that OsNFR5 is required for rice root cell invasion by *M. oryzae*, which further motivated me to investigate rice leaf response to *M. oryzae* in the absence of OsNFR5. This involved inoculating WT and *nfr5* mutant rice leaf with *M. oryzae* Guy11 (WT) conidia in two types of experiments, 1) a time-course leaf sheath inoculation assay to monitor fungal invasion at early (26 hpi) and late (30 hpi) time points, and 2) a leaf spray infection assay to monitor disease necrosis at 6 dpi.

Microscopic monitoring of infected rice leaf sheath cells showed an early penetration of primary invasive fungal hyphae in the first leaf sheath cell at 26 hours post inoculation (hpi) (Figure 2.14A), but not in *nfr5* mutants, where hyphal penetration of the first leaf sheath cell was not seen. Instead, appressoria still attached to conidia *via* the germ tube were seen on the epidermal leaf sheath surface in the mutant (Figure 2.14C). With prolonged incubation, secondary invasive bulbous hyphae filled up individual WT leaf sheath cells at 30 hpi (Figure 2.14B), whereas primary invasive hyphae were just seen invading the first leaf sheath cell in *nfr5* mutants (Figure 2.14D), suggesting that *M. oryzae* penetration of epidermal leaf sheath cells was delayed in the absence of *OsNFR5*. Importantly, mutants of *OsCERK1* and *OsCEBiP* were used as positive controls in this experiment because of their established function in immunity signalling during *M. oryzae* rice leaf infection. As expected, increased susceptibility to *M. oryzae* in *cerk1* and *cebip* rice leaf sheath cells were seen, confirming the involvement of both RLK and RLP in immunity signalling.

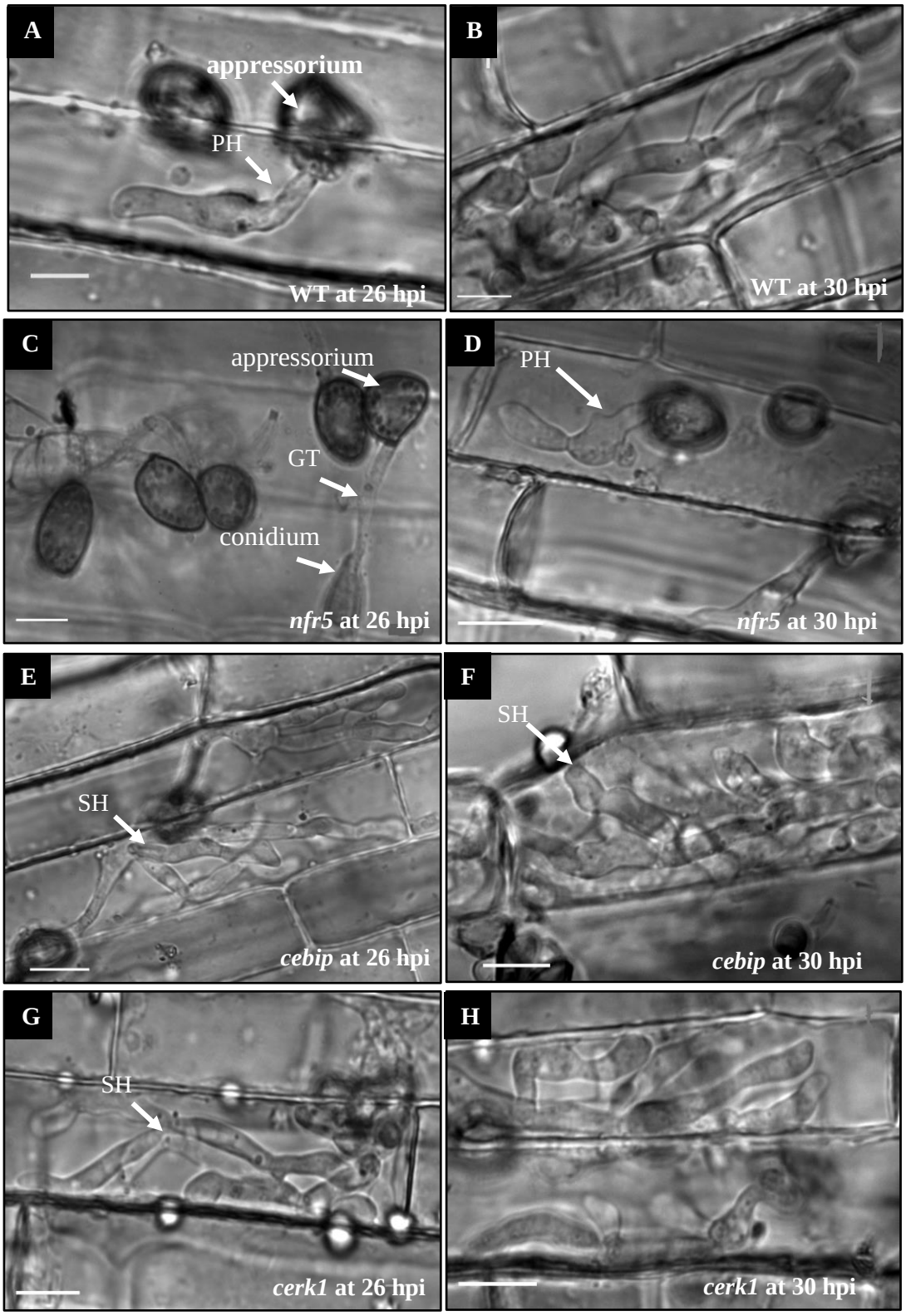

Figure 2.14: Microscopic images of *M. oryzae* (Guy11) infected rice leaf sheath cells. Primary invasive hypha (PH) invades the first cell in the WT at 26 hpi, but not in *nfr5* mutants, where conidia (C) still attached to appressoria (A) through the germ tube (GT) and no penetration are seen (**A, C**). Secondary invasive hyphae (SH) filled up individual WT leaf sheath cells at 30 hpi, but not in *nfr5* mutants, where the primary hypha had just invaded the first cell (**B, D)**. In both *cebip* and *cerk1*, a rapid progression in *M. oryzae* infection was seen at both time points (**E-H**). Representative of ~9 images per genotype (with three biological replicates per experiment) in two independent time-course experiments. Scale bar = 50µm.

To ascertain whether *M. oryzae* infection is delayed in the absence of *OsNFR5*, a rice leaf spray inoculation experiment was performed, and the average number of necrotic lesions was calculated after 6 dpi. On *nfr5* mutant leaves, significantly fewer and less expanded (area) necrotic disease lesions/5 cm had formed compared to both WT and *cerk1* mutant, which were used as positive controls in the experiment (Figure 2.15; Figure 2.16). Interestingly, a second independent experiment (not shown) confirmed the phenotypes observed in *nfr5*, as well as in *cerk1* and *cebip* mutants, together, suggesting that OsNFR5 promotes *M. oryzae* rice leaf infection. Notably, CO39 (a highly susceptible cultivar) was used as a positive control in one experiment to ensure that the experimental design was robust. All mutants (*nfr5*, *cerk1* and *cebip*) however, are in the Nipponbare genetic background.

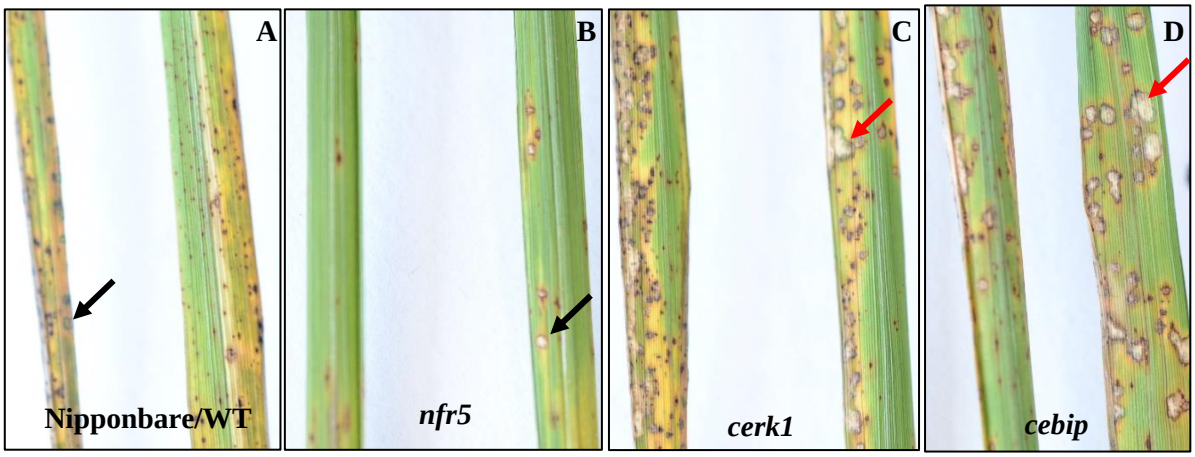

Figure 2.15: Necrotic disease lesion formation on *M. oryzae* inoculated rice leaves. Fewer necrotic disease lesions are seen on *nfr5* mutant leaves (**B**) compared to the WT (**A**). *cerk1* and *cebip* mutants (**C-D**) showed the highest number of expanded necrotic disease lesions (red arrow), confirming increased susceptibility of the host plant to *M. oryzae* in the absence of CERK1 and CEBiP. Leaf samples are from three plants per genotype per experiment (in two independent experiments).

Table 8	**WT (CO39)**	**WT (Nipponbare)**	***cerk1***	***nfr5***
Number of Leaf Samples	11	17	14	15
Number of Lesions/5 cm	513	379	554	209
Average Number of Lesions	**47**	**22**	**40**	**14**

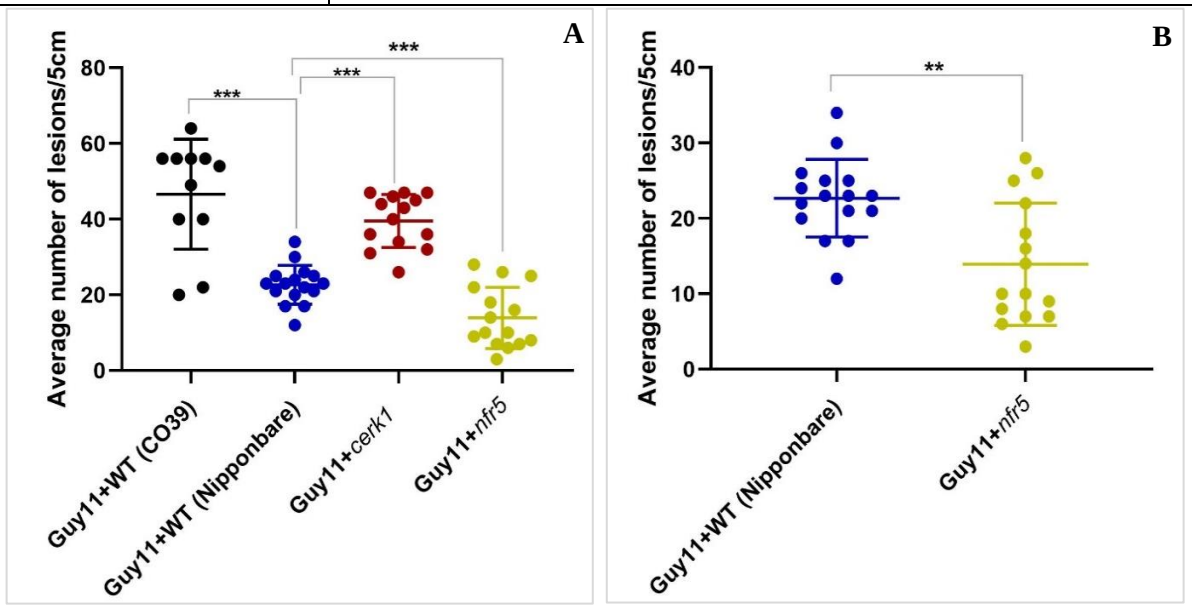

Figure 2.16: Quantification of necrotic disease lesion formation in WT and LysM-RLK mutant rice leaf. The table shows the average number of lesions/5 cm of leaf sample in four gentoypes (Nipponbare, CO39, *cerk1* and *nfr5*. As a highly suceptible rice cultivar, CO39 showed the highest average number of lesions (47) followed by *cerk1* (40), Nipponbare (22) and *nfr5* mutants (14), which had significantly fewer number of necrotic lesions compared to the other genotypes (**A-B**). Dots represent the number of disease lesions/5 cm formed on the leaf surface of each tested genotype. Asterisks indicate significant differences in the average number of lesions/5 cm of infected leaves among different genotypes. (ANOVA and *t*-test, *, $P < 0.05$; **, $P < 0.01$; ***, $P < 0.001$, n.s., $P > 0.05$). Two independent experiments (with three plants per genotype) were performed.

2.6. Discussion

The efforts described in this chapter addressed the role of plant membrane receptors known for leaf immunity and root nodule signalling during AM symbiosis, as well as rice root infection by *M. oryzae*. Plant membrane receptors. such as the LysM receptor-like kinases (CERK1 and NFR5) and receptor-like proteins (CEBiP) have been generally well-studied in the context of endosymbiosis and immunity, but not for rice root colonisation by *M. oryzae*. In this study, an

important new role was found for CERK1, NFR5 and CEBiP during rice root colonisation by *M. oryzae* and for NFR5 during rice leaf infection by *M. oryzae*.

CERK1 has been shown to be indispensable for inducing early symbiotic signalling responses during AM symbiosis, especially since AM colonisation was severely reduced in *cerk1* knockout (Miyata et al., 2014) and RNAi (Zhang et al., 2015) mutant rice roots at early, but not the later stages of infection. This is also well known in legumes, where *L. japonicus* NFR1 (the closest homologue of OsCERK1) interacts with LjNFR5 to perceive and transduce signals that lead to nodulation and rhizobia symbiosis (Madsen et al., 2003; Radutoiu et al., 2003).

Consistent with these findings, my results revealed severe phenotypes including clusters of hyphopodia (still with attached extra-radical hyphae), low levels of mycorrhization and reduced expression of AM marker genes in *cerk1* mutant roots at early colonisation (3 wpi) with *R. irregularis* (Figure 2.1C). With prolonged co-cultivation however, the total level of fungal colonisation in both *cerk1* and WT roots were not significantly different, although clusters of hyphopodia were still seen in the mutant at 5 wpi (Figure 2.1E). These results confirm that OsCERK1 is a key requirement for early AM symbiosis signalling and supports previous findings.

In contrast to CERK1, studies have suggested that OsCEBiP does not participate in AM symbiosis as *cebip* mutants inoculated with *R. irregularis* established symbiosis normally (Miyata et al., 2014). This is inconsistent with my observations, which showed severe phenotypes including clusters of hyphopodia (with attached extra-radical hyphae) (Figure 2.6), extremely low levels of colonisation (Figure 2.7), and significantly reduced levels of AM marker gene expression in *cebip* mutant roots inoculated with *R. irregularis* at 3 wpi (Figure 2.9). Importantly, the observed hyphopodia phenotype in *cebip* mutants (Figure 2.6B) closely resembles those seen in *cerk1* mutants (Figure 2.1B) during early colonisation, whereby the fungus successfully forms a hyphopodium on the rice root surface but is unable to penetrate the epidermal cell layer. In both mutants (*cebip* and *cerk1*), extra-radical hyphae are mostly still attached to the fungus, and if penetration of the epidermal layer eventually occurs, intra-radical hyphal proliferation appears to be restricted within the epidermal cell, especially at early colonisation (Figure 2.6B).

Consistent with the difficulty to penetrate the rice root surface after hyphopodia formation, total AM fungal root length colonisation was significantly reduced ($P<0.001$) in *cebip* mutants

relative to the WT at both 3 and 5 wpi (Figure 2.7A, 2.7B). Molecular quantification experiments also revealed a significant reduction in AM marker gene expression in *cebip* mutants at 3 wpi (Figure 2.9A-D) but not at 5 wpi, except for *AM3*, which was significantly reduced at this later time point. This inconsistency between the fungal colonisation data and AM marker gene expression levels at 5 wpi may be due unequal distribution of all rice root samples (crown, large lateral and fine lateral roots) during the different experiments, as well as variations in the values of the biological replicates as indicated by the error bars (Figure 2.9E, 2.9G, 2.9H). The uneven distribution of AM colonisation within rice root systems has been demonstrated. Crown roots (CRs) are weakly colonised; large lateral roots (LLRs) are strongly colonised; and fine lateral roots (FLRs) are not colonised (Gutjahr and Paszkowski, 2013; Gutjahr et al., 2009; Rebouillat et al., 2009). This differential colonisation indicates that reciprocal root-fungal signalling events prior to, or during colonisation, and plant physiological changes in response to colonisation are root-type specific (Gutjahr and Paszkowski, 2009).

In addition, morphological characterization of internal fungal colonisation structures by WGA staining revealed a possible slight reduction in hyphal branching in *cebip* mutants compared to the wild-type, although this requires further investigation. Considering the observed phenotypes, which are more prominent during early colonisation (3 wpi), it may be logical to suggest that OsCEBiP is also required for early induction of symbiotic signalling, especially since OsCEBiP is structurally known to directly bind chitin oligosaccharides prior to forming complexes with OsCERK1 during immunity signalling (Kaku et al., 2006; Shinya et al., 2012; Kouzai et al., 2014).

With respect to rice root colonisation by *M. oryzae*, my observations suggest that all three LysM-RLKs (*OsCERK1* and *OsNFR5*) and RLP (*OsCEBiP*) may be required for efficient intracellular proliferation of the pathogen in rice roots. *cerk1* mutant roots inoculated with GFP-expression *M. oryzae* conidia revealed striking phenotypes, including 31% of fungal invasive hyphae which appeared dead and trapped inside rice root cells at 4 and 7 dpi, respectively (Figure 2.4B, 2.4F, 2.4H). The morphology of *M. oryzae* invasive hyphae in *nfr5* mutant rice roots also looked abnormal, in that, they were mostly bulbous, ring-shaped and trapped inside, with swellings in places where they occasionally crossed cell junctions (Figure 2.12). Interestingly, no fungal morphological aberration was seen in *cebip* mutant roots, and unlike *cerk1* mutants, the number of dead fungal hyphae in both *cebip* and *nfr5* mutants was infinitesimally low and not different from the WT (Table 2 and 3). Gene expression analysis revealed a drastic overall reduction in the molecular biomass of *M. oryzae* in all three mutants

(*cerk1*, *cebip* and *nfr5*) at both early and late colonisation stages (Figure 2.5, 2.11, 2.13), strongly implicating the LysM-RLKs and RLP as compatibility factors for *M. oryzae* rice root colonisation.

Although the role of the receptor kinase OsNFR5 during AM symbiosis was not re-tested under my experimental conditions due to lack of time, published findings show that OsNFR5 does not participate in AM symbiotic signalling responses (Miyata et al., 2016). The role of OsNFR5 during rice leaf infection by *M. oryzae* had also not been previously studied. Interestingly, both rice leaf sheath and leaf spray infection assays showed a distinctive suppression of *M. oryzae* invasion in *nfr5* mutant leaf tissue. As expected at the early infection stage (26 hpi), primary fungal hypha invaded the first cell in the WT epidermal leaf sheath (Figure 2.14A), but not in *nfr5* mutants, where appressoria connected to conidia were seen on the leaf sheath epidermal surface, with no sign of penetration (Figure 2.14C). At the later stage of infection (30 hpi), bulbous, branched hyphae filled up individual WT leaf sheath cells (Figure 2.14B), only then was the primary hypha seen invading the first cell in *nfr5* mutants (Figure 2.14D), suggesting a delay in fungal penetration. These data are supported by the rice leaf spray infection assay, which revealed the presence of significantly less average number of disease lesions (per 5 cm) on *nfr5* mutant leaves compared to the WT (Figure 2.15) or *cerk1* and *cebip* (Figure 2.14E-H), which were highly susceptible to the pathogen during rice leaf infection. Interestingly, these results demonstrate a role of OsNFR5 as a compatibility factor for *M. oryzae* penetration and invasion of rice leaf tissue.

Altogether, the results presented in this chapter provide clear evidence that common requirements exist for mutualistic and detrimental fungi in rice roots. A novel role of OsCERK1 during rice root intracellular colonisation by *M. oryzae* was discovered and the dual responsibility of OsCERK1 in AM symbiosis and immunity signalling was confirmed. The similar range of phenotypes observed in *M. oryzae* and *R. irregularis* colonised *cerk1* mutant rice roots was quite intriguing. For instance, in *R. irregularis* colonised *cerk1* mutants, rice root surface penetration was mostly hindered as evidenced by clusters of hyphopodia and fungal colonisation was significantly reduced at 3 wpi. Similarly, dead and restricted invasive *M. oryzae* hyphae were seen in *cerk1* rice root cells, followed by a drastic overall reduction in fungal colonisation at early and late infection stages. With respect to rice leaf infection, *M. oryzae* inoculated *cerk1* mutants resulted in a significant increase in disease susceptibility, all together, suggesting that CERK1 represents a common receptor for chitooligosaccharide-based signals produced by mycorrhizal fungi and other beneficial and harmful microbes.

Furthermore, this study confirmed the role of OsCEBiP in immunity signalling in the leaf and led to unexpected new findings implicating OsCEBiP function in rice root colonisation by *M. oryzae* and *R. irregularis*. In common with *cerk1* mutant roots, *cebip* mutants inoculated with *R. irregularis* showed clusters of hyphopodia on the rice root surface, signifying root penetration difficulties, which reflected in the extremely low mycorrhization levels shown by qRT-PCR at 3 wpi. In contrast to *cerk1* mutants though, *M. oryzae* colonised *cebip* rice roots did not reveal any distinct dead or restricted invasive proliferating fungal hyphae, although significantly less fungus was molecularly measured in the mutant. These results suggest that OsCEBiP may be involved in early symbiotic signalling, as well as for compatibility during rice root invasion by *M. oryzae*.

Although my findings with CEBiP and arbuscular mycorrhization contradict existing reports (Miyata et al., 2014), the phenotypic observations, which resemble AM phenotypes in *cerk1* mutants, strongly suggests that OsCEBiP probably perceives and directs chitin signalling during early AM symbiosis. Studies have suggested that OsCEBiP binds longer chain chitin-oligosaccharides such as heptamers or octamers, which are not necessary for AM symbiosis (Miyata et al., 2014), however, it is possible that OsCEBiP forms a complex with OsCERK1 or other plasma membrane receptors to perceive a mixture of symbiotic signals including Myc-LCOs, which are longer chain chitin molecules, to activate the CSSP. This is supported by the lack of intracellular domains, which strongly suggests that OsCEBiP requires partner proteins to form a functional receptor complex for successful signal transduction as shown in immunity signalling, where it partners with OsCERK1. OsCERK1, on the other hand, lacks the ability to bind chitin oligosaccharides although it possesses an active intracellular kinase domain and can transduce symbiotic or immunity signals, suggesting the possibility of an OsCERK1-OsCEBiP complex formation in AM symbiosis. This model also applies in the case of *M. oryzae* rice root invasion, where all three LysM-RLKs/RLP are shown to be required for efficient invasion and intracellular accommodation. Several possibilities could be that OsCERK1 and OsCEBiP form a complex with each other or individually with other unknown partners to perceive and transduce signals leading to rice root colonisation by *M. oryzae*. OsNFR5 is an unlikely candidate in this case because it has an inactive intracellular kinase domain and is unable to interact with OsCEBiP. Heterodimerization with OsCERK1 is also unlikely as BiFC (Bimolecular Fluorescence Complementation) assays, which is used to visualise protein interactions in living cells, failed to show any evidence of interaction (Miyata et al., 2016). This

means that OsNFR5 requires another partner protein to recognize chitooligosaccharide-based signals during *M. oryzae* rice root invasion.

As with LjNFR5, which has a high affinity for binding Nod-LCOs but requires LjNFR1 to transduce the signal for nodulation and rhizobia symbiosis, OsNFR5 (LjNFR5 homologue) may also perceive signals that are similar to Nod-LCOs from *M. oryzae* but it must partner with another receptor protein to activate downstream signalling responses that would permit fungal accommodation in the root. This aligns well with findings that OsNFR5 may also be required for compatibility rather than immunity signalling during rice leaf infection by *M. oryzae*. Unlike OsCERK1 and OsCEBiP, which play opposite roles in immunity and compatibility depending on the different plant organs (immunity in leaf infection and compatibility in root infection). OsNFR5 acts as a compatibility factor in both scenarios, suggesting its role in the perception of specific signals from *M. oryzae*. These findings altogether, provide deep insight into the shared roles of LysM-RLKs and RLP during AM symbiosis and *M. oryzae* invasion of rice root and leaf tissue. It also describes a unique organ-specific function of plasma membrane receptors, which may be further explored for the development of new crop improvement and disease control strategies.

CHAPTER 3

Overlapping Transcriptome Signatures in Response to *R. irregularis* and *M. oryzae* Rice Root Colonisation

3.1. Introduction

Plant cells host a variety of mutualistic and detrimental microbes by forming intracellular accommodation structures, which appear similar at the cellular level. It is well-established that the arbuscular mycorrhizal fungi engage in symbiosis with more than 70% of all existing higher plants (Wang and Qiu, 2006). The symbiont provides mineral nutrients such as phosphorus to its host plant, and in return, receives from the plant, carbohydrate obtained through photosynthesis. Plant carbohydrates are also known to be very attractive to root-infecting filamentous pathogens such as fungi and oomycetes.

Although mutualistic fungi and pathogens (including oomycete pathogens such as *Phytophthora palmivora* and *Hyaloperonospora arabidopsidis*, downy mildew) are far apart in the end process of their interaction with plant (in that one supports plant growth and development while the other leads to disease) their root colonisation mechanisms can be very similar. This similarity is mostly seen at the initial stages of plant infection whereby both mutualistic and detrimental microbes use common strategies such as spore adhesion, appressorium formation and penetration to enter the plant host tissue (for review, see Panstruga, 2003). The fungal symbiont forms a pre-penetration apparatus, which guides the fungal invasion through the cell lumen, a process that occurs similarly in the root epidermal or the inner cortical cells, preceding arbuscule formation (Genre et al., 2005; Genre et al., 2008). Arbuscules are surrounded by a plant-derived peri-arbuscular membrane (PAM), which provides a unique interface for mineral nutrient exchange in the symbiosis.

Similarly, oomycete pathogens project specialized hyphae known as haustoria inside living host cells, which they use to suppress the plant host defence, as well as to acquire nutrients (O'Connell and Panstruga, 2006). As the oomycete pathogen grows inside the host cell, the haustorium becomes enveloped by a plant-derived extrahaustorial membrane (EHM), which serves as a physical barrier to separate the pathogen from the host cell cytoplasm and engulfs the extrahaustorial matrix in between (Lu et al., 2012). This feature is also peculiar to the *M.*

oryzae invasive hypha, which is surrounded by a plant-derived extra-invasive hyphal membrane (EIHM) during intracellular growth in rice roots (Marcel et al., 2010).

Interestingly, the process of accommodating microbe infection structures, whether symbiotic or pathogenic, involves a substantial developmental reprogramming or reorganization of the host plant cell. The striking similarities between mutualistic and detrimental microbe accommodation structures inside the host cell have also led to speculations that both associations depend on similar or overlapping genetic programmes (Parniske, 2000). To this end, shared genetic elements such as the *Nod Factor Perception, NFP* (Rey et al., 2013), *Reduced Arbuscular Mycorrhization 2, RAM2* (Wang et al., 2012; Gobbato et al., 2013) and the *Chitin Elicitor Receptor Kinase 1, CERK1* (Miyata et al., 2014; Zhang et al., 2015) have been found to function during beneficial and pathogenic plant-microbe interactions. In addition, a common set of genes have been associated with rice root colonisation by the symbiont *R. irregularis* and the pathogens, *Fusarium monoliforme* and *M. oryzae*, indicating a conserved response to fungal colonisation but the roles of the genes for compatibility remain unknown (Guimil et al., 2005).

The aim of this chapter was to identify a common set of genes that are co-upregulated during rice root colonisation by *R. irregularis* and *M. oryzae*. In contrast to the study of Guimil et al. (2005), which utilized a qPCR-based analysis to examine the differential expression of 224 mycorrhiza-inducible genes (identified by whole-transcriptome analysis) in root-pathogen interactions, this work involved the comparison of whole genome transcriptomics data from rice roots during interaction with *R. irregularis* (Gutjahr et al., 2015) and progressive root infection by *M. oryzae* (Marcel et al., 2010). It identified a set of commonly regulated genes that may be involved in determining compatibility and enabling accommodation of symbiotic and detrimental fungi in rice roots. By applying a variety of phenotypic and molecular analyses, it is hoped that this study will provide new insight into the function of the selected genes during rice root colonisation by both symbiotic and pathogenic fungi.

3.2. Results

3.2.1. Identification of genes commonly induced during rice root intracellular accommodation by *R. irregularis* and *M. oryzae*

To identify genes that are co-upregulated during rice root colonisation by *R. irregularis* and *M. oryzae*, two independent transcriptomics studies by Gutjahr et al. (2015) and Marcel et al. (2010) were compared.

3.2.2. Transcriptome comparison

Gutjahr et al. (2015) identified a total of 1,179 transcripts that accumulated differentially in the crown roots (CR) and large lateral roots (LLR) at 7 weeks post inoculation (wpi) with and without (mock-inoculated) *R. irregularis*, whereas Marcel et al. (2010) revealed 2,000 genes that are differentially expressed in all root types (infected *versus* non-infected/mock inoculated) with *M. oryzae* at 6 days post inoculation (dpi). Notably, 7 wpi and 6 dpi were considered for this analysis because both microbes intracellularly colonise rice roots at this stage. Specifically, *R. irregularis* grows both inter- and intracellularly inside the host root, with enriched numbers of arbusculated cortical cells, whereas *M. oryzae* grows intracellularly across all root types.

The first step was to overlay these two datasets using MS-Excel software to identify a common set of 498 differentially expressed genes (False Discovery Rate, FDR < 0.05) between both plant-fungal interactions (Figure 3.1). To ensure the selection of a robust dataset, stringent filtering conditions were applied to identify genes with moderate to high expression levels and with distinct changes in transcript level. Specifically, background expression was set at 50, which is equivalent to the mean values of the negative controls plus four times the standard deviation (as *per* Guimil et al., 2005).

Importantly, genes were considered as upregulated by mycorrhizal or *M. oryzae* colonisation if they showed a ≥ 2-fold change in expression level in colonised versus non-colonised/mock-inoculated plants at 7 wpi and 6 dpi, respectively. A total of 116 and 226 genes in mycorrhizal and *M. oryzae* inoculated rice roots, respectively, met this criterion (Figure 3.1). From the upregulated genes, a common set of 78 that were co-upregulated in both interactions were selected. Although 48 out of these 78 genes were still upregulated, they were unsuitable because of their high basal expression level (> 50 as explained above) and were therefore, filtered out.

Our interest in genes with low transcript levels in mock plants was driven by our initial plans to produce reporter lines where background expression would have interfered. The removal of 48 genes with high transcript levels in mock plants resulted in a total of 30 co-upregulated genes in both mycorrhizal and *M. oryzae* rice root interactions.

Since the goal of this data comparison exercise was to identify genes that are significantly co-upregulated during rice root invasion by both mutualistic and detrimental fungi, only genes with ≥ 2.5-fold change increase were selected. This resulted in a common set of 8 co-upregulated gene candidates, including an Exo70 exocyst protein, a lectin receptor-like kinase and a group of DUF538 domain containing protein of unknown function (Table 4). Three gene types were selected for further investigation based on the known roles of their homologues and orthologues in symbiosis (e.g. *MtExo70*) and immunity (e.g. *LecRLK*). In general, little is known about the third selected gene type, i.e. encoding DUF538 domain containing proteins of unknown function and they have not been studied in the context of either symbiosis or immunity. However, this analysis identified 4 out of 11 *DUF538* genes expressed in rice as co-upregulated during rice root interactions with *R. irregularis* and *M. oryzae*, making the superfamily of genes an attractive candidate for further analysis.

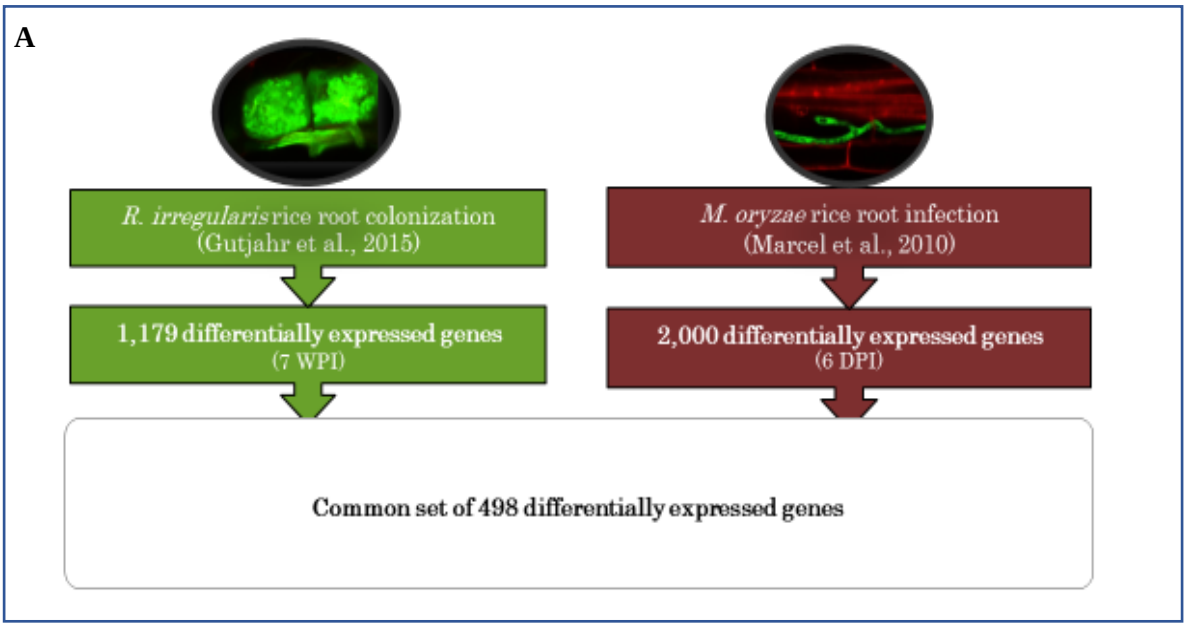

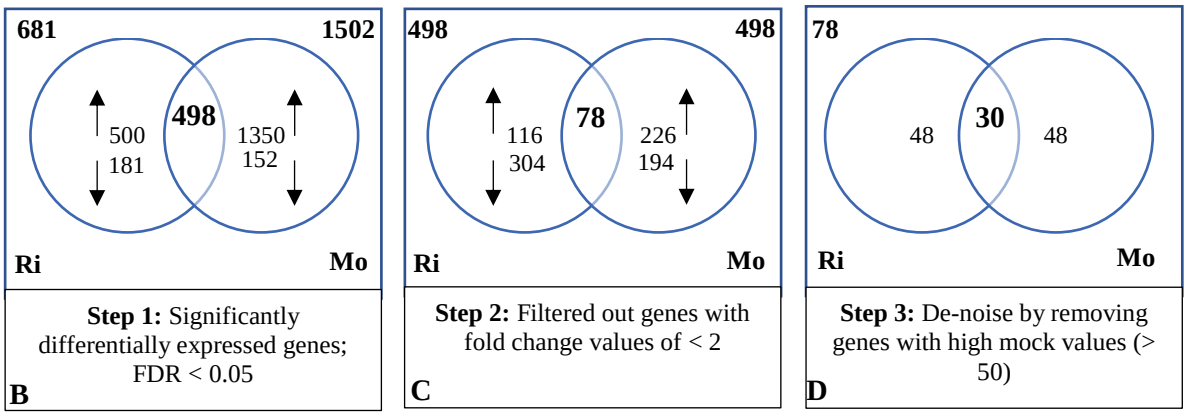

Figure 3.1: A flowchart showing the selection of co-upregulated genes during *R. irregularis* and *M. oryzae* rice root interactions. Transcriptional profiling of genes expressed during *R. irregularis* and *M. oryzae* intracellular colonisation of rice roots (**A**). Gutjahr et al. (2015) identified 1,179 differentially expressed genes in CR and LLRs at 7 wpi with and without *R. irregularis* (green) and Marcel et al. (2010) identified 2,000 genes differentially expressed at 6 dpi of rice roots with and without *M. oryzae* (red). Computational analysis revealed a common set of 498 differentially expressed genes in both interactions from which 116 and 226 were upregulated in *R. irregularis* and *M. oryzae*, respectively (**B**). Following a stringent filtering criterion, genes with Fold Change, FC < 2 were filtered out, leaving a total common set of 78 genes (**C**). Genes with high basal expression level (> 50) were removed (**D**) leading to the selection of top nine genes that are significantly upregulated in both interactions (Table below).

Gene Locus ID (LOC)	Description	Expression (Ri; CR+LLR; 7 wpi)	Expression (Mock; CR+LLR; 7 wpi)	FC (Ri/Mock)	Expression (+ Mag; 6 dpi)	Expression (Mock; 6 dpi)	FC (Mag/Mock)
Os11g38240	DUF538 domain containing protein, putative, expressed	602	18	**33**	104	12	**9**
Os07g02920	DUF538 domain containing protein, putative, expressed	583	18	**32**	342	24	**14**
Os11g38210	DUF538 domain containing protein, putative, expressed	284	13	**22**	186	11	**17**
Os07g02880	DUF538 domain containing protein, putative, expressed	888	49	**18**	381	48	**8**

Os02g12230	hypothetical protein	77	14	**6**	141	22	**6**
Os02g11880	conserved hypothetical protein	278	35	**8**	106	21	**5**
Os07g38800	lectin-like receptor kinase, putative, expressed	240	39	**6**	349	40	**9**
Os11g01050	exo70 exocyst complex subunit domain containing protein, expressed	234	45	**5.2**	95	25	**3.8**

Table 4: Top gene candidates co-upregulated during rice root infection with *R. irregularis* and *M. oryzae*. Genes were selected based on the fold change (FC) expression values (antilog) of *R. irregularis* (Ri) and *M. oryzae* (Mag) inoculated versus non-inoculated samples. Ri inoculated and inoculated rice root types (CR and LLR) were compared at 7 wpi, whereas Mag inoculated and non-inoculated rice roots (all types) were compared at 6 dpi. Genes strongly induced during Ri and Mag colonisation were selected based on the ratio of their FC (≥ 2.5) expression in inoculated versus mock samples. Seven out of the 8 genes are hypothetical proteins and DUF538 domain containing proteins of unknown function, whereas two genes, *OsExo70-H3b (LOC_Os11g01050)* and *OsLecRLK (LOC_Os07g38800)* have been relatively well studied in rice plants.

3.3. Characterization of *OsExo70-H3b* exocyst protein

3.3.1. Phylogenetic characterization of the plant Exo70 exocyst gene superfamily

Studies estimate that there are about 43 Exo70 exocysts in *O. sativa* compared to 23 in *Arabidopsis thaliana* (Synek et al., 2006; Cvrčková et al., 2012). To identify the position of OsExo70-H3b, a phylogenetic tree was generated using the amino acid sequences of 23 rice Exo70 exocysts available in the rice genome annotation database. The failure to identify 43 rice Exo70 exocysts as indicated by Synek et al. (2006) may be due to annotation errors on the different databases, where multiple exo70 exocysts are given the same accession and locus identification numbers. Nonetheless, the phylogenetic characterization identified nine OsExo70 exocyst subgroups (Exo70A-Exo70I), which clustered into 9 different clades (Figure 3.2).

OsExo70-H3b belongs to the OsExo70-H clade, which further diverged into two subgroups, OsExo70-H1 and OsExo70-H3 (red highlight in Figure 3.2). From these two subgroups are (OsExo70-H1a and OsExo70-H1b) and (OsExo70-H3a and OsExo70-H3b), which seem to code for identical proteins as formerly described by Synek et al. (2006). Considering the

proximity and amino acid sequence similarity (99%) of OsExo70-H3b and its closest homologue OsExo70-H3a, it is very likely that the gene is either duplicated or there is an annotation error in the genome database. Further experimentation by Southern blot analysis for instance, will help to clarify whether there is one or multiple copies of *OsExo70-H3b* in the rice genome as that may contribute to gene redundancy effects during functional studies.

Importantly, since MtExo70I is associated with the development of the sub-domain of the peri-arbuscular membrane during AM symbiosis (Zhang et al., 2015), we were interested to determine how OsExo70-H3b relates to Medicago Exo70I. Interestingly, my phylogenetic analysis revealed that OsExo70-H3b and MtExo70-I belong to two different clades (H and I) that are distant from each other (red highlight in Figure 3.3). It also identified an OsExo70-I, the closest MtExo70-I homologue, the corresponding gene of which is not induced during *R. irregularis* or *M. oryzae* rice root colonisation as indicated by the transcriptomics analysis.

Finally, to determine the distribution of OsExo70-H3b type proteins across monocotyledonous and dicotyledonous species, a Reciprocal Blast Search Strategy (RBS) was applied. An initial blast search of the full-length amino acid sequence of OsExo70-H3b using the NCBI protein blast software showed that only 10 hits had site coverage of 50% and above, with E values ranging from 0.0 to 4e-110. Nevertheless, a reciprocal blast search produced nine OsExo70-H3b homologues/orthologues in different monocot species including *Elaeis guineensis* (African palm oil), *Phoenix dactylifera* (Date palm), *Setaria italic* (Foxtail millet), *Aegilops tauschii* (goat grass), *Hordeum vulgare* (barley), *Brachypodium distachyon* (a grass species), Sorghum (*Sorghum bicolor*), *Zea mays* (maize), and *Oryza brachyantha* (Figure 3.4). We found the closest orthologue of OsExo70-H3b to be an *O. brachyantha* (wild rice) Exo70 exocyst, which is particularly interesting because the completely sequenced genome of *O. brachyantha* provides high-quality reference for future functional and evolutionary studies of OsExo70-H3b. Interestingly, no OsExo70-H3b homologue was found in either mycorrhizal or non-mycorrhizal dicotyledons, suggesting that *OsExo70-H3b* gene may have a monocot-specific function.

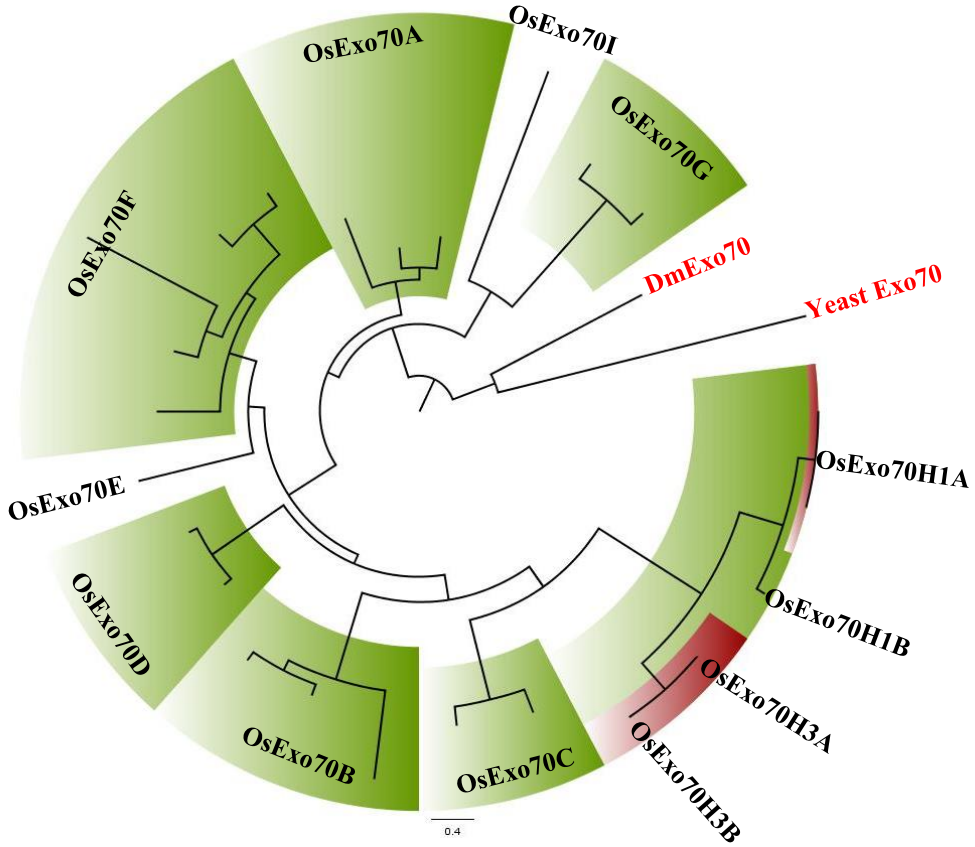

Figure 3.2: A maximum-likelihood phylogenetic tree of *O. sativa* Exo70 exocyst protein superfamily. The tree shows nine subgroups of *Oryza sativa* Exo70s clustering into 9 distinct clades (Exo70A-I). Clades are represented in 7 slices (green) and two individual nodes OsExo70I and OsExo70E (not-highlighted). The clade containing the target gene (*OsExo70-H3b*) is highlighted in red. *OsExo70I* and *OsExo70E* appear as single copy genes in rice as previously suggested. Two outgroups *Saccharomyces cerevisiae* (Yeast) and *Drosophila melanogaster* (Dm) Exo70 exocysts are highlighted in red.

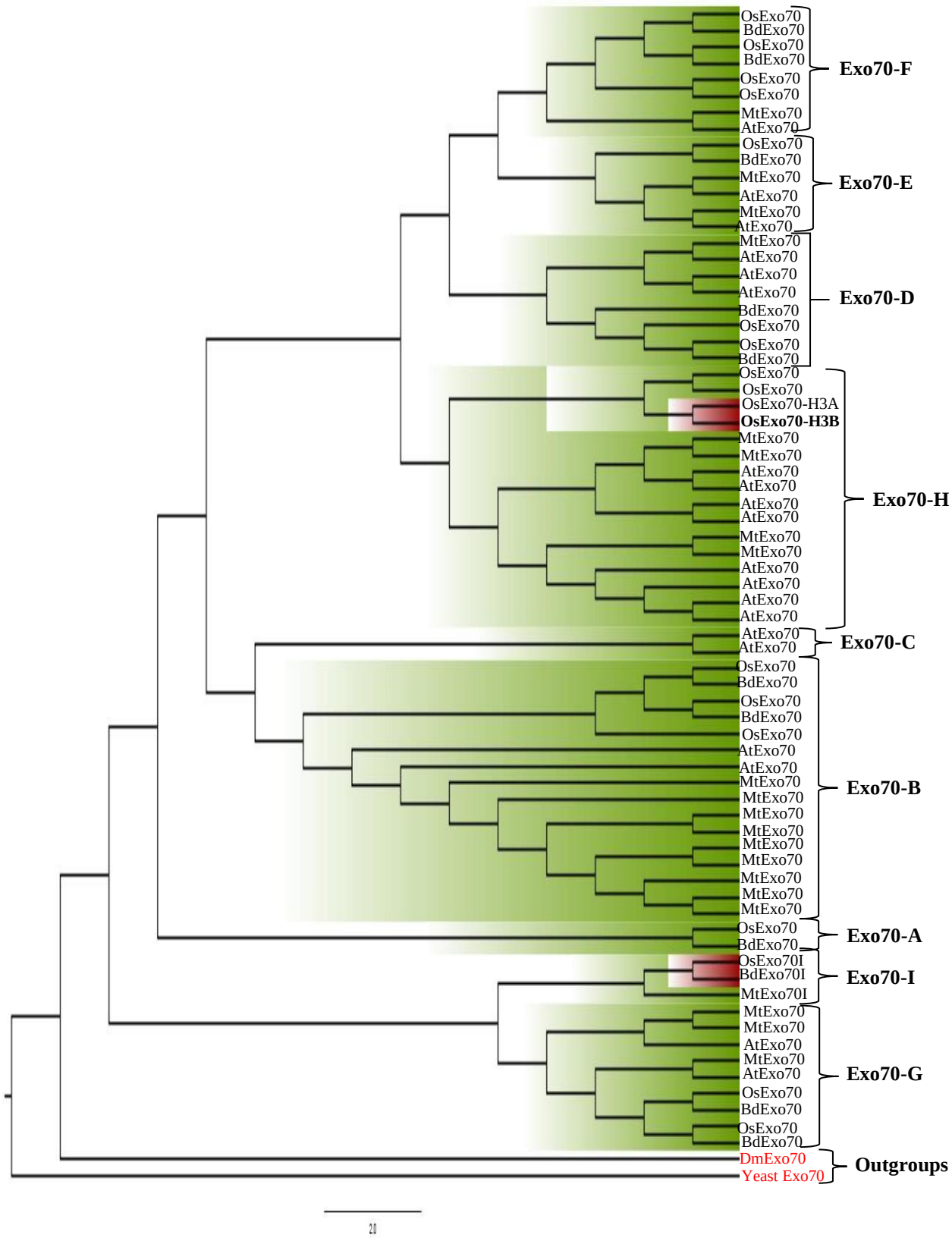

Figure 3.3: Maximum-likelihood phylogenetic tree of *O. sativa* Exo70 exocyst protein superfamily. The tree shows the position of OsExo70-H3b in relation to exo70 exocysts in other plant species (*Arabidopsis thaliana*, *Medicago truncatula* and *Brachypodium distachyon*). OsExo70-H3b (red) is in the Exo70-H clade and clusters with other Exo70-H groups from both dicotyledons and monocotyledons, although OsExo70-H3b and three of its closest homologues seem to have slightly diverged from the H-group. Exo70-I (red) from rice, *Medicago* and *Brachypodium* cluster together in the same clade, with a clear distance from the location of OsExo70-H3b, suggesting that it is not an

orthologue of the MtExo70-I, which is required for development of a subdomain of the peri-arbuscular membrane during AM symbiosis (Zhang et al., 2015).

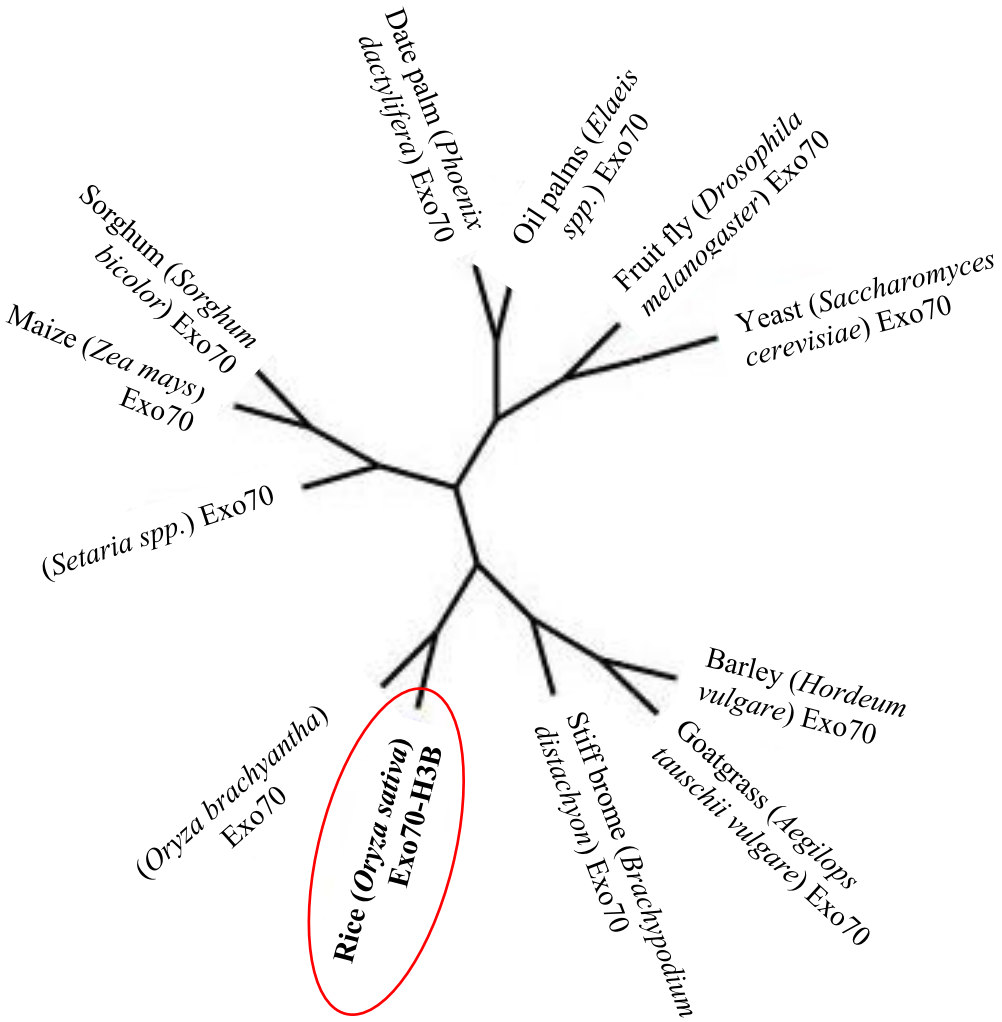

Figure 3.4: A maximum-likelihood phylogenetic tree showing OsExo70-H3b orthologues in nine monocot species. *O. branchyantha* Exo70 appeared to be the closest orthologue of OsExo70-H3b (indicated in red circle). Interestingly, no dicot homologue was found in the search. Two outgroups *Saccharomyces cerevisiae* (Yeast) and *Drosophila melanogaster* Exo70 exocysts are highlighted in red.

3.3.2. *Exo70-H3B* is induced during rice root colonisation by both *R. irregularis* and *M. oryzae*

Following the identification of *OsExo70-H3b* as a possible gene candidate involved in AM symbiosis and *M. oryzae* rice root colonisation (Figure 3.1; Table 4), it was necessary to validate the Affymetrix microarray data by qRT-PCR. This was done using gene-specific qRT-PCR primers to quantify the expression level of *OsExo70-H3b* in *R. irregularis* and *M. oryzae* colonised and non-colonised rice roots at 7 wpi and 7 dpi, respectively. A 12-fold increase in *OsExo70-H3b* transcript level ($P < 0.01$) was observed in mycorrhized roots relative to non-mycorrhized roots (Figure 3.5B) and a 0.45-fold increase in the transcript level of the same gene ($P < 0.05$) was seen in *M. oryzae* inoculated roots compared to non-inoculated roots at 7 wpi and 7 dpi, respectively (Figure 3.5C). Both gene expression analyses confirmed the Affymetrix microarray data, which showed a 5- and 3.8-fold-change increase in *Rhizophagus* and *Magnaporthe* inoculated *versus* non-inoculated rice roots, respectively (Table 4), although the qPCR results showed a much reduced *OsExo70-H3b* transcript level in *M. oryzae* inoculated versus non-inoculated rice roots. In addition, when compared to *R. irregularis* colonised roots, both experiments (Affymetrix microarray and qPCR) showed that the level of expression of *OsExo70-H3b* was significantly lower in *M. oryzae* colonised roots, suggesting that OsExo70-H3b may be more involved in the intracellular colonisation of the symbiont in rice roots (as shown with MtExo70I, Zhang et al., 2015) than with the pathogen in rice roots.

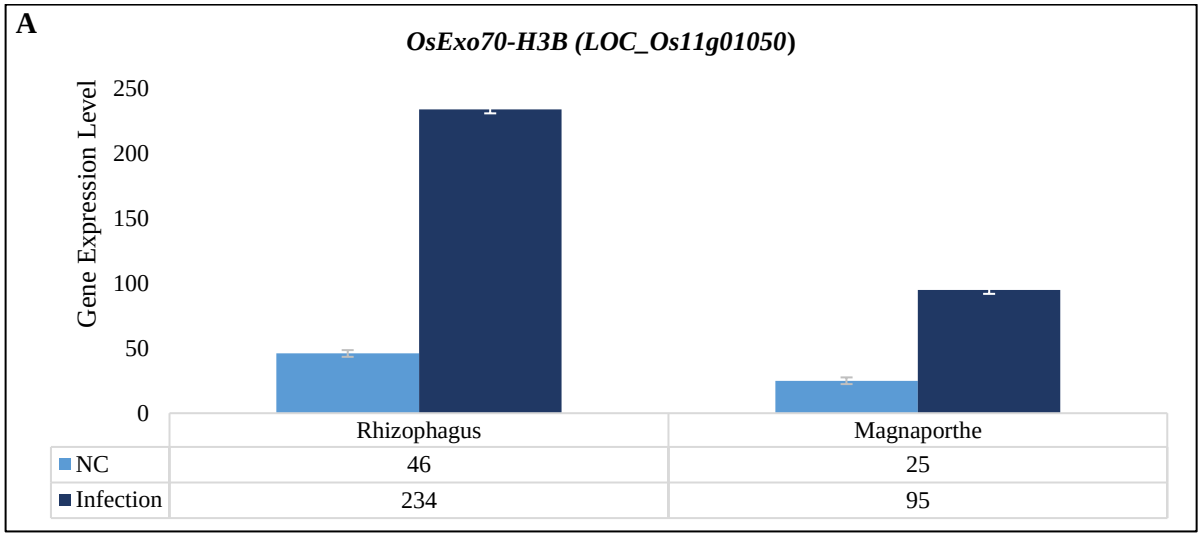

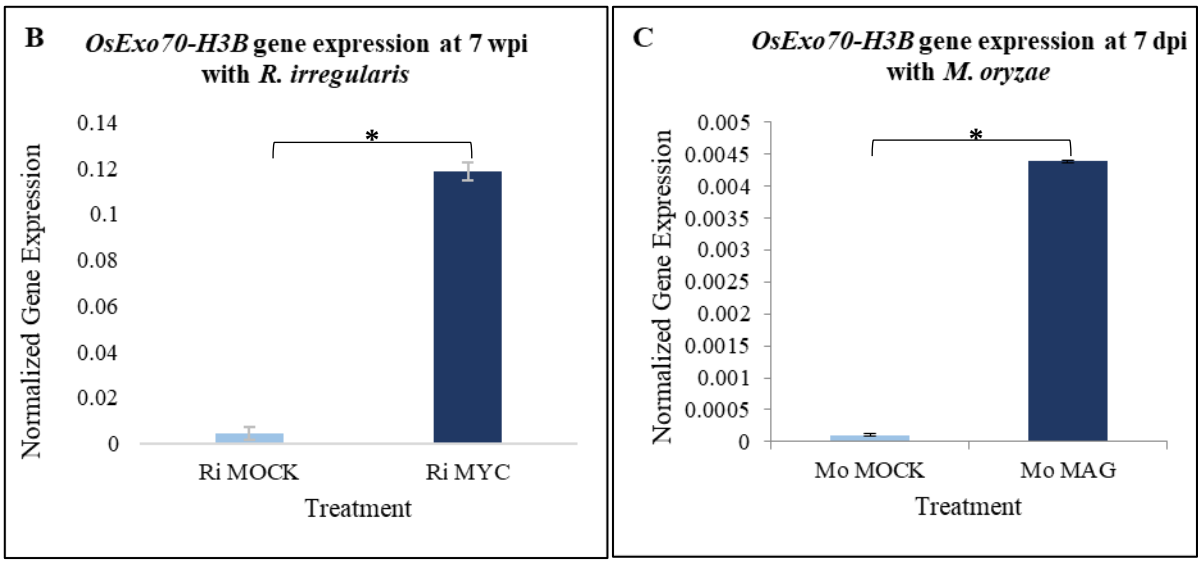

Figure 3.5: *OsExo70-H3B* gene expression analysis in *R. irregularis* and *M. oryzae* inoculated and non-inoculated rice roots. *OsExo70-H3B* gene expression level was determined by Affymetrix microarray data (**A**) and validated by qRT-PCR (**B, C**). Expression levels by qRT-PCR were normalized to the expression of *O. sativa* Cyclophilin. Bars represent the means of three biological replicates (n = 1) ± SEM. Asterisks indicate significant differences between expression levels in colonised and non-colonised roots. NC = Non-colonised. (*t*-test, *, P < 0.05; **, P < 0.01; ***, P < 0.001, n.s., P > 0.05).

3.3.3. Towards evaluating the biological function of *OsExo70-H3B* during rice root colonisation by *R. irregularis* and *M. oryzae*

Following the molecular confirmation that *OsExo70-H3b* is co-induced in *R. irregularis* and *M. oryzae* colonised rice roots, I wished to evaluate the biological role of the gene using T-DNA insertion mutant lines of *OsExo70-H3B (2D-31114)*. The mutant lines were ordered from Kyung Hee University, Korea (Yi and An, 2013) and analysed by genotyping using gene-specific primers (Exo70 P1 and Exo70 P2) in combination with T-DNA border primers (LB or RB) as instructed (Figure 3.6).

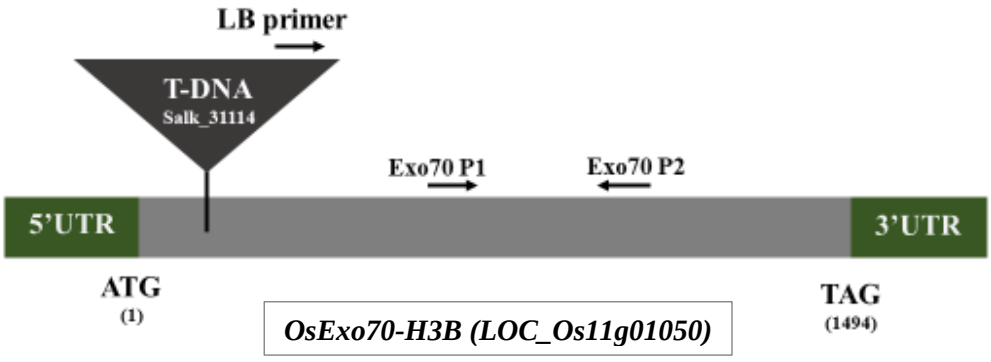

Figure 3.6: Schematic diagram of T-DNA insertion. Green and grey boxes indicate UTR regions and exons, respectively. T-DNA of vector is represented by triangle. Exo70 P1 and Exo70 P2 are gene-specific primers and LB is left-border primer of T-DNA insertion (modified from Yi and An, 2003).

Thirty T-DNA insertion mutant seeds of *OsExo70-H3b* were received and pre-germinated for genotyping and seed production. Only 19 seeds germinated and were genotyped. The expected genotypic distribution based on Mendelian genetics was a 1:2:1 ratio (i.e. 25% WT + 50% Heterozygotes + 25% Homozygous for mutation); however, the genotypic distribution observed from the 19 germinated seedlings was as follows: 8 WT + 11 Heterozygous + 0 Homozygous (Figure 3.7). Unfortunately, due to very poor seed setting and low germination rate, a larger number of plants could not be produced, and amongst those produced, no homozygous *OsExo70-H3b* plants were recovered.

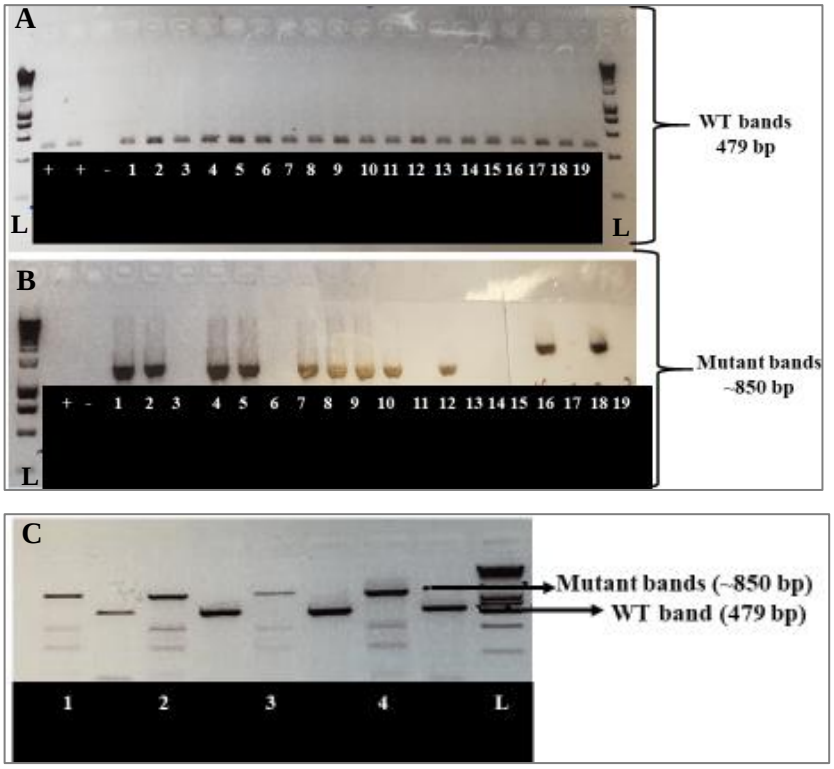

Figure 3.7: Genotypic characterization of *OsExo70-H3B* T-DNA insertion mutant lines. Agarose gel electrophoresis shows genotyping results for *OsExo70-H3B* (2D-31114) T-DNA insertion lines (**A-C**). Genotyping with OsExo70-H3b gene-specific primers shows amplification of WT bands in WT (Nipponbare – denoted as +) and all 19 plants at T2 generation (**A**). Genotyping with T-DNA border primers (RB2) plus one gene specific primer (OsExo70-H3b-R) reveals 11 heterozygous mutants (**B**) because all seedlings had a WT band as shown in above gel (**A**) at T2 generation. Four (out of 11) heterozygous plants were further cultivated and genotyped at T3 generation, and all plants had both the WT and heterozygote allele (**C**). L = 1 kb Ladder.

3.3.4. Discussion

Exo70 exocyst is part of an exocyst complex comprising eight subunits - Sec3, Sec5, Sec6, Sec8, Sec10, Sec15, Exo70 and Exo84. The exocyst complex was first discovered in the budding yeast *Saccharomyces cerevisiae* (Novick et al., 1980; TerBush et al., 1996), and was later purified from the rat brain (Hsu et al., 1996). Studies show that the exocyst is recruited to sites of active exocytosis and membrane expansion, where it mediates the tethering of secretory vesicles to the plasma membrane prior to soluble N-ethylmaleimide-sensitive factor (NSF) attachment protein receptor (SNARE)-mediated exocytic fusion (Hsu et al., 1996). Land plants also possess a large family of Exo70 genes unlike other eukaryotes such as *opisthokonts*, where Exo70 is encoded by a single gene (Cvrčková et al., 2001; Cvrčková et al., 2012; Vukašinović et al., 2014).

In plants, Exo70 exocysts are thought to contribute to polarized pollen tube development, root hair growth, cell wall material deposition, cell plate initiation and maturation, defence and autophagy (Synek et al., 2006; Fendrych et al., 2010; Kulich et al., 2013) and arbuscular mycorrhizal symbiosis (Zhang et al., 2015). The multiplicity of Exo70 paralogues within land plants has been associated with different processes, including cell-specific exocytosis within differentiating plant tissues; differential exocytosis or trafficking pathways within a single cell, especially those with more cortical recycling domains present, and exocytosis due to stress-responses to pathogen attack or abiotic stress (for review, see Zarky et al., 2013). Studies in *Arabidopsis* showed that homozygote mutants of the *AtExo70A1* gene exhibited phenotypic defects, such as impaired polar growth of root hairs and stigmatic papillae, suggesting the role of Exo70 in cell and organ morphogenesis (Synek et al., 2010). The *Oryza sativa Exo70A1* gene is associated with normal vascular bundle formation and mineral transport in rice as mutations in the *Rls2* gene, which encodes OsExo70A1 resulted in irregular vascular bundles and perturbed mineral nutrient transport in rice (Tu et al., 2015).

The role of Exo70 in symbiosis has also been highlighted. For instance, Genre et al. (2012) showed that vesicle exocytosis (which involves exocyst proteins) opposite the tips of growing hyphae leads to the extension of the peri-fungal membrane surrounding the intracellular hyphae in the legume *Medicago truncatula* and the non-legume *Daucus carota*. The *Medicago truncatula* Exo70 exocyst protein known as MtExo70i has also been linked with normal development of the branch domain of the peri-arbuscular membrane (PAM) during arbuscule development as MtExo70i mutants exhibited an abnormal arbuscule phenotype with aberrant hyphal growth (Zhang et al., 2015). More specifically, the arbuscules of *mtexo70i* mutants had

short, random hyphal branches with an uneven width and frequently swollen at the tip. The arbuscules were surrounded by a PAM but with limited incorporation of PAM-resident ABC transporters (STR and STR2) in the branch domain, indicating that Exo70I activity is crucial during the early branching phase of the arbuscule, perhaps through the secretion of PAM-resident proteins (Zhang et al., 2015).

Exo70 exocyst function has also been associated with plant defence and pathogen response. For instance, two *Arabidopsis* Exo70 exocyst genes, *AtExo70B2* and *AtExo70H1* were shown to be non-redundantly involved in plant defence responses against three different pathogens, e.g. *Pseudomonas syringae* pv. *maculicola*, *P. syringae* pv. *tomato* and *Hyaloperonospora parasitica* (Pecenokova et al., 2011). Messenger RNAs from both exocysts were strongly up-regulated upon stimulation with the fungus *Blumeria graminis* f. sp *hordei*, *P. syringae* and elicitors, such as *elf18* (elicitor peptide derived from the bacterial elongation factor), and exposure of *AtExo70B2* mutants to the non-host *Blumeria graminis f. sp hordei* resulted in cell wall thickenings (papillae) due to accumulation of extensive vesicular compartments on the cytoplasmic side, suggesting a defect in vesicle tethering or fusion (Pecenkova et al., 2011). Fungal penetration efficiency was not affected in this interaction, but infection by *Blumeria graminis* of a host plant (barley) that had a transiently silenced *Exo70F1*-like exocyst enhanced fungal penetration, implying a possible function of some Exo70 exocysts in disease resistance (Pecenkova et al., 2011). Furthermore, two *Oryza sativa* Exo70 exocyst subunits, Exo70F2 and Exo70F3 have been associated with plant immunity based on their interaction with *M. oryzae* effectors (Fujisaki et al., 2015). In this scenario, OsExo70F3 specifically interacts with the AVR-Pii effector to trigger Pii-dependent resistance in the rice-*M. oryzae* pathosystem (Fujisaki et al., 2015). AVR-Pii is a small (70 amino acid) secreted protein of *M. oryzae* (Yoshida et al., 2009) and Pii is a cognate rice resistance locus encoding a pair of CC (coiled-coil)-NB (nucleotide-binding domain)-LRR (leucine rich repeat) type NLR (nucleotide-binding and leucine-rich repeat-containing) proteins (Takagi et al., 2013).

Considering the known roles of Exo70 exocysts in plant-microbe symbiotic and detrimental interactions, we speculate that the target gene, *OsExo70-H3b*, may also be involved in a secretory pathway required for the assembly of the PAM and EIHM during rice root colonisation by *R. irregularis* and *M. oryzae*, respectively. Although Exo70 exocysts have been associated with defence responses in plants, it is highly unlikely that OsExo70-H3b will function in immunity during *M. oryzae* during rice root infection since the fungus seems to adopt an endophytic, rather than a pathogenic lifestyle in the root. For this reason, the

involvement of OsEx70-H3b for intracellular accommodation of *R. irregularis* and *M. oryzae* fungal hyphae in rice roots would be a more appropriate speculation, hence the various analyses performed here. First, was a phylogenetic characterization to determine how OsExo70-H3b relates to the symbiotic MtExo70i, as well as other rice and non-rice Exo70 exocysts, e.g. AtExo70H1 and AtExo70H2, which are involved in disease resistance. Second, was a molecular analysis of *OsExo70-H3b* function in rice roots inoculated with *R. irregularis* and *M. oryzae*, respectively, to validate the gene expression data presented by the Affymetrix microarray experiment. And third was a functional study utilising a T-DNA insertion mutant of *OsExo70-H3b* to better understand its biological role during rice root colonisation by both fungi.

In this study, a rice Exo70 exocyst (*OsExo70-H3b*) which is induced during rice root colonisation by both mutualistic (*R. irregularis*) and detrimental (*M. oryzae*) fungi was identified. According to my phylogenetic characterization, *OsExo70-H3b* exocyst is a member of the Exo70 exocyst superfamily of genes, which consists of 43 members that cluster into nine subgroups (Exo70A-Exo70I) (Figure 3.2) in rice, as previously reported (Synek et al., 2006). I found that OsExo70-H3b belongs to the Exo70-H exocyst group, which consists of four exocysts (OsExo70-H3b and OsExo70-H3a, OsExo70-H1a and OsExo70-H1b) that maintain very close proximity with each other (Figure 3.2). At the amino acid sequence level, OsExo70-H3b (Os11g01050) and its closest homologue, OsExo70-H3a (Os12g01040) share 99% similarity, indicating the possibility of an annotation error or a duplication event of *OsExo70-H3b* in the rice genome. Further analysis with the Southern blot technique will clarify whether one or multiple copies of *OsExo70-H3b* gene are present in the rice genome, and is therefore, recommended. As the phylogenetic characterization did not identify any close homologue of OsExo70-H3b in both mycorrhizal and non-mycorrhizal dicotyledonous plant species, it is possible that OsExo70-H3b may have a monocotyledon-specific function.

In addition, the closest homologue of MtExo70I, which is involved in the development of the sub-domain of the arbuscule (Zhang et al., 2015) was found in rice (OsExo70I). However, unlike *MtExo70I*, which is induced in AM symbiosis, *OsExo70I* is not induced during rice root invasion by either *R. irregularis* or *M. oryzae* based on our gene expression profile. Quantitative RT-PCR experiments validated the Affymetrix microarray data, which showed the co-induction of *OsExo70-H3b* during *R. irregularis* and *M. oryzae* rice root colonisation (Figure 3.5B, 3.5C). This suggests that OsExo70-H3b may have a functional role in AM symbiosis, as well as rice root interactions with *M. oryzae*.

Attempts to functionally characterize T-DNA insertion mutant lines for *OsExo70-H3b* were hampered by the inability to recover homozygous mutant individuals due to a possible lethal effect, which implies that Exo70-H3b plays an essential role. This possibility is supported by studies in *A. thaliana*, which linked a homozygous mutation of *AtExo70A1* to the development of smaller organs, loss of apical dominance and dramatically reduced fertility, thereby implicating AtExo70A1 function in cell and organ morphogenesis (Synek et al., 2006). Further support is rendered by studies linking the function of AtExo70A1 to the regulation of vesicle trafficking in tracheary element differentiation in *A. thaliana* (Li et al., 2013). Mutants of *AtExo70I* led to aberrant xylem development, dwarfed and nearly sterile plants with very low fertility, reduced cell expansion, and decreased water potential and hydraulic transport (Li et al., 2013).

Although a full functional analysis could not be performed due to the failure to recover homozygous mutant lines of *OsExo70-H3b*, the expression profile presented here, provide an indication that the Exo70-H3b exocyst protein may play a role during rice root colonisation by *R. irregularis* and *M. oryzae*. For AM symbiosis and in analogy to other work, OsExo70-H3b may be involved in the biogenesis of the plant-derived peri-arbuscular membrane (PAM) through vesicle trafficking and exocytosis opposite the tips of growing hyphae, thus resulting in the extension of the PAM as shown in *M. truncatula* and the non-legume *D. carota* (Genre et al., 2012). More specifically, OsExo70-H3b may be involved in the early branching phase of arbuscule development as shown in *M. truncatula*, where *exo70i* mutants failed to support normal arbuscule development and limited the incorporation of the PAM-resident ABC transporters (required for arbuscule development and functional symbiosis), STR and STR2 (Zhang et al., 2010) into the PAM (Zhang et al., 2015). The study also showed that MtExo70I accumulated in spatially restricted zones adjacent to the PAM at arbuscule branch tips, where it interacts with an arbuscule-specific protein known as Vapyrin (Pumplin et al., 2010; Zhang et al., 2015). Considering the spatial location of Exo70I and its ability to interact with Vapyrin, it was suggested that Vapyrin probably acts as a scaffold protein that recruits or maintains Exo70I adjacent to the PAM at the hyphal tips (Zhang et al., 2015). It is possible that OsExo7-H3b functions in a similar fashion as MtExo70I, but more experimental analysis must be carried out to determine its specific role during AM symbiosis.

With respect to detrimental plant-microbe interactions, the role of some Exo70 exocysts such as AtExo70B2, AtExo70H1, OsExo70F2 and OsExo70F3 have been associated with plant

defence and pathogen response (Pecenokova et al., 2011; Fujisaki et al., 2015). AtExo70B2 has also been associated with controlling PAMP signalling potentially through recycling signalling proteins (Stegmann et al., 2012). In its signalling role, AtExo70B2 targets the plant U-box-type ubiquitin ligase 22 (PUB22), which act in collaboration with PUB23 and PUB24 to negatively regulate PAMP-triggered responses (Stegmann et al., 2012). Although Exo70 activity has not been studied during rice root invasion by *M. oryzae*, my experiments suggest that OsExo70-H3b may be required in cellular processes involving the development of plant-fungal interfaces such as the EIHM to accommodate the pathogen in rice roots.

3.4. Characterization of the candidate lectin receptor-like kinase (LecRLK)

3.4.1. Phylogenetic characterization of plant lectin receptor-like kinases

Lectin receptor-like kinases are represented by 75 members in *Arabidopsis* and more than 173 members in rice, with no homologues found in yeast and human genomes (Hervé et al., 1996). To determine the position of the target LecRLK (Os07g38800), a phylogenetic tree was produced using amino acid sequences of all rice LecRLKs available on the rice genome database. All genes clustered into three major classes or types based on their lectin domains, e.g. L-, G- and C-types. The majority of the LecRLK superfamily clustered within the L- or G-type clade, with only one LecRLK belonging to the C-type. Interestingly, we identified our candidate OsLecRLK (Os07g38800) as an L-type LecRLKs (Figure 3.8A), with a close homologue/paralogue in the *O. sativa* family (Os07g38820) and an orthologue in the *Oryza brachyantha* family (Figure 3.8B). As with OsExo70-H3b, no orthologues of OsLecRLK (Os07g38800) were found in either mycorrhizal or non-mycorrhizal dicotyledonous plants, suggesting that OsLecRLK (Os07g38800), like the *OsExo70-H3b* exocyst gene, may have a monocot-specific function.

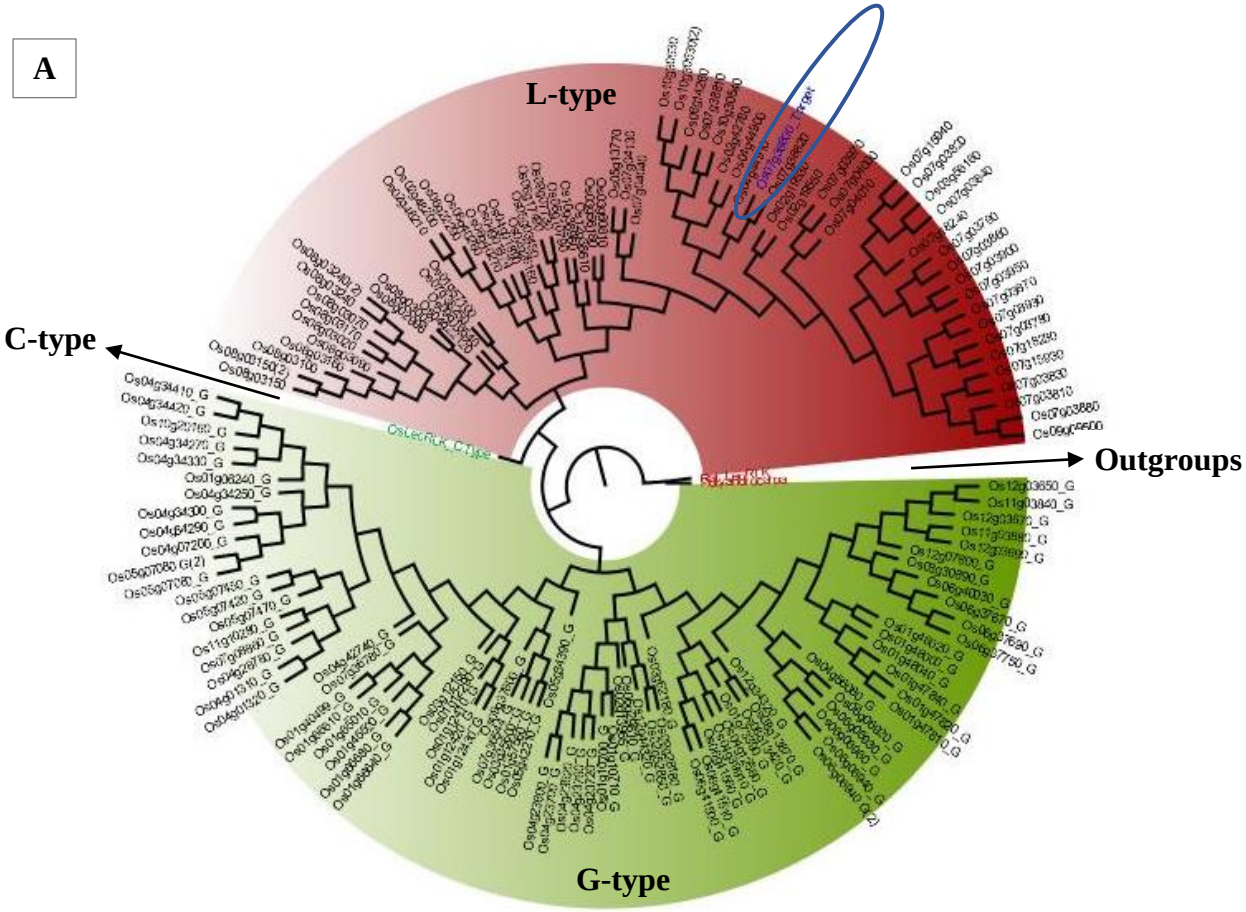
A
L-type
C-type
Outgroups
G-type

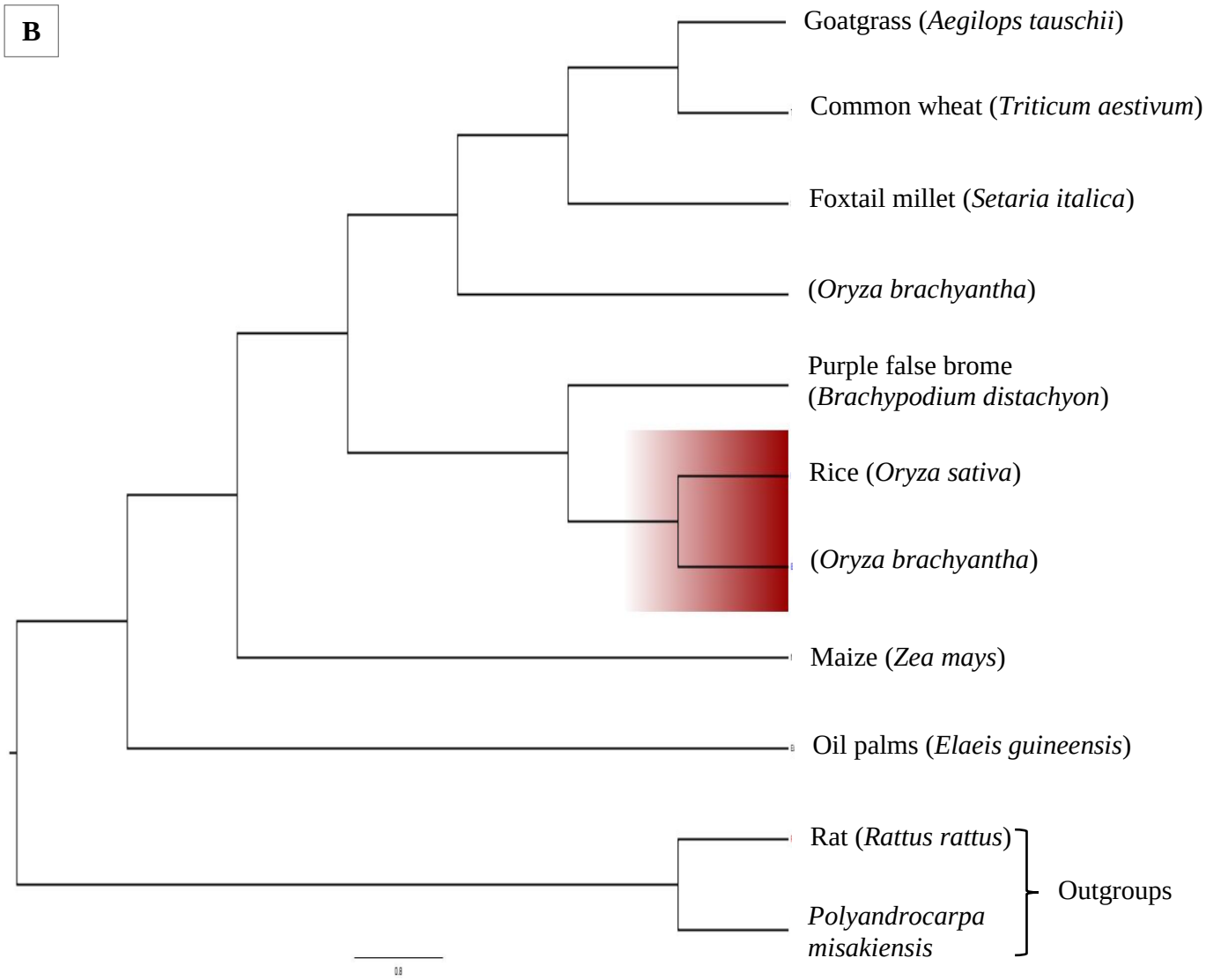

Figure 3.8: A maximum-likelihood phylogenetic tree of OsLecRLK superfamily of genes. All assessed OsLecRLKs clustered into 3 subgroups/clades (G-type - green, L-type – red, and the C-type) based on their extracellular lectin domains (**A**). Only one C-type LecRLK was identified. Phylogenetic tree showing OsLecRLK orthologues (**B**). An *O. brachyantha* LecRLK was identified as the closest homologue. Two outgroups *Rattus rattus* and *Polyandrocarpa misakiensis* (indicated as the non-highlighted slice in A) were used in the phylogenetic analysis.

3.4.2. *OsLecRLK (Os07g38800)* is induced in rice roots upon exposure to *R. irregularis* and *M. oryzae*

To validate the Affymetrix microarray data, which showed that *OsLecRLK (Os07g38800)* is highly co-upregulated during rice root colonisation by *R. irregularis* (FC = 6) and *M. oryzae* (FC = 9) (Table 4, Figure 3.9), a qRT-PCR was performed. This resulted in a 28-fold increase ($P < 0.01$) in *OsLecRLK (Os07g38800)* transcript level in *R. irregularis* colonised roots relative to the mock at 7 wpi, and a 6-fold increase ($P < 0.01$) in *M. oryzae* colonised rice roots compared to the corresponding mock at 7 dpi (Figure 3.9B, 3.9C). These results confirm the Affymetrix microarray data.

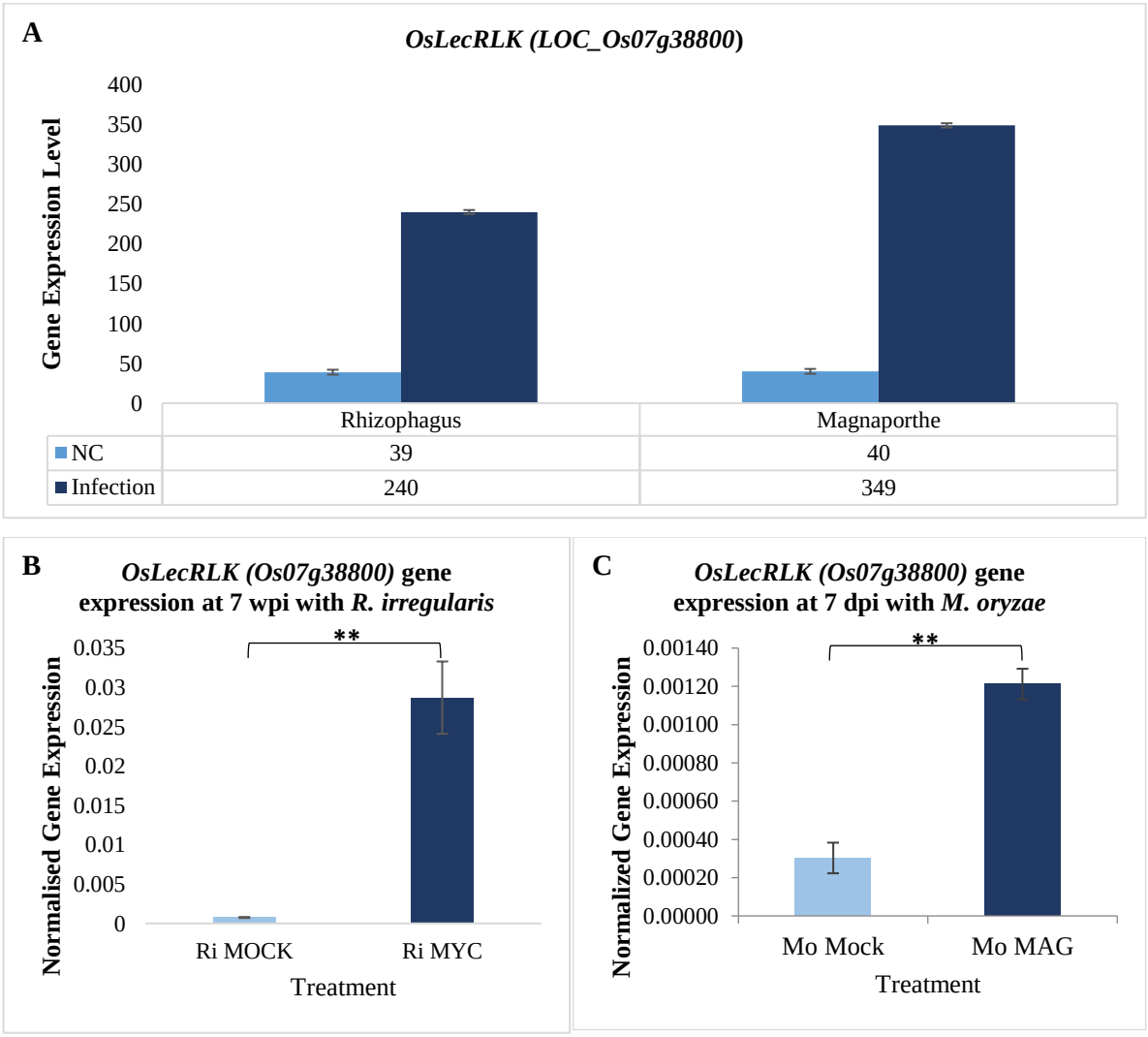

Figure 3.9: *OsLecRLK (Os07g38800)* gene expression analysis in *R. irregularis* and *M. oryzae* inoculated and non-inoculated rice roots. *OsLecRLK (Os07g38800)* transcript level was significantly increased in rice roots colonised by both fungi at 7 wpi and 7 dpi, respectively (**B-C**), validating the Affymetrix microarray data (**A**). *OsLecRLK (Os07g38800)* expression level was normalized to the expression of *O. sativa* Cyclophilin. Bars represent the means of three biological replicates (n = 1) ±

SD. Asterisks indicate significant differences between expression levels in colonised and non-colonised roots. (*t*-test, *, P < 0.05; **, P < 0.01; ***, P < 0.001, n.s., P > 0.05). NC = Non-colonised.

3.4.3. Investigating the functional role of *OsLecRLK (Os07g38800)* during rice root colonisation by *R. irregularis* and *M. oryzae*

Since my analyses indicated that *OsLecRLK (Os07g38800)* gene is highly induced during rice root colonisation by *R. irregularis* and *M. oryzae* fungi, it was necessary to determine the role of OsLecRLK during colonisation of rice roots by both fungi. To this end, T-DNA insertion mutant seeds of *OsLecRLK_Os07g38800* (4A-20704) were obtained from the Korean T-DNA collection and genotyped.

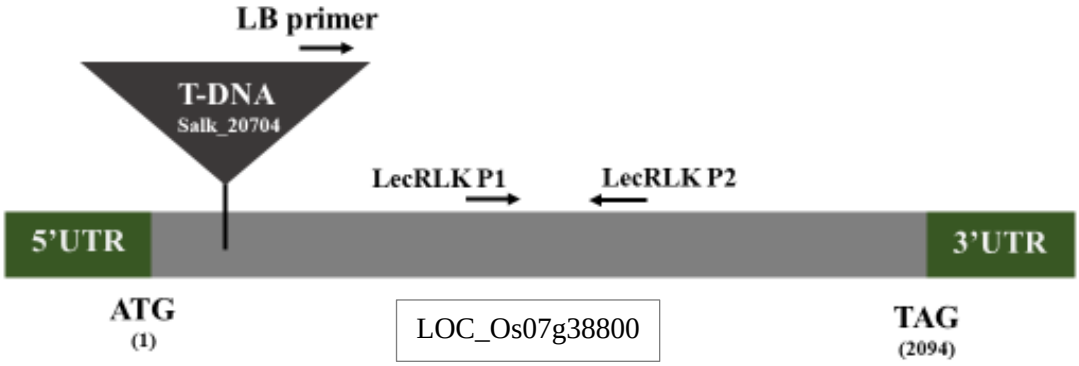

Figure 3.10: Schematic diagram of T-DNA insertion. Green and grey boxes indicate UTR regions and exons, respectively. T-DNA of vector is represented by triangle. LecRLK P1 and LecRLK P2 are gene-specific primers and LB is left-border primer of T-DNA insertion (modified from Yi and An, 2003).

Out of 40 seeds, 33 (83%) germinated and were genotyped using both gene-specific primers and T-DNA insertion primers as suggested by Yi and An, 2013. Unfortunately, only WT alleles were amplified in all seedlings (Figure 3.11), indicating that the seed batch may have contained all wild-types due to a mix-up or the unsuccessful integration of the T-DNA insert.

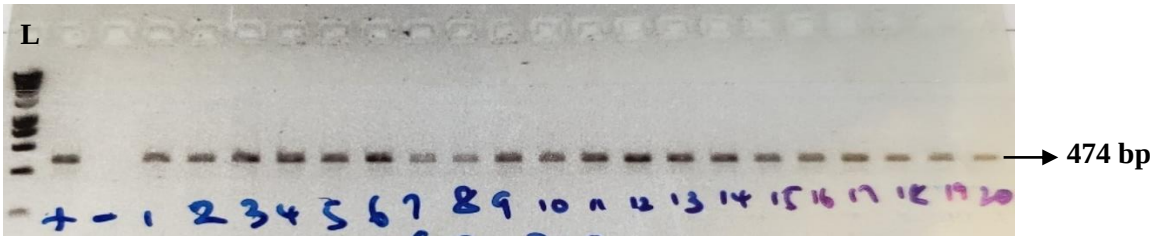

Figure 3.11: Genotypic characterization of *OsLecRLK (Os07g38800)* T-DNA insertion mutant lines (4A-20704). The presence of only wild-type bands is seen on the gel. Positive control (+) was genomic DNA from a corresponding WT plant, whereas the negative control (-) was the PCR master mix with water only. L = DNA Ladder (1 kb).

3.4.4. Discussion

Plant lectin receptor-like kinases (LecRLKs) belong to a class of receptor-like kinases comprising of three major domains; an extracellular or N-terminal lectin domain, an intermediate transmembrane domain, and a C-terminal kinase domain. They are divided into three classes - G-type, C-type and L-type LecRLKs and this classification is based on the properties of their lectin motifs (Shiu and Bleecker, 2001). G-type LecRLKs have a lectin domain homologous to the mannose-specific lectins of bulb species, and they have been associated with self-complementarity in flowering plants, seed germination (Cheng et al., 2013), innate immunity and disease resistance (Liu et al., 2015). C-type LecRLKs contain a calcium-dependent lectin motif, and only one member has been identified in both Arabidopsis and rice (*Oryza sativa*), with their function remaining largely unknown (Bellande et al., 2017). Although legume lectins are abundant in legume seeds, they are not legume-specific because related genes were found in other plants and animals. Structural studies indicate that legume lectins are small calcium-/Manganese-containing (glyco) proteins with a conserved tertiary structure composed of three β-sheets (Loris et al., 1998). Their carbohydrate-binding specificity usually varies due to variability around a conserved core of residues defining a monosaccharide binding site. They can be dimeric or tetrameric, and some of them undergo an oligomerization process that leads to the creation of one or multiple binding sites for hydrophobic ligands, such as adenine, related cytokinins and auxins (Bouckaert et al., 1999). *In vivo*, the actual ligands of legume lectins are more complex glycans including simple sugars and hydrophobic hormones (Loris, 2002).

Due to the close resemblance of the L-type LecRLKs to legume lectins, their involvement in saccharide signal recognition and transduction have been proposed, although studies in

Arabidopsis suggest they are unlikely receptors for small sugars due to their poorly conserved sugar-binding site (Hervé et al., 1996). The better conserved hydrophobic-binding site of the L-type LecRLKs lends support to their involvement in the recognition of either small hydrophobic hormones or more complex glycans (Barre et al., 2002). Accumulation of defence-related metabolites such as nicotine, diterpene-glucosides and trypsin-protease was affected due to the silencing of LecRLK1 in *Nicotiana attenuata* (Gilardoni et al., 2011) and their roles have been implicated in various physiological processes, such as protein sorting, recognition, embryogenesis, and development.

The L-type LecRLK comprises of an extracellular kinase domain that resembles the carbohydrate-binding protein of the legume lectin family. They were first described in *Arabidopsis* and are thought to play a role in transduction pathways involving carbohydrate and plant hormone signals (Hervé et al., 1996). A comprehensive expression analysis of all the L-type LecRLKs (Bouwmeester and Govers, 2009) revealed that most of the LecRLK genes are not or weakly expressed in all tissues and developmental stages in *Arabidopsis thaliana*, except for three genes; *LecRK-I.9 (*Does Not Respond to Nucleotides 1 or DORN1 eATP receptor (Choi et al., 2014)), *LecRK-IV.1* and *LecRK-VIII.1*, whose transcripts are found in all tissues (for review, see Bellande et al., 2017). By contrast, the expression of many genes change in response to various stimuli such as hormones, abiotic stress and elicitors.

Consistent with the above, the lectin receptor-like kinase gene *NbLRK1* from *Nicotiana benthamiana* is associated with the recognition of *Phytophthora infestans* INF1 elicitor and the mediation of INF1-induced cell death (Kanzaki et al., 2008). Similarly, the L-type cell surface lectin receptor-like kinase LecRK-1.9 in *Arabidopsis* is linked to enhanced resistance to *P. infestans* in the Solanaceous plants potato and *N. benthamiana* (Bouwmeester et al., 2014). Overexpression of *LecRK-1.9* strengthened cell adhesion, which hindered penetration and intracellular proliferation of *P. infestans*. With respect to AM symbiosis, not much is known about the role of LecRLKs, however, a study identified a family of nine *MtLecRLK* genes, some of which are speculated to be involved in a signalling pathway that possibly requires rhizobial-lipo-chitooligosaccharides to establish legume-rhizobia symbiosis (Navarro-Gochicoa et al., 2003).

This sub-chapter aimed to investigate the role of the target *OsLecRLK* gene *(Os07g38800)* during rice root colonisation by both *R. irregularis* and *M. oryzae*. It involved the phylogenetic characterization of the target gene to identify which class of LecRLKs it belongs to and its

relationship with other plant LecRLKs, especially those identified to play a role in symbiosis and plant infection by detrimental microbes. Functional studies using T-DNA insertion mutant lines were also performed to better understand the biological role of the gene during rice root colonisation by both fungi. The study led to the identification of a novel putative L-type *OsLecRLK (Os07g38800)* that is upregulated during *R. irregularis* and *M. oryzae* rice root invasion. Based on our phylogenetic characterization, OsLecRLK (Os07g38800) has close paralogues and orthologues in other monocotyledonous plants and grasses including *Zea mays*, *Brachypodium*, *Aegilops sp*., *Triticum aestivum*, and *O. brachyantha*, which is its closest homologue (Figure 3.8B). Interestingly, no homologue was found in eudicot species, implying that *OsLecRLK (Os07g38800)* has a monocot-specific function.

Consistent with the Affymetrix microarray data (Table 4), gene expression validation experiments by qRT-PCR revealed a significant increase ($P < 0.01$) of *OsLecRLK (Os07g38800)* transcript level in both *R. irregularis* and *M. oryzae* inoculated rice roots (Figure 3.9B, 3.9C). Unfortunately, functional analysis was not possible due to the lack of suitable stable transgenic knockout lines of the target gene.

So far, results obtained from this study point towards a role of OsLecRLK (Os07g38800) during rice root colonisation by *R. irregularis* and *M. oryzae*. This is supported by very few studies, which have shown the involvement of LecRLK genes in symbiosis and plant innate immunity. For example, some members of a family of nine *M. truncatula* LecRLK genes were speculated to be involved in a signalling pathway that possibly requires rhizobial-lipo-chitooligosaccharides to establish legume-rhizobia symbiosis. The enhanced expression of the MtLecRLK genes in *Medicago* roots indicated that they may play a role in the regulation of nodulation, but probably not through Nod factor binding (Navarro-Gochicoa et al., 2003). Some G-type rice LecRLKs have also been linked to resistance to attacks by herbivorous insects, such as the Brown Planthopper (BPH) and the rice pathogens *M. oryzae* and *Xanthomonas oryzae*, the causative agent of bacterial blight (Cheng et al., 2013). In particular, a gene cluster, *Bph3*, encoding lectin receptor kinases was found to confer broad-spectrum resistance to the brown planthopper insect and *M. oryzae* (Liu et al., 2015). Together with these studies, our preliminary data suggest a role for *OsLecRLK (Os07g38800)* gene in AM symbiosis and rice root interaction with *M. oryzae*, but further investigation is required to fully understand the specific function of the gene in both plant-fungal microbe interactions.

3.5. Exploring the role of DUF538 genes during rice root colonisation by *R. irregularis* and *M. oryzae*

The DUF538 protein superfamily is made up of several plant proteins of unknown function. They have a molecular weight of 19-21 kDa and encode about 170 amino acids (Gholizadeh 2016). The *DUF538* superfamily of genes is widely distributed across monocotyledonous and dicotyledonous plant species (Gholizadeh 2011; Takahashi et al., 2013). In *Arabidopsis thaliana*, DUF538 protein has a three-dimensional petal-like structure, with its protein structure dominated by β-strands. Their function has largely been predicted using genome annotation tools, as well as cloning from plants challenged with various environmental stimuli such as nutrient deficiency and mild drought, as well as crown gall and mixed elicitors (Gholizadeh and Baghbankkohnehrouz, 2010).

DUF538 proteins are suggested to play a role in the regulation of different stress responses in plants due to their predicted high phosphorylation potential (Nakagami et al., 2010). This was supported by the activation of the redox system of plant cells by an exogenously applied fusion form of DUF538 protein using a plant tissue abrading material (Gholizadeh 2011). Although thorough experimental investigations to understand the function of DUF538 proteins have not been performed, a structural study predicted plant DUF538 proteins to be homologues to the Bactericidal Permeability Increasing (BPI) proteins found in the immune system of mammals (Gholizadeh and Kohnehrouz, 2013). BPI are thought to provide the first line of defence against different pathogens including bacteria, fungi, viruses and parasites. However, no association with symbiosis or accommodation of detrimental microbes in plant roots has yet been found.

3.5.1. Characterisation of the DUF538 superfamily of genes

The RiceXPro database predicts that the rice genome contains about 29 DUF538 proteins of unknown function, with 11 DUF538 proteins expressed. It is not however, entirely clear how many of these genes are present in other plant species. From my transcriptome comparison analysis (Figure 3.1), four of these *DUF538* genes (*Os07g2880, Os07g02920, Os11g38210* and *Os11g38240*) were co-upregulated during rice root colonisation by both *R. irregularis* and *M. oryzae* (Table 5); however, gene expression validation experiments by qRT-PCR (Figure 3.12) confirmed the co-upregulation of three *DUF538* genes (*Os07g02880, Os07g02920* and

Os11g38210) during rice root colonisation by *R. irregularis* and *M. oryzae* at 7 wpi and 7 dpi, respectively. Based on their expression profile from both the Affymetrix microarray and qRT-PCR experiments, three genes were selected for functional studies.

Gene Locus ID (LOC)	Description	Expression (Ri; CR+LLR; 7 wpi)	Expression (Mock; CR+LLR; 7 wpi)	FC (Ri/Mock)	Expression (Mag; 6 dpi)	Expression (Mock; 6 dpi)	FC (Mag/Mock)
Os11g38240	DUF538 domain containing protein, putative, expressed	602	18	**33**	104	12	**9**
Os07g02920	DUF538 domain containing protein, putative, expressed	583	18	**32**	342	24	**14**
Os11g38210	DUF538 domain containing protein, putative, expressed	284	13	**22**	186	11	**17**
Os07g02880	DUF538 domain containing protein, putative, expressed	888	49	**18**	381	48	**8**

Table 5: Affymetrix microarray data showing the expression profile of four *DUF538* genes during rice root colonisation by *R. irregularis* (Ri) and *M. oryzae* (Mag). Ri inoculated and non-inoculated rice root types (CR and LLR) were compared at 7 wpi, whereas Mag inoculated, and non-inoculated roots were compared at 6 dpi. These *DUF538* genes were strongly co-upregulated (FC ≥ 2.5) during rice root colonisation by both fungi.

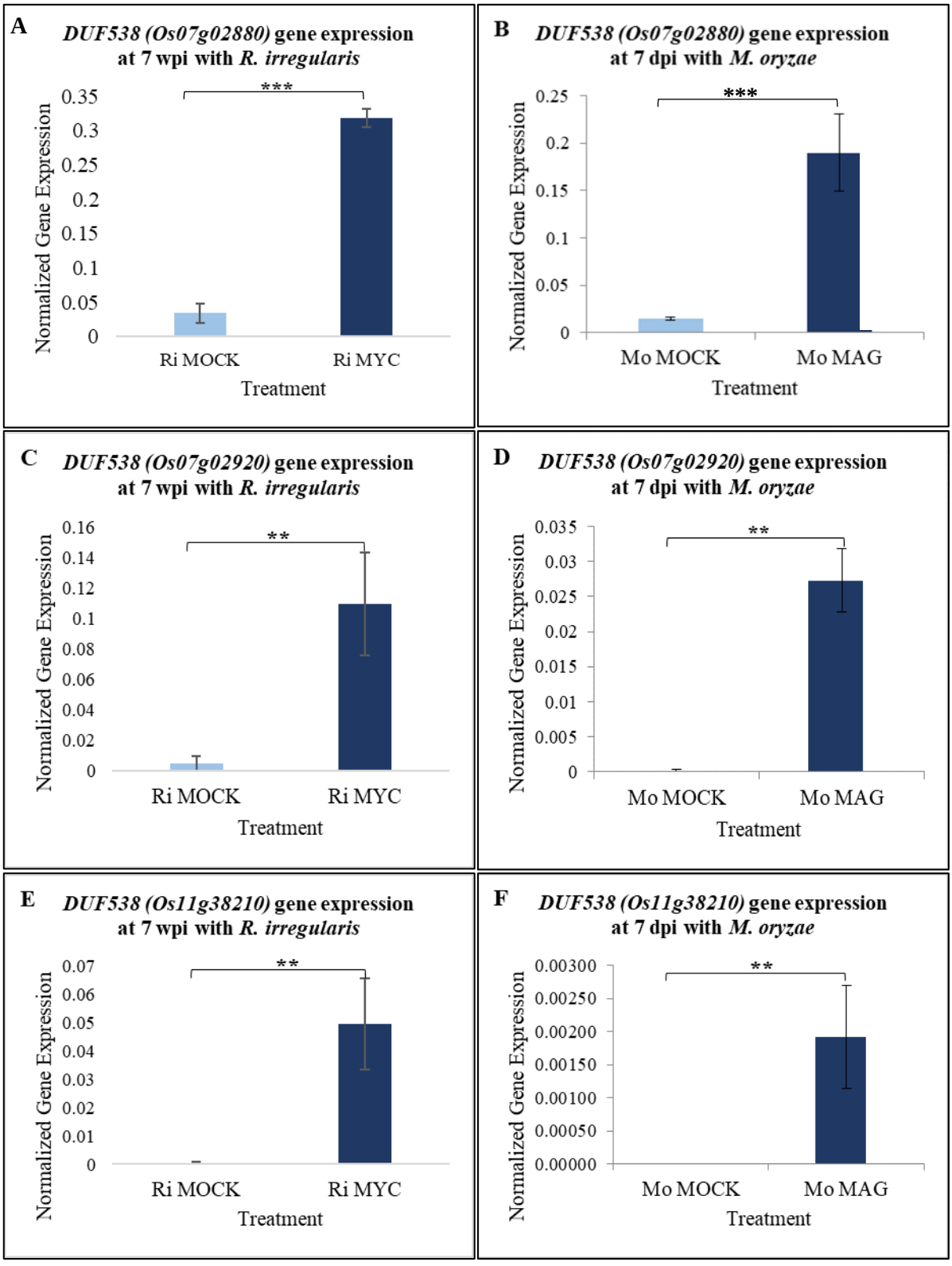

Figure 3.12: *DUF538* gene expression analysis in *R. irregularis* and *M. oryzae* inoculated and non-inoculated rice roots. The transcript levels of the three rice *DUF538* genes (*Os07g02880*, *Os07g02920* and *Os11g38210*) genes were measured by qRT-PCR and normalized to the expression of Cyclophilin (**A-F**). Bars represent the means of three biological replicates (n = 1) ± SEM. Asterisks indicate significant differences between expression levels in colonised and non-colonised roots. (*t*-test, *, $P < 0.05$; **, $P < 0.01$; ***, $P < 0.001$, n.s., $P > 0.05$).

Following the validation and selection of three strongly co-upregulated *DUF538* (Figure 3.12), the transcriptional activity of the other eight *DUF538* genes during rice root colonisation by both *R. irregularis* and *M. oryzae* was monitored by qRT-PCR. The results show that an additional three *DUF538* genes (*07g02900, 07g02690* and *11g38240*) and four *DUF538* genes (*07g02900, 07g02690, 07g02940* and *07g02850*) were induced during rice root colonisation by *R. irregularis* and *M. oryzae*, respectively (Figure 3.13, 3.14). On the other hand, five *DUF538* genes (*07g02940, 07g02850, 07g02700, 07g02870* and *11g38220*) and four *DUF538* genes (*07g02700, 07g02870, 11g38220* and *11g38240*) were not induced during rice root interactions with *Rhizophagus* and *Magnaporthe*, respectively (Table 6). Taken together, the qPCR-based gene expression analysis showed that 5 (out of 11) *DUF538* genes were co-induced during rice root interactions by both fungi; one gene (*11g38240*) was exclusively induced by *R. irregularis*, two genes (*07g02940* and *07g02850*) were solely induced by *M. oryzae*, whereas three genes (*07g02700, 07g02870* and *11g38220*) were not induced by either fungus (see Table 6 for summary).

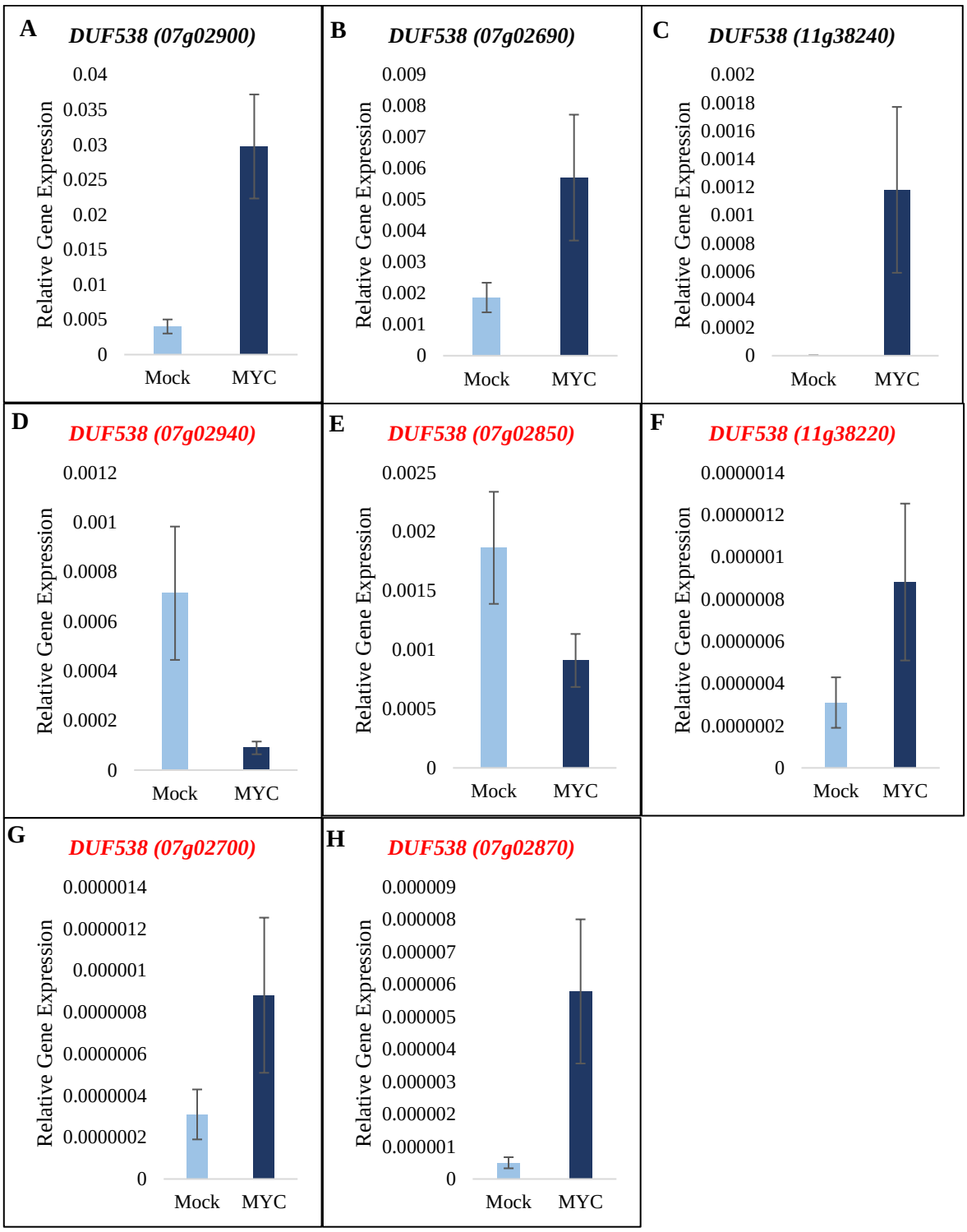

Figure 3.13: Molecular quantification of *DUF538* transcript levels in *R. irregularis* colonised and non-colonised rice roots. Expression of *DUF538* genes was normalised to the expression (geomean) of three *O. sativa* housekeeping genes (*Cyclophilin*, *GAPDH* and *Ubiquitin*). During rice root colonisation by *R. irregularis*, three genes were induced (**A-C**) and two genes were not induced (**D-E**, indicated in red) and three genes were extremely lowly expressed but perhaps at a detectable level (**F, G, H**). Bars represent the means of three biological replicates (n = 1) ± SEM.

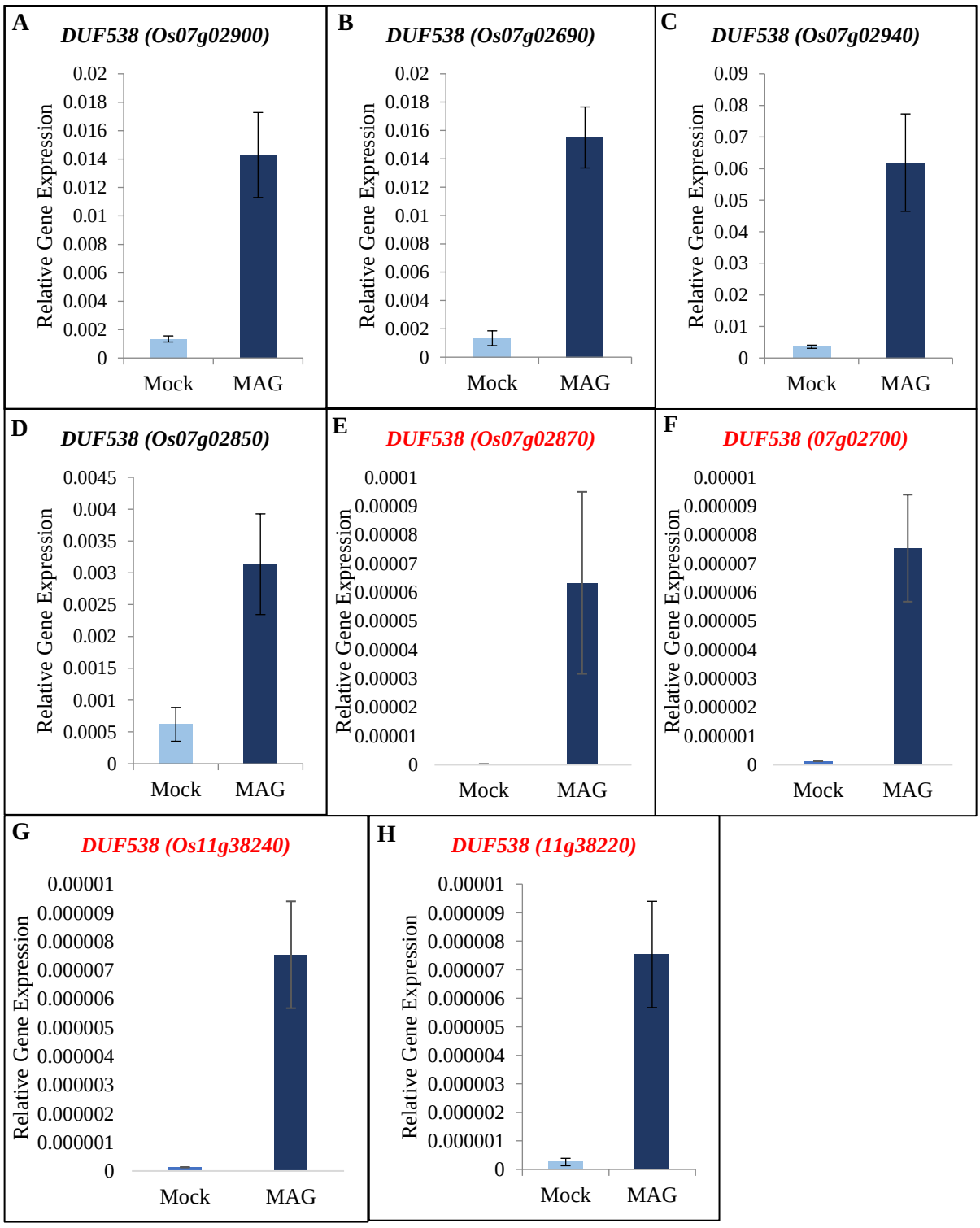

Figure 3.14: Molecular quantification of *DUF538* transcript levels in *M. oryzae* colonised (MAG) and non-colonised (Mock) rice roots. Expression of *DUF538* genes was normalised to the expression (geomean) of three *O. sativa* housekeeping genes (*Cyclophilin*, *GAPDH* and *Ubiquitin*). Four genes were induced (**A-D**), one gene was very lowly expressed (**E**) and the transcript of three genes were not detectable by qPCR (**F, G, H**; indicated in red) in *M. oryzae* colonised rice roots. Bars represent the means of three biological replicates (n = 1) ± SEM.

Gene Locus ID (LOC)	Description	Expression (Ri)	Expression (Mock)	Fold change	Expression (Mag)	Expression (Mock)	Fold change
Os07g02880 (Affymetrix)	DUF538 domain containing protein, putative, expressed	888	49	**18**	381	48	**8**
qPCR		Induced	NI		Induced	NI	
Os07g02920 (Affymetrix)	DUF538 domain containing protein, putative, expressed	583	18	**32**	342	24	**14**
(qPCR)		Induced	NI		Induced	NI	
Os11g38210 (Affymetrix)	DUF538 domain containing protein, putative, expressed	284	13	**22**	186	11	**17**
(qPCR)		Induced	NI		Induced	NI	
Os11g38240 (Affymetrix)	DUF538 domain containing protein, putative, expressed	602	18	**33**	104	12	**9**
(qPCR)		Induced	NI		NI	NI	
Os07g02960 (Affymetrix)	DUF538 domain containing protein, putative, expressed	1626	111	**15**	699	50	**14**
(qPCR)		Induced	NI		Induced	NI	
Os07g02850 (Affymetrix)	DUF538 domain containing protein, putative, expressed	683	89	**8**	379	53	**7**
(qPCR)		NI	NI		Induced	NI	
Os07g02870 (Affymetrix)	DUF538 domain containing protein, putative, expressed	11	13	**0.8**	Not found		
(qPCR)		NI			NI		
Osg07g02940 (Affymetrix)	DUF538 domain containing protein, putative, expressed	1455	180	**8**	Not found		
(qPCR)		NI			Induced	NI	
Os07g02700 (Affymetrix)	DUF538 domain containing protein, putative, expressed	Not found			Not found		
(qPCR)		NI	NI		NI	NI	
Os07g02900 (Affymetrix)	DUF538 domain containing protein, putative, expressed	Not found			Not found		
(qPCR)		Induced	NI		Induced	NI	
Os11g38220 (Affymetrix)	DUF538 domain containing protein, putative, expressed	Not found			Not found		
(qPCR)		NI	NI		NI	NI	

Table 6: Affymetrix microarray and qPCR-based gene expression profile of 11 *DUF538* genes in *R. irregularis* and *M. oryzae* colonised and non-colonised rice roots. The table shows the fold change

gene expression values of all *DUF538* genes in inoculated and non-inoculated rice roots as shown by the Affymetrix microarray data. Affymetrix gene expression data were validated by qRT-PCR. Induced genes are denoted as 'Induced', whereas non-induced genes are denoted as 'NI'. Genes that were not found in the Affymetrix microarray database (for both fungal interactions) are denoted 'Not found'.

3.5.2. Phylogenetic analysis of DUF538 proteins

A phylogenetic characterization of the rice DUF538 proteins was performed. This showed the clustering of the DUF538 proteins into two major clades based on the two chromosomes, 7 and 11, on which the corresponding genes are found. The eight DUF538s on chromosome 7 clustered in one clade, whilst the three DUF583s on chromosome 11 formed the other clade. As revealed by my molecular analysis, two *M. oryzae* specific DUF538 proteins (07g02850 and 07g02940) clustered in one clade whilst the only mycorrhizal-specific DUF538 *Os11g38240* was found on a separate clade (Figure 3.15). Interestingly, the five *DUF538* genes that were co-upregulated by *R. irregularis* and *M. oryzae* (green highlight on Figure 3.15), clustered within the two major clades, although four of them on chromosome 7 clustered together with the two *M. oryzae*-specific *DUF538* genes. Three *DUF538* genes absent in the Affymetrix microarray data and which were not expressed in either of the plant-fungal interactions based on the qPCR analysis, appeared close to each other on the phylogenetic tree (red highlight, Figure 3.15), although it is not exactly clear whether this has any relevance to the biological function of the *DUF538* superfamily of genes.

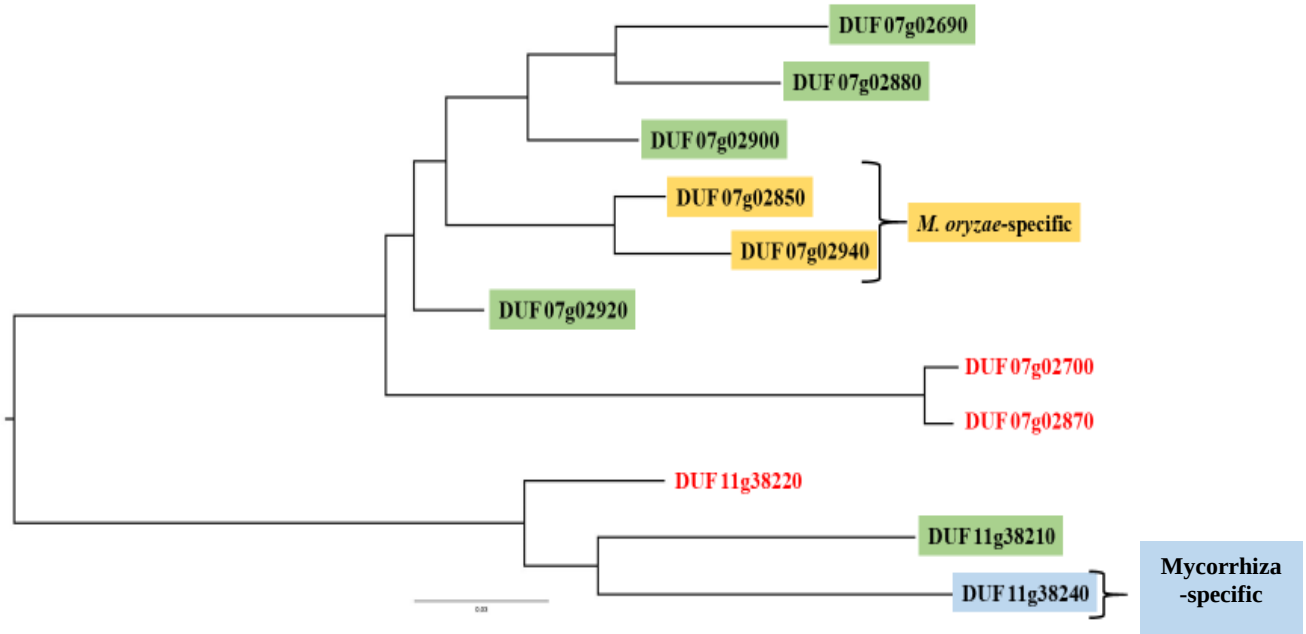

Figure 3.15: Maximum-likelihood phylogenetic tree showing the clustering of 11 DUF538s expressed in *O. sativa*. The DUF538 proteins cluster into two major clades based on the two chromosomes in which their corresponding genes are found. *M. oryzae*-specific DUF538s (yellow) cluster together on a clade separate from the mycorrhiza-specific DUF538 protein (blue). Five DUF538s (green) are co-induced by both fungi, whilst three DUF538s (red) are not induced by either fungus.

3.5.3. The functional role of *OsDUF538* genes during rice root colonisation by *R. irregularis* and *M. oryzae*

To understand whether OsDUF538 proteins of unknown function have any biological function during the colonisation of rice roots by *R. irregularis* and *M. oryzae*, multiplex CRISPR-Cas9 gene editing technology was employed to perturb *OsDUF538* gene function in rice. Although gene expression analyses showed that only five *OsDUF538* genes (*Os07g02880*, *Os07g02920*, *Os07g02690*, *Os07g02900* and *Os11g38210*) are significantly co-upregulated in both *Rhizophagus* and *Magnaporthe* rice root interactions, the ideal reverse genetics approach would have been to knockout all 11 *DUF538* genes expressed in rice to avoid any redundancy effect. While this appeared challenging, it was decided to design a multiplex CRISPR-Cas9 approach to simultaneously edit as many *DUF538* genes as possible in parallel. This was done using a single guide RNA designed from one *DUF538* gene (*Os07g02880*), which is co-induced in rice root colonisation by both *R. irregularis* and *M. oryzae*. The *DUF538* genes have a high level of similarly at the nucleotide sequence level (Figure 3.16), thus permitting the targeting of multiple of *DUF538* genes with a single guide RNA.

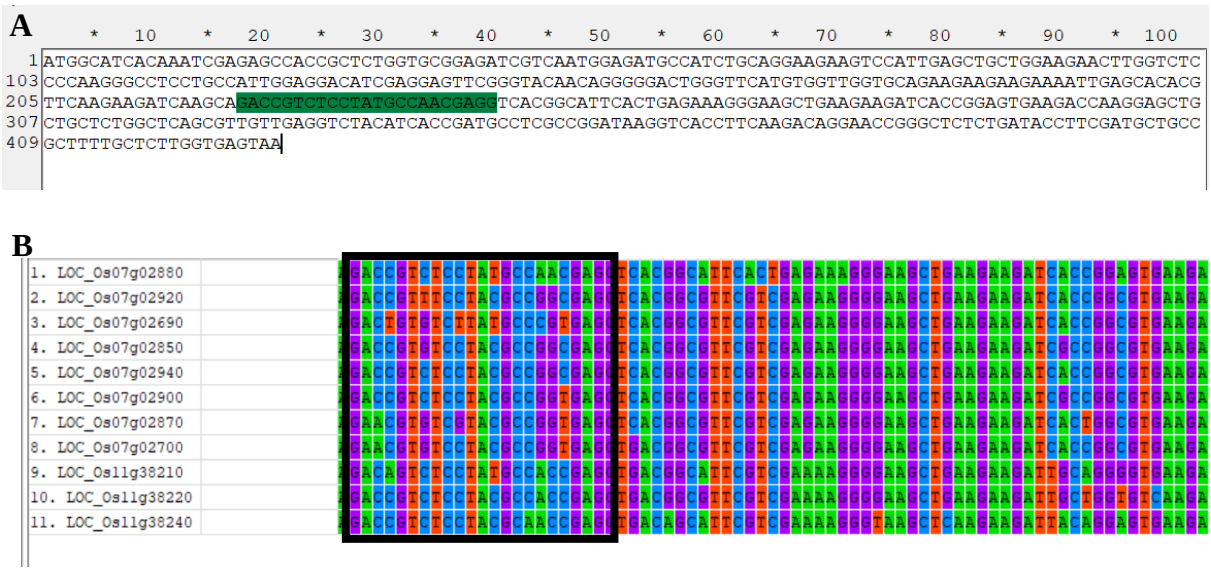

Figure 3.16: A schematic showing the nucleotide sequence of *OsDUF538* genes. The single guide RNA sequence of *DUF538 (Os07g02880)* is shown in the gene coding sequence (CDS) region (**A**). Alignment of all 11 rice DUF538 genes reveals highly conserved regions (**B**). The sgRNA sequence region is highlighted in the black box.

The single guide RNA (**GAC CGT CTC CTA TGC CAA CG AGG**) used for the gene editing consists of 23 nucleotide sequences including three base Protospacer Adjacent Motif (PAM) site (green). The sequence is located at positions 222 to 245 from the *DUF538_Os07g02880* transcription start site (ATG) in the rice genome (Figure 3.17). An alignment of all 11 DUF538 gene (Figure 3.16B) and protein (not shown) sequences revealed highly conserved regions among the genes.

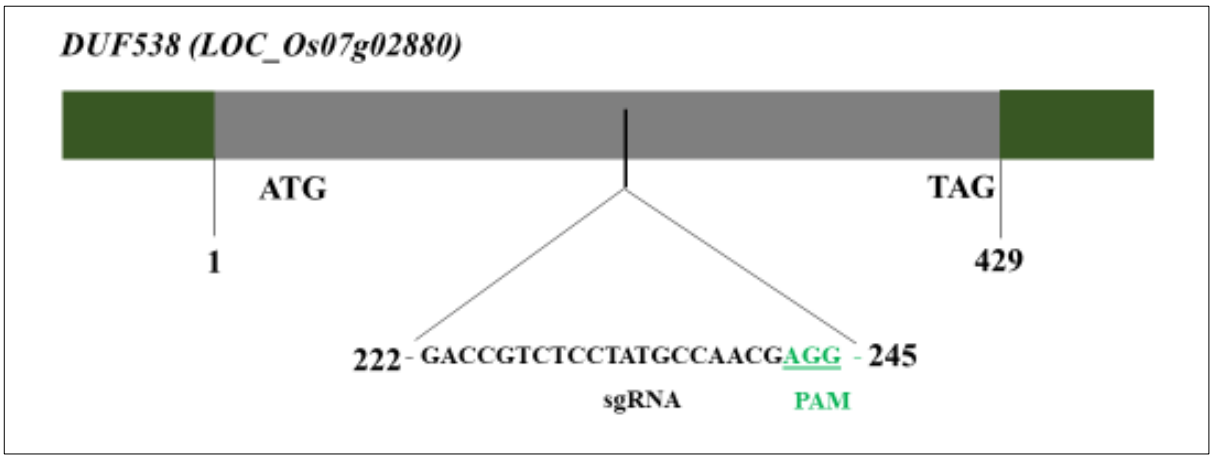

Figure 3.17: A schematic diagram showing the sgRNA sequence position in the CDS region of DUF538 (Os07g02880). The CDS region (429 base pairs) begins with a transcription start site (ATG) and ends with a stop codon (TAG). The sgRNA with a PAM site (green) is located between 222 to 245 in the CDS region.

Following the introduction of the single guide RNA (sgRNA) sequence into an entry vector (Figure 3.18A), and subsequent ligation with a destination vector (Figure 3.18B) containing cas9, successful constructs (see appendix for final construct) were introduced into rice seedlings by agrobacterium transformation. A total of 31 primary transformants and four empty vector control plants were produced. Initial screening of the primary regenerants by genotyping and Sanger sequencing led to the identification of successful gene editing events in seven seedlings at the T0 generation (Figure 3.19). Four of these lines were characterized further at the T2 generation (Table 7).

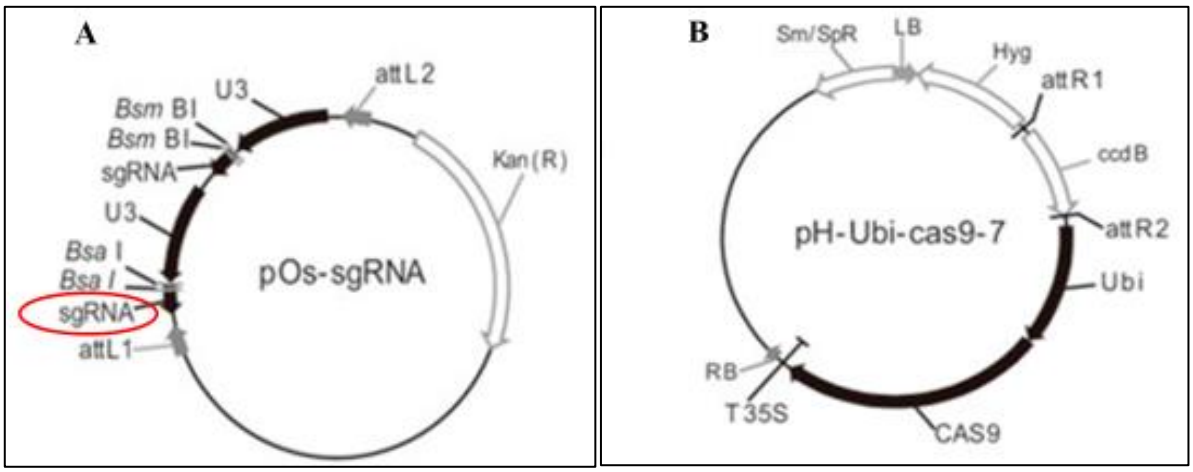

Figure 3.18: Schematic diagram of the vectors used for the CRISPR-Cas9 gene editing. The sgRNA was introduced into the entry vector and subsequently ligated (via an LR reaction) to the destination vector, which contains Cas9. (Schematic was modified from Miao et al., 2013).

T0 generation	***DUF538 (Os07g02880)***
UP87.18A	1 bp insertion
UP87.13	4 bp del
UP87.4	7 bp del
UP87.3	5 bp del + single base substitutions
UP87.1	15 bp del
UP87.11	5 bp del + single base substitutions

A

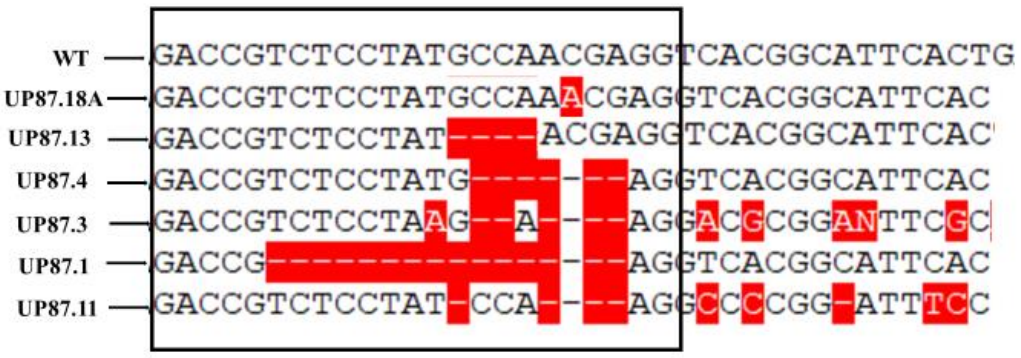

Figure 3.19: DUF538 genes with successful edits in the target sgRNA region. Genotyping and sequencing of genomic DNA from the CRISPR-Cas9 primary regenerants revealed editing events, mainly deletions, insertions and single base substitutions within the sgRNA region (shown in box) of the *DUF538 (Os07g02880)* gene (A).

At the next generation (T2), genotyping by sequencing were performed on the four selected lines. This also included a test for the presence or absence of Cas9 nuclease activity. Interestingly, a few more *DUF538* genes were edited in the plants (Table 7), with Cas9 either present or absent in the different segregating plant populations. The highest number of edited genes were seen in the *duf538.up87.13* gene edited line. One of these lines (*duf538.up87.13*$^{+}$) still had Cas9 nuclease function and failed to produce seeds (Figure 3.20), whereas the line without Cas9 activity (*duf538.up87.13*$^{-}$) produced seeds and was phenotyped (Figure 3.25).

T2 generation	**Os07g02880**	**Os07g02920**	**Os07g02900**	**Os07g02850**	**Os07g02690**	**Os07g02940**	**Os07g02870**	**Os07g02700**	**Os11g38210**	**s11g38220**	**Os11g38240**
UP87.1 (-Cas9)	-	-	-	-	-	-	+	+	-	-	-
UP87.11 M1 (-Cas9)	+ (4bp del)	-	-	-	-	-	-	+	-	+	-
UP87.13 M3 (+Cas9)	+ (4bp del & 1 base sub)	-	+	+	+	-	+	+	+	-	-
UP87.13 M7 (-Cas9)	++++	-	+	-	+	-	+	+	+	+	-
UP87.18b M7 (-Cas9)	+	-	+	-	-	-	-	+	+	-	+

Table 7: Genotyping by sequencing data of selected CRISPR-Cas9 *OsDUF538* gene edited plants at T2 generation. (+) indicates the presence of a single base mutation (deletion, insertion or substitution) whereas (-) indicates the occurrence of no mutation. (++++) indicates there is a 4 bp insertion.

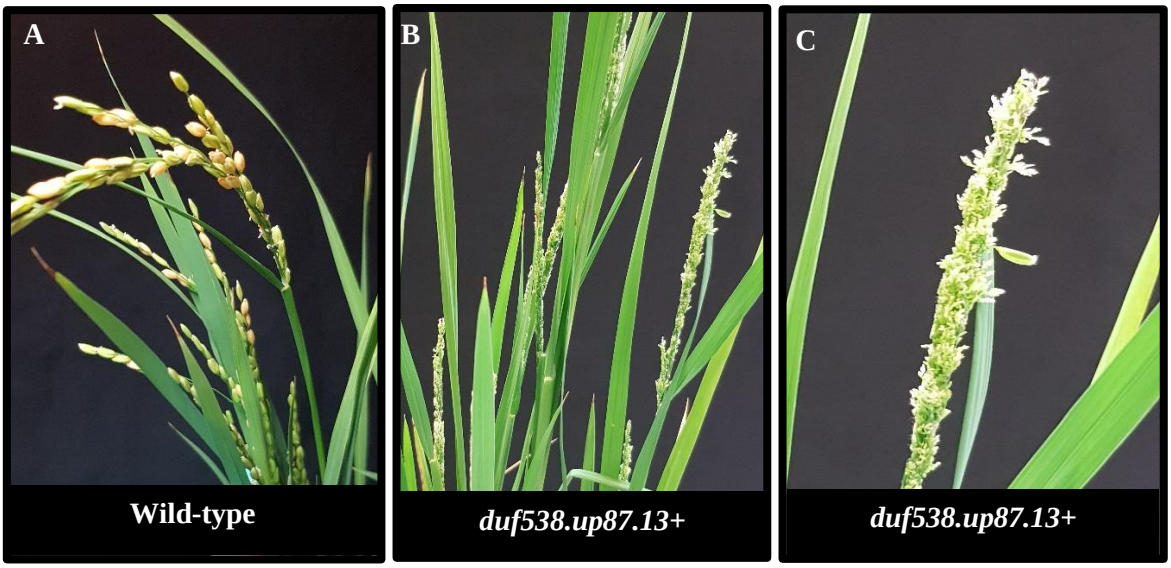

Figure 3.20: CRISPR-Cas9 gene edited *duf538.up87.13*$^{+}$ rice plants. The mutant line failed to produce seeds at the T2 generation (**B-C**) compared to the wild-type (**A**). It had the highest number of successfully edited genes, possibly due to the presence of Cas9 into the next generation.

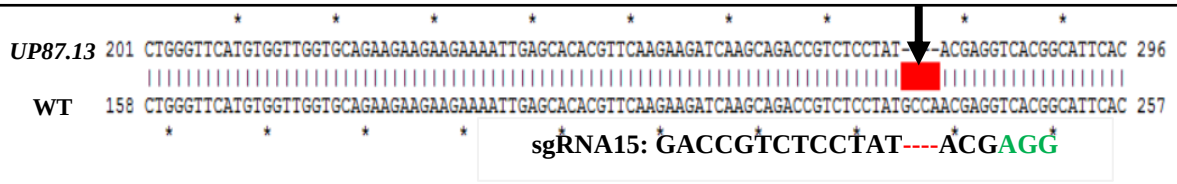

Figure 3.21: A schematic showing the sequence alignment of WT (Nipponbare) and CRISPR-Cas9 gene edited *UP87.13* (*duf538.up87.13)* plant at T0. Sanger sequencing revealed a 4 bp deletion mutation (red highlight) in the single guide RNA region of the *OsDUF538 (Os07g02880)* target gene, which is located in the middle of the gene CDS region (see Figure 3.16). The sgRNA protospacer adjacent motif (PAM) sequence is indicated in green.

Another interesting gene editing event was seen in the *UP87.1* line, which had a 15 bp deletion in the sgRNA region of *DUF538 (Os07g02880)* at T0 (Figure 3.21). However, the primary regenerant of this line was only able to produce two seeds after a very long delay (i.e. when other regenerants were at T2 generation). One seed germinated and was propagated for seed production (T2). Seedlings from five seeds (*UP87.1*, T2 generation) were genotyped and sequenced to determine how many of the *DUF538* genes were edited and whether the plants still possessed Cas9 activity. Interestingly, Cas9 activity had been lost from all the genotyped plants, but also, the 15 bp deletion detected in the primary regenerant (Figure 3.19) was no longer seen in these T2 plants. Instead, a single base substitution and deletion were found in two *OsDUF538* genes (*Os07g02700* and *Os07g02870*) (Table 7), which are not induced in rice roots by either *R. irregularis* or *M. oryzae* as shown by our molecular analysis. The absence of the 15 bp deletion in the T2 plants may be attributed to the poor seed production and low seed number in a segregating plant population.

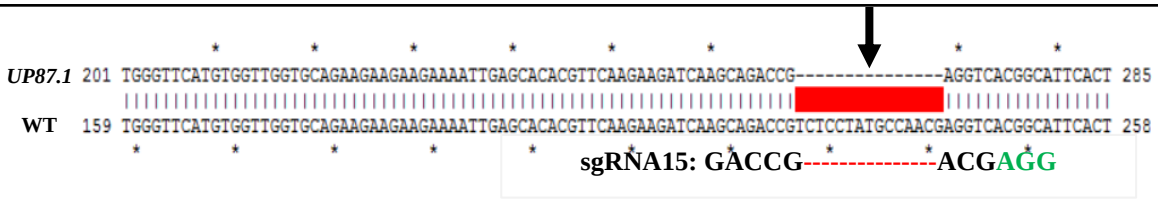

Figure 3.22: A schematic showing the sequence alignment of WT (Nipponbare) and CRISPR-Cas9 gene edited *UP87.1* plant at T0. Sanger sequencing revealed a 15 bp deletion mutation (red highlight) in the single guide RNA region of the *OsDUF538 (Os07g02880)* target gene, which is in the middle of the gene CDS region. The sgRNA protospacer adjacent motif (PAM) sequence is indicated in green.

The *UP87.11* gene edited line successfully had a 4 bp deletion (homozygous) in the sgRNA region of the target *DUF538 (Os07g02880)* gene at T0, with functional Cas9 nuclease activity (Figure 3.22). Upon propagation to the T2 generation, the 4 bp deletion in the sgRNA region of *DUF538 (Os07g02880)* was retained, but an additional DUF538 gene (*Os07g02700*), which is not induced by *R. irregularis* or *M. oryzae* was edited with several types of mutations, especially single base substitutions. Five bases were substituted inside the sgRNA region and several others occurred across the CDS region of this gene (Figure 3.23). Due to the loss of Cas9 activity in the T2 generation, this plant was phenotyped as shown in subchapter 3.5.4.

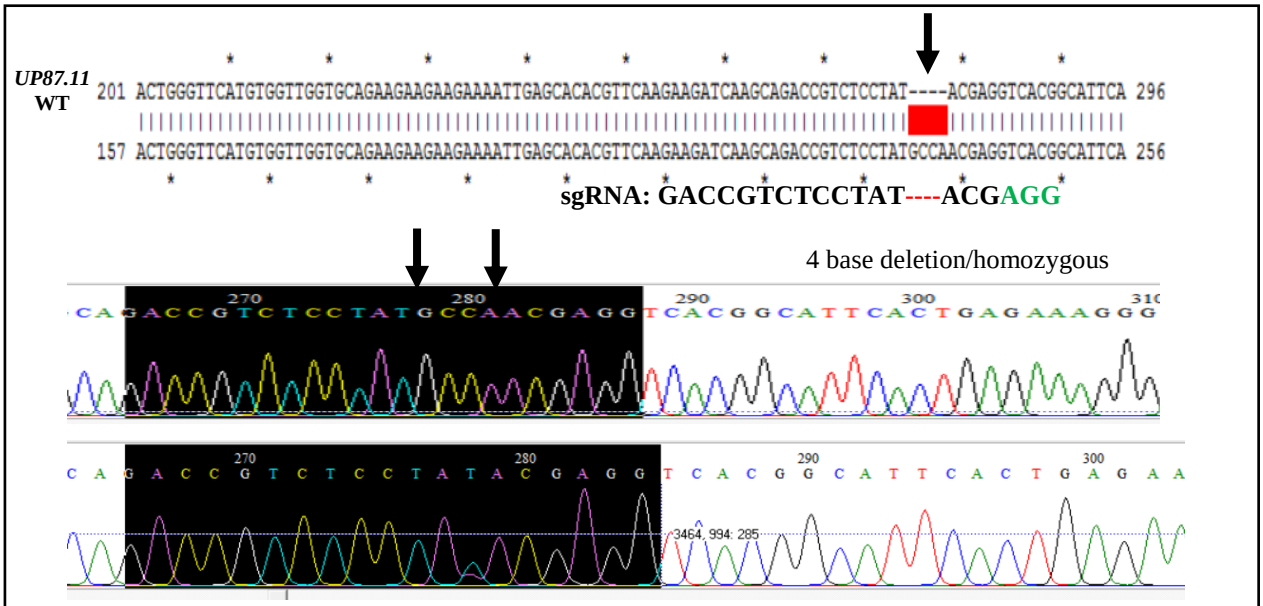

Figure 3.23: A schematic showing the sequence alignment of WT (Nipponbare) and CRISPR-Cas9 gene edited *UP87.11* plant at T0. Sanger sequencing revealed a 4 bp homozygous deletion mutation (red/black highlight with arrows) in the sgRNA region of the *OsDUF538 (Os07g02880)* target gene. The sgRNA protospacer adjacent motif (PAM) sequence is indicated in green.

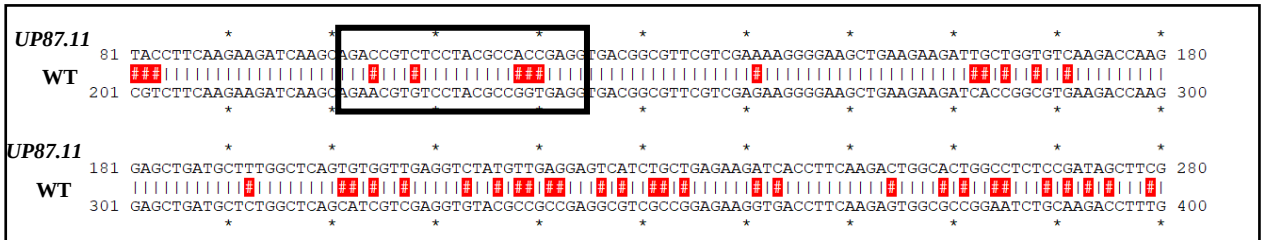

Figure 3.24: An alignment of the CDS region of WT and *UP87.11* gene edited CRISPR-Cas9 plants. Sanger sequencing revealed several single base substitutions in the CDS region of *DUF538 (Os07g02700)*. The sgRNA region is highlighted in rectangular box.

3.5.4. Phenotypic characterization of *R. irregularis* inoculated *OsDUF538* CRISPR-Cas9 gene edited plants

To determine whether perturbation in *DUF538* gene function caused any phenotypic aberration in rice roots inoculated with *R. irregularis* or *M. oryzae*, four mutant lines were selected and phenotyped based on the number of edited *DUF538* genes. Four mutant lines were phenotyped after colonisation experiments with *R. irregularis* (*duf538.up87.11*, *duf538.up.13 and duf538.up.18b*) and *M. oryzae* (*duf538.up87.18b* and *duf538.up87.1*). Following trypan blue staining of colonised rice roots at 5 wpi, total root length colonisation by *R. irregularis* structures was quantified. Experimental results showed no difference in the total level of colonisation in *duf538.up87.11* plants compared to the WT (Figure 3.25). However, a significant reduction ($P < 0.01$) in the total level of colonisation was seen in *duf538.up87.13* and *duf538.up87.18b* compared to the wildtype (Figure 3.26, 3.27).

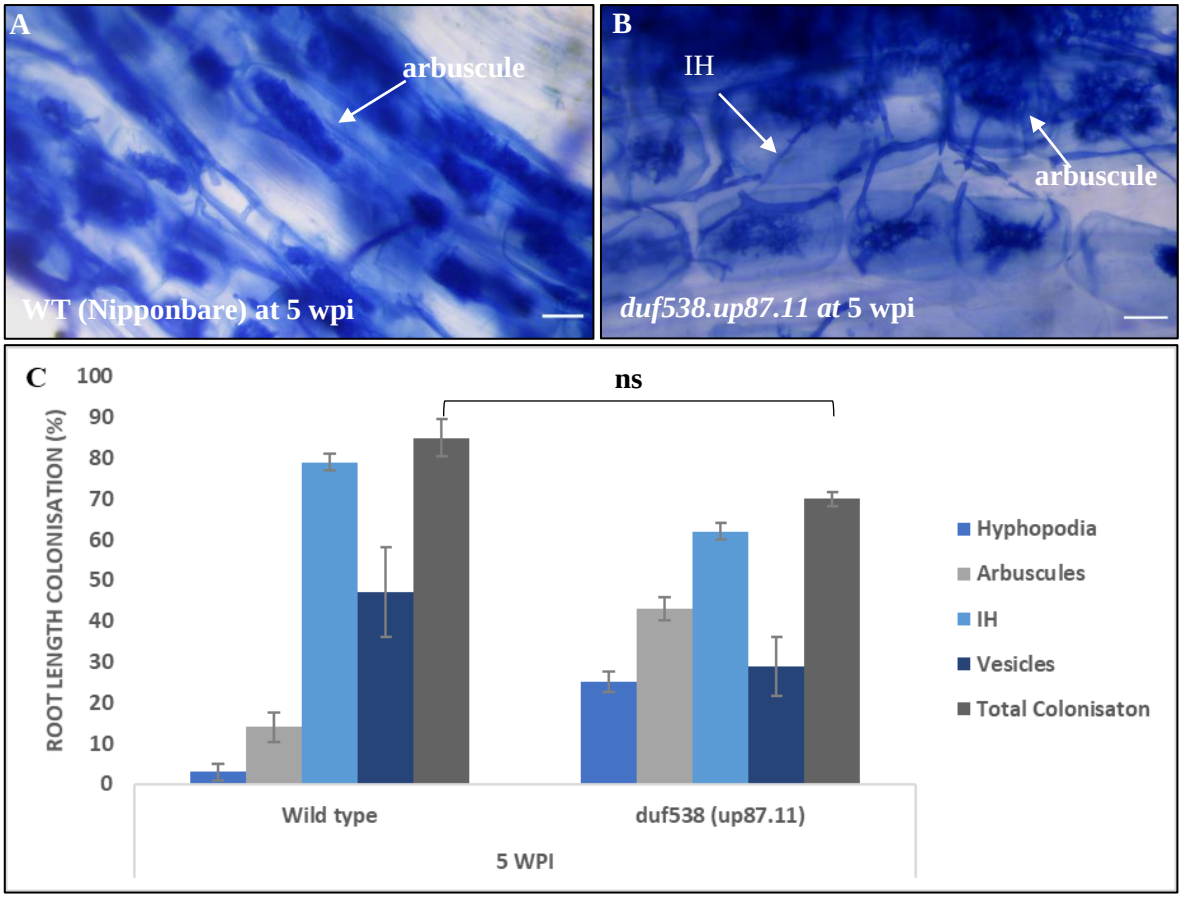

Figure 3.25: Quantification of fungal infection structures in WT and *duf538.up87.11* CRISPR-Cas9 gene edited mutant lines. The occurrence of fungal colonisation structures such as hyphopodia, vesicles, arbuscules (arrow) and intra-radical hypha (IH) in trypan blue-stained root pieces is shown as percentage of the total number of root pieces assessed (**C**). Fungal infection structures in the WT (**A**) and mutant (**B**) were quantified at 5 wpi. Bars represent the average of 3 biological replicates ± SEM

(in one experiment). Asterisks indicate significant differences between the WT and *duf538.up87.11*. (Student's *t*-test; *, P < 0.05; **, P < 0.01; ***, P < 0.001, ns, not significant). Scale bar = 10 µm.

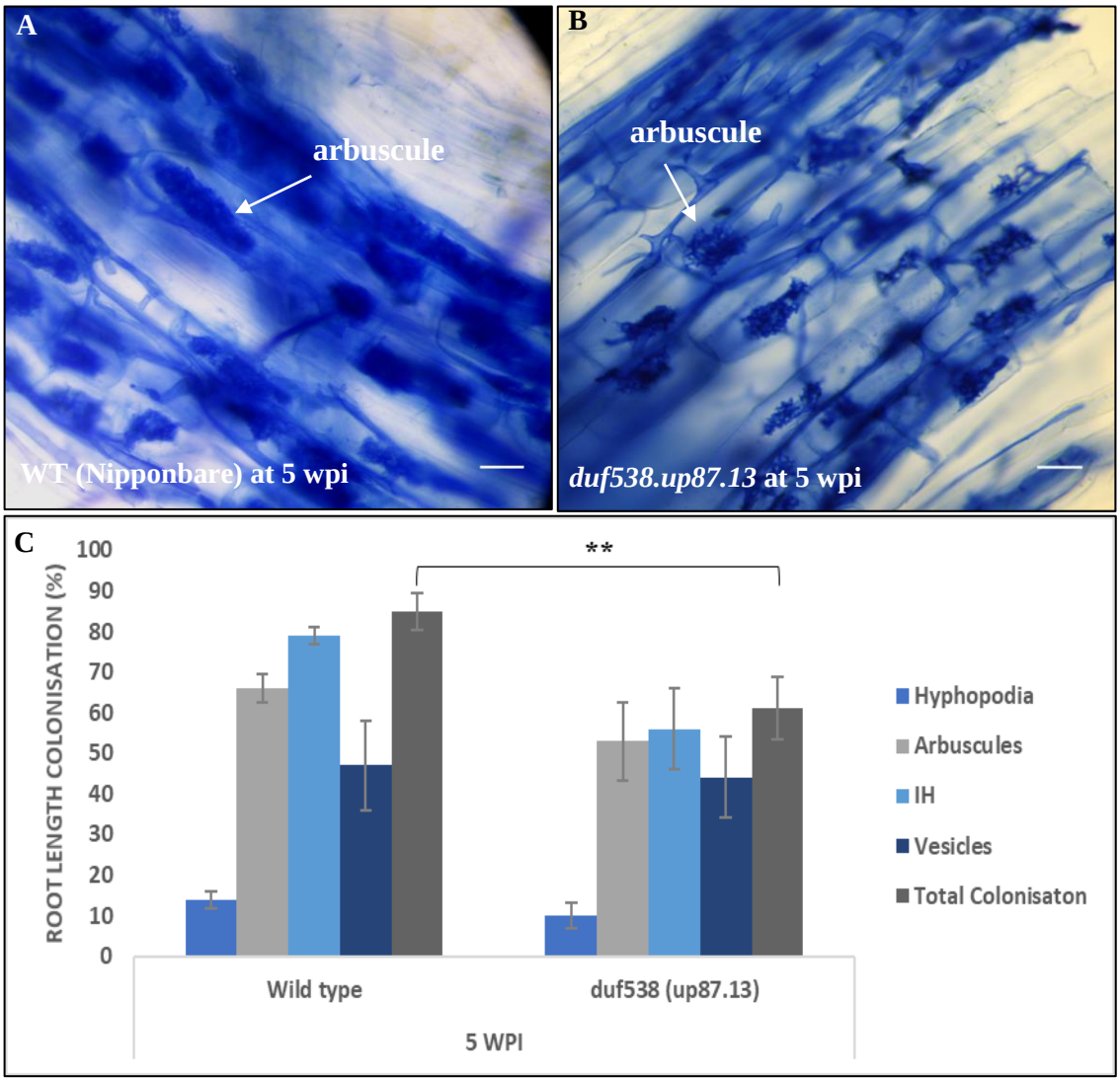

Figure 3.26: Quantification of fungal infection structures in WT and *duf538.up87.13* CRISPR-Cas9 gene edited mutant lines. Fungal infection structures are seen in the WT (**A**) and mutant (**B**) at 5 wpi. Root length colonisation shows a 24% reduction (P < 0.01) in total fungal colonisation in *duf538.up87.13* mutants relative to the WT (**C**). Bars represents the average of three biological replicates ± SEM (in one experiment). Asterisks indicate significant differences between the WT and *duf538.up87.13* (Student's *t*-test; *, P < 0.05; **, P < 0.01; ***, P < 0.001). Scale bar = 10 µm.

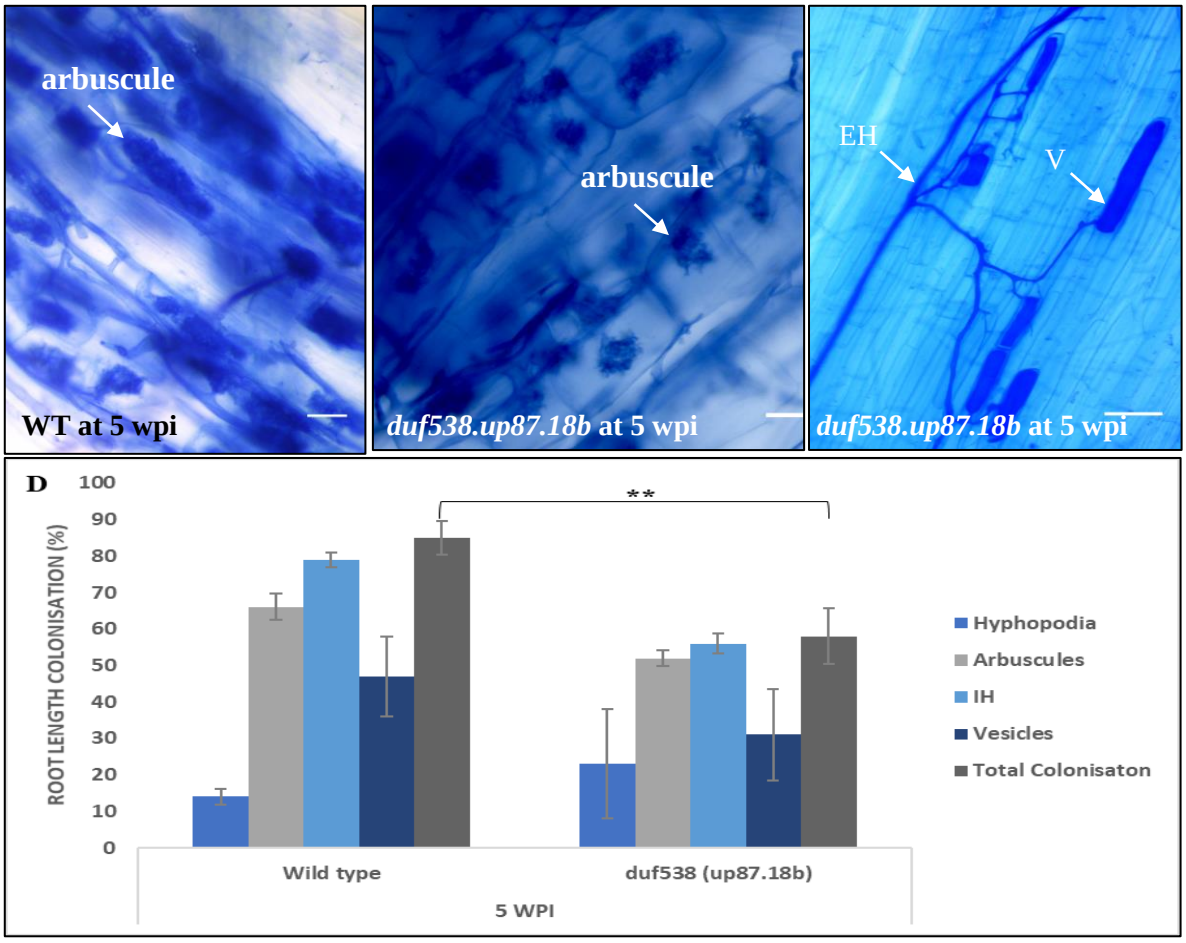

Figure 3.27: Quantification of fungal infection structures in WT and *duf538.up87.18b* CRISPR-Cas9 gene edited mutant lines. Fungal infection structures, e.g. arbuscules are seen in the WT (**A**) and mutant (**B**) at 5 wpi. In addition, vesicles (V) connected to extraradical hyphae (**C**) are seen in the mutants. Root length colonisation shows a 27% reduction ($P < 0.01$) in total fungal colonisation in *duf538.up87.18b* mutants relative to the WT (**D**). Bars represents the avearge of three biological replicates ± SEM (in one experiment). Asterisks indicate significant differences between the WT and *duf538.up87.13* (Student's *t*-test; *, $P < 0.05$; **, $P < 0.01$; ***, $P < 0.001$). Scale bar = 10 µm.

3.5.5. Phenotypic characterization of the *M. oryzae* colonisation of *OsDUF538* CRISPR-Cas9 gene edited plants

To determine whether *M. oryzae* colonisation of gene edited *duf538* rice lines was altered relative to the WT plants, two mutant lines (*duf538.up87.1* and *duf538.up87.18b*) were selected and inoculated with *M. oryzae*. These lines were selected based on the number of edited *DUF538* genes (Table 7) and availability of seeds. Also, due to the shortage of time to produce enough seeds, other *duf538* mutant lines were not fully characterized with regards to their *M. oryzae* infection phenotype. Notably, *duf538.up87.18b* was the only mutant line assessed for both *Magnaporthe* and mycorrhizal phenotypes. Following a time-course experiment, live-cell confocal imaging of inoculated *duf538.up87.1* and *duf538.up87.18b* root pieces revealed no

obvious phenotypic difference between the mutants and the WT at 4- and 7 dpi, respectively (Figure 3.28). GFP-expressing *M. oryzae* grew intracellularly, crossing over from cell to cell in both mutants and the WT at both time points. qPCR-based gene expression analysis showed no significant difference in the level of *M. oryzae* colonisation in the mutants relative to the WT (Figure 3.29). The level of fungal colonisation was determined by quantifying the expression of three *M. oryzae* housekeeping genes (*MoActin*, *MoTubulin* and *Mo40s8*), which are constitutively expressed in rice roots colonised by *M. oryzae* (Figure 3.29).

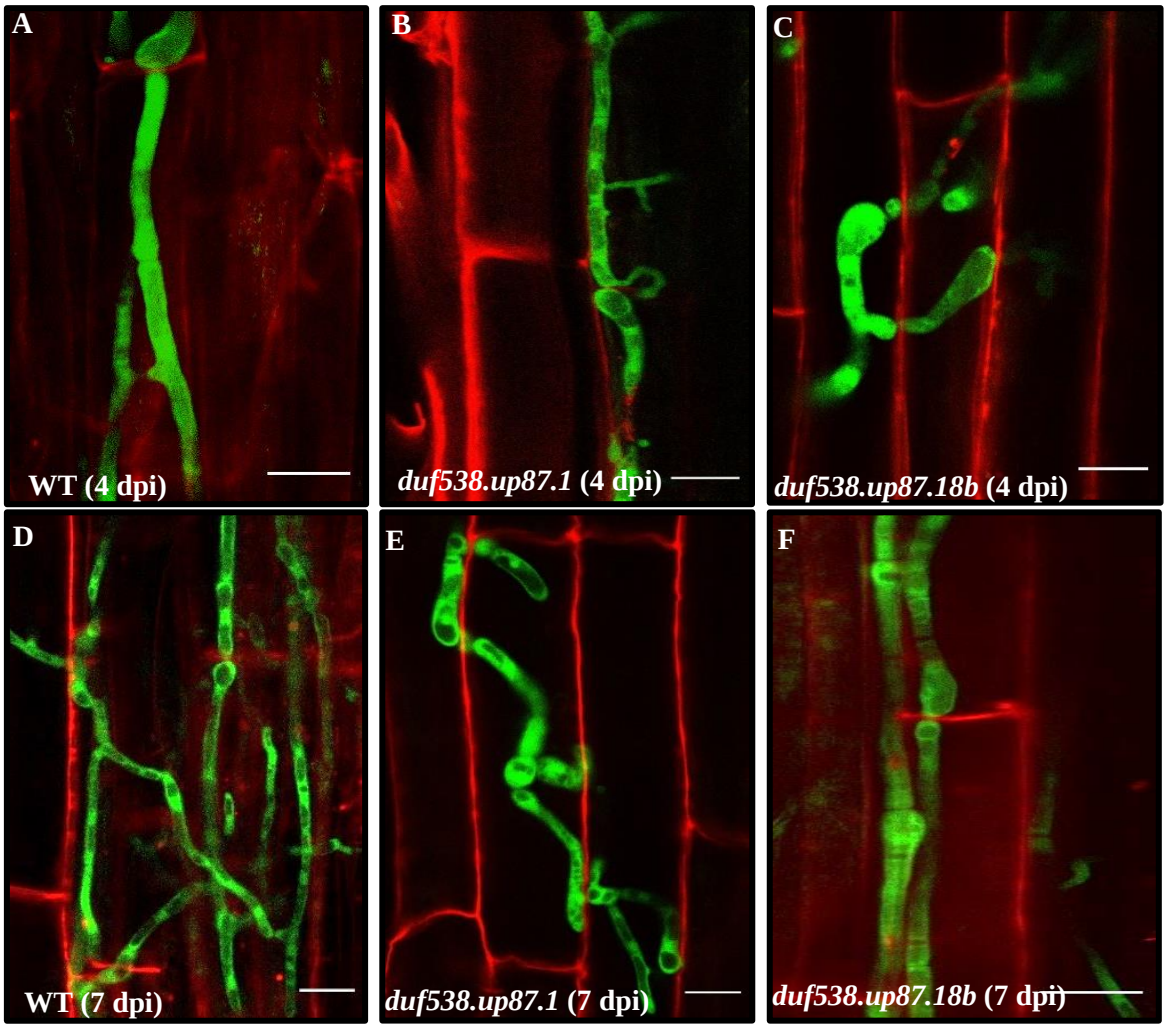

Figure 3.28: Live-cell confocal imaging of *M. oryzae* colonised WT and *duf538* CRISPR-Cas9 mutant rice lines. *M. oryzae* proliferates from cell to cell in both the WT and *duf538* mutants at 4 and 7 dpi, respectively (**A-F**). (Scale bar = 50µm). Images represent three biological replicates in one experiment.

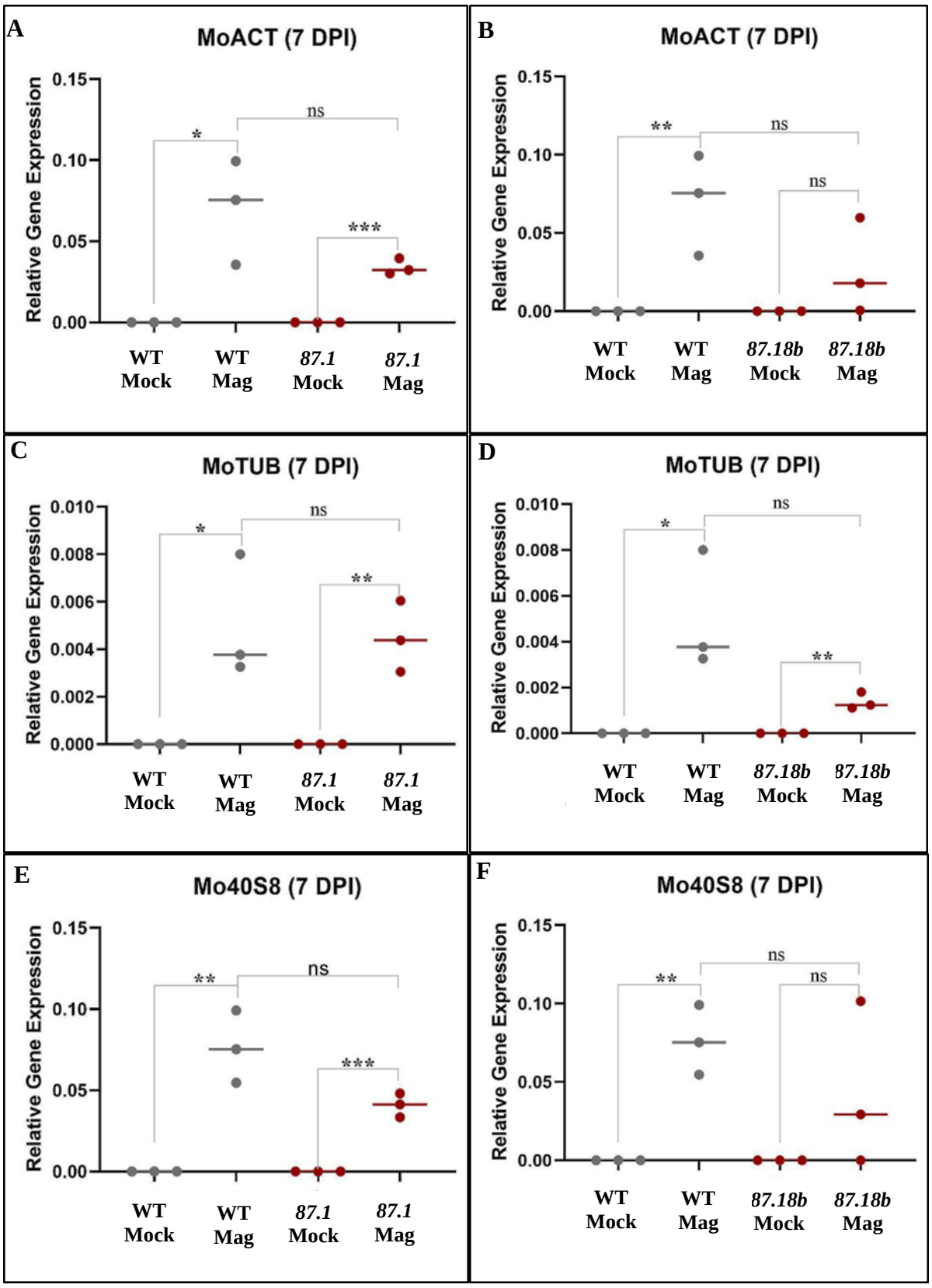

Figure 3.29: Quantification of *M. oryzae* molecular biomass in colonised WT and *duf538* CRISPR-Cas9 mutant rice roots at 7 dpi. The expression levels of three *M. oryzae* housekeeping genes (*MoActin*, *MoTubulin* and *Mo40s8* ribosomal protein) were normalized to the expression of three rice housekeeping genes (*Actin*, *GAPDH* and *Ubiquitin)*. Bars represent means of three biological replicates ± SEM (in one experiment). Asterisks indicate significant differences between expression levels in *M. oryzae* colonised versus non-colonised roots of the same genotype. (ANOVA, *, $P < 0.05$; **, $P < 0.01$; ***, $P < 0.001$, n.s., $P > 0.05$).

3.5.6. Discussion

In this sub-chapter, I discovered a novel subset of rice *DUF53*8 domain containing proteins of unknown function, which are induced in response to colonisation by both *R. irregularis* and *M. oryzae*. These genes (*Os07g02880*, *Os07g02920* and *Os11g38210*) were identified through computational analysis of two independent, previously published transcriptomic studies (Marcel et al., 2010; Gutjahr et al., 2015). qPCR-based gene expression analysis confirmed the co-induction of these genes (*Os07g02880, Os07g02920* and *Os11g38210*), as well as two other *DUF538 genes* (*Os07g02960* and *Os07g02900*) during rice root interaction with both mutualistic and detrimental fungi (Figure 3.12, 3.13 and 3.14). These two additional genes were initially excluded by the filtering criteria set during the Affymetrix microarray data merging and gene selection process due to their high mock background (> 50) (Figure 3.1). However, gene expression analysis classified all 11 *OsDUF538* genes into four categories based on their expression pattern (Table 6). They are as follows; Mycorrhiza-specific *DU538* gene (*Os07g38240*), *Magnaporthe*-specific *DUF538* gene (*Os07g02850* and *Os07g02940*), not induced by either fungus (*Os07g02700, Os07g02870* and *Os11g38220*), and co-induced by both fungi (*Os07g02880*, *Os07g02920*, *Os07g02960*, *Os07g02900* and *Os11g38210*).

Considering that the biological role of *DUF538* genes in rice interactions with microbes is not yet known, we utilized a reverse genetics approach to investigate their function during rice root colonisation by *R. irregularis* and *M. oryzae*. This involved the application of a multiplex CRISPR-Cas9 gene editing approach using a single guide RNA, which was designed based on the close nucleotide sequence homology of the *OsDUF538* gene candidates. Surprisingly, this approach led to the successful targeting of up to seven *OsDUF538* genes (*duf538.up87.13*) as revealed by Sanger sequencing (Table 7). Several editing events were also seen in different combinations in other plants, but a few plants were selected for further characterization based on the number of genes successfully edited (Table 7).

Functional characterization revealed a possible subtle phenotype for *R. irregularis* but not for *M. oryzae* in one assessed *duf538 (duf538.up87.18b)* mutant line. The mutant lines *duf538.up87.18b* and *duf538.up87.13* were successfully edited in seven and five DUF538 genes, respectively (Table 7, Figure 3.19). Interestingly, both mutant roots showed a 24% ($P < 0.01$) and 27% ($P < 0.01$) reduction in colonisation by *R. irregularis* compared to the WT (Figure 3.26, 3.27). In contrast, no phenotypic difference was seen between the WT and two inoculated *duf538* mutant (*duf538.up87.18b* and *duf538.up87.1*) roots inoculated with *M.*

oryzae and assessed by live-cell confocal imaging (Figure 3.28) and qPCR (Figure 3.29). The absence of a phenotype in *M. oryzae* inoculated *duf538* mutant lines may be due to the combination of edited *DUF538* genes, which may be involved in rice root colonisation by *R. irregularis* and not *M. oryzae*. As the role of *DUF538* genes are relatively unknown in plant-microbe interactions, it is difficult to speculate the exact function of the genes, however, developing a more robust reverse genetics strategy to knock out all *DUF538* genes would perhaps, be the preferred approach to study the functional relevance of the genes during rice root colonisation by both fungi.

CHAPTER 4

General Discussion and Future Perspectives

The overall findings of this study support the hypothesis that there are common mechanisms of accommodation for both mutualistic and detrimental fungi in rice roots. While the first set of findings describe a novel shared role of plasma membrane receptor kinases during rice root colonisation by both *R. irregularis* and *M. oryzae* (Chapter 2), the transcriptome comparison in Chapter 3 led to the identification of new plant gene candidates that may be required for intracellular accommodation of both fungi in rice roots.

As is already known, rice roots engage in symbiosis with ancient symbiotic fungi such as *R. irregularis*, whilst resisting invasion of the detrimental fungus *M. oryzae*, which causes rice blast disease *via* leaf infection. Rice roots also associate with *M. oryzae*, where the pathogen utilises simple non-melanised hyphopodia to invade the roots (Sesma and Osbourn, 2004) as opposed to the mechanical force it uses to penetrate the leaf following melanised appressoria formation (Ryder and Talbot, 2015). It is quite fascinating how *M. oryzae* behaves during root colonisation, which in many aspects, resembles *R. irregularis* rice root colonisation. For example, the pathogen exhibits an extended biotrophic lifestyle in the root, where it does not seem to cause any loss of host cell viability (Marcel et al., 2010), perhaps until it migrates to the aerial parts of the plant (Sesma and Osbourn, 2014). In the leaf, it quickly switches to necrotrophy when the secondary invasive fungal hyphae invade new cells, causing necrotic disease lesions (Wilson and Talbot, 2009; Fisher et al., 2012). This difference in behaviour raises the question of whether *M. oryzae* adopts an endophytic lifestyle during rice root colonisation, possibly as a disguise to bypass the plant defence machinery whilst entering the host.

Understanding common plant genes and developmental programmes that support the accommodation of *M. oryzae* in rice roots is important, especially since the pathogen, in some ways, mimics *R. irregularis* colonisation in the root, although with no evidence of benefits to the plant. Nonetheless, it is possible that *M. oryzae* utilises a gene set that enables intracellular accommodation of *R. irregularis* in rice roots during AM symbiosis to advance its entry into the host root, hence the relevance of the findings made in this study.

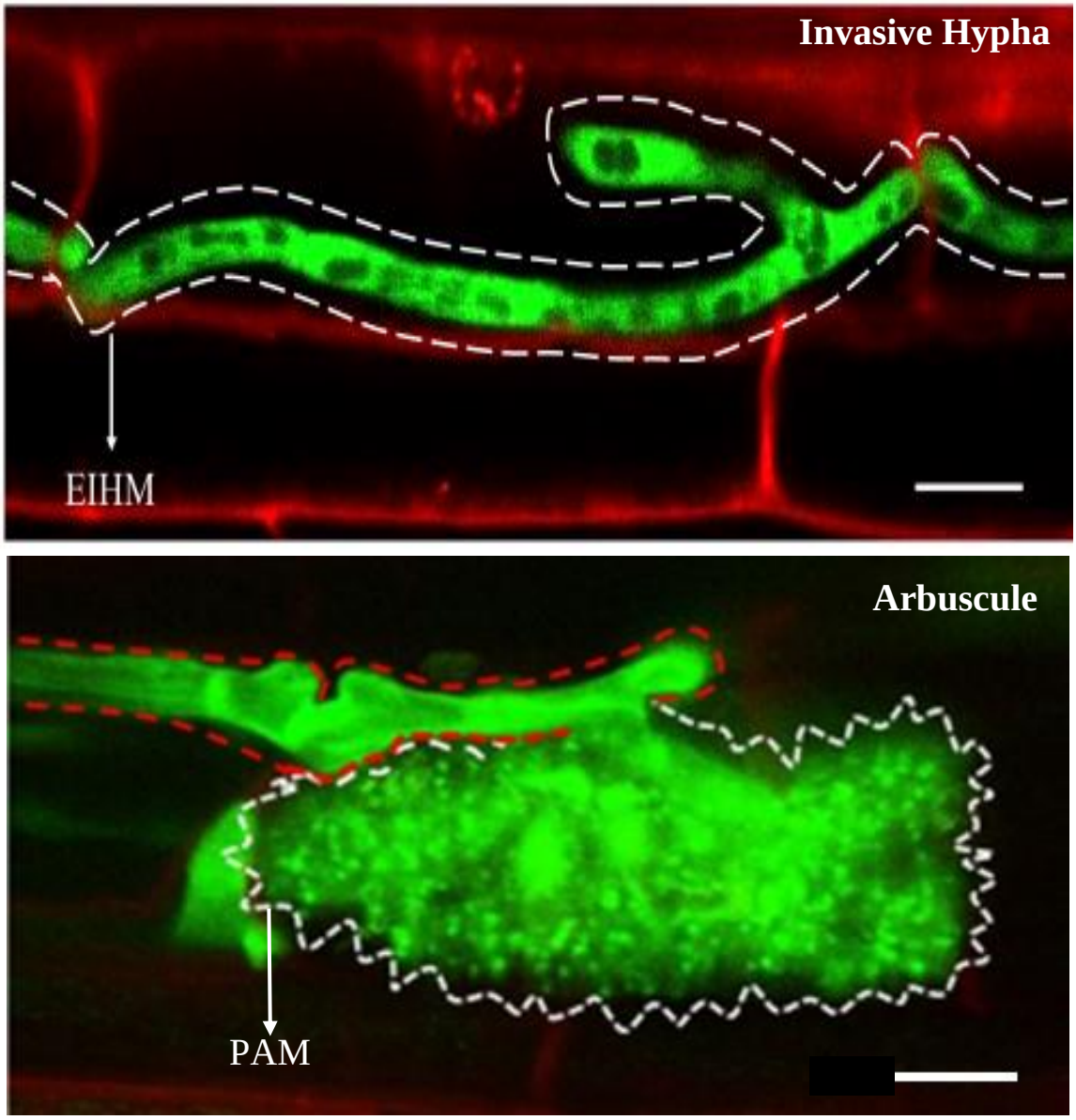

Figure 4.1: Confocal images showing the invasive hypha and arbuscule of *M. oryzae* and *R. irregularis* during rice root colonisation, respectively. *R. irregularis* forms arbuscules in inner cortical cells, whereas an *M. oryzae* invasive hypha grows intracellularly across all rice root types Arbuscules are surrounded by a plant-derived peri-arbuscular membrane (PAM), which is the site for nutrient exchange in the symbiosis, whilst *M. oryzae* is enveloped in a plant-derived extra-invasive hyphal membrane (EIHM), which is attributed to its prolonged biotrophic lifestyle in rice roots. *OsExo70-H3b* and *OsDUF538* may be involved in the biogenesis of the PAM and EIHM, which are crucial for intracellular accommodation of the fungi in rice roots. Scale bar = 50µm. Micrograph obtained using a modified protocol described in Marcel et al. (2010) and Kobae and Ohtomo (2016), respectively.

4.1. Plasma membrane receptors are involved in recognition and signalling during rice root invasion by *R. irregularis* and *M. oryzae*

In this study, plants carrying a mutation in *OsCERK1* displayed a mycorrhizal phenotype, with clusters of hyphopodia seen on the rice root surface, as well as significantly reduced levels of colonisation compared to the WT at early (3 wpi) colonisation (Chapter 2). Fungal colonisation of rice roots progressed normally at the later time point, with no qualitative differences in the infection structures observed at both time points. These results indicate a delay in the onset of mycorrhization in *cerk1* mutants compared to the wild-type and suggest that OsCERK1 is required for early AM symbiotic signalling as previously proposed (Miyata et al., 2014; Zhang et al., 2014).

The mycorrhiza phenotype seen in *cebip* mutants (which presented with clusters of hyphopodia on rice root surface and significantly low mycorrhization levels, especially during early colonisation relative to the WT) was unexpected. The striking similarity between the phenotypes seen in AM colonised *cerk1* and *cebip* mutants could suggest that *OsCERK1* and *OsCEBiP* function together to perceive and elicit symbiotic signals in AM symbiosis. This concept has been demonstrated in plant immunity signalling, where OsCERK1 and OsCEBiP form a receptor complex to perceive long-chain chitooligosaccharides (CO8) and activate defence responses in rice (Shimizu et al., 2010). In this scenario, OsCEBiP directly binds chitin oligosaccharides but is unable to elicit chitin signals due to the absence of an intracellular kinase domain (Shimizu et al., 2010). It therefore partners with OsCERK1, which does not bind chitin oligosaccharides, but can transduce signals *via* its intracellular kinase domain (Shinya et al., 2015; Liu et al., 2016).

In AM symbiosis OsCERK1 interacts with an unknown receptor kinase or protein to perceive mycorrhizal CO or LCO, and subsequently activates symbiotic signalling. However, in search of a possible interactor, both OsCEBiP and OsNFR5 were ruled out because *oscebip* and *osnfr5* mutants established symbiosis normally (Miyata et al., 2016). The failure to observe a phenotype in *cebip* mutants in the previous study is a stark contrast to our experimental findings, which suggest a role for OsCEBiP in AM symbiosis. A possible explanation for the discrepancy may be the experimental conditions used in the different studies, especially since both studies used the same mutant genotype (homologous recombination knockout mutants). Notably, our mycorrhizal experiments with *cebip* mutants was performed in a Petri dish system, which is considered a closed system, in that it retains more solution/water compared to the cone

system that is more efficient in water drainage. Although it is difficult to estimate the contribution this has to the observed mycorrhiza phenotypes in *cebip* because the experiments were performed in parallel with *cerk1* mutants and WT rice plants, more experiments will help to rule out possible artefactual effects.

Furthermore, this study identified a novel function of *OsCERK1, OsCEBiP* and *OsNFR5* during rice root invasion by *M. oryzae*. Rice plants with a mutation in each of the three LysM-RLKs/RLP displayed interesting phenotypes during *M. oryzae* rice root invasion at early (4 dpi) and late (7 dpi) colonisation stages (Chapter 2). In all mutants, fungal colonisation was significantly reduced ($P < 0.01$) compared to the WT at both time points, and except for colonised *cebip* roots, qualitative differences in fungal infection structures were seen in both *cerk1* and *nfr5* mutant roots at both time points. A striking phenotype was seen in *cerk1* mutant roots, where 31% of *M. oryzae* invasive fungal hyphae appeared dead and trapped inside rice root cells compared to the wild-type and *nfr5* and *cebip* mutants (5 %). In *nfr5* mutants, *M. oryzae* invasive hyphae appeared bulbous, ring-shaped and restricted inside rice root cells, with hyphal swellings in places where the fungus crossed cell wall junctions. These phenotypes suggest that all LysM-RLKs/RLP studied here act as compatibility factors during rice root invasion by the biotrophic pathogen *M. oryzae*, although the differences in the mutant phenotypes imply that they serve slightly different functions. For example, the hyphal death during intracellular growth of *M. oryzae* in *cerk1* mutants suggests that CERK1 is required for the sustenance of hyphal viability, which supports an endophytic lifestyle of *M. oryzae* during intracellular growth in rice roots. Alternatively, the fungal hyphal death may be a programmed cell death triggered by the host defence machinery to reduce or prevent disease symptoms, in the case where *M. oryzae* is perceived as a necrotrophic pathogen during intracellular growth in the root. This has been shown in *Arabidopsis*, where the host cells induced cell death in the necrotrophic fungus *Botrytis cinerea* by producing a phytolexin called camalexin (Shlezinger et al., 2011). The fungal anti-apoptotic machinery can protect the fungus from the host-induced programmed cell death, but it is unclear whether this example applies to other plant-parasitic microbe interactions.

Importantly, the predicted function of the plasma membrane receptors during *M. oryzae* rice root colonisation as shown in this study is surprising, especially since OsCERK1 and OsCEBiP play an opposite role during rice leaf infection with *M. oryzae*, where they activate immunity signalling to protect the plant, rather than enable infection. It also raises questions about how the plant perceives *M. oryzae* during root entry and whether the biotrophic pathogen releases

different types of signals depending on the plant organ they invade. With respect to this, studies have shown that the varying degree of polymerization (dp) of chitooligosaccharides (CO) released from microbial cell walls can determine the type of responses the microbes elicit. For example, in its unmodified form, COs (dp = 6-8) are strong inducers of plant immunity (Stacey and Shibuya, 1997; Kouzai et al., 2014; Liang et al., 2014), whereas the short chain COs (dp = 4-5) can trigger symbiotic signalling (Genre et al., 2013). When acetylated (lipo-chitooligosaccharides or LCOs) or further modified, COs can act as Nod factors to initiate legume-rhizobia symbiosis or as Myc-factors to initiate AM symbiosis (Liang et al., 2014). Undecorated chitin tetrasaccharide (CO4) and pentasaccharide (CO5) in germinating spore exudates (GSEs) of AM fungi are also found to elicit nuclear Ca^{2+} spiking. Ca^{2+} spiking can also be triggered by long-chain chitin oligosaccharides (> heptamers), which trigger immune responses, but to a lesser degree (Kaku et al., 2006; Genre et al., 2013).

Considering the influence of CO types in symbiotic and defence responses, one may speculate that *M. oryzae* releases a mixture of different types of microbial signals from its cell wall. These signals may vary in their chemical composition and abundance, and may cause the host cell to respond differently, depending on whether the signal is from leaf or root tissue. One possibility is that during rice root infection, *M. oryzae* secretes both short chain COs and LCOs similar to AM fungi (Akcapinar et al., 2015), and this may trigger 'endophyte-like' signals, thus permitting fungal invasion and intracellular accommodation. Unmodified long-chain COs (e.g. CO8) have been shown to induce immunity signalling during *M. oryzae* rice leaf infection (Akiyama and Hayashi, 2006). If this were the case in the root, then OsCERK1 could act as a common receptor to recognise and transduce the signal, possibly in partnership with OsCEBiP or other plasma membrane receptors. It is also probable that OsCEBiP may bind to chitin oligosaccharides released by *M. oryzae*, and through a receptor complex formation with OsCERK1 or another interactor with an active kinase domain, elicit signals that allow invasion of *M. oryzae* in the root. In the same way, OsNFR5 may bind 'Myc-LCO-like' signals from *M. oryzae*, and in collaboration with another receptor with an active intracellular kinase domain, activate signalling responses that enable *M. oryzae* to intracellularly colonise rice roots. It may be important to note that the interaction between OsNFR5 and OsCERK1 is highly unlikely because protein-protein interaction studies failed to observe the heterodimerization between both LysM-RLKs, although this was tested in *Nicotiana benthamiana* leaves (Miyata et al., 2016). However, OsNFR5 can cooperate with another receptor partner such as OsRLK1, OsRLK4, OsRLK5 or OsRLK7, which are expressed in roots (Shimizu et al., 2010; Miyata et al., 2016) to permit *M. oryzae* invasion of rice roots. Protein-protein interaction studies in

homologous systems will help to identify the interactors of OsNFR5 during *M. oryzae* rice root colonisation.

Another novel finding made in this study is that OsNFR5 acts as a compatibility factor for *M. oryzae* rice leaf infection rather than a defence receptor as described for OsCERK1. This is a particularly interesting finding because it suggests that OsNFR5 serves as a common receptor for perceiving a specific signal from *M. oryzae*, regardless of the plant organ the pathogen invades. This hypothesis is supported by our finding that OsNFR5 is required for the intracellular colonisation of *M. oryzae* in rice roots, but not for rice root colonisation by the symbiont *R. irregularis* (Miyata et al., 2016). However, it highlights the varying function of OsNFR5 in microbial signal perception, which has been shown in previous studies. For example, MtNFP (OsNFR5 homologue) was found to be involved in Myc-LCO-induced lateral root formation, changes in transcription and nuclear Ca^{2+} oscillations (Maillet et al., 2011; Czaja et al., 2012; Sun et al., 2015), but not for mycorrhization (Radutoiu et al., 2003; Amor et al., 2003; Zhang et al., 2015) or Myc-CO-induced nuclear calcium oscillations (Genre et al., 2013; Sun et al., 2015). However, an NFP orthologue in *Parasponia andersonii*, the only non-leguminous plant that can establish rhizobial symbiosis, was also found to play a role in both rhizobial and AM symbioses (Op den Camp et al., 2011). Both NFP and NFR5 orthologues in tomato (SLK10) were associated with successful arbuscular mycorrhizal colonisation (Buendia et al., 2016), but not OsNFR5 (Miyata et al., 2016), and MtNFP was shown to play a role in the perception of pathogenic signals leading to immunity against oomycete pathogens in *M. truncatula* (Rey et al., 2013). These opposing findings, in addition to ours, again support the notion that *M. oryzae* probably releases signals varying in structure, chemical composition and abundance, which may influence the host cell to respond differently, depending on whether the signal is from leaf or root tissue.

Overall, the interconnectivity of the downstream signalling responses of LysM-RLKs and RLP may involve an evolutionarily conserved process, especially since rhizobial symbiosis with leguminous plants was established on the basis of AM symbiosis (Parniske 2008). Consistent with this is the finding that the kinase domain of CERK1 homologues from non-leguminous AM symbiosis-participating plants were able to trigger the nodulation programme in *L. japonicus* (Miyata et al., 2014). The substantial similarity in the amino acid sequences of AtCERK1/OsCERK1/LjNFR1/MtLYK3 (Zhu et al., 2006; Zhang et al., 2007), and the fact that CERK1 also triggers both symbiotic and defence responses also support the view of a possible evolutionary relationship (Nakagawa et al., 2011). Interestingly, the findings that *OsCERK1*

and *OsCEBiP* are co-required for symbiotic and defence responses, as well as for *M. oryzae* rice root invasion provide strong support for a close evolutionary relationship between these different biological responses.

A concluding line of thought to explain the varying roles of plasma membrane receptors during *M. oryzae* invasion of rice roots is that *M. oryzae* may in fact adopt an endophytic lifestyle in the root. This may explain the related strategies the plant uses to allow accommodation of the fungus in its root *via* plasma membrane receptors, which often serve as 'gatekeepers' to decide which microbe to allow or restrict entry. For example, *OsCERK1* and *OsCEBiP* act together to launch a defence response against *M. oryzae* infection in the leaf but allow its entry in the root. By contrast, OsNFR5 allows entry of the pathogen through the leaf, but also through the root. This is consistent with a recent finding that demonstrated the role of two *Lotus japonicus* LysM genes, *Lys13* and *Lys14* in positively regulating the intracellular colonisation of the endophytic fungus *Fusarium solani* strain K (*FsK*). The study suggests that the LysM genes may act as entry receptors for successful passage of *FsK* through the rhizodermis in the legume root (Skiada et al., 2019), a role that may be related to that of OsNFR5 in the interaction with *M. oryzae*.

Suggestions for the future would be to experimentally identify the types of chitin oligosaccharide signals produced by *M. oryzae* and whether this determines how the host plant perceives and allows intracellular accommodation of the fungus in its roots. Another interesting experiment may be to determine whether the nutrient status of the plant influences the plant's response to allow entry of biotrophic pathogens, alongside mutualistic ones *via* the root. This is particularly important because *in vitro* cultures of *M. oryzae* and rice seedlings are performed under nutrient starvation (up to 21 days), and it may be that under this condition the plant allows invasion of all types of microbes, whether mutualistic or pathogenic in search of nutrients. Other experiments including reactive oxygen species (ROS) and phosphorylation assays will help to elucidate the *M. oryzae* hyphal death responses observed in *cerk1* mutant rice roots, as well as RNA sequencing experiments to monitor the differential regulation of genes in *O. sativa* LysM-RLK/RLP mutants (*cerk1*, *cebip* and *nfr5*) relative to the WT. This could potentially lead to the identification of novel genes involved in downstream processes leading to the accommodation of *R. irregularis* and *M. oryzae* during rice root colonisation.

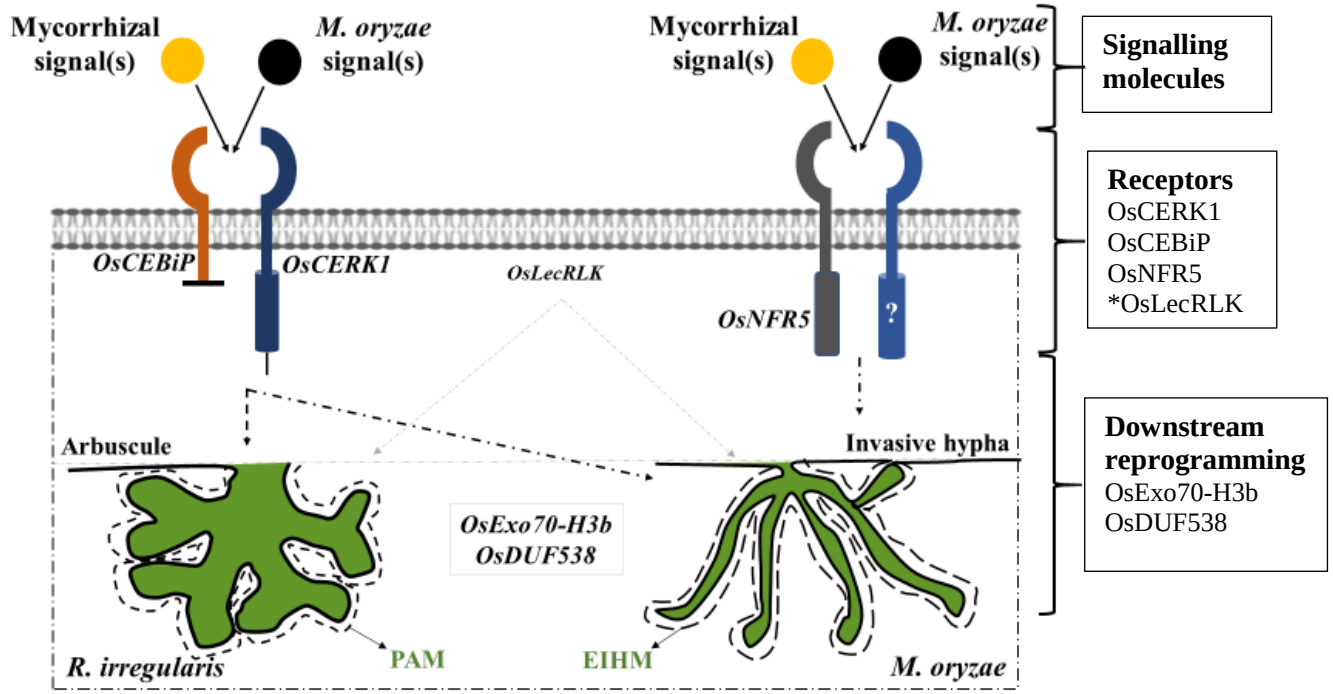

Figure 4.2: Working model for the functional role of LysM-RLKs/RLP during *R. irregularis* and *M. oryzae* colonisation of rice root cells. The plasma membrane receptors form complexes with known and unknown receptor partners to perceive and transduce signals leading to symbiosis and/or defence responses in the host plant. Here, OsCERK1 interacts with OsCEBiP to elicit both symbiotic and immunity signals, as well as signals leading to intracellular accommodation of *M. oryzae* in rice root cells. Although the function of *OsLecRLK (Os07g38800)*, *OsExo70-H3b* and *OsDUF538* are not yet known, we speculate that *LecRLK* probably interacts with another RLK to induce symbiotic and/or defence responses, whereas the other two genes are involved in downstream processes leading to the accommodation of *R. irregularis* and *M. oryzae* in rice roots.

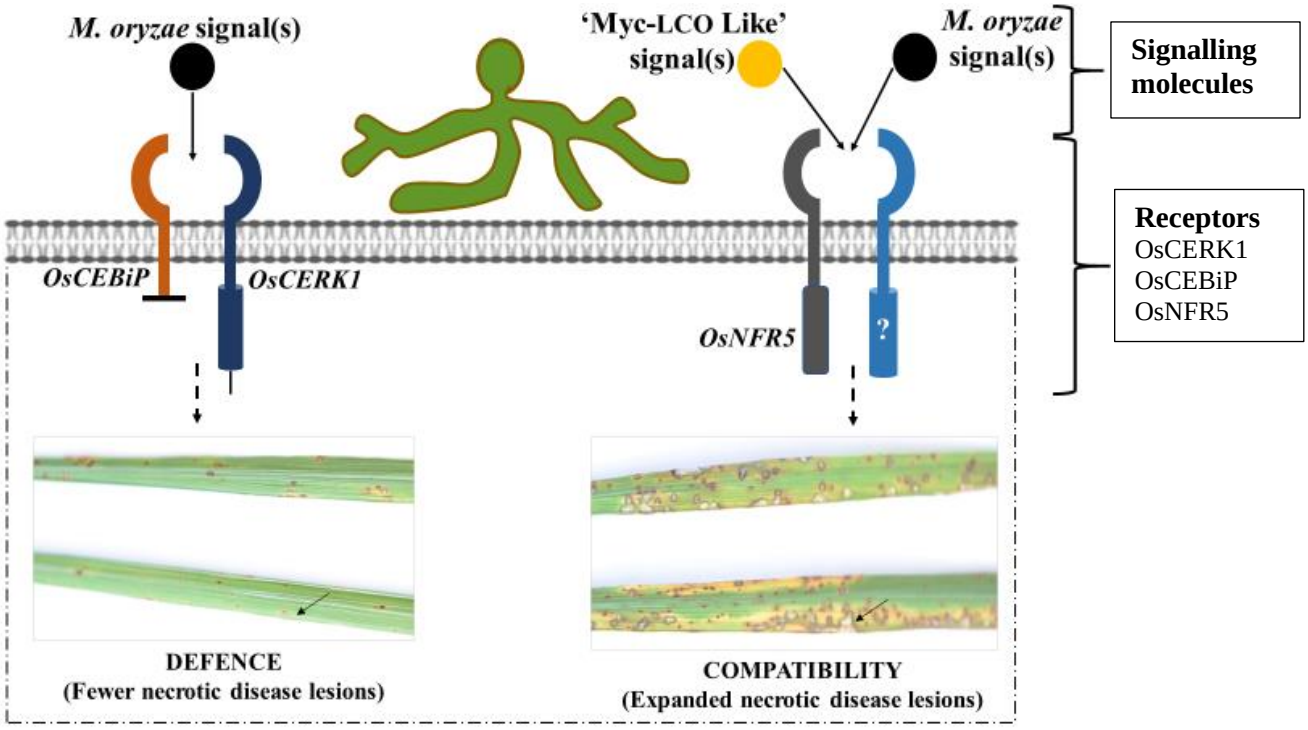

Figure 4.3: Working model for the functional role of LysM-RLKs/RLP during *M. oryzae* rice leaf infection. OsCERK1 and OsCEBiP form hetero-complexes to activate immunity signalling (Kouzai et al., 2014), whereas *OsNFR5* cooperates with an unknown receptor partner to perceive signals enabling the compatibility of *M. oryzae* during rice leaf infection.

4.2. Overlaps in the transcriptional responses to *R. irregularis* and *M. oryzae* rice root colonisation

Some studies have shown that microbial pathogens can exploit plant programmes or genes controlling beneficial plant-microbe interactions such as AM symbiosis to facilitate their invasion of the host root. A recent example was a reduction in the reproductive success of the downy mildew pathogen *Hyaloperonospora arabidopsidis* (*Hpa*) due to mutations in three *A. thaliana*-related common symbiosis genes (Symbiosis Receptor-like Kinase, SYMRK; nuclear-envelope localised cation channel, POLLUX, and the nucleoporin NUP107-160 complex), which are essential for symbiotic signal transduction and arbuscular mycorrhiza development (Reid et al., 2019). Similarly, the perturbation of *M. truncatula RAM2* gene, which is required for normal AM fungal infection within the root cortex failed to elicit appressoria formation by *Phytophthora palmivora* at the root surface, suggesting that RAM2 it is required for root invasion by the oomycete pathogen (Wang et al., 201). A shared role of the GRAS protein gene RAD1 in AM symbiosis and *P. palmivora* root interaction (Rey et al., 2017), as

well as for OsCERK1 in AM symbiosis and immunity signalling during *M. oryzae* rice leaf infection (Kouzai et al., 2014) has also been found.

In this study, a set of genes commonly regulated in response to infection by both *R. irregularis* and *M. oryzae* were identified. The genes include an *OsExo70-H3b* (*Os11g01050*), *OsLecRLK* (*Os07g38800*) and *OsDUF538* genes encoding proteins with a 'domain of unknown function'. None of these genes have been studied in the context of symbiosis or rice root invasion by a parasitic fungus. However, considering the significant co-induction of these gene candidates in rice roots colonised by both *R. irregularis* and *M. oryzae* (Chapter 3), we speculate that the genes may be involved in processes required to accommodate both fungi in rice root cells. Two *duf538* CRISPR-Cas9 mutant lines exhibited reduced mycorrhizal colonisation but did not result in any phenotype in *M. oryzae* colonised rice roots, although more quantitative and qualitative experiments are required to determine whether this gene has any biological function during rice root interactions with both mutualistic and detrimental fungi. Phylogenetic analysis revealed that all three candidate genes are members of superfamily of genes.

Although the functional role of *OsExo70-H3b (11g01050)* during rice root colonisation by the symbiont *R. irregularis* and pathogen *M. oryzae* was not fully evaluated in this study, I postulate that the gene may be involved in the biogenesis of the perifungal membranes (peri-arbuscular membrane, PAM and extra-invasive hyphal membrane, EIHM) of both fungi. Related work demonstrated by previous studies implicate Exo70 exocyst complexes in symbiosis (Zhang et al., 2015), and more specifically, in root hair tip growth and development of the perifungal membrane (Genre et al., 2012). Both plant-derived membranes (PAM and EIHM) envelope the fungi as they grow and proliferate inside rice roots. The PAM surrounds the arbuscules and is produced as an extension of the host plasmalemma (Parniske 2008; Pumplin and Harrison, 2009; Genre and Bonfante, 2010). TEM (Transmission Electron Microscopy) and *in vivo* GFP imaging revealed that pre-penetration responses and construction of the PAM are associated with extensive membrane dynamics involving the main components of the exocytic machinery as well as the Golgi apparatus (Genre et al., 2012).

Pre-penetration responses apply to all root cells that undergo AM colonisation, and experimental evidence indicate that all elements of the secretory pathway accumulate inside the PPA at the point of cell entry by AM fungus (Genre et al., 2012). The route of intracellular fungal growth is marked by an extension of the ER cisternae and concentration of the Golgi apparatus activity. More importantly, three v-SNARE (soluble-N-ethylmaleimide-sensitive

factor attachment protein receptor) proteins of the vesicle-associated membrane protein 72 (VAMP72) family and a member of the exocyst concentrate in the PPA cytoplasm, showing that it is the site of intense exocytosis (Genre et al., 2012). Consistent with this finding, Zhang et al. (2015) showed the involvement of a *M. truncatula* Exo70I in the development of the fine branch domain of the arbuscule. Mutants of MtExo70I developed normal trunk domain but had reduced arbuscule branching and aberrant hyphal branches. Consequentially, the mutants experienced premature formation of septa, arbuscule collapse and significantly smaller arbuscules than the wild-type (Zhang et al., 2015). Since Exo70 exocysts play a key role in tethering post-Golgi vesicles prior to exocytic fusion (He and Guo, 2009), MtExo70I was predicted to play a major role in the biogenesis of the PAM (Zhang et al., 2015). In this role, it is possible that MtExo70I as well as *OsExo70-H3b* are required for secretion of a signal into the peri-arbuscular apoplast or specific placement of a receptor in the PAM as suggested by Zhang et al. (2015). This has been shown in *Arabidopsis*, where an Exo70B1 regulates PAMP signalling possibly by recycling signalling protein (Stegmann et al., 2012). MtExo70I was found to interact with Vapyrin, a protein of unknown function required for arbuscule development, perhaps to recruit or maintain Exo70I in a specific position near the PAM at the hyphal tips (Zhang et al., 2015). Although MtExo70I homologue in rice (*OsExo70I*) is not induced in rice roots by *R. irregularis* or *M. oryzae*, it is possible that *OsExo70-H3b* functions similarly to MtExo70I during PAM development. Further analysis will help to confirm this.

With regards to plant responses to pathogens, two *Arabidopsis* Exo70 exocysts (Exo70H1 and Exo70B2) were associated in defence responses against the fungal pathogen *Blumeria graminis* f. sp. *hordei* (Pečenková et al., 2011; Stegmann et al., 2012). Mutants of AtExo70B2 showed a defect in vesicle tethering or fusion but fungal penetration efficiency was not affected (Pečenková et al., 2011). By contrast, enhanced penetration of the same pathogen occurred when it infected its host, barley, which had a transiently silenced *Exo70F1* (Ostertag et al., 2013), suggesting the role of Exo70s in plant immunity. Although this strategy may not necessarily apply to *M. oryzae* during rice root infection because the fungus does not seem to exhibit a pathogenic lifestyle, it is possible that Exo70 exocysts, including our OsExo70-H3b may serve as a hub for endomembrane trafficking, secreting proteins to positions of hyphal tip growth as postulated by Zarsky et al. (2013). This is obvious during rice leaf infection, where *M. oryzae* secretes fungal effector proteins into the host cytoplasm or the extracellular compartments such as the apoplast (Giraldo et al., 2013). Apoplastic effectors are generally dispersed and retained within the EIHM compartment, which is linked with filamentous fungal apical hyphal tip growth involving the Spitzenkörper, the organizing centre where growing

fungal hyphal tips are fed with vesicles (Giraldo et al., 2013). Vesicle transport to the growing hyphal tips is aided by an exocyst complex via a process known as exocytosis. Although it is not clear whether *M. oryzae* secretes cytoplasmic or apoplastic effectors during rice root infection, the fact that the fungus is enveloped by the EIHM throughout intracellular growth in the root (Marcel et al., 2010), indicates that the Exo70 exocyst complex may have a function in the biogenesis of this important membrane. Further studies, including the generation and characterization of CRISPR-Cas9 mutant lines, will unfold the exact biological role of OsExo70-H3b during intracellular accommodation of *M. oryzae* in rice roots.

In addition to *OsExo70-H3b*, this study identified a new putative L-type (Legume-type) lectin receptor-like kinase (07g38800) that is co-induced during *R. irregularis* and *M. oryzae* colonisation of rice roots (Chapter 3). Based on the level of induction in the gene transcript in inoculated rice roots, I speculate that the *OsLecRLK (Os07g38800)* gene may be involved in the accommodation of both beneficial and detrimental fungi within rice root cells. As a putative cell-surface receptor kinase, OsLecRLK is likely to be involved in the recognition and transduction of extracellular signals. This is consistent with the finding that the intracellular kinase domains of LecRLKs constitute receptor-like kinases, indicating a role in signalling (Bellande et al., 2017). The expression of many L-type LecRLKs change in response to various stimuli such as hormones, abiotic stresses and a variety of elicitors (Bellande et al., 2017), and strong induction and repression of such genes are particularly seen in response to pathogens, which suggests a role for L-type LecRLKs in defence responses (Gouhier-Darimont et al., 2013; Bouwmeester et al., 2011; Liu et al., 2015; Wang et al., 2016). Only a few genes have been associated with plant development. For example, the *small, glued-together (SGC) Lectin RLK1*, which is required for proper pollen development in *Arabidopsis* (Wan et al., 2008) and a *Medicago truncatula LecRLK* (*MtLecRK1*), which is associated with an increase in nodule number during legume-rhizobia symbiosis (Navarro-Gochicoa et al., 2003). Future experiments, including the generation of CRISPR-Cas9 mutants of *OsLecRLK (07g38800)* will help to decipher the functional role of OsLecRLK (Os07g38800) during rice root colonisation by both *R. irregularis* and *M. oryzae*.

Finally, this study identified a subset of *DUF538* genes (*Os07g02880, Os07g02920, Os07g02690, Os07g02900 and Os11g38210*) that are induced during rice root colonisation by both *R. irregularis* and *M. oryzae*. While a significant reduction ($P < 0.01$) in the level of *R. irregularis* colonisation was seen in two selected *duf538* CRISPR-Cas9 mutant lines, no effect was seen with *M. oryzae*, suggesting that the genes successfully edited in the selected mutant

lines may have been those required for the accommodation of the symbiont rather than the pathogen in rice roots. This is a vague speculation as knowledge of plant DUF538 gene function is very scarce, except for very few reports about their expression in plants under various stressful stimuli such as bacteria and elicitors (Gholizadeh and Kohnehrouz, 2013). The application of a multiplex CRISPR-Cas9 gene editing technology in this study was an innovative approach aimed to knockout as many as the 11 *OsDUF538* genes expressed in rice plants to avoid compensatory effects during functional characterisation. Unfortunately, the mutant lines were not fully characterised to determine whether *OsDUF538* genes are involved in AM symbiosis and the colonisation of rice roots by *M. oryzae*. Future studies should focus on a comprehensive quantitative and qualitative characterization of non-characterised *OsDUF538* CRISPR-Cas9 lines to determine the number of genes mutated and whether a crossbreeding approach may result in more mutated genes for functional analysis. A preferred approach would be to generate a strategy to simultaneously knockout all *OsDUF538* genes, although this remains a challenge due to the splitting of the gene family in two rice chromosomes (7 and 11). Understanding the functional role of these interesting subset of proteins of unknown function would be a novel and important contribution to the field of plant-microbe interactions.

4.3. Conclusions and future direction

A long-standing hypothesis has been that plant pathogens exploit genetic pathways established in the ancient arbuscular mycorrhizal symbiosis to facilitate their invasion of the host plant. While very few studies support this hypothesis, many questions still arise. Interestingly, the work presented in this thesis provide evidence to show that plant pathogens and symbionts have genetic commonalities that enable their recognition, invasion and accommodation in the host root. First, transcriptome comparison experiments identified a new common set of genes (*OsExo70-H3B, OsLecRLK* and *OsDUF538*) that are associated with rice root invasion by the symbiont *R. irregularis* and the pathogen *M. oryzae*. Second, a novel function was found for three LysM receptor-like kinases (*OsCERK1* and *OsNFR5*) and protein (*OsCEBiP*) during *M. oryzae* intracellular colonisation of rice roots, as well as for *OsCEBiP* in AM symbiosis. Third, an unexpected new role was found for *OsNFR5* during rice leaf infection by *M. oryzae*, where the LysM-RLK acts as a compatibility factor, rather than a defence receptor. These findings reveal two major sets of genes and proteins that are involved in microbial signal recognition at

the cell surface (LysM-RLKs/RLP) and possibly for downstream processes (OsExo70-H3b and OsDUF538) leading to the accommodation of both symbiont and pathogen in rice roots. Excitingly, OsCERK1 and OsCEBiP emerged as a putative co-receptor complex commonly required for AM symbiosis, defence and intracellular accommodation of *M. oryzae* in rice roots, supporting the hypothesis that common mechanisms of accommodation exist for symbiotic and detrimental fungi in rice roots. To confirm receptor complex formation between OsCERK1 and OsCEBiP in AM symbiosis, protein-protein interaction studies using Yeast 2 Hybrid or other methods is highly recommended. Further experiments are also recommended to identify the receptor partner for OsNFR5 during rice root and leaf invasion by *M. oryzae*. Although previous findings showed that BiFC assays failed to observe a complex formation between OsCERK1 and OsNFR5 (Miyata et al., 2014), the experiment was performed in a heterologous system. It is possible that other types of experiment such as co-immunoprecipitation assays used to show the interaction between the LRR receptor-like protein kinases BAK1 and FLS2 in *Arabidopsis* (Chinchilla et al., 2007) may provide answers to the receptor complex formation between the studied rice RLKs and RLP during AM symbiosis and *M. oryzae* colonisation of rice root and leaves. Finally, the utilisation of more mutant alleles and additional experiments are recommended to confirm the reproducibility of these results, which may be further explored for engineering disease-resistant rice crops.

CHAPTER 5

Materials and Methods

5.1. Plant and Fungal Material

Wild-type japonica rice (*Oryza sativa* cv Nipponbare, Dong Jin and Hwayoung), wild-type *R. irregularis* spores (generated in Paszkowski's Lab, University of Cambridge), wild-type *Magnaporthe oryzae* Guy11 strain and ToxA-promoter-driven eGFP-transformed *M. oryzae* strains (kindly provided by Prof. N. J. Talbot's Lab at the Sainsbury Laboratory, Norwich) were used in all plant and fungal experiments. *oscerk1*, *oscebip* and *osnfr5* knockout mutant seeds were generously provided by Naoto Shibuya (Department of Life Sciences, School of Agriculture, Meiji University, Kawasaki, Kanagawa, Japan). The mutants were used in studies by Miyata et al. (2014).

5.2. Plant Growth

5.2.1. Seed Sterilization and Germination

Following the de-husking of rice seeds with a manual grinder, seeds were sterilized for 30 minutes in 3.5% (w/v) sodium hypochlorite on a Heidolph Polymax 1040 platform shaker (Schwaback, Germany). The sodium hypochlorite solution was removed, and seeds (9-12 seeds per genotype, depending on the experiment) were washed three times with autoclaved distilled water. For *Rhizophagus irregularis* inoculation experiments, seeds were transferred onto 0.6% (w/v) autoclaved water agar plates in 90 mm Petri-dishes and sealed with micropore tape. For *Magnaporthe oryzae* inoculation experiments, about 10 seeds (per plate) were transferred into 1% (w/v) autoclaved solid Bacto-agar plates in 120 mm square Petri-dishes and sealed with micropore tape. Plates were incubated at 30^{o}C for 3-4 days (depending on the germination rate) or until the seminal root and coleoptile were seen. Bacto-agar plates containing sterilized seeds for *M. oryzae* inoculation were incubated vertically at 30^{o}C in the dark for 4 days to promote root growth. Plants were then grown vertically in a controlled environment growth chamber with a 16-h light/8-h dark photoperiod at 28/24^{o}C for another 8-10 days prior to inoculation. All procedures were carried out under a sterile flow hood.

5.2.2. Plant Watering and Fertilization

Inoculated rice seedlings in sand (see 5.3.1) were watered with distilled water for two weeks (three times a week), after which they were fertilised with low phosphate Hoagland solution (Table 9), two times a week, and with water only once a week.

Table 9: Low phosphate (B – 25M) Hoagland solution

Solution	Chemical	M.W.	mL in final ½ Hoagland (1L)
A	KNO_3	101.11	
	$Ca(NO_3)_2.4H_2O$	236.15	25
	$MgSO_4.7H_2O$	240.48	
B	KH_2PO_4	136.09	5
	KCl	74.56	
C	Fe-Citrate	-	5
D	$MnSO_4.H_2O$	169.02	
	$ZnSO_4.7H_2O$	287.54	0.5
	$CuSO_4.5H_2O$	249.68	
E	$Na_2B_4O7.10H_2O$	381.4	0.5
	$(NH_4)_6Mo_7O_{24}.4H_2O$	1235.86	

5.3. Fungal Culture and Plant Inoculation Assays

5.3.1. Rice root inoculation with *Rhizophagus irregularis*

Pre-germinated rice seedlings (from 5.2.1) were carefully transferred into plastic cones/conical flasks (2.5 cm diameter; 12 cm depth) or Petri-dishes (30 mm) containing autoclaved-sterilized sand. One millilitre of *R. irregularis* spores (250 spores per Petri-dish or 300 spores per cone) contained in a suspension mixture with autoclaved distilled water was added onto the sand at a depth of approximately 1 cm from the rim of the cone, and more sand was added to the cone to

cover the roots of the seedlings. Inoculated plants were incubated or grown in a controlled growth chamber set at 12-h light/12-h dark cycle at 28ºC-day/24ºC-night cycle.

5.3.2. *R. irregularis* Spore Extraction

R. irregularis spores were grown on hairy carrot roots (describe in Raj et al., 2016) cultured on bacto-agar cultures incubated at 25ºC in the dark. To harvest spores, carrot root cultures on solid agar medium were cut into pieces (using a sterile blade) and placed in a citrate buffer solution at a 3:1 ratio (Table 10). The spore-citrate buffer mixture was stirred with a magnetic stirrer and plate for one hour to allow the solid agar to dissolve. The dissolved solution was then sieved through a 500 µm mesh to first remove root pieces, before extracting the spores through a second sieve with a 45 µm mesh. Extracted spores were washed with sterile distilled water and added into a 50 ml Falcon tube using a sterile Pasteur pipette. To count the number of spores per ml, 10 µl of spore solution were placed on a slide or haemocytometer and counted under a Nikon light microscope. Rice seedlings were inoculated with 250-300 spores per plant.

Table 10: Citrate Buffer Solution

Chemical	Final Concentration
Citric acid	0.1 M
Sodium citrate	0.1 M
Distilled H_2O	90 ml
Adjusted to pH 6 using small volumes of citric acid or sodium citrate to a final volume of 100 ml	

5.3.3. *Magnaporthe oryzae* Culture and Spore Production

M. oryzae spores or conidia were produced by culturing mycelium (contained on small pieces of sterile filter paper) on Complete Medium™ (Talbot et al., 1993) at 26ºC (16-h light/8-h dark cycle). Spores were harvested from 7-10-day old cultures by adding 3 millilitres of sterile distilled water onto the culture plates, then carefully scaping the spore-containing mycelia with sterile L-shaped spreaders (Fisher Scientific). Conidia suspension was filtered into sterile Falcon tubes using Miracloth (GLife Tech), followed by a centrifugation step for 5 minutes

(10,000 rpm). The supernatant was discarded, and spores rinsed with sterile water prior to counting under the microscope.

5.3.4. *Magnaporthe oryzae* Rice Root Infection Assay

To inoculate rice roots, 14-day old seedlings were placed horizontally on top of a sterile filter paper placed on 1% (w/v) sterile solidified bacto-agar in square Petri-dishes (120 mm). Using a pipette, fungal spores (~$5x10^3$ spores per root) were spread to cover the entire root length. Plates were then sealed with parafilm to avoid evaporation and placed in a controlled growth chamber (16h-light/8-h dark) for 4 to 7 days.

5.3.5. *Magnaporthe oryzae* Rice Leaf Spray Infection Assay

For *M. oryzae* rice leaf assay, two-week-old rice seedlings were uniformly sprayed with *M. oryzae* conidial suspension at a concentration of 2 x 10^{-5} conidia per millilitre in 0.2% Tween 20 (v/v). The inoculated plants were placed in a chamber with 90% humidity and 24-h darkness and then returned to the normal plant growth conditions (12-hour light/12-hour dark photoperiod). After six days, the disease lesion progression was observed and calculated based on the protocol described in Valent et al. (1991). This experiment was repeated two times with similar results.

5.3.6. *Magnaporthe oryzae* Rice Leaf Sheath Infection Assay

Rice leaf sheath inoculation assays were conducted by excising and inoculating leaf sheaths from 4-6-week-old rice seedlings with a conidial suspension of 5×10^4 conidia per millilitre in 0.2% Tween 20 (v/v). The inoculated leaf sheaths were placed in a growth chamber at 24-26^{o}C, 12-h light/12-h dark photoperiod, followed by a microscopic observation at different time points. M. oryzae infection was scored according to the four infection (Level 0, just appressoria without penetration; Level 1, with penetration peg or primary IH; Level 2, with sparse secondary IH restricted in the first infected rice cell; Level 3, with abundant IH in the initial and even neighbouring rice cells) described in Nie et al. (2019). Two assays were conducted independently, with three biological replicates.

5.4. Phenotypic Characterization Assay

5.4.1. Trypan blue staining for quantification of *R. irregularis* colonised rice roots

Rice plants (4-6 weeks, depending on the experimental objective) planted in cones or Petri-dishes were harvested by gently pulling out the plants from the soil. Following thorough washing with sterile distilled water, root samples were cut, mixed/shuffled (to avoid selecting specific root types), placed in 10% (w/v) potassium hydroxide (KOH) contained in 2 ml Eppendorf tubes, and heated for 30 minutes at 98^{o}C. After heating, KOH was removed, and root pieces washed three times with sterile distilled water. This was followed by incubation of root pieces in 0.3M HCl (w/v) at room temperature for 15-30 minutes, after which they were placed in fresh Eppendorf tubes containing 1 ml of 0.1% (w/v) trypan blue solution (Table 11). Samples were heated for 8 minutes at 95^{o}C and root pieces removed from trypan blue solution and mounted on slides (ten 1 cm-root pieces from one plant) with the addition of droplets of 50% (w/v) acidic glycerol. Coverslips were placed on top of the mounted slides and sealed with nail varnish to prevent evaporation.

Table 11: Trypan blue staining solution

Solution	Composition (Final Concentration)
KOH	10% (w/v)
HCl	0.3 M
Trypan blue	0.1% (v/v) (in 2:1:1 mix of lactic acid/glycerol/distilled H_2O)
Acidic glycerol	50% v/v) (1:1 mix of glycerol/0.3M HCl)

5.4.2. Wheat Germ Agglutinin (WGA) Staining

To investigate the morphology of *R. irregularis* in colonised rice root, colonised plants were stained with WGA (Alexa Fluor^{TM} 488; Invitrogen W11261) as follows: rice roots were harvested, and 3-4 pieces of individual roots placed in 50% (w/v) ethanol for at least 4 hours. Root pieces were then removed from ethanol and placed in 20% (w/v) KOH for 2-3 days at room temperature. Following the removal of 20% KOH, root pieces were rinsed thoroughly with distilled water and incubated in 0.1M HCl (w/v) for at least one hour at room temperature.

The acid solution was then removed, and root pieces rinsed with distilled water first, then with phosphate-buffered saline (PBS). Following this step, root pieces were stained with WGA by placing them in Eppendorf tubes containing a final concentration of 0.2 µg/ml WGA-PBS solution for at least 6 hours in the dark. For long-term storage, stained root samples were wrapped in foil and stored at -4^{o}C.

5.5. Microscopy

5.5.1. Microscopic quantification of *R. irregularis* in colonised rice roots

To quantify the level of fungal colonisation in rice roots, mounted root pieces (5.4.1) were viewed under a light microscope (Nikon Labohot) at a magnification of 200x. For each 1-cm root length, fungal structures (e.g. extracellular hyphae, hyphopodia, intra-radical hyphae, arbuscules, vesicles and spores) were scored as present or absent at 10 positions or field of vision. Notably, all fungal structures except for extracellular hyphae and spores, were scored as positive colonisation. Once all 10 pieces of roots (from one plant) were scored (10 points or field of vision each), the total level of fungal colonisation per plant was calculated. At least three plant biological replicates (per genotype) were used in every experiment. Images of fungal colonisation were captured using the same microscope. For all experimental assays, the different mutants with their corresponding wild-type were tested in parallel using the same fungal inoculum and *in vitro* growth conditions to ensure that the observed phenotypes were comparable.

5.5.2. Confocal microscopy to monitor rice root intracellular colonisation by *R. irregularis* and *M. oryzae*

R. irregularis and *M. oryzae* colonised rice roots were monitored using a Leica TCS SP8 confocal microscope. *R. irregularis* colonised rice roots were stained with Wheat Germ Agglutinin to enable monitoring of the morphology of internal fungal structures while the monitoring of GFP-expressing *M. oryzae* in colonised rice roots did not require any staining. Root pieces were stained for 5 minutes with 15 µM Propidium iodide (PI), which stains and outlines the plant cell wall structure. eGFP excitement and emission wavelengths were 488 nm and 509 nm, respectively.

5.6. Molecular Techniques

5.6.1. Genomic DNA extraction

Rice leaf samples (100 mg) from one-week old seedlings were collected, placed in 2 ml Eppendorf tubes containing 2-3 sterile glass beads and frozen in liquid nitrogen. Using a Qiagen Tissue Lyser II (Cat No./ID: 85300), leaf samples were lysed for 2 minutes (with brief pulses at 30 second intervals). To extract genomic DNA, 200 ml of sucrose-based extraction buffer (Table 12) was added into each 2 ml tube, followed by a brief vortex and incubation at 98^{o}C in a heat block for 10 minutes. Tubes containing lysed DNA samples were centrifuged for 5 minutes at 13,000 rpm and DNA was stored at 4^{o}C until use.

Table 12: Genomic DNA Extraction Buffer

	M. W.	**Final**
TRIS-HCl, pH 8	74.54	50 mM
EDTA, pH 8		40 mM
Sucrose		0.75 M
UltraPure™ water (ThermoFisher 10977035)		

5.6.2. Genotyping by Polymerase Chain Reaction (PCR)

Plant materials used for fungal inoculation experiments were genotyped by PCR using a standard PCR reaction mixture (Table 13). PCR reactions were performed in a thermocycler using appropriate annealing temperatures for primers used. Available primers were used in combination with newly designed primers (Table 14) depending on the genotyping assay. Amplified PCR products were analysed by agarose gel electrophoresis, followed by product visualization using a UV transilluminator.

Table 13: Primer sequences used for genotyping

Primer Name	Primer Sequence
OsCERK1 (Os08g42580) Self-generated	**F:** CACCAACATGGCGGATCTCT **R:** AGCTGCCTGTACTGCACAAA
OsCEBiP (Os03g04110) Self-generated	**F:** CAGTCAAACAAACACCAAGCCT **R:** GTCACCCCGTACTTGGCAG
OsNFR5 (Os02g09960) (Miyata et al., 2014)	**F:** AGCACCGTGACAGCCAGCTCCAAATGG **R:** GGAGCTATTGCTGTCGAATCTGT **R**(HPT): CTTCTCGACAGACGTCGCGGTGAGTTC
DUF538 (Os07g02880)	**F:** TCCATCACCAACAATCTCTCA **R:** ACTGGAACAGATGCAGGAAT
DUF538 (Os07g02920)	**F:** CTCACAACCCATTTGCACAC **R:** TGGTGACCTAAGATAGTGGCTTT
DUF538 (Os07g02690)	**F:** ACATCCAATGGCATCACAAA **R:** TGCAATTGAATACAAAAAGATGG
DUF538 (Os07g02850)	**F:** CCAACTCGATCTCAGCATCA **R:** CCTTCTTCCCTCCCTACGAT
DUF538 (Os07g02900)	**F:** TCACCAACAATCTCTCACCAA **R:** GGACTTGCAGTCTTGCATCA
DUF538 (Os07g02940)	**F:** GCTCCAAGACTTCCATTGCT **R:** CCTTAATTAAACATGCAAAACAGTG
DUF538 (Os07g02870)	**F:** GAAGTCCATCGAGCTTCTGG **R:** AGCTTGGTCCAAAGGTACTGA
DUF538 (Os07g02700)	**F:** GCAGGAAGAAGTCCATCGAG **R:** GCGTCAAAGGTCTTGCAGAT
DUF538 (Os11g38210)	**F:** TGCTGAAATGGCAGCTAAGA **R:** ACCATAAAACATGGGGGAAA
DUF538 (Os11g38220)	**F:** CAAGCTCCAAACAAGCCATT **R:** TTCCCTCGGATGTTCAGTTC
DUF538 (Os11g38240)	**F:** CACAAGCTCCAAACAGACCA **R:** GGCTGAACATTTAGCCACCA
CAS9 (self-generated)	**F:** CGATCAGCTTGTCGGAGTTG **R:** GACGTGGACCATATTGTGCC

F = Forward**; R** = Reverse

Note: All DUF538 primers were self-generated.

Table 14: PCR reaction mixes and solutions

Reagent	Final Concentration
H_2O	
Betaine	5 M
Go Taq green buffer	5X
template	75 ng/µl
dNTP	2.5 mM
$MgCl_2$	50 mM
F primer	10 µM
R primer	10 µM
GotaqG2 Flexi DNA Polymerase (Promega M7801)	5 U/µl
Total	**20**

Table 15: PCR reaction programme

	Initial Denaturation	Denaturation	Annealing	Extension	Final Extension	Hold
Temp. (°C)	96	96	Specific Primer	72	72	16
Time	2 m	30 s	30 s	60 s	10 m	
		35 cycles				

5.6.3. RNA Extraction

Rice tissue material (300 mg) harvested for gene expression analysis was immediately placed in 2 ml Eppendorf tubes containing 2-3 steel beads and frozen in liquid nitrogen. Frozen tissue was ground in a Qiagen tissue lyser (set at a frequency of 27 seconds) for 2-4 minutes. RNA extraction was then performed using a standard Trizol protocol (Table 16). Following treatment with LiCl buffer (4 M LiCl, 20 mM tris-HCl pH7.5, 10 mM EDTA) and incubation at 20^{o}C for one hour, precipitated single stranded RNA samples were centrifuged at 13,000 rpm for 20 minutes followed by a washing step with 75% (w/v) ethanol. RNA pellets were airdried,

resuspended in 20 µl of RNase-free water and quantified using a nanodrop reader. To check the integrity of the RNA, samples were run on agarose (2.5%, w/v) gel electrophoresis and imaged using a DNA gel documentation system. Intact RNA samples produced clear 28S and 18S ribosomal RNA bands.

Table 16: Trizol Solution

Reagent	Concentration in Trizol
Guanidium Thiocyanate	0.8 M
Ammonium Thiocyanate	0.4 M
Sodium Acetate (pH 5)	0.1 M
Glycerol	5% (v/v)
Phenol (pH 5)	38% (v/v)

5.6.4. cDNA Synthesis

Following RNA quality check, RNA samples were treated with DNase 1 (Sigma-Aldrich) at 25^{o}C for 20 minutes to remove genomic DNA contamination. A 'RT' PCR reaction with *O. sativa* cyclophilin DNA primers was run on RNA to ensure that no genomic DNA contamination was present. Following this confirmatory test, cDNA was made using the First Strand cDNA synthesis with SuperScript II Reverse Transcriptase (Invitrogen) following the manufacturer's guide. To estimate the amount of cDNA made, another PCR reaction (using OsGAPDH primers) was run.

5.6.5. Gene Expression Analysis by Quantitative Real-Time Polymerase Chain Reaction

Gene expression analysis was performed using cDNA (5.6.4.) and specific primers (Table 17) for each experiment. For each qPCR reaction, three *O. sativa* housekeeping genes (*Cyclophilin*, *GAPDH* and *Ubiquitin*) were run and their C_t values used to normalize the Ct expression values of the genes of interest using a Geometric Mean calculator, which provided accurate measurements.

Table 17: Primer sequences used for qPCR

Primer Name	Primer Sequence
OsCERK1	**F:** TGGAATCGTGTACATCCCCG **R:** AGCTCCCTTCCCTGGTGATT
OsCEBiP	**F:** GTTGGAGACTACTGCAACTCT **R:** GTACAAGTGCCACTCATCCTCT
OsNFR5	**F:** ACGCGTTCGAGAGGCTATG **R:** TATCTAGCTGCCACCTCGTTC
MoACT	**F:** CAGATGTGGATCTCGAAGCA **R:** GCCCAACATCTCGGTTTATC
MoTUB	**F:** CTGCCATCTTCCGTGGAAAGG **R:** GACGAAGTACGACGAGTTCTTG
Mo40s8	**F:** GCTCACTACCGCCAGAAGC **R:** ACGGACGGTGTGAATGCG
RiEF	**F:** GCTATTTTGATCATTGCCGCC **R:** TCATTAAAACGTTCTTCCGACC
OsUbiquitin	**F:** CATGGAGCTGCTGCTGTTCTAG **R:** CAGACAACCATAGCTCCATTGG
OsGAPDH	**F:** CTGATGATATGGACCTGAGTCTACTTTT **R:** CAACTGCACTGGACGGCTTA
OsCyclophilin	**F:** GTGGTGTTAGTCTTTTTATGAGTTCGT **R:** ACCAAACCATGGGCGATCT
OsAM1	**F:** ACCTCGCCAAAATATATGTATGCTATT **R:** TTTGCTTGCCACACGTTTTAA
OsAM3	**F:** CTGTTGTTACATCTACGAATAAGGAGAAG **R:** CAACTCTGGCCGGCAAGT
OsPT11	**F:** GAGAAGTTCCCTGCTTCAAGCA **R:** CATATCCCAGATGAGCGTATCATG
OsAM14	**F:** CCAACACCGTTGCAAGTACAATAC **R:** GCACTTTGAAATTGGACTGTAAGAAA
DUF538 (Os07g02880)	**F:** GAGGTCTACATCACCGATGC **R:** CAGATTTGCACCATCTCTAGCTT
DUF538 (Os07g02920)	**F:** CTCGCCGGAGAAGGTCAC **R:** AAGTACATGGTGACCTAAGATAGTGG

DUF538 (Os07g02690)	**F:** AGGTCTACCTCGCCGATGC **R:** TGAGTCTTGTCATCATTTCTTACTCC
DUF538 (Os07g02850)	**F:** CACCTTCAAGACGGGAACC **R:** AAGCTTGCATGTCTCGACTTT
DUF538 (Os07g02900)	**F:** CTCGCCGGAGAAGGTCAC **R:** TTAAGATTAAGGACTTGCAGTCTTGC
DUF538 (Os07g02940)	**F:** GACTGGAACTGGGCTCTCTG **R:** GCAATACAGAGATACAACAGTACATGG
DUF538 (Os07g02870)	**F:** CGAGCCGCCAATTTCATT **R:** GAAATCCTCGGCAACTGACT
DUF538 (Os07g02700)	**F:** GTCGCCGGAGAAGGTGAC **R:** TTCCATCCTTCTTTGACACG
DUF538 (Os11g38210)	**F:** GATGAGTCTTCTGCTGGGAAG **R:** ACCATAAAACATGGGGGAAA
DUF538 (Os11g38220)	**F:** TGTTGAGGAGTCATCTGCTG **R:** TTCCCTCGGATGTTCAGTTC
DUF538 (Os11g38240)	**F:** AGGAGTCATCTGCTGGGAAG **R:** TGAAAAGAAAGCCCAAGTGAG

Table 18: qPCR master mix

Reagent	**Final Concentration**
H_2O	
GoTaq colourless buffer	5X
dNTP	10 mM
$MgCl_2$	25 nM
Primer mix (F+R)	3 µM
SYBR green (made in house)	10X
GoTaq Flexi	5 U/µl
DNA template	1 µl

Table 19: qPCR reaction programme

	Initial Denaturation	Denaturation	Annealing	Extension	Final Denaturation
Temp. (°C)	96	96	59	72	95
Time	10 m	30 s	60 s	30 s	1 m
		40 cycles			

5.6.6. Generation of CRISPR-Cas9 constructs

To generate constructs for the multiplex CRISPR-Cas9 approach to edit the DUF538 genes, the pENTRY vector (Figure 3.18A) was digested with the restriction enzyme (Bsa1) for two hours at 37^{o}C and the products run on an 0.7% (w/v) agarose gel. Digested plasmid DNA was purified using a gel extraction and purification kit (NuceloSpin^{R} Plasmid DNA, RNA and Protein Purification Kit, Machery-Nagel, Catalog# 740588.250), after which a ligation reaction using T4 ligase was performed to ligate the single guide (sg) RNA (GAC CGT CTC CTA TGC CAA CG) to the pENTRY vector. Ligated plasmid vector was transformed in competent *E. coli* (DH5α/Top 10) cells for one hour at 37^{o}C, followed by plating on Luria-Bertani (LB) agar containing 50 ml/ml kanamycin (Table 20) and incubation at 37^{o}C overnight. Following the overnight incubation, two colonies were selected and further grown in suspension culture overnight at 37^{o}C before a mini-prep was performed. Purified pENTRY vector containing the sgRNA was then introduced into a pDESTINATION vector (Figure 3.18B) through an LR reaction following the instruction manual (Gateway LR Clonase^{TM} II, Invitrogen 11791-020). This was followed by transformation in competent *E. coli* (DH5α/Top 10) cells and an overnight incubation at 37^{o}C. A colony PCR was then performed using the sgRNA-F primer and the pZmUbi-R (*Zea mays* ubiquitin promoter primer) primers (Table 21) to confirm successful constructs prior to rice transformation. Notably, the single guide RNA sequence was designed using the free CRISPR-P (2.0) online webtool.

Table 20: Media and antibiotics for bacteria culture/selection

Media	Composition	Quantity
LB selection medium (100 ML)	Tryptone	1 g
	Yeast extract	0.5 g
	NaCl	0.5 g
	d.i. H_2O	100 ml
	Stock antibiotic	(1000X) 100 µl
LB blue/white selection plates (100 ml)	selection medium	100 ml
	Agarose	1 g
	X-gal (20 mg/ml)	100 µl
	IPTG (100 mM)	100 µl
Stock spectinomycin (1000X)	Spectinomycin	50 mg
	d.i. H_2O	1 ml
Stock kanamycin (1000X)	Kanamycin	50 mg
	d.i H_20	1 ml

d.i. water = Distilled water

Table 21: CRISPR-Cas9 sgRNA Primers

Primer Name	Primer Sequence (Forward)	Primer Sequence (Reverse)
sgRNA15-F	GACCGTCTCCTATGCCAACG	
sgRNA15-R	CGTTGGCATAGGAGACGGTC	
ZmUbi		GACCATGTCTAACTG TTC AT

5.6.7. Genotyping by Sequencing

CRISPR-Cas9 mutant plants were genotyped by Sanger sequencing to detect the presence or absence of mutations. First, genomic DNA was extracted from the plants (Table 12) followed by PCR using gene-specific primers (Table 13). Amplified DNA samples were sequenced using the Sanger sequencing technology (Source Biosciences, Cambridge) and sequencing results analysed using free online software (Ape and Serial Cloner).

5.7. Statistical analysis

Two-way ANOVA followed by Tukey's *post-hoc* test was used in gene expression analysis data. Student's *t*-test was used in all pairwise comparisons. One-way ANOVA was used in comparisons between 3 or more independent (unrelated) groups (i.e. average number of lesion quantification). Statistical analyses used are indicated in detail in the corresponding Figures/Figure legends.

5.8. Computational analysis

Phylogenetic analysis was performed using the Molecular Evolutionary Genetic Analysis (MEGA) software. Protein sequences were identified from the rice genome annotation database (http://rice.plantbiology.msu.edu/) and sequence alignment performed using the ClustalW sequence alignment tool available on the MEGA software. To avoid bias, regions with extensive alignment gaps or predicted unreliability were removed. Model selection was performed to select the best substitution model (e.g. the Jones-Taylor-Thornton, JTT model plus Gamma distributed rate) for constructing the trees. Phylogenetic trees were built using the Maximum Likelihood statistical method with a bootstrap method of 1000 replications. Trees were viewed using the FigTree phylogenetic tree viewer software.

For selection of gene candidates after transcriptome comparison in Chapter 3, two independent transcriptomics studies (Gutjahr et al., 2015 and Marcel et al., 2010) were compared. Gutjahr's data identified a total of 1,179 transcripts accumulated differentially in the CR, crown roots and LLR, large lateral roots at 7 weeks post inoculation (wpi) with and without (mock-inoculated) *R. irregularis*, whilst Marcel's data revealed 2,000 genes that are differentially expressed in all root types infected and non-infected (mock inoculated) with *M. oryzae* at 6 days post inoculation (dpi).

By overlaying these two data sets using MS-Excel software, a common set of 498 genes that are differentially expressed in both *R. irregularis* and *M. oryzae* rice root interactions were identified (Figure 3.1). Overlaying of cells was done using the 'conditional formatting' tool bar in MS-Excel, which allows a manual setting of rules for highlighting cells. By setting the rule to highlight cells with the same Locus ID, similar genes were selected in both whole genome transcriptome datasets, i.e. for *R. irregularis* and *M. oryzae*. Gene IDs that were not highlighted were not present in both independent datasets and were, therefore, removed. This resulted in a total common set of 498 genes.

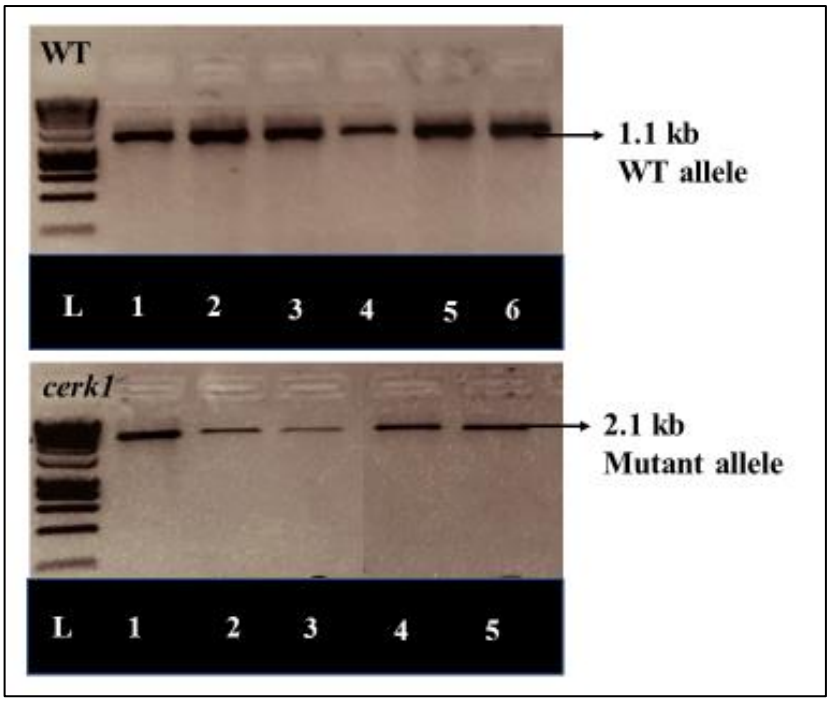

Figure A1: Genotyping results showing WT (1.1 kb) and *oscerk1* (2.1 kb) mutant alleles using self-generated primers listed in Table 13.

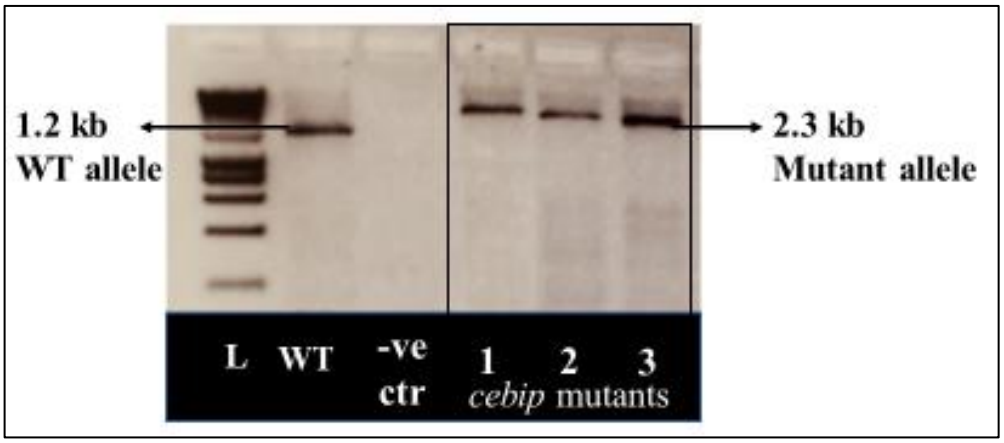

Figure A2: Genotyping results showing WT (1.2 kb) and *oscebip* (2.3 kb) mutant alleles using self-generated primers listed in Table 13.

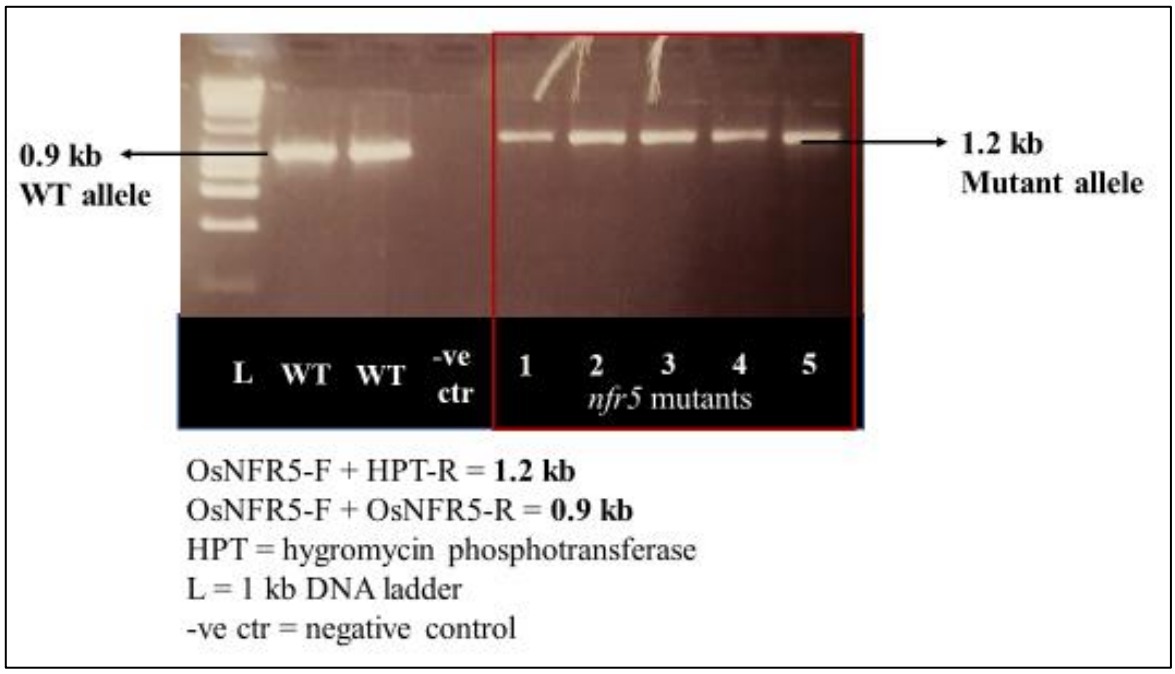

Figure A3: Genotyping results showing alleles WT (0.9 kb) and *osnfr5* (1.2 kb) mutant alleles using primer sets described in Miyata et al. (2014).

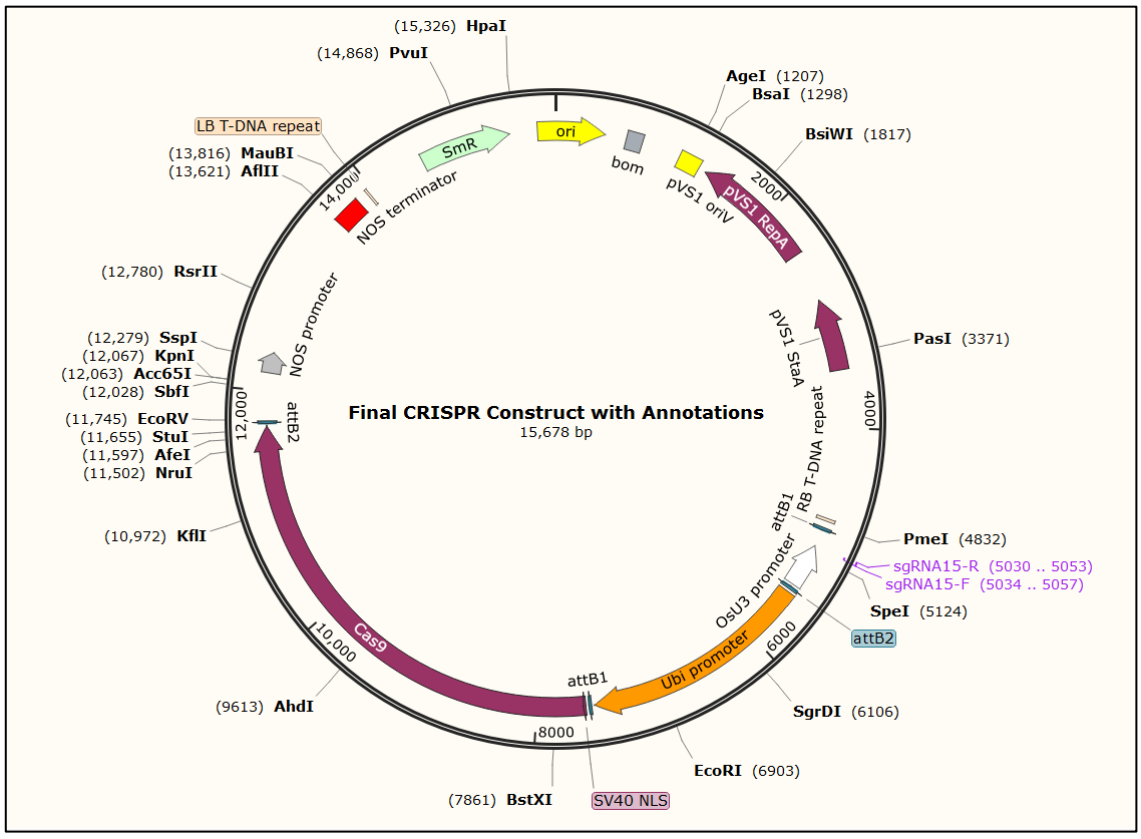

Figure A4: *In silico* representation of the final OsDUF538 CRISPR-Cas9 final construct prior to rice transformation.

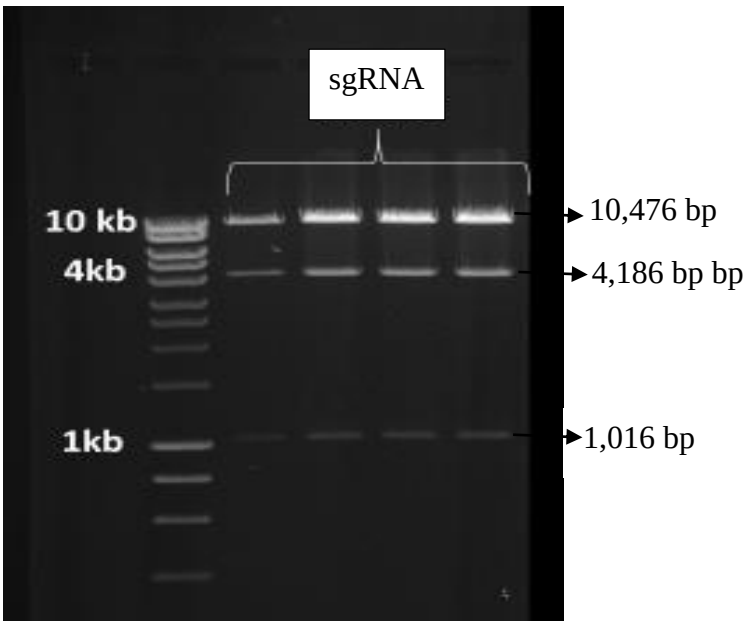

Figure A5: Restriction enzyme digest of *OsDUF538* CRISPR-Cas9 final construct (shown in A4) prior to rice transformation. The restriction enzyme *Nco1* (NEB # R3193S) generated three expected DNA fragments (1,016 bp, 4,186 bp and 10,476 bp) which matched the size of the final construct (15,678 kb). The final construct was sent to NIAB for rice transformation.

LIST OF FIGURES

LIST OF TABLES

REFERENCES

Akcapinar, G. B., Kappel, L., Sezerman, O. U. & Seidl-Seiboth, V. Molecular diversity of LysM carbohydrate-binding motifs in fungi. Curr. Genet. 61, 103–113 (2015).

Akiyama, K. & Hayashi, H. Strigolactones: Chemical signals for fungal symbionts and parasitic weeds in plant roots. Handb. Environ. Chem. Vol. 5 Water Pollut. 97, 925–931 (2006).

Akiyama, K., Matsuzaki, K. I. & Hayashi, H. Plant sesquiterpenes induce hyphal branching in arbuscular mycorrhizal fungi. Nature 435, 824–827 (2005).

Al-Babili, S. & Bouwmeester, H. J. Strigolactones, a Novel Carotenoid-Derived Plant Hormone. Annu. Rev. Plant Biol. 66, 161–186 (2015).

Alder, A. et al. The path from β-carotene to carlactone, a strigolactone-like plant hormone. Science. 335, 1348–1351 (2012).

Alexander, T., Toth, R., Meier, R. & Weber, H. C. Dynamics of arbuscule development and degeneration in onion, bean, and tomato with reference to vesicular–arbuscular mycorrhizae in grasses. Can. J. Bot. 67, 2505–2513 (1989).

Ali, R. et al. Death don't have no mercy and neither does calcium: *Arabidopsis* Cyclic Nucleotide Gated Channel 2 and innate immunity. Plant Cell 19, 1081–1095 (2007).

Alvarez, F. J. & Konopka, J. B. Identification of an N-acetylglucosamine transporter that mediates hyphal induction in *Candida albicans*. Mol. Biol. Cell 18, 965–975 (2007).

Amor, B. Ben et al. The NFP locus of *Medicago truncatula* controls an early step of Nod factor signal transduction upstream of a rapid calcium flux and root hair deformation. Plant J. 34, 495–506 (2003).

Antolín-Llovera, M. et al. Knowing your friends and foes - plant receptor-like kinases as initiators of symbiosis or defence. New Phytol. 204, 791–802 (2014).

Antolín-Llovera, M., Ried, M. K., Binder, A. & Parniske, M. Receptor Kinase Signaling Pathways in Plant-Microbe Interactions. Annu. Rev. Phytopathol. 50, 451–473 (2012).

Ao, Y. et al. OsCERK1 and OsRLCK176 play important roles in peptidoglycan and chitin signaling in rice innate immunity. Plant J. 80, 1072–1084 (2014).

Ardourel, M. et al. *Rhizobium meliloti* lipooligosaccharide nodulation factors: Different structural requirements for bacterial entry into target root hair cells and induction of plant symbiotic developmental responses. Plant Cell 6, 1357–1374 (1994).

Arrighi, J. F. et al. The *Medicago truncatula* lysine motif-receptor-like kinase gene family includes NFP and new nodule-expressed genes. Plant Physiol. 142, 265–279 (2006).

Augé, R. M., Toler, H. D. & Saxton, A. M. Arbuscular mycorrhizal symbiosis alters stomatal conductance of host plants more under drought than under amply watered conditions: a meta-analysis. Mycorrhiza 25, 13–24 (2014).

Balestrini, R. & Bonfante, P. Cell wall remodeling in mycorrhizal symbiosis: A way towards biotrophism. Frontiers in Plant Science 5, 1–10 (2014).

Barre, A., Hervé, C., Lescure, B. & Rougé, P. Lectin receptor kinases in plants. Critical Reviews in Plant Sciences 21, 379–399 (2002).

Becker, M., Becker, Y., Green, K. & Scott, B. The endophytic symbiont *Epichloë festucae* establishes an epiphyllous net on the surface of *Lolium perenne* leaves by development of an expressorium, an appressorium-like leaf exit structure. New Phytol. 211, 240–254 (2016).

Bellande, K., Bono, J. J., Savelli, B., Jamet, E. & Canut, H. Plant lectins and lectin receptor-like kinases: How do they sense the outside? International Journal of Molecular Sciences 18, (2017).

Bensmihen, S., de Billy, F. & Gough, C. Contribution of NFP LysM domains to the recognition of Nod factors during the *Medicago truncatula/Sinorhizobium meliloti* symbiosis. PLoS One 6, (2011).

Besserer, A., Bécard, G., Jauneau, A., Roux, C. & Séjalon-Delmas, N. GR24, a synthetic analog of strigolactones, stimulates the mitosis and growth of the arbuscular mycorrhizal fungus *Gigaspora rosea* by boosting its energy metabolism. Plant Physiol. 148, 402–413 (2008).

Besserer, A. et al. Strigolactones stimulate arbuscular mycorrhizal fungi by activating mitochondria. PLoS Biol. 4, 1239–1247 (2006).

Böhnert, H. U. et al. A putative polyketide synthase/peptide synthetase from *Magnaporthe grisea* signals pathogen attack to resistant rice. Plant Cell 16, 2499–2513 (2004).

Boller, T. & Felix, G. A Renaissance of Elicitors: Perception of Microbe-Associated Molecular Patterns and Danger Signals by Pattern-Recognition Receptors. Annu. Rev. Plant Biol. 60, 379–406 (2009).

Bonfante, P. & Genre, A. Arbuscular mycorrhizal dialogues: Do you speak 'plantish' or 'fungish'? Trends in Plant Science 20, 150–154 (2015).

Borghi, L., Kang, J., Ko, D., Lee, Y. & Martinoia, E. The role of ABCG-type ABC transporters in phytohormone transport. Biochem. Soc. Trans. 43, 924–930 (2015).

Bouckaert, J., Hamelryck, T., Wyns, L. & Loris, R. Novel structures of plant lectins and their complexes with carbohydrates. Current Opinion in Structural Biology 9, 572–577 (1999).

Boulos, L., Prévost, M., Barbeau, B., Coallier, J. & Desjardins, R. Live/Dead (®) BacLight $^{(TM)}$: Application of a new rapid staining method for direct enumeration of viable and total bacteria in drinking water. J. Microbiol. Methods 37, 77–86 (1999).

Bourett, T. M. & Howard, R. J. In vitro development of penetration structures in the rice blast fungus *Magnaporthe grisea*. Can. J. Bot. 68, 329–342 (1990).

Bouwmeester, H. J., Matusova, R., Zhongkui, S. & Beale, M. H. Secondary metabolite signalling in host-parasitic plant interactions. Current Opinion in Plant Biology 6, 358–364 (2003).

Bouwmeester, H. J., Roux, C., Lopez-Raez, J. A. & Bécard, G. Rhizosphere communication of plants, parasitic plants and AM fungi. Trends in Plant Science 12, 224–230 (2007).

Bouwmeester, K. et al. The lectin receptor kinase LecRK-I.9 is a novel *Phytophthora* resistance component and a potential host target for a RXLR effector. PLoS Pathog. 7, (2011).

Bouwmeester, K. & Govers, F. Arabidopsis L-type lectin receptor kinases: Phylogeny, classification, and expression profiles. J. Exp. Bot. 60, 4383–4396 (2009).

Brader, G., Compant, S., Mitter, B., Trognitz, F. & Sessitsch, A. Metabolic potential of endophytic bacteria. Current Opinion in Biotechnology 27, 30–37 (2014).

Bravo, A., Brands, M., Wewer, V., Dörmann, P. & Harrison, M. J. Arbuscular mycorrhiza-specific enzymes FatM and RAM2 fine-tune lipid biosynthesis to promote development of arbuscular mycorrhiza. New Phytol. 214, 1631–1645 (2017).

Breuillin-Sessoms, F. et al. Suppression of arbuscule degeneration in *Medicago truncatula* phosphate transporter4 mutants is dependent on the ammonium transporter 2 family protein AMT2;3. Plant Cell 27, 1352–1366 (2015).

Brewer, P. B. et al. Lateral branching oxidoreductase acts in the final stages of strigolactone biosynthesis in *Arabidopsis.* Proc. Natl. Acad. Sci. U. S. A. 113, 6301–6306 (2016).

Broghammer, A. et al. Legume receptors perceive the rhizobial lipochitin oligosaccharide signal molecules by direct binding. Proc. Natl. Acad. Sci. U. S. A. 109, 13859–13864 (2012).

Bruno, M. et al. Insights into the formation of carlactone from in-depth analysis of the CCD8-catalyzed reactions. FEBS Lett. 591, 792–800 (2017).

Brutus, A., Sicilia, F., Macone, A., Cervone, F. & De Lorenzo, G. A domain swap approach reveals a role of the plant wall-associated kinase 1 (WAK1) as a receptor of oligogalacturonides. Proc. Natl. Acad. Sci. U. S. A. 107, 9452–9457 (2010).

Buendia, L., Wang, T., Girardin, A. & Lefebvre, B. The LysM receptor-like kinase SlLYK10 regulates the arbuscular mycorrhizal symbiosis in tomato. New Phytol. 210, 184–195 (2016).

Buist, G., Steen, A., Kok, J. & Kuipers, O. P. LysM, a widely distributed protein motif for binding to (peptido)glycans. Molecular Microbiology 68, 838–847 (2008).

Bureau, C. et al. A protocol combining multiphoton microscopy and propidium iodide for deep 3D root meristem imaging in rice: Application for the screening and identification of tissue-specific enhancer trap lines. Plant Methods 14, (2018).

Cao, Y. et al. The kinase LYK5 is a major chitin receptor in *Arabidopsis* and forms a chitin-induced complex with related kinase CERK1. Elife 3, (2014).

Capoen, W. et al. Nuclear membranes control symbiotic calcium signaling of legumes. Proc. Natl. Acad. Sci. U. S. A. 108, 14348–14353 (2011).

Carbonnel, S. & Gutjahr, C. Control of arbuscular mycorrhiza development by nutrient signals. Front. Plant Sci. 5, (2014).

Carotenuto, G. et al. The rice LysM receptor-like kinase OsCERK1 is required for the perception of short-chain chitin oligomers in arbuscular mycorrhizal signaling. New Phytol. 214, 1440–1446 (2017).

Catoira, R. et al. Four genes of *Medicago truncatula* controlling components of a Nod factor transduction pathway. Plant Cell 12, 1647–1665 (2000).

Chabaud, M., Venard, C., Defaux-Petras, A., Bécard, G. & Barker, D. G. Targeted inoculation of *Medicago truncatula in vitro* root cultures reveals MtENOD11 expression during early stages of infection by arbuscular mycorrhizal fungi. New Phytol. 156, 265–273 (2002).

Chabaud, M. et al. Arbuscular mycorrhizal hyphopodia and germinated spore exudates trigger Ca2+ spiking in the legume and nonlegume root epidermis. New Phytol. 189, 347–355 (2011).

Charpentier, M. et al. *Lotus japonicus* Castor and Pollux are ion channels essential for perinuclear calcium spiking in legume root endosymbiosis. Plant Cell 20, 3467–3479 (2008).

Charpentier, M. et al. Nuclear-localized cyclic nucleotide-gated channels mediate symbiotic calcium oscillations. Science. 352, 1102–1105 (2016).

Cheng, X. et al. A rice lectin receptor-like kinase that is involved in innate immune responses also contributes to seed germination. Plant J. 76, 687–698 (2013).

Chinchilla, D., Bauer, Z., Regenass, M., Boller, T. & Felix, G. The Arabidopsis receptor kinase FLS2 binds flg22 and determines the specificity of flagellin perception. Plant Cell 18, 465–476 (2006).

Chinchilla, D. et al. A flagellin-induced complex of the receptor FLS2 and BAK1 initiates plant defence. Nature 448, 497–500 (2007).

Choi, J. et al. Identification of a plant receptor for extracellular ATP. Science. 343, 290–294 (2014).

Choi, W. & Dean, R. A. The Adenylate Cyclase Gene MAC1 of *Magnaporthe grisea* Controls Appressorium Formation and Other Aspects of Growth and Development. Plant Cell 9, 1973 (1997).

Christensen, M. J. & Voisey, C. R. The biology of the endophyte/grass partnership. New Zeal. Grassl. Assoc. Endophyte Symp. (2007).

Christensen, M. J. Variation in the ability of Acremonium endophytes of *Lolium perenne, Festuca arundinacea* and *F. pratensis* to form compatible associations in the three grasses. Mycol. Res. 99, 466–470 (1995).

Christensen, M. J., Ball, O. J. P., Bennett, R. J. & Schardl, C. L. Fungal and host genotype effects on compatibility and vascular colonization by *Epichloe festucae*. Mycol. Res. 101, 493–501 (1997).

Chumley, F. G. Genetic Analysis of Melanin-Deficient, Nonpathogenic Mutants of *Magnaporthe grisea*. Mol. Plant-Microbe Interact. 3, 135 (1990).

Clarke, V. C., Loughlin, P. C., Day, D. A. & Smith, P. M. C. Transport processes of the legume symbiosome membrane. Front. Plant Sci. 5, (2014).

Collemare, J. et al. *Magnaporthe grisea* avirulence gene ACE1 belongs to an infection-specific gene cluster involved in secondary metabolism. New Phytol. 179, 196–208 (2008).

Cook, C. E., Whichard, L. P., Turner, B., Wall, M. E. & Egley, G. H. Germination of witchweed (striga lutea lour.): Isolation and properties of a potent stimulant. Science. 154, 1189–1190 (1966).

Cook, D. E., Mesarich, C. H. & Thomma, B. P. H. J. Understanding Plant Immunity as a Surveillance System to Detect Invasion. Annu. Rev. Phytopathol. 53, 541–563 (2015).

Cook, R. J. Take-all of wheat. Physiological and Molecular Plant Pathology 62, 73–86 (2003).

Couto, D. & Zipfel, C. Regulation of pattern recognition receptor signalling in plants. Nat. Rev. Immunol. 16, 537–552 (2016).

Cvrckova, F., Elias, M., Hala, M., Obermeyer, G. & Zarsky, V. Small GTPases and conserved signalling pathways in plant cell morphogenesis: From exocytosis to the exocyst. in Cell Biology of Plant and Fungal Tip Growth 328, 105–122 (2001).

Cvrčková, F. et al. Evolution of the land plant exocyst complexes. Front. Plant Sci. 3, (2012).

Czaja, L. F. et al. Transcriptional responses toward diffusible signals from symbiotic microbes reveal MtNFP- and MtDMI3-dependent reprogramming of host gene expression by arbuscular mycorrhizal fungal lipochitooligosaccharidesspi. Plant Physiol. 159, 1671–1685 (2012).

David-Schwartz, R. et al. Identification of a novel genetically controlled step in mycorrhizal colonization: Plant resistance to infection by fungal spores but not extra-radical hyphae. Plant J. 27, 561–569 (2001).

De Cuyper, C. et al. From lateral root density to nodule number, the strigolactone analogue GR24 shapes the root architecture of Medicago truncatula. J. Exp. Bot. 66, 137–146 (2015).

De Cuyper, C. & Goormachtig, S. Strigolactones in the rhizosphere: Friend or foe? Molecular Plant-Microbe Interactions 30, 683–690 (2017).

de Guillen, K. et al. Structure Analysis Uncovers a Highly Diverse but Structurally Conserved Effector Family in Phytopathogenic Fungi. PLoS Pathog. 11, (2015).

De Wit, P. J. G. M. How plants recognize pathogens and defend themselves. Cellular and Molecular Life Sciences 64, 2726–2732 (2007).

Den Camp, R. O. et al. LysM-type mycorrhizal receptor recruited for rhizobium symbiosis in nonlegume Parasponia. Science. 331, 909–912 (2011).

Denarie, J. Rhizobium Lipo-Chitooligosaccharide Nodulation Factors: Signaling Molecules Mediating Recognition and Morphogenesis. Annu. Rev. Biochem. 65, 503–535 (1996).

Devers, E. A., Teply, J., Reinert, A., Gaude, N. & Krajinski, F. An endogenous artificial microRNA system for unraveling the function of root endosymbioses related genes in *Medicago truncatula*. BMC Plant Biol. 13, (2013).

D'Haeze, W. & Holsters, M. Nod factor structures, responses, and perception during initiation of nodule development. Glycobiology 12, (2002).

Dickson, S. The Arum-Paris continuum of mycorrhizal symbioses. New Phytol. 163, 187–200 (2004).

Downie, J. A. & Walker, S. A. Plant responses to nodulation factors. Current Opinion in Plant Biology 2, 483–489 (1999).

Eaton, C. J. et al. Disruption of signaling in a fungal-grass symbiosis leads to pathogenesis. Plant Physiol. 153, 1780–1794 (2010).

Ebbole, D. J. *Magnaporthe* as a Model for Understanding Host-Pathogen Interactions. Annu. Rev. Phytopathol. 45, 437–456 (2007).

Eckardt, N. A. Chitin signaling in plants: Insights into the perception of fungal pathogens and rhizobacterial symbionts. Plant Cell 20, 241–243 (2008).

El Ghachtouli, N., Martin-Tanguy, J., Paynot, M. & Gianinazzi, S. First report of the inhibition of arbuscular mycorrhizal infection of *Pisum sativum* by specific and irreversible inhibition of polyamine biosynthesis or by gibberellic acid treatment. FEBS Lett. 385, 189–192 (1996).

Endre, G. et al. A receptor kinase gene regulating symbiotic nodule development. Nature 417, 962–966 (2002).

Evangelisti, E., Rey, T. & Schornack, S. Cross-interference of plant development and plant-microbe interactions. Current Opinion in Plant Biology 20, 118–126 (2014).

Farman, M. L. & Leong, S. A. Chromosome walking to the AVR1-CO39 avirulence gene of *Magnaporthe grisea*: Discrepancy between the physical and genetic maps. Genetics 150, 1049–1058 (1998).

Faulkner, C. et al. LYM2-dependent chitin perception limits molecular flux via plasmodesmata. Proc. Natl. Acad. Sci. U. S. A. 110, 9166–9170 (2013).

Feddermann, N. et al. The PAM1 gene of petunia, required for intracellular accommodation and morphogenesis of arbuscular mycorrhizal fungi, encodes a homologue of VAPYRIN. Plant J. 64, 470–481 (2010).

Felix, G., Duran, J. D., Volko, S. & Boller, T. Plants have a sensitive perception system for the most conserved domain of bacterial flagellin. Plant J. 18, 265–276 (1999).

Fendrych, M. et al. The *Arabidopsis* exocyst complex is involved in cytokinesis and cell plate maturation. Plant Cell 22, 3053–3065 (2010).

Fisher, M. C. et al. Emerging fungal threats to animal, plant and ecosystem health. Nature 484, 186–194 (2012).

Fisher, R. F. & Long, S. R. Rhizobium-plant signal exchange. Nature 357, 655–660 (1992).

Flematti, G. R., Ghisalberti, E. L., Dixon, K. W. & Trengove, R. D. A compound from smoke that promotes seed germination. Science. 305, 977 (2004).

Fliegmann, J. & Felix, G. Immunity: Flagellin seen from all sides. Nat. Plants (2016).

Floss, D. S. et al. A Transcriptional Program for Arbuscule Degeneration during AM Symbiosis Is Regulated by MYB1. Curr. Biol. 27, 1206–1212 (2017).

Floss, D. S., Levy, J. G., Lévesque-Tremblay, V., Pumplin, N. & Harrison, M. J. DELLA proteins regulate arbuscule formation in arbuscular mycorrhizal symbiosis. Proc. Natl. Acad. Sci. U. S. A. 110, (2013).

Foo, E. & Davies, N. W. Strigolactones promote nodulation in pea. Planta 234, 1073–1081 (2011).

Freeman, J. & Ward, E. *Gaeumannomyces graminis*, the take-all fungus and its relatives. Molecular Plant Pathology 5, 235–252 (2004).

Fujisaki, K. et al. Rice Exo70 interacts with a fungal effector, AVR-Pii, and is required for AVR-Pii-triggered immunity. Plant J. 83, 875–887 (2015).

Garvey, K. J., Saedi, M. S. & Ito, J. Nucleotide sequence of Bacillus phage ø29 genes 14 and 15: Homology of gene 15 with other phage lysozymes. Nucleic Acids Res. 14, 10001–10008 (1986).

Gaulin, E., Jacquet, C., Bottin, A. & Dumas, B. Root rot disease of legumes caused by *Aphanomyces euteiches*. Molecular Plant Pathology 8, 539–548 (2007).

Genre, A. et al. Multiple exocytotic markers accumulate at the sites of perifungal membrane biogenesis in arbuscular mycorrhizas. Plant Cell Physiol. 53, 244–255 (2012).

Genre, A. & Bonfante, P. The making of symbiotic cells in arbuscular mycorrhizal roots. in Arbuscular Mycorrhizas: Physiology and Function 57–71 (2010). doi:10.1007/978-90-481-9489-6_3

Genre, A. et al. Short-chain chitin oligomers from arbuscular mycorrhizal fungi trigger nuclear Ca2+ spiking in *Medicago truncatula* roots and their production is enhanced by strigolactone. New Phytol. 198, 190–202 (2013).

Genre, A., Chabaud, M., Faccio, A., Barker, D. G. & Bonfante, P. Prepenetration apparatus assembly precedes and predicts the colonization patterns of arbuscular mycorrhizal fungi within the root cortex of both *Medicago truncatula* and *Daucus carota*. Plant Cell 20, 1407–1420 (2008).

Genre, A., Chabaud, M., Timmers, T., Bonfante, P. & Barker, D. G. Arbuscular mycorrhizal fungi elicit a novel intracellular apparatus in *Medicago truncatula* root epidermal cells before infection. Plant Cell 17, 3489–3499 (2005).

Genre, A. & Russo, G. Does a common pathway transduce symbiotic signals in plant–microbe interactions? Front. Plant Sci. 7, (2016).

Geurts, R., Xiao, T. T. & Reinhold-Hurek, B. What Does It Take to Evolve A Nitrogen-Fixing Endosymbiosis? Trends in Plant Science 21, 199–208 (2016).

Gholizadeh, A. & Kohnehrouz, B. B. Identification of DUF538 cDNA clone from Celosia cristata expressed sequences of nonstressed and stressed leaves. Russ. J. Plant Physiol. 57, 247–252 (2010).

Gholizadeh, A. Heterologous expression of stress-responsive DUF538 domain containing protein and its morpho-biochemical consequences. Protein J. 30, 351–358 (2011).

Gholizadeh, A. Chlorophyll Binding Ability of Non-chloroplastic DUF538 Protein Superfamily in Plants. Proc. Natl. Acad. Sci. India Sect. B - Biol. Sci. 88, 967–976 (2018).

Gholizadeh, A. DUF538 protein superfamily is predicted to be chlorophyll hydrolyzing enzymes in plants. Physiol. Mol. Biol. Plants 22, 77–85 (2016).

Gholizadeh, A. & Kohnehrouz, S. B. DUF538 protein super family is predicted to be the potential homologue of bactericidal/permeability-increasing protein in plant system. Protein J. 32, 163–171 (2013).

Gilardoni, P. A., Hettenhausen, C., Baldwin, I. T. & Bonaventure, G. Nicotiana attenuata lectin receptor kinase1 suppresses the insect-mediated inhibition of induced defense responses during manduca sexta herbivory. Plant Cell 23, 3512–3532 (2011).

Giraldo, M. C. et al. Two distinct secretion systems facilitate tissue invasion by the rice blast fungus *Magnaporthe oryzae*. Nat. Commun. 4, (2013).

Gleason, C. et al. Nodulation independent of rhizobia induced by a calcium-activated kinase lacking autoinhibition. Nature 441, 1149–1152 (2006).

Gobbato, E. et al. A GRAS-type transcription factor with a specific function in mycorrhizal signaling. Curr. Biol. 22, 2236–2241 (2012).

Gobbato, E. et al. RAM1 and RAM2 function and expression during Arbuscular Mycorrhizal Symbiosis and *Aphanomyces euteiches* colonization. Plant Signal. Behav. 8, (2013).

Gómez-Gómez, L. & Boller, T. FLS2: An LRR receptor-like kinase involved in the perception of the bacterial elicitor flagellin in *Arabidopsis*. Mol. Cell 5, 1003–1011 (2000).

Gómez-Gómez, L. & Boller, T. Flagellin perception: A paradigm for innate immunity. Trends in Plant Science 7, 251–256 (2002).

Gomez-Roldan, V. et al. Strigolactone inhibition of shoot branching. Nature 455, 189–194 (2008).

Gomez-Roldan, V., Roux, C., Girard, D., Bécard, G. & Puech-Pagés, V. Strigolactones: Promising plant signals. Plant Signal. Behav. 2, 163–164 (2007).

Gong, B. Q. et al. Rice Chitin Receptor OsCEBiP Is Not a Transmembrane Protein but Targets the Plasma Membrane via a GPI Anchor. Molecular Plant 10, 767–770 (2017).

Gough, C., Cottret, L., Lefebvre, B. & Bono, J. J. Evolutionary history of plant LysM receptor proteins related to root endosymbiosis. Front. Plant Sci. 9, (2018).

Gough, C. & Cullimore, J. Lipo-chitooligosaccharide signaling in endosymbiotic plant-microbe interactions. Mol. Plant-Microbe Interact. 24, 867–878 (2011).

Gouhier-Darimont, C., Schmiesing, A., Bonnet, C., Lassueur, S. & Reymond, P. Signalling of *Arabidopsis thaliana* response to Pieris brassicae eggs shares similarities with PAMP-triggered immunity. J. Exp. Bot. 64, 665–674 (2013).

Groth, M. et al. NENA, a *Lotus japonicus* homolog of Sec13, is required for rhizodermal infection by arbuscular mycorrhiza fungi and rhizobia but dispensable for cortical endosymbiotic development. Plant Cell 22, 2509–2526 (2010).

Güimil, S. et al. Comparative transcriptomics of rice reveals an ancient pattern of response to microbial colonization. Proc. Natl. Acad. Sci. U. S. A. 102, 8066–8070 (2005).

Gust, A. A., Willmann, R., Desaki, Y., Grabherr, H. M. & Nürnberger, T. Plant LysM proteins: Modules mediating symbiosis and immunity. Trends in Plant Science 17, 495–502 (2012).

Gutjahr, C. et al. Arbuscular Mycorrhiza-Specific Signaling in Rice Transcends the Common Symbiosis Signaling Pathway. Plant Cell 20, 2989–3005 (2008).

Gutjahr, C., Casieri, L. & Paszkowski, U. *Glomus intraradices* induces changes in root system architecture of rice independently of common symbiosis signaling. New Phytol. 182, 829–837 (2009).

Gutjahr, C. et al. Rice perception of symbiotic arbuscular mycorrhizal fungi requires the karrikin receptor complex. Science. 350, 1521–1524 (2015).

Gutjahr, C. et al. Presymbiotic factors released by the arbuscular mycorrhizal fungus Gigaspora margarita induce starch accumulation in *Lotus japonicus* roots: Rapid report. New Phytol. 183, 53–61 (2009).

Gutjahr, C. & Parniske, M. Cell and Developmental Biology of Arbuscular Mycorrhiza Symbiosis. Annu. Rev. Cell Dev. Biol. 29, 593–617 (2013).

Gutjahr, C. & Paszkowski, U. Multiple control levels of root system remodeling in arbuscular mycorrhizal symbiosis. Frontiers in Plant Science 4, (2013).

Gutjahr, C. et al. The half-size ABC transporters STR1 and STR2 are indispensable for mycorrhizal arbuscule formation in rice. Plant J. 69, 906–920 (2012).

Gutjahr, C. et al. Transcriptome diversity among rice root types during asymbiosis and interaction with arbuscular mycorrhizal fungi. Proc. Natl. Acad. Sci. U. S. A. 112, 6754–6759 (2015).

Hamer, J. E., Valent, B. & Chumley, F. G. Mutations at the smo genetic locus affect the shape of diverse cell types in the rice blast fungus. Genetics (1989).

Hamer, J. E., Howard, R. J., Chumley, F. G. & Valent, B. A mechanism for surface attachment in spores of a plant pathogenic fungus. Science. (1988). doi:10.1126/science.239.4837.288

Hamer, J. E. & Talbot, N. J. Infection-related development in the rice blast fungus *Magnaporthe grisea*. Curr. Opin. Microbiol. (1998). doi:10.1016/S1369-5274(98)80117-3

Hann, D. R. & Rathjen, J. P. Early events in the pathogenicity of *Pseudomonas syringae* on *Nicotiana benthamiana*. Plant J. (2007). doi:10.1111/j.1365-313X.2006. 02981.x

Harris, J. M., Wais, R. & Long, S. R. Rhizobium-Induced Calcium Spiking in *Lotus japonicus*. Mol. Plant-Microbe Interact. (2007). doi:10.1094/mpmi.2003.16.4.335

Harrison, M. J. Molecular and cellular aspects of the arbuscular mycorrhizal symbiosis. Annu. Rev. Plant Physiol. Plant Mol. Biol. (1999). doi: 10.1146/annurev.arplant.50.1.361

Harrison, M. J. Cellular programs for arbuscular mycorrhizal symbiosis. Current Opinion in Plant Biology (2012). doi: 10.1016/j.pbi.2012.08.010

Harrison, M. J. Signaling in the arbuscular mycorrhizal symbiosis. Annu. Rev. Microbiol. (2005). doi: 10.1146/annurev.micro.58.030603.123749

Harrison, M. J., Dewbre, G. R. & Liu, J. A phosphate transporter from *Medicago truncatula* involved in the acquisition of phosphate released by arbuscular mycorrhizal fungi. Plant Cell (2002). doi:10.1105/tpc.004861

Hayakawa, Y., Ishikawa, E., Shoji, J. ya, Nakano, H. & Kitamoto, K. Septum-directed secretion in the filamentous fungus *Aspergillus oryzae*. Mol. Microbiol. (2011). doi:10.1111/j.1365-2958.2011. 07700.x

Hayashi, T. et al. A dominant function of CCaMK in intracellular accommodation of bacterial and fungal endosymbionts. Plant J. (2010). doi:10.1111/j.1365-313X.2010. 04228.x

He, B. & Guo, W. The exocyst complex in polarized exocytosis. Current Opinion in Cell Biology (2009). doi: 10.1016/j.ceb.2009.04.007

Heese, A. et al. The receptor-like kinase SERK3/BAK1 is a central regulator of innate immunity in plants. Proc. Natl. Acad. Sci. (2007). doi:10.1073/pnas.0705306104

Heider, M. R. & Munson, M. Exorcising the Exocyst Complex. Traffic (2012). doi:10.1111/j.1600-0854.2012. 01353.x

Hervé, C., Dabos, P., Galaud, J. R., Rougé, P. & Lescure, B. Characterization of an *Arabidopsis thaliana* gene that defines a new class of putative plant receptor kinases with an extracellular lectin-like domain. J. Mol. Biol. (1996). doi:10.1006/jmbi.1996.0286

Hijikata, N. et al. Polyphosphate has a central role in the rapid and massive accumulation of phosphorus in extraradical mycelium of an arbuscular mycorrhizal fungus. New Phytologist (2010). doi:10.1111/j.1469-8137.2009. 03168.x

Horváth, B. et al. *Medicago truncatula* IPD3 is a member of the common symbiotic signaling pathway required for rhizobial and mycorrhizal symbioses. Mol. Plant-Microbe Interact. (2011). doi:10.1094/MPMI-01-11-0015

Howard, R. J. & Valent, B. Breaking and entering: Host Penetration by the Fungal Rice Blast Pathogen *Magnaporthe grisea*. Annu. Rev. Microbiol. (2002). doi: 10.1146/annurev.micro.50.1.491

Hsu, S. C. et al. The mammalian brain rsec6/8 complex. Neuron (1996). doi:10.1016/S0896-6273(00)80251-2

Iizasa, E., Mitsutomi, M. & Nagano, Y. Direct binding of a plant LysM receptor-like kinase, LysM RLK1/CERK1, to chitin in vitro. J. Biol. Chem. (2010). doi:10.1074/jbc.M109.027540

Ivanov, S. et al. Rhizobium-legume symbiosis shares an exocytotic pathway required for arbuscule formation. Proc. Natl. Acad. Sci. U. S. A. (2012). doi:10.1073/pnas.1200407109

Ivanov, S. & Harrison, M. J. A set of fluorescent protein-based markers expressed from constitutive and arbuscular mycorrhiza-inducible promoters to label organelles, membranes and cytoskeletal elements in Medicago truncatula. Plant J. (2014). doi:10.1111/tpj.12706

Javot, H., Penmetsa, R. V., Terzaghi, N., Cook, D. R. & Harrison, M. J. A *Medicago truncatula* phosphate transporter indispensable for the arbuscular mycorrhizal symbiosis. Proc. Natl. Acad. Sci. U. S. A. (2007). doi:10.1073/pnas.0608136104

Jeong, D.-H. et al. T-DNA Insertional Mutagenesis for Activation Tagging in Rice. Plant Physiol. (2002). doi:10.1104/pp.014357

Jin, Y. et al. DELLA proteins are common components of symbiotic rhizobial and mycorrhizal signalling pathways. Nat. Commun. (2016). doi:10.1038/ncomms12433

Jones, J. D. G. & Dangl, J. L. The plant immune system. Nature (2006). doi:10.1038/nature05286

Jumpponen, A. & Trappe, J. M. Dark septate endophytes: A review of facultative biotrophic root-colonizing fungi. New Phytol. (1998). doi:10.1046/j.1469-8137.1998. 00265.x

Jung, S. C., Martinez-Medina, A., Lopez-Raez, J. A. & Pozo, M. J. Mycorrhiza-Induced Resistance and Priming of Plant Defenses. J. Chem. Ecol. (2012). doi:10.1007/s10886-012-0134-6

Kaku, H. et al. Plant cells recognize chitin fragments for defense signaling through a plasma membrane receptor. Proc. Natl. Acad. Sci. (2006). doi:10.1073/pnas.0508882103

Kämpfer, P. The Family Streptomycetaceae, Part I: Taxonomy. in The Prokaryotes (2006). doi:10.1007/0-387-30743-5_22

Kanamori, N. et al. A nucleoporin is required for induction of Ca2+ spiking in legume nodule development and essential for rhizobial and fungal symbiosis. Proc. Natl. Acad. Sci. U. S. A. (2006). doi:10.1073/pnas.0508883103

Kang, S. The PWL Host Specificity Gene Family in the Blast Fungus *Magnaporthe grisea*. Mol. Plant-Microbe Interact. (2011). doi:10.1094/mpmi-8-0939

Kankanala, P., Czymmek, K. & Valent, B. Roles for Rice Membrane Dynamics and Plasmodesmata during Biotrophic Invasion by the Blast Fungus. Plant cell online (2007). doi:10.1105/tpc.106.046300

Kanzaki, H. et al. NbLRK1, a lectin-like receptor kinase protein of *Nicotiana benthamiana*, interacts with *Phytophthora infestans* INF1 elicitin and mediates INF1-induced cell death. Planta (2008). doi:10.1007/s00425-008-0797-y

Kee, Y. et al. Subunit structure of the mammalian exocyst complex. Proc. Natl. Acad. Sci. U. S. A. (1997). doi:10.1073/pnas.94.26.14438

Kershaw, M. J. & Talbot, N. J. Genome-wide functional analysis reveals that infection-associated fungal autophagy is necessary for rice blast disease. Proc. Natl. Acad. Sci. U. S. A. (2009). doi:10.1073/pnas.0901477106

Kevei, Z. et al. 3-Hydroxy-3-methylglutaryl coenzyme A reductase1 interacts with NORK and is crucial for nodulation in *Medicago truncatula*. Plant Cell (2007). doi:10.1105/tpc.107.053975

Kistner, C. & Parniske, M. Evolution of signal transduction in intracellular symbiosis. Trends Plant Sci. (2002). doi:10.1016/S1360-1385(02)02356-7

Kistner, C. et al. Seven *Lotus japonicus* genes required for transcriptional reprogramming of the root during fungal and bacterial symbiosis. Plant Cell (2005). doi:10.1105/tpc.105.032714

Kobae, Y. & Ohtomo, R. An improved method for bright-field imaging of arbuscular mycorrhizal fungi in plant roots. Soil Sci. Plant Nutr. (2016). doi:10.1080/00380768.2015.1106923

Koga, H., Christensen, M. J. & Bennett, R. J. Incompatibility of some grass-Acremonium endophyte associations. Mycol. Res. (1993). doi:10.1016/S0953-7562(09)81292-6

Koga, H. Hypersensitive death, autofluorescence, and ultrastructural changes in cells of leaf sheaths of susceptible and resistant near-isogenic lines of rice in relation to penetration and growth of *Pyricularia oryzae*. Can. J. Bot. (2007). doi:10.1139/b94-180

Kohlen, W. et al. The tomato carotenoid cleavage dioxygenase8 (SlCCD8) regulates rhizosphere signaling, plant architecture and affects reproductive development through strigolactone biosynthesis. New Phytol. (2012). doi:10.1111/j.1469-8137.2012. 04265.x

Koltai, H. et al. A tomato strigolactone-impaired mutant displays aberrant shoot morphology and plant interactions. J. Exp. Bot. (2010). doi:10.1093/jxb/erq041

Kosuta, S. et al. A Diffusible Factor from Arbuscular Mycorrhizal Fungi Induces Symbiosis-Specific MtENOD11 Expression in Roots of *Medicago truncatula*. Plant Physiol. (2003). doi:10.1104/pp.011882

Kosuta, S. et al. Differential and chaotic calcium signatures in the symbiosis signaling pathway of legumes. Proc. Natl. Acad. Sci. U. S. A. (2008). doi:10.1073/pnas.0803499105

Kouzai, Y. et al. Targeted Gene Disruption of OsCERK1 Reveals Its Indispensable Role in Chitin Perception and Involvement in the Peptidoglycan Response and Immunity in Rice. Mol. Plant-Microbe Interact. (2014). doi:10.1094/mpmi-03-14-0068-r

Kouzai, Y. et al. CEBiP is the major chitin oligomer-binding protein in rice and plays a main role in the perception of chitin oligomers. Plant Mol. Biol. (2014). doi:10.1007/s11103-013-0149-6

Krajinski, F. et al. The H+-ATPase HA1 of *Medicago truncatula* is essential for phosphate transport and plant growth during arbuscular mycorrhizal symbiosis. Plant Cell (2014). doi:10.1105/tpc.113.120436

Kretzschmar, T. et al. A petunia ABC protein controls strigolactone-dependent symbiotic signalling and branching. Nature (2012). doi:10.1038/nature10873

Kuhn, H., Küster, H. & Requena, N. Membrane steroid-binding protein 1 induced by a diffusible fungal signal is critical for mycorrhization in *Medicago truncatula*. New Phytol. (2010). doi:10.1111/j.1469-8137.2009. 03116.x

Kulich, I. et al. Arabidopsis exocyst subunits SEC8 and EXO70A1 and exocyst interactor ROH1 are involved in the localized deposition of seed coat pectin. New Phytol. (2010). doi:10.1111/j.1469-8137.2010. 03372.x

Kumar, V., Kumar, A., Pandey, K. D. & Roy, B. K. Isolation and characterization of bacterial endophytes from the roots of Cassia tora L. Ann. Microbiol. (2015). doi:10.1007/s13213-014-0977-x

Kunze, G. The N Terminus of Bacterial Elongation Factor Tu Elicits Innate Immunity in *Arabidopsis* Plants. Plant Cell Online (2004). doi:10.1105/tpc.104.026765

Kwak, Y. S. & Weller, D. M. Take-all of wheat and natural disease suppression: A review. Plant Pathology Journal (2013). doi:10.5423/PPJ.SI.07.2012.0112

Labeda, D. P. Multilocus sequence analysis of phytopathogenic species of the genus streptomyces. Int. J. Syst. Evol. Microbiol. (2011). doi:10.1099/ijs.0.028514-0

Lanfranco, L., Fiorilli, V. & Gutjahr, C. Partner communication and role of nutrients in the arbuscular mycorrhizal symbiosis. New Phytologist (2018). doi:10.1111/nph.15230

Lefebvre, B. et al. Role of N-glycosylation sites and CXC motifs in trafficking of *Medicago truncatula* Nod factor perception protein to plasma membrane. J. Biol. Chem. (2012). doi:10.1074/jbc.M111.281634

Leppyanen, I. V. et al. Receptor-like kinase LYK9 in *Pisum sativum* L. Is the CERK1-like receptor that controls both plant immunity and AM symbiosis development. Int. J. Mol. Sci. (2018). doi:10.3390/ijms19010008

Leuchtmann, A., Schardl, C. L. & Siegel, M. R. Sexual Compatibility and Taxonomy of a New Species of Epichloe Symbiotic with Fine Fescue Grasses. Mycologia (2007). doi:10.2307/3760595

Lévy, J. et al. A Putative Ca2+and Calmodulin-Dependent Protein Kinase Required for Bacterial and Fungal Symbioses. Science. (2004). doi:10.1126/science.1093038

Li, L. et al. The FLS2-associated kinase BIK1 directly phosphorylates the NADPH oxidase RbohD to control plant immunity. Cell Host Microbe (2014). doi: 10.1016/j.chom.2014.02.009

Li, S. et al. EXO70A1-mediated vesicle trafficking is critical for tracheary element development in *Arabidopsis*. Plant Cell (2013). doi:10.1105/tpc.113.112144

Li, X. et al. Dark septate endophytes isolated from a xerophyte plant promote the growth of *Ammopiptanthus mongolicus* under drought condition. Sci. Rep. (2018). doi:10.1038/s41598-018-26183-0

Liang, Y. et al. Lipochitooligosaccharide recognition: An ancient story. J. Physiol. (2014). doi:10.1111/nph.12898

Limpens, E. et al. LysM Domain Receptor Kinases Regulating Rhizobial Nod Factor-Induced Infection. Science. (2003). doi:10.1126/science.1090074

Lindow, S. E. & Brandl, M. T. Microbiology of the phyllosphere. Applied and Environmental Microbiology (2003). doi:10.1128/AEM.69.4.1875-1883.2003

Liu, S. et al. Molecular Mechanism for Fungal Cell Wall Recognition by Rice Chitin Receptor OsCEBiP. Structure (2016). doi: 10.1016/j.str.2016.04.014

Liu, T. et al. Chitin-induced dimerization activates a plant immune receptor. Science. (2012). doi:10.1126/science.1218867

Liu, W. et al. Strigolactone biosynthesis in *Medicago truncatula* and rice requires the symbiotic GRAS-type transcription factors NSP1 and NSP2. Plant Cell (2011). doi:10.1105/tpc.111.089771

Liu, Y. et al. A gene cluster encoding lectin receptor kinases confers broad-spectrum and durable insect resistance in rice. Nature Biotechnology (2015). doi:10.1038/nbt.3069

Lo Presti, L. et al. Fungal Effectors and Plant Susceptibility. Annu. Rev. Plant Biol. (2015). doi:10.1146/annurev-arplant-043014-114623

Lohmann, G. V. et al. Evolution and regulation of the lotus japonicus LysM receptor gene family. Mol. Plant-Microbe Interact. (2010). doi:10.1094/MPMI-23-4-0510

Loris, R. Principles of structures of animal and plant lectins. Biochimica et Biophysica Acta - General Subjects (2002). doi:10.1016/S0304-4165(02)00309-4

Lu, D. et al. A receptor-like cytoplasmic kinase, BIK1, associates with a flagellin receptor complex to initiate plant innate immunity. Proc. Natl. Acad. Sci. U. S. A. (2010). doi:10.1073/pnas.0909705107

Lu, Y. J. et al. Patterns of plant subcellular responses to successful oomycete infections reveal differences in host cell reprogramming and endocytic trafficking. Cell. Microbiol. (2012). doi:10.1111/j.1462-5822.2012. 01751.x

Luginbuehl, L. H. et al. Fatty acids in arbuscular mycorrhizal fungi are synthesized by the host plant. Science. (2017). doi:10.1126/science. aan0081

Luginbuehl, L. H. & Oldroyd, G. E. D. Understanding the Arbuscule at the Heart of Endomycorrhizal Symbioses in Plants. Current Biology (2017). doi: 10.1016/j.cub.2017.06.042

Maclean, A. M., Bravo, A. & Harrison, M. J. Plant Signaling and Metabolic Pathways Enabling Arbuscular Mycorrhizal Symbiosis. Plant Cell (2017). doi:10.1105/tpc.17.00555

Madsen, E. B. et al. Autophosphorylation is essential for the in vivo function of the *Lotus japonicus* Nod factor receptor 1 and receptor-mediated signalling in cooperation with Nod factor receptor 5. Plant J. (2011). doi:10.1111/j.1365-313X.2010. 04431.x

Madsen, E. B. et al. A receptor kinase gene of the LysM type is involved in legume perception of rhizobial signals. Nature (2003). doi:10.1038/nature02045

Madsen, L. H. et al. The molecular network governing nodule organogenesis and infection in the model legume *Lotus japonicus*. Nat. Commun. (2010). doi:10.1038/ncomms1009

Maeda, D. et al. Knockdown of an arbuscular mycorrhiza-inducible phosphate transporter gene of *Lotus japonicus* suppresses mutualistic symbiosis. Plant Cell Physiol. (2006). doi:10.1093/pcp/pcj069

Maillet, F. et al. Fungal lipochitooligosaccharide symbiotic signals in arbuscular mycorrhiza. Nature (2011). doi:10.1038/nature09622

Mandyam, K. & Jumpponen, A. Seeking the elusive function of the root-colonising dark septate endophytic fungi. Stud. Mycol. (2005). doi:10.3114/sim.53.1.173

Marcel, S., Sawers, R., Oakeley, E., Angliker, H. & Paszkowski, U. Tissue-Adapted Invasion Strategies of the Rice Blast Fungus *Magnaporthe oryzae*. Plant Cell (2010). doi:10.1105/tpc.110.078048

Markmann, K., Giczey, G. & Parniske, M. Functional adaptation of a plant receptor-kinase paved the way for the evolution of intracellular root symbioses with bacteria. PLoS Biol. (2008). doi: 10.1371/journal.pbio.0060068

Martin-urdiroz, M., Oses-ruiz, M., Ryder, L. S. & Talbot, N. J. Investigating the biology of plant infection by the rice blast fungus. Fungal Genet. Biol. (2015). doi: 10.1016/j.fgb.2015.12.009

Mentlak, T. A. et al. Effector-Mediated Suppression of Chitin-Triggered Immunity by Magnaporthe oryzae Is Necessary for Rice Blast Disease. Plant Cell (2012). doi:10.1105/tpc.111.092957

Miao, J. et al. Targeted mutagenesis in rice using CRISPR-Cas system. Cell Research (2013). doi:10.1038/cr.2013.123

Miller, J. B. & Oldroyd, G. E. D. The Role of Diffusible Signals in the Establishment of Rhizobial and Mycorrhizal Symbioses. in (2012). doi:10.1007/978-3-642-20966-6_1

Miller, J. B. et al. Calcium/calmodulin-dependent protein kinase is negatively and positively regulated by calcium, providing a mechanism for decoding calcium responses during symbiosis signaling. Plant Cell (2013). doi:10.1105/tpc.113.116921

Miwa, H., Sun, J., Oldroyd, G. E. D. & Downie, J. A. Analysis of Nod-factor-induced calcium signaling in root hairs of symbiotically defective mutants of *Lotus japonicus*. Mol. Plant. Microbe. Interact. (2006). doi:10.1094/MPMI-19-0914

Miya, A. et al. CERK1, a LysM receptor kinase, is essential for chitin elicitor signaling in *Arabidopsis*. Proc. Natl. Acad. Sci. (2007). doi:10.1073/pnas.0705147104

Miyata, K. et al. Evaluation of the role of the LysM receptor-like kinase, OsNFR5/OsRLK2 for AM symbiosis in rice. Plant Cell Physiol. (2016). doi:10.1093/pcp/pcw144

Miyata, K. et al. The bifunctional plant receptor, OsCERK1, regulates both chitin-triggered immunity and arbuscular mycorrhizal symbiosis in rice. Plant Cell Physiol. (2014). doi:10.1093/pcp/pcu129

Mohd, S. et al. Endophytic fungi *Piriformospora indica* mediated protection of host from arsenic toxicity. Front. Microbiol. (2017). doi:10.3389/fmicb.2017.00754

Moscatiello, R. et al. The intracellular delivery of TAT-aequorin reveals calcium-mediated sensing of environmental and symbiotic signals by the arbuscular mycorrhizal fungus *Gigaspora margarita*. New Phytol. (2014). doi:10.1111/nph.12849

Mosquera, G., Giraldo, M. C., Khang, C. H., Coughlan, S. & Valent, B. Interaction Transcriptome Analysis Identifies *Magnaporthe oryzae* BAS1-4 as Biotrophy-Associated Secreted Proteins in Rice Blast Disease. Plant Cell Online (2009). doi:10.1105/tpc.107.055228

Mukherjee, A. & Ané, J.-M. Germinating Spore Exudates from Arbuscular Mycorrhizal Fungi: Molecular and Developmental Responses in Plants and Their Regulation by Ethylene. Mol. Plant-Microbe Interact. (2010). doi:10.1094/mpmi-06-10-0146

Murray, J. D. et al. Vapyrin, a gene essential for intracellular progression of arbuscular mycorrhizal symbiosis, is also essential for infection by rhizobia in the nodule symbiosis of *Medicago truncatula*. Plant J. (2011). doi:10.1111/j.1365-313X.2010. 04415.x

Nadal, M. & Paszkowski, U. Polyphony in the rhizosphere: Presymbiotic communication in arbuscular mycorrhizal symbiosis. Current Opinion in Plant Biology (2013). doi: 10.1016/j.pbi.2013.06.005

Nadal, M. et al. An N-acetylglucosamine transporter required for arbuscular mycorrhizal symbioses in rice and maize. Nat. Plants 3, 17073 (2017).

Nagahashi, G. & Douds, D. D. The effects of hydroxy fatty acids on the hyphal branching of germinated spores of AM fungi. Fungal Biol. (2011). doi: 10.1016/j.funbio.2011.01.006

Nagy, R. et al. The characterization of novel mycorrhiza-specific phosphate transporters from *Lycopersicon esculentum* and *Solanum tuberosum* uncovers functional redundancy in symbiotic phosphate transport in solanaceous species. Plant J. (2005). doi:10.1111/j.1365-313X.2005. 02364.x

Nakagami, H. et al. Large-Scale Comparative Phosphoproteomics Identifies Conserved Phosphorylation Sites in Plants. Plant Physiol. (2010). doi:10.1104/pp.110.157347

Nakagawa, T. & Imaizumi-Anraku, H. Rice arbuscular mycorrhiza as a tool to study the molecular mechanisms of fungal symbiosis and a potential target to increase productivity. Rice (2015). doi:10.1186/s12284-015-0067-0

Nakagawa, T. et al. From defense to symbiosis: Limited alterations in the kinase domain of LysM receptor-like kinases are crucial for evolution of legume-Rhizobium symbiosis. Plant J. (2011). doi:10.1111/j.1365-313X.2010. 04411.x

Navarro-Gochicoa, M. T. et al. Characterization of Four Lectin-Like Receptor Kinases Expressed in Roots of *Medicago truncatula*. Structure, Location, Regulation of Expression, and Potential Role in the Symbiosis with *Sinorhizobium meliloti*. Plant Physiol. (2003). doi:10.1104/pp.103.027680

Newsham, K. K., Fitter, A. H. & Watkinson, A. R. Arbuscular Mycorrhiza Protect an Annual Grass from Root Pathogenic Fungi in the Field. J. Ecol. (1995). doi:10.2307/2261180

Nie, H. Z. et al. The secreted protein MoHrip1 is necessary for the virulence of *Magnaporthe oryzae*. Int. J. Mol. Sci. (2019). doi:10.3390/ijms20071643

Novick, P., Field, C. & Schekman, R. Identification of 23 complementation groups required for post-translational events in the yeast secretory pathway. Cell (1980). doi:10.1016/0092-8674(80)90128-2

O'Connell, R. J. & Panstruga, R. Tête à tête inside a plant cell: Establishing compatibility between plants and biotrophic fungi and oomycetes. New Phytologist (2006). doi:10.1111/j.1469-8137.2006. 01829.x

Oldroyd, G. E. D. & Downie, J. A. Calcium, kinases and nodulation signalling in legumes. Nature Reviews Molecular Cell Biology (2004). doi:10.1038/nrm1424

Oldroyd, G. E. D. & Long, S. R. Identification and characterization of nodulation-signaling pathway 2, a gene of *Medicago truncatula* involved in nod factor signaling. Plant Physiol. (2003). doi:10.1104/pp.102.010710

Oldroyd, G. E. D., Mitra, R. M., Wais, R. J. & Long, S. R. Evidence for structurally specific negative feedback in the nod factor signal transduction pathway. Plant J. (2001). doi:10.1046/j.1365-313X.2001. 01149.x

Oldroyd, G. E. D. Speak, friend, and enter: Signalling systems that promote beneficial symbiotic associations in plants. Nature Reviews Microbiology (2013). doi:10.1038/nrmicro2990

Oldroyd, G. E. D. D., Murray, J. D., Poole, P. S. & Downie, J. A. The Rules of Engagement in the Legume-Rhizobial Symbiosis. Annu. Rev. Genet. (2011). doi:10.1146/annurev-genet-110410-132549

Oldroyd, G. E. D. & Downie, J. A. Coordinating Nodule Morphogenesis with Rhizobial Infection in Legumes. Annu. Rev. Plant Biol. (2008). doi: 10.1146/annurev.arplant.59.032607.092839

Orbach, M. J., Farrall, L., Sweigard, J. A., Chumley, F. G. & Valent, B. A Telomeric Avirulence Gene Determines Efficacy for the Rice Blast Resistance Gene Pi-ta. Plant Cell (2007). doi:10.2307/3871102

Ostertag, M., Stammler, J., Douchkov, D., Eichmann, R. & Hückelhoven, R. The conserved oligomeric Golgi complex is involved in penetration resistance of barley to the barley powdery mildew fungus. Mol. Plant Pathol. (2013). doi:10.1111/j.1364-3703.2012. 00846.x

Oteng, J. W. and Sant'Anna, R. International Rice Commission Newsletter Vol. 48. Available at: http://www.fao.org/3/x2243t/x2243t05.htm. (Accessed: 15th April 2019)

Pangesti, N., Pineda, A., Pieterse, C. M. J., Dicke, M. & van Loon, J. J. A. Two-way plant mediated interactions between root-associated microbes and insects: from ecology to mechanisms. Front. Plant Sci. (2013). doi:10.3389/fpls.2013.00414

Panstruga, R. Establishing compatibility between plants and obligate biotrophic pathogens. Current Opinion in Plant Biology (2003). doi:10.1016/S1369-5266(03)00043-8

Parniske, M. Arbuscular mycorrhiza: The mother of plant root endosymbioParniske, M. (2008). Arbuscular mycorrhiza: The mother of plant root endosymbioses. Nat. Rev. Microbiol. 6: 763–775.ses. Nat. Rev. Microbiol. (2008). doi:10.1038/nrmicro1987

Parniske, M. Intracellular accommodation of microbes by plants: A common developmental program for symbiosis and disease? Current Opinion in Plant Biology (2000). doi:10.1016/S1369-5266(00)00088-1

Parniske, M. Arbuscular mycorrhiza: The mother of plant root endosymbioses. Nature Reviews Microbiology (2008). doi:10.1038/nrmicro1987

Paszkowski, U. A journey through signaling in arbuscular mycorrhizal symbioses 2006. New Phytologist (2006). doi:10.1111/j.1469-8137.2006. 01840.x

Paszkowski, U., Jakovleva, L. & Boller, T. Maize mutants affected at distinct stages of the arbuscular mycorrhizal symbiosis. Plant J. (2006). doi:10.1111/j.1365-313X.2006. 02785.x

Paszkowski, U., Kroken, S., Roux, C. & Briggs, S. P. Rice phosphate transporters include an evolutionarily divergent gene specifically activated in arbuscular mycorrhizal symbiosis. Proc. Natl. Acad. Sci. U. S. A. (2002). doi:10.1073/pnas.202474599

Pečenková, T., Marković, V., Sabol, P., Kulich, I. & Zárský, V. Exocyst and autophagy-related membrane trafficking in plants. Journal of Experimental Botany (2017). doi:10.1093/jxb/erx363

Peiter, E. et al. The Medicago truncatula DMI1 Protein Modulates Cytosolic Calcium Signaling. PLANT Physiol. (2007). doi:10.1104/pp.107.097261

Perfect, S. E. & Green, J. R. Infection structures of biotrophic and hemibiotrophic fungal plant pathogens. Molecular Plant Pathology (2001). doi:10.1046/j.1364-3703.2001. 00055.x

Petutschnig, E. K., Jones, A. M. E., Serazetdinova, L., Lipka, U. & Lipka, V. The Lysin Motif Receptor-like Kinase (LysM-RLK) CERK1 is a major chitin-binding protein in *Arabidopsis thaliana* and subject to chitin-induced phosphorylation. J. Biol. Chem. (2010). doi:10.1074/jbc.M110.116657

Pimprikar, P. et al. A CCaMK-CYCLOPS-DELLA complex activates transcription of RAM1 to regulate arbuscule branching. Curr. Biol. (2016). doi: 10.1016/j.cub.2016.01.069

Pimprikar, P. & Gutjahr, C. Transcriptional Regulation of Arbuscular Mycorrhiza Development. Plant and Cell Physiology (2018). doi:10.1093/pcp/pcy024

Poovaiah, B. W., Du, L., Wang, H. & Yang, T. Recent advances in calcium/calmodulin-mediated signaling with an emphasis on plant-microbe interactions. Plant Physiology (2013). doi:10.1104/pp.113.220780

Popp, C. & Ott, T. Regulation of signal transduction and bacterial infection during root nodule symbiosis. Current Opinion in Plant Biology (2011). doi: 10.1016/j.pbi.2011.03.016

Poulsen, K. H. et al. Physiological and molecular evidence for Pi uptake via the symbiotic pathway in a reduced mycorrhizal colonization mutant in tomato associated with a compatible fungus. New Phytol. (2005). doi:10.1111/j.1469-8137.2005. 01523.x

Price, N. P. J. et al. Broad-host-range Rhizobium species strain NGR234 secretes a family of carbamoylated, and fucosylated, nodulation signals that are O-acetylated or sulphated. Mol. Microbiol. (1992). doi:10.1111/j.1365-2958. 1992.tb01793.x

Pumplin, N. & Harrison, M. J. Live-cell imaging reveals periarbuscular membrane domains and organelle location in *Medicago truncatula* roots during arbuscular mycorrhizal symbiosis. Plant Physiol. (2009). doi:10.1104/pp.109.141879

Pumplin, N. et al. *Medicago truncatula* Vapyrin is a novel protein required for arbuscular mycorrhizal symbiosis. Plant J. (2010). doi:10.1111/j.1365-313X.2009. 04072.x

Radutoiu, S. et al. LysM domains mediate lipochitin-oligosaccharide recognition and Nfr genes extend the symbiotic host range. EMBO J. (2007). doi: 10.1038/sj.emboj.7601826

Radutoiu, S. et al. Plant recognition of symbiotic bacteria requires two LysM receptor-like kinases. Nature (2003). doi:10.1038/nature02039

Raj, B. M., Kumar, R. B., Rao, G. V. & Murthy, K. S. R. An optimised in vitro protocol for mass production of *Rhizophagus irregularis* spores - for sustainable agriculture. African J. Bacteriol. Res. (2017). doi:10.5897/JBR2016.0214

Ranf, S. et al. Microbe-associated molecular pattern-induced calcium signaling requires the receptor-like cytoplasmic kinases, PBL1 and BIK1. Ann. Bot. (2014). doi:10.1186/s12870-014-0374-4

286. Read, N. D. Exocytosis and growth do not occur only at hyphal tips. Molecular Microbiology (2011). doi:10.1111/j.1365-2958.2011. 07702.x

Rebouillat, J. et al. Molecular genetics of rice root development. Rice (2009). doi:10.1007/s12284-008-9016-5

Rech, S. S., Heidt, S. & Requena, N. A tandem Kunitz protease inhibitor (KPI106)-serine carboxypeptidase (SCP1) controls mycorrhiza establishment and arbuscule development in *Medicago truncatula*. Plant J. (2013). doi:10.1111/tpj.12242

Rey, T. et al. NFP, a LysM protein controlling Nod factor perception, also intervenes in *Medicago truncatula* resistance to pathogens. New Phytol. (2013). doi:10.1111/nph.12198

Rey, T. & Schornack, S. Interactions of benefi cial and detrimental root colonizing filamentous microbes with plant hosts. Genome Biology (2013). doi:10.1186/gb-2013-14-6-121

Rich, M. K. et al. The petunia GRAS transcription factor ATA/RAM1 regulates symbiotic gene expression and fungal morphogenesis in arbuscular mycorrhiza. Plant Physiol. (2015). doi:10.1104/pp.15.00310

Ried, M. K., Antolín-Llovera, M. & Parniske, M. Spontaneous symbiotic reprogramming of plant roots triggered by receptor-like kinases. Elife (2014). doi:10.7554/eLife.03891

Rillig, M. C. et al. Plant root and mycorrhizal fungal traits for understanding soil aggregation. New Phytologist (2015). doi:10.1111/nph.13045

Robatzek, S. et al. Molecular identification and characterization of the tomato flagellin receptor LeFLS2, an orthologue of Arabidopsis FLS2 exhibiting characteristically different perception specificities. Plant Mol. Biol. (2007). doi:10.1007/s11103-007-9173-8

Roche, P. et al. Molecular basis of symbiotic host specificity in rhizobium meliloti: nodH and nodPQ genes encode the sulfation of lipo-oligosaccharide signals. Cell (1991). doi:10.1016/0092-8674(91)90290-F

Ruyter-Spira, C., Al-Babili, S., van der Krol, S. & Bouwmeester, H. The biology of strigolactones. Trends in Plant Science (2013). doi: 10.1016/j.tplants.2012.10.003

Ryder, L. S. & Talbot, N. J. Regulation of appressorium development in pathogenic fungi. Current Opinion in Plant Biology (2015). doi: 10.1016/j.pbi.2015.05.013

Sagan, M., Morandi, D., Tarenghi, E. & Duc, G. Selection of nodulation and mycorrhizal mutants in the model plant *Medicago truncatula* (Gaertn.) after γ-ray mutagenesis. Plant Sci. (1995). doi:10.1016/0168-9452(95)04229-N

Saito, K. et al. Nucleoporin85 is required for calcium spiking, fungal and bacterial symbioses, and seed production in *Lotus japonicus*. Plant Cell (2007). doi:10.1105/tpc.106.046938

Santos, S. G. dos, Silva, P. R. A. da, Garcia, A. C., Zilli, J. É. & Berbara, R. L. L. Dark septate endophyte decreases stress on rice plants. Brazilian J. Microbiol. (2017). doi: 10.1016/j.bjm.2016.09.018

Sasse, J. et al. Asymmetric localisations of the ABC transporter PaPDR1 trace paths of directional strigolactone transport. Curr. Biol. (2015). doi: 10.1016/j.cub.2015.01.015

Saunders, D. G. O., Aves, S. J. & Talbot, N. J. Cell cycle-mediated regulation of plant infection by the rice blast fungus. Plant Cell (2010). doi:10.1105/tpc.109.072447

Schardl, C. L., Scott, B., Florea, S. & Zhang, D. Epichloë Endophytes: Clavicipitaceous Symbionts of Grasses. in The Mycota (2009). doi:10.1007/978-3-540-87407-2_15

Schauser, L. et al. Symbiotic mutants deficient in nodule establishment identified after T-DNA transformation of Lotus japonicus. Mol. Gen. Genet. (1998). doi:10.1007/s004380050831

Schechter, L. M. et al. Multiple Approaches to a Complete Inventory of Pseudomonas syringae pv. tomato DC3000 Type III Secretion System Effector Proteins. Mol. Plant-Microbe Interact. (2007). doi:10.1094/mpmi-19-1180

Schirawski, J. & Perlin, M. H. Plant–microbe interaction 2017—the good, the bad and the diverse. International Journal of Molecular Sciences (2018). doi:10.3390/ijms19051374

Schmitz, A. M. & Harrison, M. J. Signaling events during initiation of arbuscular mycorrhizal symbiosis. Journal of Integrative Plant Biology (2014). doi:10.1111/jipb.12155

Schwartz, S. H., Qin, X. & Loewen, M. C. The biochemical characterization of two carotenoid cleavage enzymes from Arabidopsis indicates that a carotenoid-derived compound inhibits lateral branching. J. Biol. Chem. (2004). doi:10.1074/jbc.M409004200

Sesma, A. & Osbourn, A. E. The rice leaf blast pathogen undergoes developmental processes typical of root-infecting fungi. Nature (2004). doi:10.1038/nature02880

Seto, Y. et al. Carlactone is an endogenous biosynthetic precursor for strigolactones. Proc. Natl. Acad. Sci. U. S. A. (2014). doi:10.1073/pnas.1314805111

Sharda, J. N. & Koide, R. T. Can hypodermal passage cell distribution limit root penetration by mycorrhizal fungi? New Phytol. (2008). doi:10.1111/j.1469-8137.2008. 02600.x

Shibuya, N. & Minami, E. Oligosaccharide signalling for defence responses in plant. Physiol. Mol. Plant Pathol. (2001). doi:10.1006/pmpp.2001.0364

Shimizu, T. et al. Two LysM receptor molecules, CEBiP and OsCERK1, cooperatively regulate chitin elicitor signaling in rice. Plant J. (2010). doi:10.1111/j.1365-313X.2010. 04324.x

Shimoda, Y. et al. Rhizobial and fungal symbioses show different requirements for calmodulin binding to calcium calmodulin-dependent protein kinase in *Lotus japonicus*. Plant Cell (2012). doi:10.1105/tpc.111.092197

Shinya, T. et al. Functional characterization of CEBiP and CERK1 homologs in *Arabidopsis* and rice reveals the presence of different chitin receptor systems in plants. Plant Cell Physiol. (2012). doi:10.1093/pcp/pcs113

Shinya, T., Nakagawa, T., Kaku, H. & Shibuya, N. Chitin-mediated plant-fungal interactions: Catching, hiding and handshaking. Current Opinion in Plant Biology (2015). doi: 10.1016/j.pbi.2015.05.032

Shiu, S. H. & Bleecker, A. B. Plant receptor-like kinase gene family: diversity, function, and signaling. Science's STKE: signal transduction knowledge environment (2001).

Shlezinger, N., Goldfinger, N. & Sharon, A. Apoptotic-like programed cell death in fungi: The benefits in filamentous species. Frontiers in Oncology (2012). doi:10.3389/fonc.2012.00097

Shlezinger, N. et al. Anti-apoptotic machinery protects the necrotrophic fungus botrytis cinerea from host-induced apoptotic-like cell death during plant infection. PLoS Pathog. (2011). doi: 10.1371/journal.ppat.1002185

Simon, L., Bousquet, J., Lévesque, R. C. & Lalonde, M. Origin and diversification of endomycorrhizal fungi and coincidence with vascular land plants. Nature (1993). doi:10.1038/363067a0

Singh, S., Katzer, K., Lambert, J., Cerri, M. & Parniske, M. CYCLOPS, A DNA-binding transcriptional activator, orchestrates symbiotic root nodule development. Cell Host Microbe (2014). doi: 10.1016/j.chom.2014.01.011

Skiada, V. et al. Colonization of legumes by an endophytic Fusarium solani strain FsK reveals common features to symbionts or pathogens. Fungal Genet. Biol. (2019). doi: 10.1016/j.fgb.2019.03.003

Smith, S. E. & Read, D. J. (David J. . Mycorrhizal symbiosis. (Academic Press, 2008).

Smith, S. & Read, D. Mycorrhizal Symbiosis. Mycorrhizal Symbiosis (2008). doi:10.1016/B978-0-12-370526-6.X5001-6

Sousa, J. A. de J. & Olivares, F. L. Plant growth promotion by streptomycetes: Ecophysiology, mechanisms and applications. Chemical and Biological Technologies in Agriculture (2016). doi:10.1186/s40538-016-0073-5

Stacey, G. & Shibuya, N. Chitin recognition in rice and legumes. in Plant and Soil (1997).

Stegmann, M. et al. The ubiquitin ligase PUB22 targets a subunit of the exocyst complex required for PAMP-triggered responses in *Arabidopsis.* Plant Cell (2012). doi:10.1105/tpc.112.104463

Stracke, S. et al. A plant receptor-like kinase required for both bacterial and fungal symbiosis. Nature (2002). doi:10.1038/nature00841

Su, Z. Z. et al. Evidence for Biotrophic Lifestyle and Biocontrol Potential of Dark Septate Endophyte *Harpophora oryzae* to Rice Blast Disease. PLoS One (2013). doi: 10.1371/journal.pone.0061332

Sun, J. et al. Activation of symbiosis signaling by arbuscular mycorrhizal fungi in legumes and riceopen. Plant Cell (2015). doi:10.1105/tpc.114.131326

Sun, Y. et al. Structural basis for flg22-induced activation of the Arabidopsis FLS2-BAK1 immune complex. Science. (2013). doi:10.1126/science.1243825

Sweigard, J. A. et al. Identification, Cloning, and Characterization of PWL2, a Gene for Host Species Specificity in the Rice Blast Fungus. Plant Cell (2007). doi:10.2307/3870097

Synek, L. et al. AtEXO70A1, a member of a family of putative exocyst subunits specifically expanded in land plants, is important for polar growth and plant development. Plant J. (2006). doi:10.1111/j.1365-313X.2006. 02854.x

Takagi, H. et al. MutMap-Gap: Whole-genome resequencing of mutant F2 progeny bulk combined with de novo assembly of gap regions identifies the rice blast resistance gene Pii. New Phytol. (2013). doi:10.1111/nph.12369

Takahashi, S. et al. The photoconvertible water-soluble chlorophyll-binding protein of Chenopodium album is a member of DUF538, a superfamily that distributes in Embryophyta. J. Plant Physiol. (2013). doi: 10.1016/j.jplph.2013.06.001

Takai, R., Isogai, A., Takayama, S. & Che, F. S. Analysis of flagellin perception mediated by flg22 receptor OsFLS2 in rice. Mol. Plant-Microbe Interact. (2008). doi:10.1094/MPMI-21-12-1635

Takeda, N. et al. Gibberellins interfere with symbiosis signaling and gene expression and alter colonization by Arbuscular Mycorrhizal fungi in *Lotus Japonicus*. Plant Physiol. (2015). doi:10.1104/pp.114.247700

Takeda, N., Maekawa, T. & Hayashi, M. Nuclear-localized and deregulated calcium- and calmodulin-dependent protein kinase activates rhizobial and mycorrhizal responses in *Lotus japonicus*. Plant Cell (2012). doi:10.1105/tpc.111.091827

Takeda, N., Sato, S., Asamizu, E., Tabata, S. & Parniske, M. Apoplastic plant subtilases support arbuscular mycorrhiza development in *Lotus japonicus*. Plant J. (2009). doi:10.1111/j.1365-313X.2009. 03824.x

Talbot, N. J. Appressoria. Current Biology (2019). doi: 10.1016/j.cub.2018.12.050

Talbot, N. J. On the Trail of a Cereal Killer: Exploring the Biology of *Magnaporthe grisea.* Annu. Rev. Microbiol. (2004). doi: 10.1146/annurev.micro.57.030502.090957

Talbot, N. J. et al. MPG1 Encodes a Fungal Hydrophobin Involved in Surface Interactions during Infection-Related Development of *Magnaporthe grisea*. Plant Cell (2007). doi:10.2307/3870210

Tamura, Y., Kobae, Y., Mizuno, T. & Hata, S. Identification and expression analysis of arbuscular mycorrhiza-inducible phosphate transporter genes of soybean. Biosci. Biotechnol. Biochem. (2012). doi:10.1271/bbb.110684

Tanaka, A. Reactive Oxygen Species Play a Role in Regulating a Fungus-Perennial Ryegrass Mutualistic Interaction. Plant cell online (2006). doi:10.1105/tpc.105.039263

TerBush, D. R., Maurice, T., Roth, D. & Novick, P. The Exocyst is a multiprotein complex required for exocytosis in Saccharomyces cerevisiae. EMBO J. (1996). doi:10.1002/j.1460-2075.1996.tb01039.x

Tian, W. et al. A calmodulin-gated calcium channel links pathogen patterns to plant immunity. Nature (2019). doi:10.1038/s41586-019-1413-y

Tirichine, L. et al. Deregulation of a Ca 2+ /calmodulin-dependent kinase leads to spontaneous nodule development. Nature (2006). doi:10.1038/nature04862

Trdá, L. et al. The grapevine flagellin receptor VvFLS2 differentially recognizes flagellin-derived epitopes from the endophytic growth-promoting bacterium *Burkholderia phytofirmans* and plant pathogenic bacteria. New Phytol. (2014). doi:10.1111/nph.12592

Tsuzuki, S., Handa, Y., Takeda, N. & Kawaguchi, M. Strigolactone-induced putative secreted protein 1 is required for the establishment of symbiosis by the arbuscular mycorrhizal fungus *Rhizophagus irregularis*. Mol. Plant-Microbe Interact. (2016). doi:10.1094/MPMI-10-15-0234-R

Tu, B. et al. Disruption of OsEXO70A1 Causes Irregular Vascular Bundles and Perturbs Mineral Nutrient Assimilation in Rice. Sci. Rep. (2015). doi:10.1038/srep18609

Tucker, S. L. & Talbot, N. J. Surface attachment an pre-penetration stage development by plant pathogenic fungi. Annu. Rev. 'Phytopathology (2001).

Upson, R., Newsham, K. K., Bridge, P. D., Pearce, D. A. & Read, D. J. Taxonomic affinities of dark septate root endophytes of *Colobanthus quitensis* and *Deschampsia antarctica*, the two native Antarctic vascular plant species. Fungal Ecol. (2009). doi: 10.1016/j.funeco.2009.02.004

Valent, B., Farrall, L. & Chumley, F. G. *Magnaporthe grisea* genes for pathogenicity and virulence identified through a series of backcrosses. Genetics (1991).

Valent, B. & Khang, C. H. Recent advances in rice blast effector research. Current Opinion in Plant Biology (2010). doi: 10.1016/j.pbi.2010.04.012

Van Der Heijden, M. G. A. et al. Mycorrhizal fungal diversity determines plant biodiversity, ecosystem variability and productivity. Nature (1998). doi:10.1038/23932

Vaneault-Fourrey, C., Barooah, M., Egan, M., Wakley, G. & Talbot, N. J. Autophagic fungal cell death is necessary for infection by the rice blast fungus. Science. (2006). doi:10.1126/science.1124550

Varma, A., Bakshi, M., Lou, B., Hartmann, A. & Oelmueller, R. Piriformospora indica: A Novel Plant Growth-Promoting Mycorrhizal Fungus. Agricultural Research (2012). doi:10.1007/s40003-012-0019-5

Venkateshwaran, M. et al. A role for the mevalonate pathway in early plant symbiotic signaling. Proc. Natl. Acad. Sci. U. S. A. (2015). doi:10.1073/pnas.1413762112

Vorholt, J. A. Microbial life in the phyllosphere. Nat. Rev. Microbiol. (2012). doi:10.1038/nrmicro2910

Vukašinović, N. et al. Dissecting a hidden gene duplication: The *Arabidopsis thaliana* SEC10 locus. PLoS One (2014). doi: 10.1371/journal.pone.0094077

Vurukonda, S. S. K. P., Giovanardi, D. & Stefani, E. Plant growth promoting and biocontrol activity of streptomyces spp. As endophytes. International Journal of Molecular Sciences (2018). doi:10.3390/ijms19040952

Wan, J. et al. A LysM Receptor-Like Kinase Plays a Critical Role in Chitin Signaling and Fungal Resistance in Arabidopsis. Plant cell online (2008). doi:10.1105/tpc.107.056754

Wan, J. et al. A lectin receptor-like kinase is required for pollen development in *Arabidopsis*. Plant Mol. Biol. (2008). doi:10.1007/s11103-008-9332-6

Wang, B. & Qiu, Y. L. Phylogenetic distribution and evolution of mycorrhizas in land plants. Mycorrhiza (2006). doi:10.1007/s00572-005-0033-6

Wang, E. et al. A common signaling process that promotes mycorrhizal and oomycete colonization of plants. Curr. Biol. (2012). doi: 10.1016/j.cub.2012.09.043

Wang, E. et al. A H + -ATPase that energizes nutrient uptake during mycorrhizal symbioses in rice and *Medicago truncatula*. Plant Cell (2014). doi:10.1105/tpc.113.120527

Wang, J. L., Li, T., Liu, G. Y., Smith, J. M. & Zhao, Z. W. Unraveling the role of dark septate endophyte (DSE) colonizing maize (*Zea mays*) under cadmium stress: Physiological, cytological and genic aspects. Sci. Rep. (2016). doi:10.1038/srep22028

Wang, Q. et al. Transcriptional Programming and Functional Interactions within the *Phytophthora sojae* RXLR Effector Repertoire. Plant Cell (2011). doi:10.1105/tpc.111.086082

Wang, Y., Nsibo, D. L., Juhar, H. M., Govers, F. & Bouwmeester, K. Ectopic expression of Arabidopsis L-type lectin receptor kinase genes LecRK-I.9 and LecRK-IX.1 in *Nicotiana benthamiana* confers *Phytophthora* resistance. Plant Cell Rep. (2016). doi:10.1007/s00299-015-1926-2

Whalley, H. J. & Knight, M. R. Calcium signatures are decoded by plants to give specific gene responses. New Phytologist (2013). doi:10.1111/nph.12087

Willmann, R. et al. Arabidopsis lysin-motif proteins LYM1 LYM3 CERK1 mediate bacterial peptidoglycan sensing and immunity to bacterial infection. Proc. Natl. Acad. Sci. (2011). doi:10.1073/pnas.1112862108

Willmann, R. et al. mediate bacterial peptidoglycan sensing and immunity to bacterial infection. Proc. Natl. Acad. Sci. U. S. A. (2011). doi: 10.1073/pnas.1112862108/-/DCSupplemental.www.pnas.org/cgi/doi/10.1073/pnas.1112862108

Wilson, R. A. & Talbot, N. J. Under pressure: Investigating the biology of plant infection by *Magnaporthe oryzae*. Nature Reviews Microbiology (2009). doi:10.1038/nrmicro2032

Xie, X. et al. Functional analysis of the novel mycorrhiza-specific phosphate transporter AsPT1 and PHT1 family from Astragalus sinicus during the arbuscular mycorrhizal symbiosis. New Phytol. (2013). doi:10.1111/nph.12188

Xie, X. Structural diversity of strigolactones and their distribution in the plant kingdom. J. Pestic. Sci. (2016). doi:10.1584/jpestics. J16-02

Xin, Z., Wang, A., Yang, G., Gao, P. & Zheng, Z. L. The Arabidopsis A4 subfamily of lectin receptor kinases negatively regulate abscisic acid response in seed germination. Plant Physiol. (2009). doi:10.1104/pp.108.130583

Xue, L. et al. Network of GRAS transcription factors involved in the control of arbuscule development in Lotus japonicus. Plant Physiol. (2015). doi:10.1104/pp.114.255430

Yan, X. & Talbot, N. J. Investigating the cell biology of plant infection by the rice blast fungus *Magnaporthe oryzae*. Current Opinion in Microbiology (2016). doi: 10.1016/j.mib.2016.10.001

Yang, S. Y. et al. Nonredundant regulation of rice arbuscular mycorrhizal symbiosis by two members of the phosphate transporter1 gene family. Plant Cell (2012). doi:10.1105/tpc.112.104901

Yang, S. Y. & Paszkowski, U. Phosphate import at the arbuscule: Just a nutrient? Molecular Plant-Microbe Interactions (2011). doi:10.1094/MPMI-06-11-0151

Yano, K. et al. CYCLOPS, a mediator of symbiotic intracellular accommodation. Proc. Natl. Acad. Sci. U. S. A. (2008). doi:10.1073/pnas.0806858105

Yi, J. & An, G. Utilization of T-DNA tagging lines in rice. J. Plant Biol. (2013). doi:10.1007/s12374-013-0905-9

Yoshida, K. et al. Association genetics reveals three novel avirulence genes from the rice blast fungal pathogen *Magnaporthe oryzae*. Plant Cell (2009). doi:10.1105/tpc.109.066324

Yu, I. C., Parker, J. & Bent, A. F. Gene-for-gene disease resistance without the hypersensitive response in *Arabidopsis dnd1* mutant. Proc. Natl. Acad. Sci. U. S. A. (1998). doi:10.1073/pnas.95.13.7819

Yu, N. et al. A della protein complex controls the arbuscular mycorrhizal symbiosis in plants. Cell Research (2014). doi:10.1038/cr.2013.167

Yuan, P., Jauregui, E., Du, L., Tanaka, K. & Poovaiah, B. W. Calcium signatures and signaling events orchestrate plant–microbe interactions. Current Opinion in Plant Biology (2017). doi: 10.1016/j.pbi.2017.06.003

Žárský, V., Kulich, I., Fendrych, M. & Pečenková, T. Exocyst complexes multiple functions in plant cells secretory pathways. Current Opinion in Plant Biology (2013). doi: 10.1016/j.pbi.2013.10.013

Zhang, Q., Blaylock, L. A. & Harrison, M. J. Two Medicago truncatula half-ABC transporters are essential for arbuscule development in arbuscular mycorrhizal symbiosis. Plant Cell (2010). doi:10.1105/tpc.110.074955

Zhang, S. & Xu, J.-R. Effectors and Effector Delivery in *Magnaporthe oryzae*. PLoS Pathog. (2014). doi: 10.1371/journal.ppat.1003826

Zhang, X.-C. X. C. et al. Molecular Evolution of Lysin Motif-Type Receptor-Like Kinases in Plants. Plant Physiol. (2007). doi:10.1104/pp.107.097097

Zhang, X. et al. The receptor kinase CERK1 has dual functions in symbiosis and immunity signalling. Plant J. (2015). doi:10.1111/tpj.12723

Zhang, X., Pumplin, N., Ivanov, S. & Harrison, M. J. EXO70I is required for development of a sub-domain of the periarbuscular membrane during arbuscular mycorrhizal symbiosis. Curr. Biol. (2015). doi: 10.1016/j.cub.2015.06.075

Zhang, Y. et al. Rice cytochrome P450 MAX1 homologs catalyze distinct steps in strigolactone biosynthesis. Nat. Chem. Biol. (2014). doi:10.1038/nchembio.1660

Zhu, H., Riely, B. K., Burns, N. J. & Ané, J. M. Tracing nonlegume orthologs of legume genes required for nodulation and arbuscular mycorrhizal symbioses. Genetics (2006). doi:10.1534/genetics.105.051185

Zipfel, C. & Oldroyd, G. E. D. D. Plant signalling in symbiosis and immunity. Nature (2017). doi:10.1038/nature22009

Zipfel, C. et al. Bacterial disease resistance in Arabidopsis through flagellin perception. Nature (2004). doi:10.1038/nature02485